SERDP ER-1376
Enhancement of In Situ Bioremediation of Energetic Compounds by Coupled Abiotic/Biotic Processes:

Final Report for 2004 - 2006

Jim E. Szecsody
Steve Comfort**
Herb L. Fredrickson*
Hardiljeet K. Boparai**
Brooks J. Devary
Karen T. Thompson*
Jerry L. Phillips
Fiona Crocker*
Don C. Girvin
C. Tom Resch
Patrick Shea**
Ashley Fischer
Lisa Durkin

August 2007

Pacific Northwest National Laboratory
Richland, Washington 99352

_____

*U.S. Army Engineer Research & Development Center
Environmental Laboratory at Waterways Experiment Station
Vicksburg, Mississippi 39180-6199

**School of Natural Resources
University of Nebraska
Lincoln, Nebraska 68583

Report Documentation Page

Form Approved
OMB No. 0704-0188

Public reporting burden for the collection of information is estimated to average 1 hour per response, including the time for reviewing instructions, searching existing data sources, gathering and maintaining the data needed, and completing and reviewing the collection of information. Send comments regarding this burden estimate or any other aspect of this collection of information, including suggestions for reducing this burden, to Washington Headquarters Services, Directorate for Information Operations and Reports, 1215 Jefferson Davis Highway, Suite 1204, Arlington VA 22202-4302. Respondents should be aware that notwithstanding any other provision of law, no person shall be subject to a penalty for failing to comply with a collection of information if it does not display a currently valid OMB control number.

1. REPORT DATE **AUG 2007**	2. REPORT TYPE	3. DATES COVERED **00-00-2007 to 00-00-2007**
4. TITLE AND SUBTITLE **Enhancement of In Situ Bioremediation of Energetic Compounds by Coupled Abiotic/Biotic Processes**		5a. CONTRACT NUMBER
		5b. GRANT NUMBER
		5c. PROGRAM ELEMENT NUMBER
6. AUTHOR(S)		5d. PROJECT NUMBER
		5e. TASK NUMBER
		5f. WORK UNIT NUMBER
7. PERFORMING ORGANIZATION NAME(S) AND ADDRESS(ES) **Pacific Northwest National Laboratory,902 Battelle Boulevard,Richland,WA,99354**		8. PERFORMING ORGANIZATION REPORT NUMBER
9. SPONSORING/MONITORING AGENCY NAME(S) AND ADDRESS(ES)		10. SPONSOR/MONITOR'S ACRONYM(S)
		11. SPONSOR/MONITOR'S REPORT NUMBER(S)

12. DISTRIBUTION/AVAILABILITY STATEMENT
Approved for public release; distribution unlimited

13. SUPPLEMENTARY NOTES

14. ABSTRACT

15. SUBJECT TERMS

16. SECURITY CLASSIFICATION OF:			17. LIMITATION OF ABSTRACT	18. NUMBER OF PAGES	19a. NAME OF RESPONSIBLE PERSON
a. REPORT **unclassified**	b. ABSTRACT **unclassified**	c. THIS PAGE **unclassified**	**Same as Report (SAR)**	**314**	

Standard Form 298 (Rev. 8-98)
Prescribed by ANSI Std Z39-18

DISCLAIMER

This report was prepared as an account of work sponsored by an agency of the United States Government. Neither the United States Government nor any agency thereof, nor Battelle Memorial Institute, nor any of their employees, makes **any warranty, express or implied, or assumes any legal liability or responsibility for the accuracy, completeness, or usefulness of any information, apparatus, product, or process disclosed, or represents that its use would not infringe privately owned rights**. Reference herein to any specific commercial product, process, or service by trade name, trademark, manufacturer, or otherwise does not necessarily constitute or imply its endorsement, recommendation, or favoring by the United States Government or any agency thereof, or Battelle Memorial Institute. The views and opinions of authors expressed herein do not necessarily state or reflect those of the United States Government or any agency thereof.

SERDP ER-1376
Enhancement of In Situ Bioremediation
of Energetic Compounds by
Coupled Abiotic/Biotic Processes:

Final Report for 2004 - 2006

Jim E. Szecsody
Steve Comfort**
Herb L. Fredrickson*
Hardiljeet K. Boparai**
Brooks J. Devary
Karen T. Thompson*
Jerry L. Phillips
Fiona Crocker*
Don C. Girvin
C. Tom Resch
Patrick Shea**
Ashley Fischer
Lisa Durkin

August 2007

Pacific Northwest National Laboratory
Richland, Washington 99352

_____

*U.S. Army Engineer Research & Development Center
Environmental Laboratory at Waterways Experiment Station
Vicksburg, Mississippi 39180-6199

**School of Natural Resources
University of Nebraska
Lincoln, Nebraska 68583

Table of Contents

List of Figures

List of Figures (Continued)

List of Figures (Continued)

List of Figures (Continued)

List of Figures (Continued)

List of Figures (Continued)

List of Tables

Acronyms

2-ADNT	2-aminodinitrotoluene, TNT degradation intermediate
4-ADNT	4-aminodinitrotoluene, TNT degradation intermediate
CL-20	2,4,6,8,10,12-Hexanitro-2,4,6,8,10,12-Hexaazaisowurzitane, CAS 135285-90-4
2,4-DANT	2,4-diaminonitrotoluene, TNT degradation intermediate
2,6-DANT	2,6-diaminonitrotoluene, TNT degradation intermediate
di/Fe	molar ratio of sodium dithionite to reducible ferrous iron in sediment dithionite is used to chemically reduce ferric iron surface phases
DCB	dithionite-citrate-bicarbonate soil extraction for ferric oxides
DNX	hexahydro-1,3-dinitroso-5-nitro-1,3,5-triazine, RDX deg. intermediate
DOD	U.S. Department of Defense
DOE	U.S. Department of Energy
EPA	U.S. Environmental Protection Agency
EPPS	N-2-hydroxyethylpiperazine propane sulfonic acid, pH buffer
ERDC	U.S Army Research and Development Center
FRC	Field Research Center at the U.S. DOE Oak Ridge Site
GC	gas chromatography
HE	high explosive
HEPES	4-(2-hydroxyethyl)-1-piperazine ethane sulfonic acid, pH buffer
HMX	1,3,5,7-tetranitro-1,3,5,7-tetrazocane, high melting explosive, CAS 2691-41-0
HPLC-UV	high performance liquid chromatography with ultraviolet detection
2-HADNT	2-hydroxyaminodinitrotoluene, TNT degradation intermediate
4-HADNT	4-hydroxyaminodinitrotoluene, TNT degradation intermediate
LC/MS	liquid chromatography/mass spectrometry
MDNA	methylene dinitramine, RDX and HMX degradation intermediate
MNX	hexahydro-1-nitroso-3,5-dinitro-1,3,5-triazine, RDX deg. intermediate
MSM	mineral salt media used for microbial experiments
4-NADB	4-nitro-2,4-diaza-butanal, RDX degradation intermediate
PIPES	1,4-piperazinediethanesulfonic acid, pH buffer
PLFA	phospholipids fatty acids
PNNL	Pacific Northwest National Laboratory, Richland, WA
PRB	permeable reactive barrier
RDX	hexahydro-1,3,5-trinitro-1,3,5-triazine, royal demolition explosive, CAS 121-8-24
SERDP	Strategic Environmental Research and Development Program
TETRYL	trinitrophenylmethylnitramine explosive, CAS 479-45-8
TAT	triaminotoluene, TNT degradation intermediate
TNT	1,3,5-trinitrotoluene, CAS 118-96-7
TNX	hexahydro-1,3,5-trinitroso-1,3,5-triazine, RDX degradation intermediate
UNL	University of Nebraska, Lincoln
UV	ultraviolet
WES	U.S. ERDC, Waterways Experiment Station, Vicksburg, MS
ZVI	zero valent iron

Acknowledgments

Executive Summary

This project was initiated by SERDP to quantify processes and determine the effectiveness of abiotic/biotic mineralization of energetics (RDX, HMX, TNT) in aquifer sediments by combinations of biostimulation (carbon, trace nutrient additions) and chemical reduction of sediment to create a reducing environment. Initially it was hypothesized that a balance of chemical reduction of sediment and biostimulation would increase the RDX, HMX, and TNT mineralization rate significantly (by a combination of abiotic and biotic processes) so that this abiotic/biotic treatment may be more efficient for remediation than biotic treatment alone in some cases. Because both abiotic and biotic processes are involved in energetic mineralization in sediments, it was further hypothesized that consideration for both abiotic reduction *and* microbial growth was need to optimize the sediment system for the most rapid mineralization rate. Results show that there are separate optimal abiotic/biostimulation aquifer sediment treatments for RDX/HMX and for TNT. Optimal sediment treatment for RDX and HMX (which have chemical similarities and similar degradation pathways) is mainly chemical reduction of sediment, which increased the RDX/HMX *mineralization* rate 100 to150 times (relative to untreated sediment), with a secondary treatment of carbon or trace nutrients, which increased the RDX/HMX mineralization rate an additional 3 to 4 times. In contrast, the optimal aquifer sediment treatment for TNT involves mainly biostimulation (glucose addition), which stimulates a TNT/glucose cometabolic degradation pathway (6.8 times more rapid than untreated sediment), with secondary treatment by chemical reduction (13 times additional rate increase). TNT is transformed to triaminotoluene, which irreversibly sorbs in reduced systems but is rapidly degraded in oxic systems. Although the TNT degradation pathway is biologically dominated, the iron-reducing conditions created by abiotic reduction of sediment promotes more rapid abiotic degradation of amino-intermediates than biodegradation of these intermediates. Chemical reduction of sediment alone is not an effective treatment for TNT (intermediates that irreversibly sorb are not produced), even though the TNT degradation rate (to 2- or 4-aminodinitrotoluene) increases.

RDX mineralization increases significantly with dithionite treatment (98x), and indicates subsurface sediment remediation by in situ chemical reduction of sediment should be highly effective. The influence of dithionite treatment in promoting RDX mineralization was far greater than biostimulation alone (i.e., either a carbon source or trace nutrients added, or with prestimulation) in experiments lasting 1 to 3 months, although it is believed that optimal prestimulation for several months should promote high degradation rates. More specifically, RDX mineralization with untreated sediment had a 31,000 h half-life, whereas anoxic biostimulation with lactate addition had a half-life of 9900 h, biostimulation with trace nutrient addition had a half-life of 14,400 h, and anoxic prestimulation with trace nutrient and carbon source addition (5600 h half-life). All oxic biostimulation studies showed slower RDX mineralization rates compared with anoxic systems. In contrast, RDX mineralization with dithionite treatment (315 h half-life) or dithionite treatment with trace nutrients (112 h half-life) were 50x to 300x more rapid (and extent as much as 78%). Additions of 5-micron zero valent iron (0.04% to 0.4% – same weight percentage as ferrous iron in dithionite-reduced sediment) to sediment achieved nearly the same RDX mineralization rates (373 h to 540 h half-life) as dithionite treated sediment.

The first four RDX transformation steps (RDX -> MNX -> DNX -> TNX -> methylene dinitramine, MDNA) were determined to be abiotic, as the addition of a bactericide to the

reduced sediment did not slow the transformation rates. These abiotic transformation steps are rapid (5 minute to 4.5 h half-life), so not rate limiting in the overall RDX to CO_2 transformation. The methylene dinitramine (MDNA) transformation rate in reduced and oxic sediments was the same, but most rapid by acid hydrolysis (i.e., aqueous degradation reaction). MDNA transformation was slower in reduced sediment relative to untreated sediment, which is an artifact of reduced sediments being more alkaline pH (8.5 to 9.2) relative to untreated sediment. MDNA was not rate-limiting in batch experiments, due to the rapid hydrolysis rate (relative to RDX mineralization) and no observed MDNA buildup. However, MDNA was measurable in some 1-D column studies, which have significantly (100x) higher soil/water ratios, because the RDX/sediment interactions can generate MDNA more rapidly than the (proportionally less) pore water can degrade. MDNA degradation, could, therefore be partially rate-limiting in aquifers at high soil/water ratios. The final RDX degradation step is formate mineralization. This reaction can occur biotically, but experiments in reduced sediments demonstrated that this is a coupled abiotic/biotic reaction. The presence of a bactericide stopped formate mineralization, and increasing amounts of sediment reduction greatly increased the formate mineralization rate (i.e., abiotic component of the reaction). Formate mineralization was quite slow in untreated sediment (7400 h half-life) with similarity to RDX mineralization (31,000 h half-life), and rapid in reduced sediment (60 h half-life) again with similarity to RDX mineralization (315 h half-life). It is likely that this formate mineralization reaction is the rate-limiting step in RDX mineralization in dithionite-reduced sediments. Therefore, the apparent strong abiotic control of RDX mineralization (i.e., the 270x increase in the RDX mineralization rate is directly proportional to the amount of dithionite treatment) is coupled reaction control (formate abiotic/biotic mineralization).

HMX mineralization in reduced sediments was predominantly a function of the amount of sediment reduction with a smaller function of biostimulation (trace nutrient or carbon addition), similar to RDX behavior. In untreated sediment, the HMX mineralization rate was very slow (half-life 7800 h), whereas in dithionite-reduced sediments, HMX mineralization was 48x more rapid (162 h half-life). Mineralization extent in reduced sediments was as much as 66.4%. The HMX degradation pathway in reduced sediment is very similar to RDX with initial attack of the nitroso- groups, forming mono-, di-, tri, then tetra-nitrosoHMX. Subsequent ring cleavage forms methylene dinitramine. The initial degradation reaction of HMX to mononitrosoHMX is an abiotic reaction, as the addition of a bactericide did not slow HMX degradation in reduced sediment. The activation energy for this initial HMX degradation reaction by dithionite-reduced sediment was calculated to be 37.5 kJ/mol, and is therefore chemically controlled. This reaction is exothermic proceeding more rapidly at colder temperatures. The average HMX transformation rate is 1.6×10^{-6} mol g^{-1} day^{-1} (half-life 48 minutes). This rate is still two to three orders of magnitude more rapid than the overall HMX mineralization rate, so is not rate limiting. Although fewer HMX intermediates were investigated, the previously described degradation of methylene dinitramine (half-life 8 h in reduced sediment) indicates that it is also not the rate limiting step. The coupled mineralization of formate, which is very slow in untreated sediment (7400 h half-life) and rapid in reduced sediment (60 h half-life) is the likely rate-limiting step for HMX mineralization.

Trinitrotoluene is rapidly degraded to 2-aminodinitrotoluene (2-ADNT) and 4-aminodinitrotoluene (4-ADNT), then 2,6-diaminonitrotoluene (2,6-DANT) and

2,4-diaminonitrotoluene (2,4-DANT), then triaminotoluene (TAT) and possibly further by a cometabolic process with glucose addition (primary treatment) and sediment reduction (secondary treatment). The final product (triaminotoluene) is difficult to measure due to irreversible sorption and rapid aqueous degradation, so it may be degraded further. This cometabolic process was previously reported by others for the treatment of *surface* soils (contained bacteria, daphnids, algae, cress plants, and earth worms), but has not been reported for subsurface sediments containing only bacteria. This amino-degradation pathway is a viable subsurface remediation technology as it produces dinitroaminotoluene and triaminotoluene products that irreversibly sorb. Although this pathway is predominantly biotic, the partial *abiotic* control was shown by degradation rate experiments with intermediates. TNT degraded more rapidly in reduced sediment relative to untreated sediment. Both 2-ADNT and 4-ADNT degraded far more rapidly upon dithionite reduction (half-life 1100 h in untreated sediment, 2.0 h in reduced sediment). In addition, both 2,4-DANT and 2,6-DANT were degraded much more rapidly in reduced sediments (half-life 40,000 h in untreated sediment, 65 h in reduced sediment). Triaminotoluene (TAT) was degraded rapidly by acid hydrolysis (half-life 3.8 h at pH 2.5; 88 h at pH 7.1; 306 h at pH 12). Therefore, TAT was likely degraded in oxic and reduced sediments, but more slowly in reduced sediments due to the increase in pH. TNT mineralization in dithionite-reduced sediments (*without* glucose cometabolic degradation) behaves very differently than RDX and HMX. TNT mineralization was very slow (>10,000 h half-life) and limited in extent in untreated and reduced sediments (<2.7% in 1400 h), and showed no trend in rate with increasing dithionite treatment of sediment. Therefore, TNT degradation in this subsurface sediment appears to be greatly enhanced predominantly by biostimulation (cometabolic degradation with glucose), which produces irreversibly sorbed triaminotoluene. Dithionite reduction of sediment accelerated this biostimulation process (by about 11x), likely due to more rapid degradation of some amino-intermediates.

The microbial population, in general, appears to be little affected by low to moderate dithionite/carbonate concentrations used to reduce sediment. High dithionite concentrations (0.1 mol/L) did cause high microbial death (90% death, as defined by PCR/DNA and AODC biomass and acetate mineralization half-life). However, the remaining population is well able to mineralize RDX and HMX intermediates, as mineralization rates are most rapid for RDX and HMX in highly reduced sediments that received the high dithionite concentration treatment. The live-dead stain showed that the microbial population decreased the most with separate dithionite exposure (i.e., no potassium carbonate), and was not as affected by exposure to carbonate or exposure to dithionite and carbonate. Dithionite treatment of sediment does result in an increase in surface ferrous iron phases for low to moderate dithionite concentrations, but treatment with a large excess of dithionite does not result in additional reductive capacity. High dithionite concentration treatments did show changes in ferrous iron phase changes, which correlated with large differences in RDX and HMX mineralization rates (much more rapidly in highly reduced sediment). Sediment redox potential (Eh) was a measurable function of dithionite treatment, but additional redox potential changes take place over time in the reduced/biostimulated sediments due to microbial activity. Long-term degradation experiments with RDX and TNT degradation both showed a significantly more reducing environment after 1000 h.

Different optimal subsurface treatments for RDX/HMX and for TNT is likely manageable for field scale remediation, as few sites have groundwater contamination of all three energetics in

the same location. RDX and HMX are common groundwater contaminants due to slow aerobic degradation in soils and vadose zone sediments, and minimal sorption. In contrast, TNT is a common soil/shallow sediment contaminant with limited TNT subsurface migration because of aerobic and anaerobic degradation in soils and significantly greater sorption. TNT groundwater contamination does occur, however, typically at sites with subsurface burial of UXO, but would generally moves significantly slower than RDX and HMX due to greater sorption.

1. Introduction

This report represents the three-year final progress report for SERDP project 1376 entitled "Enhancement of In Situ Bioremediation of Energetic Compounds by Coupled Abiotic/Biotic Processes" for the period December 2003 to December 2006. This laboratory study of energetics (TNT, RDX, HMX) subsurface fate involves research at Pacific Northwest National Laboratory (Dr. Jim Szecsody, Dr. Don Girvin, Brooks Devary, Jerry Phillips, Tom Resch, and Ashley Fisher), the U.S. Army Engineer Research & Development Center, Waterways Experiment Station (Dr. Herb Fredrickson, Dr. Fiona Crocker, and Karen Thompson), and at the University of Nebraska, Lincoln (Dr. Steve Comfort and Dr. Hardiljeet Boparai).

The general objective of the project is to stimulate energetic bioremediation in natural sediments to maximize mineralization (risk reduction) by abiotically creating an iron-reducing environment to stimulate microbial growth and promote initial abiotic degradation. This coupled biotic/abiotic technology has successfully increased the RDX mineralization rates and CL-20 (hexanitrohexaazaisowurtzitane) degradation rate by several orders of magnitude in laboratory experiments, but the mechanism and rate-limiting steps were not known prior to this study. We experimentally investigated several energetic compounds (HMX, TNT, RDX) that exhibit a wide range of subsurface reactivity, and we will determine optimal environmental and microbial conditions for mineralization (i.e., complete degradation. The technical objectives of the project are to:

- Maximize microbial growth of explosives-degrading *isolates* and natural microbial *consortiums* in a chemically reduced natural sediment under iron-reducing conditions, and quantify how changes in microbial growth impact mineralization rates (Task 1)
- Modify the abiotic sediment reduction process to maximize the energetic compound mineralization rate, which is based on the hypothesis that initial steps are abiotic followed by later biotic steps (Task 2)
- Assess the relative importance of initial *abiotic* versus *biotic* transformation of energetic compounds on the final mineralization rate using parallel experiments with live, killed, and bioaugmented microbial communities (Task 3)
- Upscale the process by aqueous flow experiments of energetic compounds through reactive porous media systems and quantify the influence of flow at these high sediment/water ratios on mineralization rates through simulations with field-relevant processes (Task 4)

At all scales, we will collect experimental data using analytical separation and measurement methods (HPLC, LC-MS, radiochemical, ^{13}C-, ^{15}N-labeled) in conjunction with reaction path and transport modeling to quantify reaction processes. Collectively, this study will provide the basis for scale-up of the coupled biotic/abiotic processes for energetic compound remediation in the subsurface environment.

The creation of iron reducing conditions in aquifer sediments was focused primarily on sediments that were chemically reduced with sodium dithionite, as this technology can be used to create a reduced zone at any depth in an aquifer. However, in addition, multiple technologies are compared, including a relatively new technology for injecting 1-5-micron size zero valent iron

particles into an aquifer using shear-thinning fluid. Large grain size zero valent iron has been previously used for coupled abiotic/biotic remediation in soils (i.e., were sediments can be mixed with zero valent iron) and to some extent in shallow aquifers where it has been determined to be some microbial activity near zero valent iron walls. However, zero valent iron walls are typically limited in depth to <50 to 100 ft by trench installation. Deeper zero valent iron walls can be installed by shear plane injection (using guar) with wells spaced 15 ft apart (i.e., process developed by GeoSierra). In addition, 1-5-micron zero valent iron particles can be injected into aquifers in a low concentration (<2%) using a shear thinning fluid to achieve a relatively uniform spatial distribution of particles (Dr. Mart Oostrom, PNNL). The shear thinning fluid is necessary to keep the very dense iron particles in suspension. Given these advances in zero valent iron to deeper aquifer applications, coupled abiotic/biotic degradation of energetics were compared between a) sediment/zero valent iron mixtures, b) dithionite-reduced sediment, and c) biostimulation (various types).

Biostimulation of aquifer sediment was conducted by: a) carbon addition (lactate, glucose, other), b) trace nutrient addition (trace metals, amino acids, vitamins), c) carbon and trace nutrient additions. Most biostimulation experiments were conducted assuming nitrogen uptake by microbes from the energetic compounds and the amount of carbon added was 20:1 relative to the nitrogen available, based on the world-wide C:N ratio of 20. However, a series of cometabolic experiments was conducted with TNT, HMX, and RDX in which a high concentration of glucose was added to aquifer sediments that simulates similar metabolic pathways that can degrade TNT. In this case the C:N ratio of added glucose was 100:1.

In this project, energetic compound microbial reactions, coupled abiotic/biotic effects, and upscaling in flowing systems were investigated over four tasks in increasingly complex systems (Table 1.1) from maximizing microbial growth (Task 1), modifying the abiotic reduction process (Task 2), assessing coupled abiotic and biotic processes (Task 3), and upscaling to flowing systems (Task 4). The proposed work is expected to provide information and a method for predicting energetic compound degradation in an abiotically enhanced microbial reducing zone in the subsurface.

Table 1.1. Tasks associated with coupled energetic remediation.

	Task 1. Microbial Growth	Task 2. Chemical Reductant	Task 3. Coupled Processes	Task 4.Reactive Transport
Goals	Task 1.1: Quantify microbial survival during abiotic sediment reduction Task 1.2: Quantify microbial growth and energetic degradation in reduced sediment with carbon addition	• Quantify sediment reduction efficiency at differing reductant and pH buffer concentration • alter the injected reductant mixture to minimize microbial death (from Task 1) and still achieve sufficient iron reduction	Task 3.1: Quantify rate-limiting abiotic and biotic processes that result in energetic mineralization Task 3.2: Determine the influence of Eh on energetic mineralization	Task 4.1: Influence of flow on coupled abiotic/biotic mineralization of energetics (1-D column experiments) Task 4.2: Determine the influence of 3-D radial injection into aquifers on efficiency of energetic
Hypotheses	Task 1.1: Microbial survival can be maximized by changes to the aqueous reductant chemistry Task 1.2: Microbial growth and energetic mineralization in iron reducing conditions uses energetics as the N-source	• a low concentration, high velocity dithionite injection (greater volume) can achieve similar reduction efficiency as a high concentration injection; necessary to limit microbial death	Task 3.1: Initial transformation of energetics is abiotic, but final mineralization is biotic Task 3.2: Reducing conditions can be created by chemical reduction of natural sediment to achieve optimum conditions for energetic mineralization	Task 4.1: Coupled mineralization rates are 10-50x slower than batch systems Task 4.2: High velocity, low concentration injection can achieve necessary reducing environment at the field scale for mineralization
Expected Results	• quantify microbial growth as a function of dithionite and pH buffer concentrations • quantify TNT/RDX/HMX mineralization rates with and without a carbon source	• significant increase in microbial survival and still achieving sufficient sediment reduction by modification of injection strategy	• determine the significance of coupled microbial/ sediment effects • assess the relative importance of abiotic versus biotic mineralization	• experimental transport data with quantified mineralization • reactive transport model with abiotic/biotic reactions • generalized injection design for field-scale remediation
PI	Fredrickson (WES)	Szecsody, Girvin (PNNL)	Comfort (UNL)	Szecsody (PNNL)

Task 1 - Microbial Growth: The goal of this task is to maximize microbial growth of explosives-degrading *isolates* and natural microbial *consortiums* in a chemically reduced natural sediment under iron-reducing conditions, and to determine the rate of microbial mineralization. We hypothesize that only some explosives-degrading bacteria survive the abiotic process of reducing iron oxides in sediment (i.e., alkaline pH, moderate ionic strength), and these microbial communities grow using energetic compound intermediates and the electron donors. Another scenario would be that the indigenous groundwater bacteria would recolonize the area as the groundwater flows through the reactive zone. Experiments will focus on microbial growth in: a) differing injection concentration conditions, and b) iron reducing conditions. Task 1.1 will focus on microbial survival at different chemical reductant (sodium dithionite) and pH buffer (potassium carbonate) concentrations) to assess what may be adversely affecting the microbial population (i.e., dithionite toxicity, ionic strength, pH). Task 1.2 will assess microbial growth in the abiotically-created iron reducing conditions with the addition of differing energetic compounds (TNT, RDX, HMX) as the sole nitrogen source and differing carbon source additions.

Summarizing the main objectives of Task 1 experiments:

Task 1.1. How does chemical reduction of sediments change microbial survival and energetic degradation. This includes various types of biomass determinations at different dithionite/carbonate concentrations.
Task 1.2. After chemical reduction, does carbon addition result in microbial growth and increased energetic degradation.
Task 1.3. Biomass changes that occur during RDX abiotic/biotic degradation are quantified (i.e., RDX carbon mass incorporation into the biomass).
Task 1.4. Microbial detachment change with the reductant solution and how does this influence energetic biodegradation

Task 2 - Abiotic Reduction Process Modification: The goal of this task is to optimize the abiotic reduction of the iron oxides in the sediments while minimizing microbial destruction. Based on results in Task 1, the abiotic reduction process will likely be modified to minimize the effects on the indigenous microbial population. It is hypothesized that the high pH and high ionic strength used for abiotic reduction (pH 10.5) has the most significant influence on microbial death. Initial experiments in this task will extend these preliminary results by testing the reduction efficiency using 0.001 to 0.1 mol/L sodium dithionite and pH buffer at differing flow rate. The flux of the reductant can remain the same at a lower concentration by increasing the flow rate. The redox capacity of the reduced sediment will be measured by oxidizing dithionite-reduced sediments with oxygen-saturated water to measure the oxygen consumption.

Summarizing the main objectives of Task 2 experiments:

Task 2.1. Geochemical characterization of dithionte-treated sediment, zero-valent treated sediment, and biostimulated sediments.
Task 2.2. Relationship between dithionite treatment extent and RDX energetic mineralization.

Task 2.3. Relationship between dithionite treatment extent and HMX energetic mineralization.

Task 2.4. Relationship between dithionite treatment extent and TNT energetic mineralization.

   Task 3 - Coupled Processes: The goal of this task is to determine the relative importance of initial *abiotic* versus *biotic* transformation of energetic compounds on the final mineralization rate. It is hypothesized that energetic compounds will initially be *abiotically* transformed, but biodegradation is required for mineralization. Experiments in this task will parallel those described in Task 1, but with live, killed, and possibly genetically-altered microbes (to alter a metabolic pathway). It is hypothesized that RDX, TNT, and HMX can be completely mineralized in a reducing environment only in the coupled abiotic/biotic system. It is further hypothesized that the rate of initial TNT degradation will be faster than that of RDX, based on differences in reduction potential and comparison of TNT and RDX biotic degradation rates (Brannon et al. 1992). Hundal (1997) also showed faster abiotic destruction kinetics of TNT than RDX in highly contaminated soils treated with zero valent iron.

   Summarizing the main objectives of Task 3 experiments:

 Task 3.1. Relative contribution of abiotic and microbial processes for energetic degradation with dithionite-treated sediments

 Task 3.2. Eh/pH conditions that will maximize energetic transformation reactions

   Task 4 - Upscaling Coupled Processes: The goal of this task is to quantify energetic compound mineralization rates in flowing porous media systems (1-D columns) and determine the influence of flow on biomineralization and applicability to field scale bioremediation. We hypothesize that biomineralization rates will be slower in flow systems relative to batch (Task 3), as bioreactivity generally is reported slower in columns, due to microbial sorption or nutrient limitations (Szecsody et al. 1993). While the nature of the reaction network (i.e., reaction identity and stoichiometry) is identical in batch and column systems, batch-derived reaction parameters can fail to accurately predict transport because transport effects can significantly influence the apparent manifestation of nonlinear or coupled reactions during advective flow. Difference in biodegradation and mineralization rates in batch and column systems will be quantified by simulation of column experiments using batch-derived parameters.

   Summarizing the main objectives of Task 4 experiments are:

 Task 4.1. RDX degradation/mineralization rate in reduced/biostimulated sediments
 Task 4.2. HMX degradation/mineralization rate in reduced/biostimulated sediments
 Task 4.3. TNT degradation/mineralization rate in reduced/biostimulated sediments

2. Background

Enhanced bioremediation of energetics and other nitroaromatic compounds in the subsurface is often successful in removing parent compounds, but mineralization (i.e., complete destruction) rates are not necessarily faster than natural biodegradation, and often too slow or nonexistent. For example, Boopathy et al. (1994) observed enhanced TNT biotransformation by seven different carbon sources but mineralization was not observed. Persistence of recalcitrant energetics (i.e., RDX and HMX) as well as intermediates of degradable energetics (TNT, CL-20) in the subsurface can last for decades and eventually lead to groundwater contamination. This is especially problematic at firing ranges because the subsurface zone is often the most contaminated (SERDP 1993). Remediating energetics in the subsurface can be accomplished with permeable reactive zones (abiotic, biotic, coupled), when contaminant residence times are sufficient to completely mineralize, or produce intermediates that can be rapidly degraded in aerobic zones downgradient.

Natural and Enhanced Biodegradation of Energetics*: Most explosives contain multiple electron-withdrawing nitro groups on either aromatic or heterocyclic rings (e.g., HMX, RDX, and TNT) or cages (e.g., CL-20). These nitro moieties cause the explosive to resist electrophilic attack by oxygenases under aerobic conditions and usually result in incomplete mineralization. Although many researchers have attempted to improve bioremediation rates by adding carbon sources to promote cometabolism, many reaction intermediates still remain recalcitrant and can be more toxic than parent compounds. Complete degradation (i.e., mineralization) is necessary to achieve full risk reduction of energetic compounds in the subsurface. Biodegradation of TNT occurs through several different metabolic pathways (McCormick 1976), and numerous investigators have examined microbial transformation of TNT and its derivatives (Lenke and Warrelmann 1998; Esteve-Núñez and Ramos 1998). Although the initial steps of TNT degradation appear to occur under both aerobic (Boopathy et al. 1994) and anaerobic conditions (Funk et al. 1993), it has been suggested that the ideal circumstances for degradation occur when TNT is subject to anaerobic conditions followed by aerobic redox conditions (e.g., Bruns-Nagel et al. 1998). Because this type of coupled anaerobic-aerobic condition is unlikely to occur naturally, TNT degradation is typically incomplete, and reaction intermediates accumulate (Comfort et al. 1995). Because the monoamino intermediates of TNT biodegradation are more toxic than TNT, enhancing complete mineralization is needed to lower toxicological risks.

Natural biodegradation (i.e., transformation of parent compound) can be enhanced by addition of a carbon source such as molasses or lactate, but this does not necessarily increase *mineralization* rates. For example, augmented TNT biodegradation at the field scale (Table 1.1) degraded TNT within a week (182 h half-life), but mineralization required 620 h. Consequently, when TNT is flowing through a bioreactive zone, there may not be enough resident time for mineralization to occur. A similar problem may occur with HMX (Table 1.1) because rapid degradation (55 h half-life) has been observed but at much slower mineralization rates (466 h half-life).

Biodegradation of RDX is typically orders of magnitude slower than TNT (Hawari 2000). In one set of laboratory experiments, amended RDX degradation was 1000-fold slower than amended TNT biodegradation (Table 1.1; Singh et al. 1998). As a consequence, complete RDX

mineralization (pathway, Figure 2.1, McCormick et al. 1981) is not observed in natural systems and occurs slowly in augmented bioremediation systems. RDX biomineralization rates observed in laboratory experiments with several sediments ranged from 570 h to 1370 h (Table 2.1). It should be noted that laboratory rates are generally 10- to 100-fold faster than can be achieved at the field scale, so these RDX mineralization rates are considerably slower than those observed for TNT mineralization at the

Figure 2.1. RDX biotic degradation path.

field scale. Although biodegradation of RDX is widely reported (Waisner et al. 2001; Binks et al. 1995; Freedmann and Sutherland 1998; McCormick et al. 1981; Ronen et al. 1998; Sheremata and Hawari 2000), the general consensus is that RDX is biodegraded cometabolically faster under anaerobic rather than aerobic conditions (Hawari 2000).

Table 2.1. Rates of biodegradation and coupled abiotic/biotic degradation of energetic compounds.

Energetic Compound	Process	Remediation System	Geochemical Conditions	Initial Compound Degradation Rate (hours)	Mineralization Rate (hours)
RDX	biodegradation	unamended Ottawa sand[1]	anaerobic, pH 7	94	1370
	biodegradation	amended Ottawa sand[1]	anaerobic, pH 7	62	570
	biodegradation	amended Pantex sediment[1]	anaerobic, pH 8	86	980
	abiotic deg.	iron-reduced Pantex sediment[2] iron-reduced, unamended	anaerobic, pH 8	0.3	--
	coupled abio./bio.	Pantex sediment[2]	anaerobic, pH 8	0.3	101, 109*
TNT	biodegradation	laboratory, microbial isolate[3]	anaerobic	0.09	
	biodegradation	field scale, amended sed.[4]	anaerobic to aerobic	182	620
	abiotic deg.	iron-reduced 2:1 clay[5]	anaerobic, pH 8	0.53	
	abiotic deg.	zero-valent iron[6]	anaerobic	0.33	
HMX	biodegradation	anaerobic sludge[7]	anaerobic	55	466
CL-20	biodegradation	augmented Ft Bliss sediment[8]	aerobic, pH 7	10.2	
	abiotic deg.	Norborne C sediment[2]	aerobic, pH 7	340	
	abiotic deg.	iron-reduced Norborne sed.[2]	anaerobic, pH 8	0.067	

[1]S. Comfort, University of Nebraska, Lincoln, unpublished data
[2]J. Szecsody, Pacific Northwest National Lab., unpublished data
[3]McCormick et al. 1976

[5]J. Amonette, Pacific Northwest National Lab., unpublished data
[6]Agrawal, A., P. Tratnyek, 1996
[7]Hawari, J. A. Halasz, S. Beaudet, 2001

Biodegradation of CL-20, a relatively new explosive, appears to occur at slower rates than TNT but orders of magnitude faster than RDX. Preliminary studies with several explosives-contaminated sediments show 10.2- to 120-h half-lives for CL-20 removal rates. CL-20 mineralization rates have not yet been investigated. Therefore, while bioremediation of some energetic compounds is viable (TNT), additional treatments are needed to achieve a viable remediation methodology for many of the other energetics.

Abiotic Degradation of Energetic: Abiotic technologies such as zero valent iron and chemically reducing natural iron in sediment have shown good success in initially degrading energetics (Singh et al. 1998; Agrawal and Tratnyek 1996; Szecsody et al. 2001, 2004), but in

some cases mineralization does not occur. For example, a purely abiotic mineralization pathway does not occur for RDX (Hawari 2000), so either sequential anaerobic/aerobic pathways or coupled abiotic/biotic processes are needed to achieve mineralization.

In most cases where energetics have been tested, abiotic degradation rates have greatly exceeded the enhanced biodegradation rates. Abiotic reduction of energetics, nitroaromatic pesticides (Tratnyek and Macalady 1989), and polyhalogenated methanes (Pecher et al. 2002) all proceed rapidly. For example, using the same natural sediment, chemically reduced sediment (i.e., abiotic process) degraded RDX 13-times faster than enhanced bioremediation (Table 2.1). Our own laboratory (using ^{14}C-labled TNT), has shown that metal-reduced TNT is >10 times faster than untreated TNT in a surface soil, but that a much larger percentage of the reduced TNT residues end up as bound (unextractable) residue (S. Comfort, unpublished data).

The abiotic reduction of TNT has not been directly compared with bioaugmentation in the same natural sediment system, but abiotic rates are at least as fast as bioaugmentation rates (Table 2.1). The use of a chemical reductant (dithionite, see reduction technology section) to reduce structural iron in clays and iron oxides has shown that TNT degradation is fairly rapid (half-life was 32 minutes, Figure 2.2; Amonette 2000). Nearly equimolar concentrations of Fe(II) and TNT were used in that experiment, so rates of mineralization in reduced natural sediments are not known.

The abiotic reduction of RDX (hexahydro-1,3,5-trinitro-1,3,5 triazine) by chemically-reduced natural sediments was 12x faster than the bioaugmentation reduction rate (Szecsody et al. 2001).   Relative to bioremediation, RDX was quickly degraded (i.e., within minutes) in batch studies using abiotic, reduced sediments (iron reducing conditions) to at least the fourth degradation product (Table 2.1). The initial reduction pathway was the same as the biotic

Figure 2.2. TNT degradation by dithionite-reduced clay (Amonette 2000).

pathway (RDX -> MNX -> DNX -> TNX, Freedman and Sutherland 1998). The observed rates in experiments averaged <3 minutes for RDX, 0.5 h for MNX, and 10 h for DNX, and 80 h for TNX to the next product. In this study, aquifer sediments used from the U.S. DOE Pantex, Texas facility (258' depth) and U.S. DOD Ft. Lewis, Washington Army Base (65' depth) yielded a fairly high redox capacity (0.4% FeII/g Pantex, 0.24% FeII/g Ft. Lewis, Vermeul et al. 2000). This mass of reducible iron represents a sufficient quantity to completely degrade (mineralize) 15 mg RDX per gram of sediment.

The RDX degradation rate was measured as a function of pH, as the rate may increase or decrease depending on the dominant mechanism. Batch experiments conducted at pH 6 through 10 showed RDX destruction was at the same rate over the pH range, indicating that lattice or structural Fe^{2+} may dominate over adsorbed Fe^{2+} as the main reductant. The data also shows that this remediation method is viable over a wide range of pH conditions in soils. This is significant as field-scale RDX sorption is small (nearly unretarded RDX migration) and relatively constant

over a pH range (Boopathy and Manning 2000; Singh et al. 1998). We also observed that reduced Pantex sediments degraded RDX quickly in packed column using relatively rapid water flow.

Coupled Biodegradation and Abiotic Degradation: Initial abiotic degradation rates of energetic compounds are considerably faster than biodegradation rates and can be coupled with biodegradation of intermediates to produce faster overall mineralization rates (Hofstetter et al. 1999; Singh, Comfort, and Shea 1999; Wildman and Alverez 2001). The RDX mineralization rate (109 h half-life) achieved in a laboratory study using biostimulation in abiotically-reduced natural sediments (see abiotic reduction technology section) were 12 times faster than biomineralization rates (1370 h half-life) in the same Pantex sediment (Table 2.1, Szecsody et al. 2001). This was, in part, due to very rapid initial degradation of RDX abiotically by ferrous iron in the natural sediment. This coupled biotic/abiotic mineralization of RDX by reduced sediment was observed in several column experiments, but the rate-limiting step is not known. These degradation rates were maintained for 260 pore volumes, illustrating that the concept of a coupled reduced zone can be maintained for a sufficient amount of time (years to decades) that this is a viable field-scale subsurface remediation technology. This mass of reducible iron represents sufficient quantity to completely degrade (mineralize) 15 mg RDX per gram of sediment.

Coupled abiotic/biotic degradation TNT with a mixture of zero-valent iron and sediment (S. Comfort, unpublished data) has shown a 10x faster mineralization rate relative to natural biodegradation. Although the coupled biotic/abiotic mineralization of other explosives by chemically-reduced sediment has not been investigated, the rapid rates of initial abiotic degradation (relative to biodegradation rates) indicates coupled processes work as well as with RDX.

While the abiotic technology used to create an in situ iron reducing environment is well understood from a number of laboratory to field studies (Szecsody et al 2004; Vermeul et al. 2002), it is still not clear why the mechanism underlying this coupled biotic/abiotic process was significantly more efficient at energetics mineralization than bioremediation alone. It is likely that abiotic and biotic processes are geochemically coupled, creating a much more efficient electron shuttling (i.e., reducing) system than an abiotic or biotic system alone. The mechanism of this efficiency involves both coupled abiotic and biotic redox reactions, as well as nutrient considerations. In one coupled system, the abiotic reduction of nitroaromatic compounds by surface-bound ferrous iron was rapid because of the presence of iron-reducing bacteria, which re-reduced the ferric to ferrous iron (i.e., parallel biotic/abiotic redox reactions; Heijman et al. 1995). In that study, the observed rate of nitroaromatic reduction was not actually controlled by the abiotic reduction rate, but rather it was controlled by the microbial regeneration of the reactive surface sites (i.e., iron reduction). In a different coupled system, RDX was abiotically reduced by zero valent iron, then it was most likely mineralized biotically by the microbial colony in the natural sediment (i.e., redox reactions in series; Singh et al. 1998).

Clearly, remediation of energetics should take advantage of the apparent rapid abiotic degradation rates of energetics by differing reducing technologies (ferrous iron, zero valent iron), as well as the biomineralization of intermediate compounds. Although it is unclear why

biomineralization rates of energetics are faster for coupled abiotic/biotic systems than purely biotic systems, one hypothesis is that intermediates offer a more available nitrogen source than the parent energetic compound. A common method of enhancing bioremediation of explosives is to introduce a carbon source, forcing the microbes to utilize the nitroaromatic as a nitrogen source.

Abiotic Sediment Reduction Technology: We propose a coupled abiotic/biotic remediation scheme for energetics where iron-reducing conditions are artificially created in situ in natural aquifer sediments (with injection of a chemical reductant discussed in this section) and biodegradation is enhanced with the injection of a carbon source near the end of the chemical injection. The geochemical processes and field-scale injection strategies for the injection of this chemical reductant are well known through a number of laboratory investigations and field-scale remediation efforts. Natural sediments have been chemically reduced in the laboratory and successfully treat energetics (RDX, TNT, CL-20, NDMA), chlorinated solvents (PCE, TCE, TCA, 1,1-DCE, cis-DCE), and metals/radionuclides (Cr, U, Tc) using actual aquifer sediments from 10 different sites that have varying depositional environments. Field-scale use of this chemical reductant technology has been demonstrated for three chromate groundwater plumes (largest is a 2300-ft wide barrier at the Hanford Site, Washington State; Fruchter et al. 2000), and a TCE plume.

The proposed technology utilizes existing iron in aquifer sediment that is chemically treated with a reductant (sodium dithionite with a pH buffer) for 24 to 60 h. The dithionite chemical treatment dissolves and reduces amorphous and some crystalline Fe^{III} oxides in sediments (Szecsody et al. 2004). The reduced Fe^{II} created by the dithionite chemical treatment appears to be present in several different Fe^{II} phases: adsorbed Fe^{II}, Fe^{II}-carbonate (siderite), and FeS (iron sulfite), although adsorbed Fe^{2+} appears to be the dominant Fe^{II} phase. Although more than one Fe^{III} phase is likely reduced in a natural sediment, each phase of iron that is reduced by sodium dithionite proceeds via the reaction:

$$S_2O_4^{-2} + 2 >Fe^{3+} + 2 H_2O <==> 2 >Fe^{2+} + 2 SO_3^{-2} + 4H^+ \qquad (1)$$
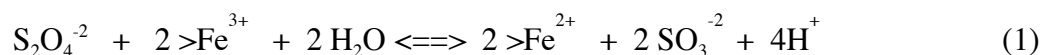
which shows that the forward rate is a function of the dithionite concentration and the square of the reducible iron concentration (rate is overall a third-order function of concentration). The aqueous Fe^{2+} produced has a high affinity for oxide surfaces, and is quickly adsorbed in neutral to slightly alkaline aquifers (pH > 7.5). Therefore, Fe^{2+} mobility in mid- to high pH, low ionic strength groundwater is extremely limited, and iron is not expected to leach from sediments during the dithionite treatment. Aqueous iron measurements in previous studies have shown <1% iron leaching even after 600 pore volumes of groundwater through a sediment column, thus a permeable redox-reactive zone is created in which contaminants flow through for decades. Iron mobility is somewhat higher during the several days of dithionite injection. Previous experimental transport studies with dithionite injection into sediments have shown 0 to 12% iron loss after 40 pore volumes of dithionite treatment. A second reaction occurs in sediments, which describes the disproportionation of dithionite in contact with sediment:

$$2 S_2O_4^{-2} + H_2O <==> S_2O_3^{-2} + 2HSO_3^- \qquad (2)$$
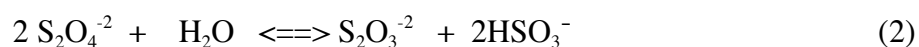
with a half-life of ~27 h, and accounts for the mass loss of dithionite that cannot be used for iron reduction. The consequence of this reaction is to limit how slowly dithionite can be reacted with (i.e., injected into) sediment in the field. While other mineral phases in natural sediments are also reduced; previous studies have shown that the redox capacity was 97% Fe^{II} phases and only 3% Mn^{II} phases.

The chemical reductant concentration used during field scale injections has ranged from 0.025 to 0.09 mol/L (sodium dithionite) and corresponding pH buffer (K_2CO_3). As discussed in Task 2, this relatively high concentration may adversely affect the microbial population, although laboratory experiments have clearly shown that there was significant microbial growth after a dithionite injection. Previous field-scale chemical injections were designed solely for abiotic reduction of iron oxides, although the injection strategy can be easily modified with a lower dithionite/pH buffer concentration and a higher flow rate to achieve similar amount of iron reduction, but with less potential impact on the microbes.

Abiotic/Biotic Reduced Zone Longevity: Once the sediment is reduced, subsequent oxidation of adsorbed and structural ferrous iron in the sediments of the permeable redox barrier occurs naturally by the inflow of dissolved oxygen through the barrier, and additionally by contaminants (TNT, RDX) and other electron acceptors present. In most subsurface systems, dissolved oxygen in water is the dominant oxidant of reduced iron species, as contaminants are generally present at lower molar concentrations relative to dissolved oxygen. Under oxygen-saturated conditions (8.4 mg L^{-1} O_2, 1 atm, 25°C), 1.05 mmol L^{-1} Fe(II) is consumed. RDX at 10 mg/L consumes the equivalent electrons of O_2 saturated water, whereas TNT at 24 mg/L consumes the equivalent electrons as O_2 saturated water. A measure of the total redox capacity of reduced sediment is achieved by oxidization of sediment (Figure 2.3), in this case by O_2 saturated water, yielding 0.4% ferrous iron species, which corresponds to 270 pore volumes of oxygen-saturated water. This redox capacity can be related to the specific field system by knowing the average aquifer concentrations of dissolved oxygen and other electron acceptors. With further knowledge of the groundwater velocity, the expected barrier longevity can be estimated. The 270 pore volume example with an assumed 1 ft/day groundwater velocity corresponds to 25 years (assumed: 30 ft wide reduced zone; no iron reducing bacteria activity). As mentioned earlier, it is likely that microbial growth utilizing the injected carbon source and energetics as the sole nitrogen source will lead to some amount of iron redox cycling. The nitroaromatic compounds are abiotically reduced by the ferrous iron (producing ferric iron), and then

Figure 2.3. Reduced sediment oxidation during flow showing a reductive capacity of 0.4% Fe(II)/g or 270 pore volumes of water.

microbes mineralize the intermediates and reduce the ferric iron back to ferrous iron, as has been shown for specific laboratory systems (Heijman et al. 1995).

10

3. Experimental and Modeling Methods

3.1 Task 1: Microbial Growth and Energetic Degradation

3.1.1 Effect of Dithionite on Soil Biomass

Experiments were set up to determine the effect of dithionite on the soil microbial community using phospholipid fatty acid (PLFA) analysis, acrodyne orange direct counts (AODC), live/dead stain, ^{14}C acetate mineralization, most probable number (MPN), and PCR amplification and DNA analysis to measure biomass. The very low biomass of Ft. Lewis soil was below the detection limits of the PLFA analysis method, therefore the soil used in the PLFA experiment was a 50:50 mixture of a Vicksburg, Mississippi topsoil and Ft. Lewis soil. Batch soil slurries at PNNL and WES were set up in a Coy anaerobic glove bag. One gram of soil was added to 3 ml of water (control) or 3 to 12 ml of a sodium dithionite/K_2CO_3 solution. The water in each tube was bubbled with ultra pure nitrogen for 30 minutes before the appropriate amount of potassium carbonate and sodium dithionite were added. There were four dithionite treatments with concentrations of 25 mM, 6 mM, 3 mM, and 0.6 mM. Concentrations of K_2CO_3 were 100 mM, 24 mM, 12 mM, and 2.4 mM, respectively. PLFA analyses were performed on the soil after 0 and 5 days of incubation. Phospholipids were extracted using the Bligh-Dyer solvent extraction method and then analyzed by GC to determine biomass (Crocker et al. 2005).

Mineralization studies were carried out aerobically by resuspending the washed soil in 3 ml MSM containing the appropriate ^{14}C substrate (^{14}C-acetate). The concentration of all substrates was 10 ppm. To measure the mineralization of each compound, disks were dipped in a 1M barium hydroxide solution and inserted into the top of each test tube cap so that ^{14}C-CO_2 would be absorbed. At appropriate time points, the disks were removed and placed in scintillation cocktail to be counted. Fresh disks with barium hydroxide were then placed in each cap. Alternatively, in experiments at PNNL, small test tubes containing 0.25 mL of 1 M NaOH were used as CO_2 traps. These mineralization studies were carried out until for times ranging from hours to 2000 h. For the live/dead stain, 0.5 ml soil slurry was mixed with 2 μl of fluorescent stains from LIVE/DEAD® *Bac*Light™ kit by Molecular Probes. This procedure makes use of a mixture of SYTO®9 (green-fluorescent nucleic acid stain) for staining all cells (live plus dead) and propidium iodide (red fluorescent nucleic acid stain) that penetrates only bacteria with damaged membranes (dead). Thus, viable cells with intact membranes fluoresce green while those with damaged membranes fluoresce red.

The AODC method relies on a DNA stain of microbes and counting individual microbes under a 1000x optical microscope with special lighting for the DNA stain. One field is shown for untreated and high dithionite treatment to illustrate that more microbes are present for the untreated sediment. The complete method involves using a phosphate buffered saline solution to desorb microbes from the sediment, then 0.2 micron filtering of the water and optical microscopy. For biomass, 20 to 30 different optical views are counted to obtain a realistic average count.

A list of the dithionite treatments conducted in batch systems and column systems (Tables 3.1 and 3.2) at both WES, PNNL, and UNL show the treatments had electron donor to acceptor ratios ranging from 0.02 to 37 (i.e., ranging from less dithionite/reducible iron to excess dithionite/reducible iron).

Table 3.1. Batch reduction experiments used to treat Ft. Lewis aquifer sediment.

exp.	sediment (g)	H2O (mL)	dithionite (mol/L)	dithionite (mol)	K_2CO_3 (mol/L)	K_2CO_3 (mol)	Fe(II) (mol)	donor/acceptor 2*di./Fe^{II} (e-/e-)
R31.1	10	30	0.050	1.50E-03	0.200	6.00E-03	7.28E-04	4.12
R31.2	10	30	0.020	6.00E-04	0.080	2.40E-03	7.28E-04	1.65
R31.3	10	30	0.012	3.60E-04	0.048	1.44E-03	7.28E-04	0.99
R31.4	10	30	0.0060	1.80E-04	0.0240	7.20E-04	7.28E-04	0.49
R31.5	10	30	0.0025	7.50E-05	0.0100	3.00E-04	7.28E-04	0.21
R31.6	10	30	0.0025	7.50E-05	0.0100	3.00E-04	7.28E-04	0.21
R31.7	10	30	0.0010	3.00E-05	0.0040	1.20E-04	7.28E-04	0.082
R31.8	10	30	0.0010	3.00E-05	0.0040	1.20E-04	7.28E-04	0.082
WES-1	1.0	3.0	0.0500	1.50E-04	0.2000	6.00E-04	7.28E-05	4.123
WES-2	1.0	3.0	0.0120	3.60E-05	0.0480	1.44E-04	7.28E-05	0.989
WES-3	1.0	3.0	0.0060	1.80E-05	0.0240	7.20E-05	7.28E-05	0.495
WES-4	1.0	3.0	0.0012	3.60E-06	0.0048	0.0000144	7.28E-05	0.099
WES-5	1.0	3.0	0.0002	7.20E-07	0.00096	2.88E-06	7.28E-05	0.020

Table 3.2. Column reduction experiments used to treat Ft. Lewis aquifer sediment.

exp.	sediment (g)	H2O (mL)	dithionite (mol/L)	dithionite (mol)	K_2CO_3 (mol/L)	K_2CO_3 (mol)	Fe(II) (mol)	donor/acceptor 2*di./Fe^{II} (e-/e-)	redox capacity (umol/g)
R14	7.92	73.22	0.1	7.32E-03	0.4	2.93E-02	5.76E-04	25.41	72.77
R15	6.56	60.648	0.1	6.06E-03	0.4	2.43E-02	4.77E-04	25.41	
R16	7.2	40.84	0.030	1.23E-03	0.120	4.90E-03	5.24E-04	4.68	67.14
R17	7.28	40.84	0.0300	1.23E-03	0.1200	4.90E-03	5.30E-04	4.63	
R18	7.73	39.055	0.0033	1.29E-04	0.0132	5.16E-04	5.63E-04	0.46	35.67
R19	7.12	39.055	0.0033	1.29E-04	0.0132	5.16E-04	5.18E-04	0.50	
R20	7.72	89.03	0.0100	8.90E-04	0.0400	3.56E-03	5.62E-04	3.170	
R21	7.04	81.19	0.0100	8.12E-04	0.0400	3.25E-03	5.12E-04	3.170	75.65
R23	17.47	172.65	0.1	1.73E-02	0.4	6.91E-02	1.27E-03	27.161	
R24	17.68	172.65	0.1	1.73E-02	0.4	6.91E-02	1.29E-03	26.838	
R25	7.36	83.903	0.003	2.52E-04	0.012	1.01E-03	5.36E-04	0.940	43.68
R26	26.75	304.95	0.003	9.15E-04	0.012	3.66E-03	1.95E-03	0.940	
R27	6.98	62.22	0.0015	9.33E-05	0.006	3.73E-04	5.08E-04	0.367	5.05
R28	27.59	245.96	0.0015	3.69E-04	0.006	1.48E-03	2.01E-03	0.368	
R29	7.24	69.615	0.0003	2.09E-05	0.0012	8.35E-05	5.27E-04	0.079	5.04
R30	29.45	283.17	0.0003	8.50E-05	0.0012	3.40E-04	2.14E-03	0.079	
R44	6.9	37.43	0.0075	2.81E-04	0.03	1.12E-03	5.02E-04	1.118	21.24
R45	97.59	529.41	0.0075	3.97E-03	0.03	1.59E-02	7.10E-03	1.118	
R46	6.9	33.969	0.0040	1.36E-04	0.016	5.44E-04	5.02E-04	0.541	27.64
R47	100.9	496.74	0.0040	1.99E-03	0.016	7.95E-03	7.34E-03	0.541	
R48	6.9	32.196	0.0018	5.80E-05	0.0072	2.32E-04	5.02E-04	0.231	
R49	94.34	440.19	0.0018	7.92E-04	0.0072	3.17E-03	6.87E-03	0.231	
R48 II	6.9	33.039	0.0018	5.95E-05	0.0072	2.38E-04	5.02E-04	0.237	
R49 II	94.34	451.72	0.0018	8.13E-04	0.0072	3.25E-03	6.87E-03	0.237	
R50	6.9	39.085	0.0005	1.95E-05	0.002	7.82E-05	5.02E-04	0.078	
R51	97.59	552.8	0.0005	2.76E-04	0.002	1.11E-03	7.10E-03	0.078	
R52			0.0005		0.002				5.39
R66	196.02	1225	0.163	2.00E-01	0.652	7.99E-01	1.43E-02	28.0	
R67+68	193.87	1179	0.0097	1.14E-02	0.0388	4.57E-02	1.41E-02	1.62	
R154	108.98	1451.5	0.1	1.45E-01	0.4	5.81E-01	7.93E-03	36.6	
R155	129.41	1031.2	0.1	1.03E-01	0.4	4.12E-01	9.42E-03	21.9	
R148	113.15	553.11	0.1	5.53E-02	0.4	2.21E-01	8.23E-03	13.4	
R147	119.83	500.76	0.1	5.01E-02	0.4	2.00E-01	8.72E-03	11.5	
R149	117.01	525.22	0.0333	1.75E-02	0.1332	7.00E-02	8.51E-03	4.11	
R150	115.1	688.1	0.01	6.88E-03	0.04	2.75E-02	8.38E-03	1.64	
R156	32.64	160.19	0.005	8.01E-04	0.02	3.20E-03	2.38E-03	0.674	
R157	30.63	235.96	0.0025	5.90E-04	0.01	2.36E-03	2.23E-03	0.529	
R151	35.35	110.68	0.00333	3.69E-04	0.01332	1.47E-03	2.57E-03	0.287	
R152	30.99	196.24	0.001	1.96E-04	0.004	7.85E-04	2.26E-03	0.174	
R153	31.63	165.69	0.000333	5.52E-05	0.001332	2.21E-04	2.30E-03	0.048	

3.1.2 Biostimulation after Dithionite Treatment and Prestimulation

Experiments were conducted under this and Task 2.2 to stimulate growth of the microbial population with the addition of a carbon source (lactate) or trace nutrients to determine if this increases the rate of energetic mineralization. In addition, under this task, acetate mineralization studies were conducted with the addition of trace nutrients to determine the effect of the addition on microbial mineralization (whereas energetic mineralization may be cause by a combination of abiotic, biotic, and coupled steps. Prestimulation experiments involved treatment of sediments with the energetic compound of interest for 200 h before initiation of an energetic degradation/ mineralization experiments. This time period allows the microbial population to acclimate to utilizing the energetic as a nitrogen or carbon source, and should increase the rate of energetic mineralization. In this prestimulation phase, a low concentration (1 mg/L) of the energetic was used.

3.1.3 Microbial Growth During RDX Mineralization: Carbon Mass Balance

A RDX degradation experiment was conducted in dithionite-reduced sediment with a set of five vials with destructive sampling at specified times to determine the amount of carbon from RDX degradation was being incorporated into biomass. RDX mineralization in dithionite-reduced sediments has been shown to mineralize as much as 78% of the carbon in RDX (results shown in Task 2.2). The question was hypothesized at the 2004 IPR that perhaps some carbon from RDX degradation was being incorporated into the microbes at early times, but by later times, microbial death may account for a portion of the final high mineralization.

The amount of RDX incorporated into microbial biomass was determined in a set of batch experiments sequential extractions. The amount of RDX and other aqueous degradation intermediates from the ^{14}C-labeled RDX that were sorbed to the microbial surface was operationally defined by two different extractions. One extraction was a phosphate-buffered saline (pbs extraction) solution used to desorb microbes from the sediment surface followed by a 0.1 micron filter. The second extraction was 1M NaOH, which should dissolve the microbial cell walls (also 0.01 micron filtered). Using these two different extractions, "sorbed" ^{14}C was defined as the unfiltered extracted mass minus the aqueous ^{14}C (filtered). The amount of carbon-14 from RDX that was incorporated into biomass (assumed to be larger organic compounds in the lysed cells) was defined as the difference between unfiltered and filtered 1M NaOH extracted carbon-14 (i.e., assuming larger organic compounds are present in portions of cell walls that are trapped by the 0.01 micron filter).

3.1.4 Microbial Detachment and Transport

Microbial biomass was measured in solution and extracted from sediment to quantify microbial attachment at differing concentrations of dithionite/carbonate. Biomass was measured by AODC or PCR/DNA.

3.2 Task 2: Abiotic Degradation Experiments

3.2.1 Quantification of RDX, CL-20, TNT, HMX, and Products (Tasks 2 and 4)

Experiments were conducted using RDX (hexahydro-1,3,5-trinitro-1,3,5-triazine, CAS 121-82-4), TNT (2,4,6-trinitrotoluene, CAS 118-96-7), and HMX (1,3,5,7-tetranitro-1,3,5,7-tetrazocane, CAS 121-82-4) were obtained as solids or in a methanol stock solution. RDX degradation products MNX (hexahydro-1-nitroso--3,5-dinitro-1,3,5 triazine), DNX (hexahydro-1,3-dinitroso--5-nitro-1,3,5 triazine), and TNX (hexahydro-1,3,5-trinitroso-1,3,5 triazine) were also obtained in methanol stock solutions for calibration standards. TNT, HMX, RDX, MNX, DNX, and TNX were measured in aqueous solution by liquid chromatography by an HPLC method (modification of EPA Method 8330, HPLC Analysis of Explosives) and by LC-MS/MS. With this HPLC system, compounds that are more polar or of lower molecular weight will elude sooner than RDX. Detection was by UV absorption at 235 nm with retention times of 6.33 min (TNX), 7.22 min (DNX), 8.53 min (MNX), 9.86 min (RDX), and 5.42 min for HMX. The specific conditions of the HPLC system include:

- Keystone NA C-18 column, 250 mm x 4.6 mm
- 40% methanol, 60% water (isocratic), degassed with continuous helium
- flow rate 0.8 mL/min, 2200 psi, HP1050 series HPLC pump
- samples in 1.5 mL HDPE vials, 50 microliter injection volume
- ultraviolet detection at 230 nm, HP1050 series multiple wavelength detector

Calibration of RDX from 0.05 mg/L to 25 mg/L (aqueous solubility ~45 mg/L) was linear. Calibration curves also exist for degradation products (RDX -> MNX -> DXN -> TNX). CL-20 and TNT were quantified on the same HPLC, but with a different mobile phase (55% methanol, 45% water) with retention times of 9.0 minutes for CL-20 and 8.2 minutes for TNT. Carbon dioxide was measured by liquid scintillation counting, by using ^{14}C labeled RDX, HMX, TNT, acetate, or formate.

3.2.2 RDX/HMX/TNT Batch Studies

Well-characterized Ft. Lewis (Tacoma, Washington) and Pantex sediments (unconfined aquifer 253-258' depth) were used to conduct time-course RDX degradation pathway and rate studies in batch systems. These experiments consist of a series of steps: a) sediment reduction by sodium dithionite for 48-120 h, b) addition of reduced sediment and the energetic-laden water to glass, septa-top vials under anaerobic conditions, and c) measurement of the energetic and degradation products of the aqueous solution at specified times. Typically 10 mg/L RDX, 5 mg/L HMX, and 20 mg/L TNT was used in separate experiments.

Samples were analyzed at times ranging from 30 seconds to 1000 h. Radiolabeled (^{14}C RDX, TNT, HMX) experiments were also conducted by a similar method, but with an additional glass trap hanging in the batch septa-top vials. These traps contained 0.25 mL of 1.0 mol/L NaOH. At specified times, the NaOH was extracted from the trap without uncapping the vial (with a needle through the septa) and counted for ^{14}C labeled carbon dioxide. The purpose of maintaining the vial seal was to keep gas phase reaction products in the system.

In some experiments, one or bactericides were added to determine the influence of microbes on the degradation or mineralization step. Bactericides used in these experiments included: a) 100 mg/L $HgCl_2$, b) gluteraldehyde, c) 2 mM ammonium molybdate tetrahydrate, d) 6 mM sodium 2-bromoethanesulfonate, e) radiation to disrupt cells. Ammonium molybdate inhibits sulfate-reducing bacteria (Oremland and Zehr 1986, whereas sodium 2-bromoethanesulfonate inhibits methanogens. Typically the bactericide was reacted with the untreated or dithionite-reduced sediment for 48 h before the experiment was initiated. The assumption of use of a bactericide is that it kills the microbes (or blocks one or more biochemical functions) without influencing the abiotic reactions in the system. It was found that the $HgCl_2$ oxidized the sediment and was not used further. Sufficient gamma radiation to disrupt cell walls was also found to oxidize the reduced sediment and was not used further. The gluteraldehyde interfered with HPLC analysis of some compounds.

3.2.3 Sediment Reduction by Dithionite and Comparison to Alternate Systems

Batch vials containing 5 to 20 g of sediment and 50 mL of water were mixed with continuous helium bubbling in an anaerobic chamber for 30 minutes before dithionite and pH buffer were added. The dithionite solution contained 0.03 to 0.10 mol L^{-1} sodium dithionite ($Na_2S_2O_4$), with 4x the dithionite concentration K_2CO_3, and 0.4x $KHCO_3$. The dithionite concentration was measured by UV absorption at 315 nm (patent 6,706,527 Szecsody 2004b). Sediment reduction studies conducted in 1-D columns consisted of injecting the dithionite solution at a steady rate into a sediment column and measuring the concentration of dithionite over time in the effluent for 48 to 160 h. The flux rate was chosen to achieve specific residence times of the dithionite solution in the column (2 h to 4 h) relative to the reduction rate (~5 to 7 h). The dry bulk density and porosity of the column was calculated from the dry and saturated column weight and column volume. The volumetric flow rate was calculated from the effluent volume and elapsed time. The electrical conductivity of the column effluent provided a second (dynamic) measure of the porosity, and was measured using a flow-through electrode and automatic data logging. The dithionite concentration was not measured in these column experiments. Instead, sediments were subsequently oxidized by air-saturated water (next section) and the mass of oxygen consumed used as a measure of the "reductive capacity" or mass of reduced iron in the sediment. This is more accurate than reductive capacity based upon dithionite measurements (Szecsody et al. 2004, 2005).

For comparison of energetic degradation/mineralization rates, dithionite-reduced sediments were compared with sediments containing small (0.04 to 0.4%) zero valent iron and to sediment systems receiving only biostimulation. Small diameter (5 micron) zero valent iron particles were used in experiments, as the technology for injection of iron into sediment with a shear thinning fluid is now available (i.e., this is an alternate technology to dithionite for deep aquifer applications). The percentage of zero valent iron addition of sediment is equivalent to the amount of ferrous iron produced by the dithionite reduction of sediment, although the zero valent iron itself is more electronegative, so is reported to degrade energetics more rapidly (although zero valent iron by itself cannot support mineralization without microbes).

RDX mineralization was also studied in various systems that received only biostimulation. The sediment biostimulation treatments included: a) oxic, no additions (oxic control), b) oxic,

carbon (lactate) addition, c) oxic, trace nutrient additions, d) anoxic, no additions (anoxic control), e) anoxic, carbon (glucose) addition, f) anoxic, carbon (glucose) and sulfate addition), g) anoxic, RDX prestimulation (acclimation), h) anoxic, RDX prestimulation and carbon (glucose) addition), i) anoxic, RDX prestimulation and trace nutrient additions. An additional control experiment was anoxic untreated sediment with bactericide addition.

3.2.4 Reductive Capacity by Sediment Oxidation in Columns

Sediment oxidation studies were also conducted in 1-D columns to determine the rate at which the dithionite-reduced sediments are oxidized and to measure of the mass of reduced iron (i.e., redox capacity). The mass of oxygen consumed over the entire experiment was used to stoichiometrically calculate the mass of ferrous iron present. While these experiments are time consuming, cost is minimized by automation (Figure 3.1). This type of column oxidation experiment approximates field conditions well, as sediment is slowly oxidized over a 2–4 week period (as opposed to batch iron extractions described below).
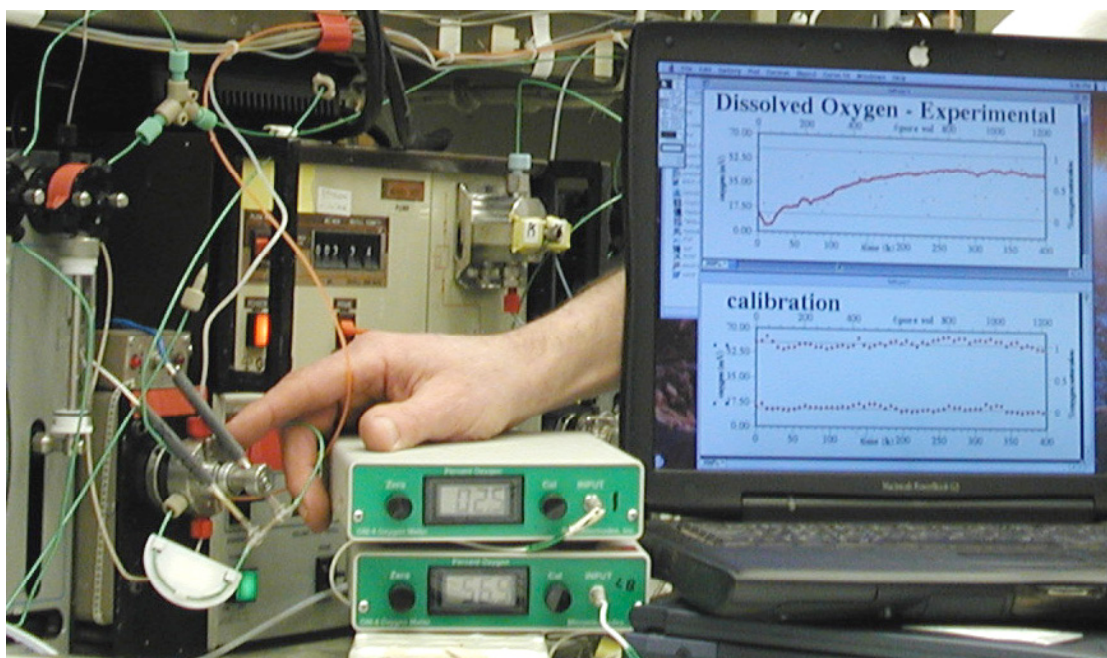
Figure 3.1. 1-D column oxidation system used to measure sediment reductive capacity (patent 6,438,501, Szecsody et al. 2002).

The dissolved oxygen levels in the experiments were monitored at the column outlet by two in-line oxygen electrodes (20 microliter flow through volume, Microelectrodes, Inc.) with automated calibration every 6 h (patent #6,706,527). This consists of two electrodes hooked up in a 6-way HPLC injection valve (Valco Industries) and 6-port Kloehn syringe pump, both controlled by a computer program (Figure 3.1). The program allows column effluent to flow through the two electrodes, then at 6-hour intervals the electrodes are pulled off line from the column and oxygen-saturated and oxygen-free water is injected through the electrodes (5 mL each). After a 1-minute equilibration time, oxygen data is recorded on a data logging board

triggered by this program. Column effluent oxygen data was recorded twice a second and averaged for two minutes and a single value recorded every two minutes (data logging with a National Instruments DAK 500 card). A typical experiment then contained 1500 to 4000 data points of column effluent data and 20 to 50 oxygen-saturated water and oxygen-free water calibration points for each of two oxygen electrodes. The columns used in these experiments were 0.765 cm diameter by 10 cm length, and the <4 mm size fraction of sediment was packed into the column. The dry bulk density and porosity was calculated from dry and wet sediment weights, and the column volume.

3.2.5 Iron Phase Extractions

Iron extractions conducted on untreated and reduced sediments from 1-D columns or batch experiments in an anaerobic chamber consisted of: a) 1 M $CaCl_2$ (Fe^{II} ion exchangeable), b) 0.5 M HCl, c) NH_2OH, HCl, d) dithionite-citrate-bicarbonate (DCB), and e) 5 M HCl. Each extraction was conducted in triplicate (standard deviations were ±3.3% to 8.3%), with additional duplication for some samples. Aqueous Fe^{II} and Fe_{total} from extractions were quantified by ferrozine, where Fe_{total} ($Fe^{II}+Fe^{III}$) samples reduced aqueous Fe^{III} to Fe^{II} by 0.025 M NH_2OH, HCl. Extracted Fe^{III} was the difference between Fe_{total} and Fe^{II}. The $FeCO_3$/FeS phase was defined by the 0.5 M HCl minus the 1 M $CaCl_2$ extraction. Amorphous and poorly crystalline Fe^{III} oxides were defined by the NH_2OH, HCl extraction, and crystalline Fe^{III} oxides were defined by the DCB minus the NH_2OH, HCl extraction. Total Fe^{II} and Fe^{III} oxides and carbonates were defined by the 5M HCl extraction (Heron et al. 1994).

3.2.6 Modeling RDX Abiotic/Biotic/Coupled Degradation

Batch experiments provided data showing the decrease of RDX by reduced sediment and the sequential increase/decrease of several degradation products. While the abiotic pathway can be assumed to be the same as the biotic pathway by a qualitative assessment of the data, modeling was used to quantify rates and possible influence of other reactions. Three different models were written to describe RDX degradation (and sorption) reactions in batch systems. The partial differential equations describing the mass fluxes of these 6 to 10 reactions were numerically solved. Three different models are currently being used to assess the degradation pathway. The first model describes only the five sequential degradation of RDX (each is a two electron transfer reaction, so all are second-order reactions). The second model assumes variable order (i.e., user specified) stoichiometry for the first four reactions. In a previous study, some experimental data indicated that the degradation reaction might not be second order. Finally, most experimental data also indicated that while RDX and subsequent degradation product mass disappeared, the appearance of a degradation products lagged relative to the disappearance of RDX. One hypothesis was that sorption may account for mass loss with no degradation, so model 3 was written to incorporate the five RDX degradation reactions and sorption of RDX, MNX, DNX, and TNX.

3.3 Task 3: Coupled Processes

The goal of this task is to determine the relative importance of initial *abiotic* versus *biotic* transformation of energetic compounds on the final mineralization rate. It is hypothesized that energetic compounds will initially be *abiotically* transformed, but biodegradation is required for mineralization. Experiments in this task will parallel those described in Task 1, but with live, killed, and possibly genetically-altered microbes (to alter a metabolic pathway). It is hypothesized that RDX, TNT, and HMX can be completely mineralized in a reducing environment only in the coupled abiotic/biotic system. It is further hypothesized that the rate of initial TNT degradation will be faster than that of RDX, based on differences in reduction potential and comparison of TNT and RDX biotic degradation rates (Brannon et al. 1992). Hundal (1997) also showed faster abiotic destruction kinetics of TNT than RDX in highly contaminated soils treated with zero valent iron.

3.3.1 Importance of Abiotic and Biotic Processes

3.3.1.1 Energetic Degradation Kinetics

Protocols used in batch experiments generally consisted of mixing 2 g of reduced Pantex sediment with 40 mL aqueous solution containing the HE of interest (RDX, HMX, and TNT). Treatments included various dithionite (10-100 mM) and K_2CO_3 (20-200 mM K_2CO_3) concentrations. For kinetic experiments, a dithionite-K_2CO_3 molar ratio of 1:2 was used for all concentrations tested.

Another experiment varied the mass of Pantex sediment (0.5 to 4.0 g) reduced with 100 mM dithionite and 400 mM K_2CO_3 to yield solid-to-solution ratios of 1:80 to 1:10. The reduced soils were then used to degrade 40 mL of RDX (20 mg L^{-1}).

To determine the effects of varying buffer concentrations, HE degradation kinetics were compared under unbuffered and buffered conditions. Specifically, dithionite (100 mM) alone, and in combination with 200, and 400 mM potassium carbonate (K_2CO_3), was used to reduce 2 g Pantex sediment in 40 mL water. The reduced sediments were then used to degrade 40 mL of 20 mg RDX L^{-1}, 3.5 mg HMX L^{-1} and 65 mg TNT L^{-1} in three separate experiments.

3.3.1.2 Contribution of Sorbed Fe^{II} to Degradation Rates

Dithionite-citrate-bicarbonate (DCB) is commonly used to extract and quantify crystalline Fe^{III} oxides in soils (Heron et al. 1994) by reducing Fe^{III} species to Fe^{II}. Extracting sediment with DCB partially removes sorbed Fe^{II} and amorphous and crystalline Fe^{III} oxides from the reduced sediment. To evaluate the effect of sorbed Fe^{II}, Pantex sediment (2 g) and 25 mL of deoxygenated water were added to 45-mL Teflon tubes and agitated overnight on a reciprocating shaker at room temperature. Fifteen mL of citrate-bicarbonate (C-B) buffer (8 parts 0.3 M citrate and 1 part 1 M bicarbonate, pH 8.5) was mixed with 100 mM dithionite and added to each suspension. The mixture was kept on a reciprocating shaker for 24 h, centrifuged and the supernatant discarded. One set of experimental units (n = 3) was then washed twice with deoxygenated water to remove excess dithionite, soluble Fe^{II} and other sulfur anions; another set

was not washed (unwashed). Fe^{II} (as $FeSO_4$, 0.35 mM) was added back into DCB treated, washed samples and the pH left unadjusted (6.8) or raised to pH 8.25.

3.3.1.3 Reductive Capacity of Reduced Sediments to Degrade RDX

The capacity of the dithionite-treated sediment to continuously degrade RDX was evaluated. This was achieved by treating 40 mL of 20 mg RDX L^{-1} with 2 g of reduced soil (100 mM dithionite, 400 mM K_2CO_3, washed twice with deoxygenated water) and measuring changes in the RDX concentration at 0, 1, 2, 4, 8, and 24 h. After the last sampling, the solutions were centrifuged and the supernatants removed. Fresh RDX (20 mg L^{-1}) solution was reseeded back into the same experimental unit (i.e., reduced soil). This reseeding occurred at 24, 48, 72, 96, and 120 h (five cycles). Changes in the RDX concentration were monitored between the reseeding cycles.

Because the reduced sediment was continuously exposed to RDX and eventually lost its reductive capacity, we determined whether the reduction capacity of sediment from the perched aquifer could be effectively regenerated (i.e., re-reduced) following exposure to energetics and oxygen. Two g of perched aquifer soil were reduced with 100 mM dithionite and 400 mM K_2CO_3. The reduced soils were then used to degrade 40 mL of 20 mg RDX L^{-1} and 65 mg TNT L^{-1} in two separate experiments. After 5 d, the tubes were centrifuged at 5000 x g for 20 min and the supernatants removed and analyzed for chemical concentrations. The sediments were extracted with methanol (10 mL) to remove and quantify adsorbed RDX and TNT. The methanol was removed and the sediments were allowed to reoxidize by keeping them outside the chamber for 2 d. The sediments were then reduced with dithionite again and used to treat solutions of RDX and TNT. This process was repeated for a total of six cycles.

3.3.1.4 Biodegradation as a Primary and Secondary Treatment for RDX and TNT

[14]C-labeled RDX and TNT solutions were treated with dithionite-reduced Ft. Lewis sediment until the RDX and TNT were undetectable by high performance liquid chromatography (HPLC). Aquifer microcosms consisting of 250-mL, wide-mouth glass jars with septa-containing screw caps were used for mineralization studies. Each experimental unit (glass jar) contained 75 g (77.6 g wet weight) of sediment and 15 mL of RDX or TNT (5 mg L^{-1}, 10,000 dpm mL^{-1}). Fifteen milliliters of RDX or TNT solution was sufficient to saturate the sediment and provided a thin film of overlying solution. Carbon dioxide traps were changed weekly and ^{14}C activity was determined by removing 0.5 mL of trapping solution, mixing with 6 mL of Ultima Gold scintillation cocktail (Packard, Meriden, Connecticut), and liquid scintillation (LS) counting. At the end of the experiment, 0.5 g of the air-dried sediment was mixed with 400 μL of Combustaid (Packard, Meriden, Connecticut), and ^{14}C bound to the solid phase was determined by combustion in a biological oxidizer (Packard, Model 306). The gas stream was trapped in a 3:2 (v/v) mixture of Carbosorb/Permaflour (Packard) and [14]CO_2 measured by liquid scintillation counting (LSC).

3.3.1.5 Methylene Dinitramine Transformation by Dithionite-Reduced Sediment

Ft. Lewis sediment (2 g) and 40 mL of deoxygenated water were added to 45-mL Teflon tubes and agitated overnight on a reciprocating shaker at room temperature. Dithionite (10 or 100 mM) and 40 or 400 mM K_2CO_3 were then added to each suspension. The mixture was kept on a reciprocating shaker for 24 h, centrifuged and the supernatant (containing dithionite and its degradation products thiosulfate, sulfate, and bisulfite) discarded. Soils were washed twice with deoxygenated water to remove excess and entrained dithionite and other sulfur compounds. Controls were prepared in a similar manner without the addition of dithionite and K_2CO_3. The reduced sediment was then used to degrade 40 mL of 20 mg MDNA L^{-1}. One set of experiments was conducted outside the chamber using untreated sediment to treat MDNA. Another treatment (control) monitored MDNA degradation in water without sediment.

3.3.1.6 Chemical Analysis

RDX, TNT, and HMX analyses were performed by HPLC (Shimadzu, Kyoto, Japan) by injecting 20 L of sample into a 4.6- by 250-mm Keystone Betasil NA column (Thermo Hypersil-Keystone, Bellefonte, Pennsylvania). The mobile phase was 50:50 methanol:water at a flow rate of 1 mL min^{-1} with spectrophotometric quantification at 220 nm. Detection limits for HE analysis by HPLC were 0.2 mg L^{-1} for RDX and HMX and 0.1 mg L^{-1} for TNT. Selected aliquots were also analyzed by liquid chromatography-mass spectrometry (LC/MS) to identify the reaction products. A BetaBasic C-18 column (Thermo Hypersil-Keystone) was used for separation on a Waters 2695 HPLC interfaced to a Micromass Quattro Micro triple quadrupole mass spectrometer with electrospray ionization (Waters Corp., Milford, Massachusetts). An isocratic mobile phase consisting of 80:20 water:isopropanol (0.5% ammonium formate) at pH 8.0.

Solutions used for iron extractions included: (a) 0.5 M HCl (Heron et al. 1994), (b) 5 M HCl, and (c) 1 M CaCl$_2$ (adsorbed Fe^{II}) (Szecsody et al. 2004). Each extraction was conducted in triplicate. Fe^{II} in supernatant solutions and from various extractions was determined spectrophotometrically using the Ferrozine method (Stookey 1970). Total Fe in the 5 M HCl extract was quantified by reducing aqueous Fe^{III} to Fe^{II} with 0.025 M NH$_2$OH$\cong$HCl and Fe^{III} was obtained from the difference between total Fe and Fe^{II}. FeCO$_3$/FeS was obtained from the difference between the 0.5 M HCl and 1 M CaCl$_2$ extractions (Szecsody et al. 2004). The minimum detection limits for RDX, HMX, and TNT were 0.2, 0.2, and 0.1 µg/L, respectively.

3.3.2 Task 3.2 Controlled Eh/pH Experiments

3.3.2.1 Fe^{II} Treatment of Explosives-Contaminated Water

Aqueous phase experiments were conducted to determine the degradation kinetics of explosives with Fe^{II}. The experiments were performed in triplicate in an anaerobic chamber (95% N$_2$: 5% H$_2$) using 45-mL Teflon centrifuge tubes as experimental units. RDX (50 μM, 40 mL), TNT (180 μM, 40 mL) and HMX (10 μM, 40 mL) were separately treated with 0.25 to 2.0 mM Fe^{II} in the presence of 50 mM EPPS buffer at pH 8.25 $\pm$ 0.1. To quantify the effects of pH, RDX (50 μM, 40 mL), TNT (180 μM, 40 mL) and HMX (10 μM, 40 mL) were treated separately with 2 mM Fe^{II} in the presence of 50 mM PIPES buffer to maintain pH 6.35 and 6.85

and 50 mM EPPS buffer for pH 7.35, 7.85, 8.25, and 8.55. The different pH levels were obtained by small additions of NaOH.

RDX (50 μM, 40 mL) degradation by 2.0 mM Fe^{II} (pH 8.25 ± 0.1) was determined in the presence or absence of oxygen by conducting experiments inside or outside of the anaerobic chamber. In a separate experiment, RDX was initially treated with Fe^{II} inside the anaerobic chamber but one-half of the experimental units were removed from the chamber after 1 h and additional Fe^{II} was added after 5 and 10 h while maintaining the pH (8.25 ± 0.1).

The effect of ferrous iron salts was compared by treating RDX (50 μM, 40 mL) with $FeCl_2$ and $FeSO_4$ (2 mM Fe^{II}) in the presence of 50 mM EPPS at pH 8.25 ± 0.1. Similar experiments compared: (I) HEPES versus EPPS buffers (50 mM, pH 8.25 ± 0.1), (II) equilibration time (0, 12, and 24 h) of Fe^{II} in EPPS buffer, and (III) filtered versus unfiltered Fe^{II} solutions (before and after dilution with buffer) on RDX transformation rates. Considering that the pH of the pore water will be alkaline and Fe^{III} will eventually be prevalent downgradient of a PRB, we determined the effect of Fe^{III} on RDX degradation at alkaline pH. In this experiment, RDX (120 $μM$, 40 mL) was treated with 1.7 mM Fe^{III} and the pH adjusted to 8.5 and 10 with 0.5 M NaOH.

3.3.2.2 RDX Degradation by Fe^{II} in the Presence of Subsurface Sediment

Subsurface (Ft. Lewis or Pantex) sediment was sterilized by autoclaving at 121°C for 30 min on three consecutive days. Twelve mL of 50 μM RDX were treated with 30 g of Pantex sediment (sterilized) and 2.0 or 7.2 mM Fe^{II}. Controls were prepared without adding Fe^{II}. Sacrifice sampling was performed. RDX degradation was also determined using Ottawa sand at pH 6.2 (unbuffered) and 7.7 (adjusted with EPPS) and in the solution at pH 6.85 (adjusted with EPPS) by 7.2 mM Fe^{II}.

3.3.2.3 Chemical and Mineralogical Analyses

For all batch experiments, temporal sampling was done by removing 1.0 mL aliquots and centrifuging at 13,000 x g for 10 min. RDX, TNT, and HMX analyses were performed by HPLC (Shimadzu, Kyoto, Japan) by injecting 20μL of sample into a 4.6- by 250-mm Keystone Betasil NA column (Thermo Hypersil-Keystone, Bellefonte, Pennsylvania). The mobile phase was 50:50 methanol:water at a flow rate of 1 mL min^{-1} with spectrophotometric quantification at 220 nm. Detection limits for HE analysis by HPLC were 0.2 mg L^{-1} for RDX and HMX and 0.1 mg L^{-1} for TNT. Selected aliquots were also analyzed by liquid chromatography-mass spectrometry (LC/MS) to identify the reaction products. A BetaBasic C-18 column (Thermo Hypersil-Keystone) was used for separation on a Waters 2695 HPLC interfaced to a Micromass Quattro Micro triple quadrupole mass spectrometer with electrospray ionization in the negative ionization mode (Waters Corp., Milford, Massachusetts). The mobile phase consisted of 80:20 water:isopropanol (0.5% ammonium formate) at pH 8.0.

Concentrations of HCl-extractable Fe^{II} in the Fe^{II}-treated RDX solutions were determined by collecting 0.5 mL of suspension and acidified with 1 mL of 1M HCl. The acidified samples were centrifuged at 13,000 X g for 10 minutes to remove solid particles. The dissolved fraction of Fe^{II} was determined by drawing 1 mL of aliquot and immediately filtering into an acidic

solution using 0.02 μm filters (Maithreepala and Doong 2004). Total Fe in the 5M HCl extract was quantified by reducing Fe^{III} to Fe^{II} by 0.025M $NH_2OH.HCl$ (Szecsody et al. 2004). Fe^{II} concentrations were determined spectrometrically using the Ferrozine method. The sorbed Fe^{II} concentration was calculated from the difference between the HCl-extractable and dissolved concentrations.

A Rigaku Mini-Flex X-Ray diffractometer (Houston, Texas) was used to monitor temporal changes in mineralogy. A scan range of 5 to 80° (2θ) at 1° min^{-1} was used. A Cobalt tube (30kV, 15 mA) was used to minimize fluorescence of Fe-rich minerals. The precipitates were filtered with 0.02 μm filter after the termination of the degradation experiments. These precipitates were completely dried under strong anaerobic conditions. The samples collected in the powdered form were immediately analyzed by XRD.

3.4 Task 4: Flow in Porous Media and Long-Term Studies

The goal of this task is to quantify energetic compound mineralization rates in flowing porous media systems (1-D columns) and determine the influence of flow on biomineralization and applicability to field scale bioremediation. We hypothesize that biomineralization rates will be slower in flow systems relative to batch (Task 3), as bioreactivity generally is reported slower in columns, due to microbial sorption or nutrient limitations (Szecsody et al. 1993). While the nature of the reaction network (i.e., reaction identity and stoichiometry) is identical in batch and column systems, batch-derived reaction parameters can fail to accurately predict transport because transport effects can significantly influence the apparent manifestation of nonlinear or coupled reactions during advective flow. Difference in biodegradation and mineralization rates in batch and column systems were quantified by simulation of column experiments using batch-derived parameters.

1-D saturated column experiments were used to derive transport-system reaction parameters to compare with batch studies (Tasks 1 and 3). The sequence of processes included RDX, TNT, and HMX degradation during flow as a function of: a) dithionite reduction (i.e., ferrous iron concentration relative to energetic concentration), b) residence time, c) temperature, and d) energetic concentration. Varying the flow velocity changes the energetic/microbial system contact time, so the intrinsic degradation and mineralization rates can be verified under different conditions. In an ideal system the intrinsic biodegradation rates would be the same under varying flow conditions, but in reality there may be secondary effects, such as nutrient limitations.

Column experiments in this task consisted of aqueous energetic (RDX, TNT, HMX) injection into a reduced sediment column at a steady flow rate and collecting effluent water for measurement of degradation products. The effluent from the column is routed into an automated 6-way multiplexing valve, which is connected to five septa-top vials and a waste bottle. The computer-controlled valve is used to alternate between routing effluent to one septa top vial for a specified time (1 to 36 h), or routed effluent to the waste bottle (4 to 72 h). This enabled anaerobic collection of effluent at specified times. Parent energetic compounds and intermediates are measured from the aqueous effluent and the extent of mineralization (carbon dioxide production) is measured with a KOH trap hanging in the sealed effluent vial, which collects all of the $^{14}CO_2$.

4. Results

4.1 Task 1. Microbial Growth and Energetic Degradation

4.1.1 Task 1.1 Microbial Biomass and Dithionite Treatment

4.1.1.1 Summary of Biomass Characterization

Characterization of microbial biomass changes that occur as a result of dithionite treatment have been conducted by measurements by phospholipid fatty acid (PFLA), live/dead stain, ^{14}C acetate mineralization, most probable number (MPN), acrodyne orange direct counts (AODC), and PCR amplification and DNA analysis.

Various microbial biomass measurements have shown that there is little change in biomass for low dithionite treatments, but there may be 90% death (i.e., order of magnitude decrease) for high (0.1 mol/L) dithionite treatment. For the Ft. Lewis subsurface sediment (composite of 50'- to 80'-depth), the natural biomass is about 10^6 CFU/mL (colony forming unit per milliliter, Figure 4.1.1, Table 4.1.1). The acrodyne orange direct count method showed some apparent increase in biomass for low dithionite treatments, then 10x death for the highest ditionite concentration. This 10x decrease in biomass is also reflected in the PCR/DNA method, which is considered the most accurate. The most probably number (MPN, shown) and phospholipid fatty acid (PFLA, not shown) methods were near detection limits, so the error in each number was large (i.e., no useful data). For a different sediment from Waterways Experiment Station, PFLA (green triangles, Figure 1) showed little change from the 7×10^8 CFU/mL natural biomass, although biomass was not measured for the highest dithionite concentration.
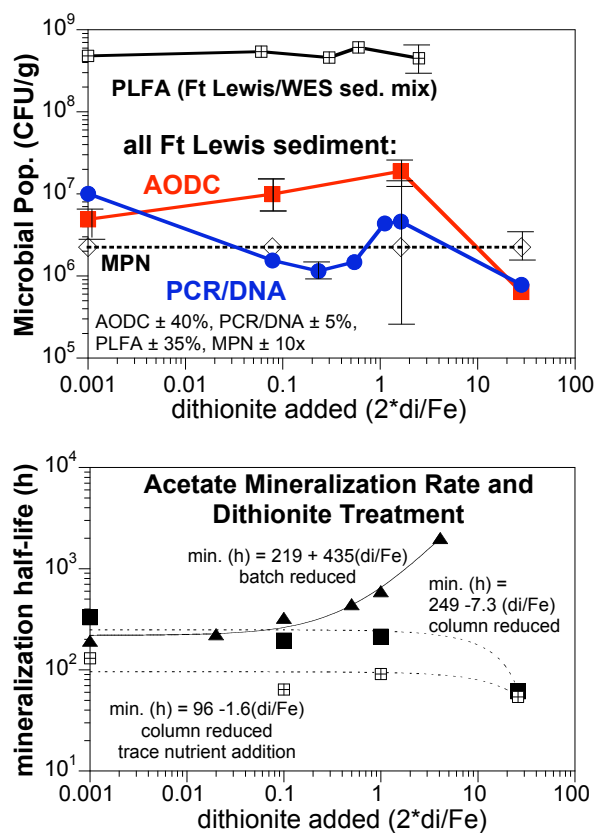
Figure 4.1.1. Dithionite treatment: a) biomass change, and b) acetate mineralization change.

The AODC method (Figure 4.1.2) relies on a DNA stain of microbes and counting individual microbes under a 1000x optical microscope with special lighting for the DNA stain. One field is shown for untreated and high dithionite treatment to illustrate that more microbes are present for the untreated sediment. The complete method involves using a phosphate buffered saline solution to desorb microbes from the sediment, then 0.2 micron

Figure 4.1.2. Acrodyne orange direct counts (AODC) for: a) untreated sediment, and b) 0.1 mol/L dithionite treatment.

filtering of the water and optical microscopy. For biomass, 20 to 30 different optical views are counted to obtain a realistic average count. This AODC method is fairly rapid and inexpensive, compared to PCR/DNA.

Table 4.1.1. Dithionite treatment and microbial population.

dithionite (mol/L)	di/Fe ratio	AODC cells/g	PCR/DNA cells/g	acetate mineralization $t_{1/2}$ (h)	w/ tr.nutr, $t_{1/2}$ (h)
0	0	$4.9\pm2.1 \times 10^6$	$1.01\pm0.05 \times 10^7$	330	130
0.0015	0.078	$9.9\pm3.8 \times 10^6$	$1.55\pm0.06 \times 10^6$	195	64
0.0032	0.23		$1.15\pm0.05 \times 10^6$		
0.007	0.54		$1.48\pm0.05 \times 10^6$		
0.013	1.11		$4.38\pm0.06 \times 10^6$		
0.02	1.62	$1.9\pm0.9 \times 10^7$	$4.63\pm0.07 \times 10^6$	213	91
0.1	28	$6.4\pm3.2 \times 10^5$	$7.82\pm0.06 \times 10^5$	61.1	54

4.1.1.2 Acetate Mineralization

Acetate mineralization rates (Figure 4.1.1b) conducted at WES and PNNL show in all cases that microbes are clearly not all dead (i.e., there is still mineralization even with extremely high dithionite concentrations). There were different trends for batch-versus column-reduced sediments, which may be cause by microbial detachment (described further in Results Section 4.1.3). The addition of trace nutrients increased the acetate mineralization rate, clearly demonstrating biostimulation can occur after dithionite treatment (described further in Results Section 4.1.2). The acetate mineralization rate appears to be inversely correlated with the exposure to dithionite, as expected (Figure 4.1.11b, batch reduction), where increasing dithionite concentration (apparently) kills some microbes, which results in a slower acetate mineralization rate. Even very a very low dithionite concentration (Figure 4.1.1b, squares; 2×10^{-4} mol/L dithionite) showed some influence relative to no exposure. Similar acetate mineralization experiments at PNNL (Figure 4.1.1b, column reduction) did show nearly the same mineralization rate for untreated sediment, but showed more rapid mineralization for increasing dithionite exposure, although the correlation was weak.

Calculation of the acetate mineralization half-lives for the batch and column reduced sediment data indeed show the same rate for untreated sediments, but differing correlation with increasing dithionite concentration. The batch reduced sediment data has an outstanding correlation (6 points, r = 0.998), indicating high dithionite concentration (0.1 mol/L) will decrease the acetate mineralization rate about 10x (from a 220 h half-life for untreated sediment to 2012 h). The column reduced sediment data shows the reverse correlation with dithionite concentration (250 h half-life for untreated sediment to 61 h for 0.1 mol/L dithionite) and the correlation is fair (r = 0.85).

A set of 240 microcosm experiments were conducted at WES in which microbial biomass was measured by phospholipid fatty acid (PFLA), live/dead stain, 14-C acetate mineralization (and RDX, TNT, CL-20 mineralization – next section) as a function of dithionite treatment concentration and as a function of dithionite treatment exposure time.

Acetate mineralization rates (Figures 4.1.3 and 4.1.4) conducted at WES and PNNL, respectively, show in all cases that microbes are clearly not all dead (i.e., there is still mineralization even with extremely high dithionite concentrations). The acetate mineralization rate appears to be inversely correlated with the exposure to dithionite, as expected (Figure 4.1.5, Table 4.1.2), where increasing dithionite concentration (apparently) kills some microbes, which results in a slower acetate mineralization rate. Even very a very low dithionite concentration (Figure 4.1.3, squares; 2 x 10^{-4} mol/L dithionite) showed some influence relative to no exposure. Similar acetate mineralization experiments at PNNL (Figure 4.1.4) did show nearly the same mineralization rate for untreated sediment, but showed more rapid mineralization for increasing dithionite exposure, although the correlation was weak. The cause of the difference between the WES and PNNL data may be the dithionite treatment methods differ (see below) in the amount of microbes washed out of the system, which increases as microbial detachment increases at higher dithionite concentrations.
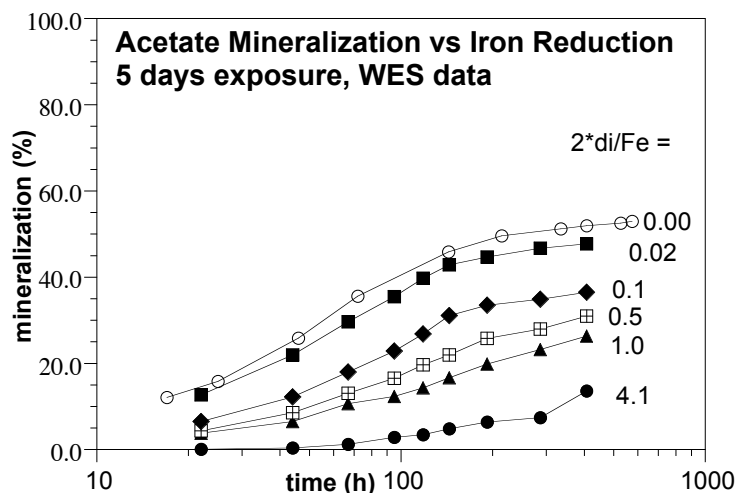
Figure 4.1.3. Acetate mineralization rate and dithionite concentration (WES data ± 0.15%).
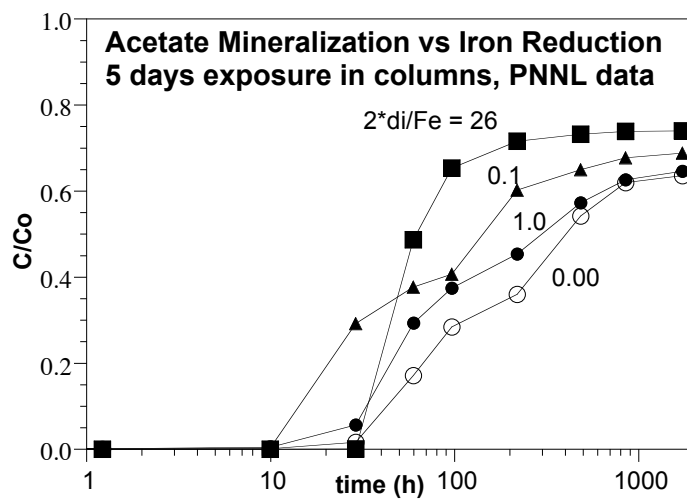
Figure 4.1.4. Acetate mineralization rate and dithionite concentration (PNNL data ± 0.2%).

Calculation of the acetate mineralization half-lives for the WES and PNNL data (Figure 4.1.5, Table 4.1.2), indeed show the same rate for untreated sediments, but differing correlation with increasing dithionite concentration.

Table 4.1.2. Acetate mineralization data for experiments at WES.

Treatment	Exposure Time (days)	Extent of Mineralization (%)	Mineralization Rate/h
Control (2*d/Fe=0)	0	52.1	0.0150
1 (2*d/Fe=4.1)	1	23.8	0.0033
1	3	19.3	0.0026
1	5	27.9	0.0015
1	10	28.0	0.0031
2 (2*d/Fe=1.0)	1	32.1	0.0036
2	3	37.6	0.0037
2	5	27.7	0.0056
2	10	29.7	0.0036
3 (2*d/Fe=0.5)	1	44.0	0.0050
3	3	40.0	0.0073
3	5	32.9	0.0073
3	10	28.2	0.0058
4 (2*d/Fe=0.1)	1	53.9	0.0100
4	3	42.4	0.0091
4	5	36.7	0.0074
4	10	25.1	0.0055
5 (2*d/Fe=.02)	1	53.9	0.0174
5	3	50.6	0.0107
5	5	47.6	0.0120
5	10	33.7	0.0085

The WES data has an outstanding correlation (6 points, r = 0.998), indicating high dithionite concentration (0.1 mol/L) will decrease the acetate mineralization rate about 10x (from a 220 h half-life for untreated sediment to 2012 h). The PNNL data shows the reverse correlation with dithionite concentration (250 h half-life for untreated sediment to 61 h for 0.1 mol/L dithionite) and the correlation is fair (r = 0.85).

To demonstrate that there is no abiotic acetate mineralization going on, dithionite reduced sediment was treated with gluteraldehyde (Figure 4.1.6), then subjected to an acetate mineralization experiment. There was <0.02% mineralization by 660 h. The control (untreated sediment with gluteraldehyde) also showed nearly no mineralization (1.9%), which is similar to results obtained by WES (<2.5% mineralization at 450 h, ^{14}C acetate with killed bacteria).
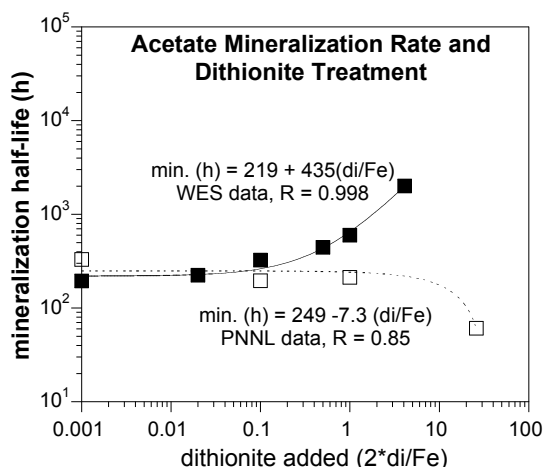
Figure 4.1.5. Acetate mineralization half-life estimation from dithionite added data (± 0.2%).
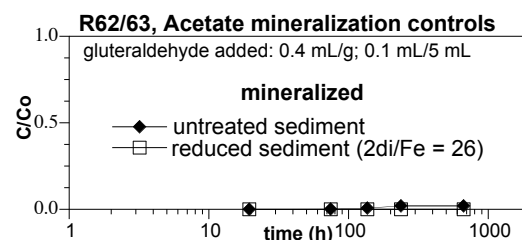
Figure 4.1.6. Acetate mineralization controls (± 0.2%).

4.1.1.3 Live/Dead State for Biomass Detection

For these treatments, the biomass in the Ft. Lewis soil using the Live/Dead strain and fluorescent microscopy and PLFAME. The biomass in this soil is very low and below the detection limits of both methods. It is not possible to simply analyze great quantities of soil with the microscopic method. The PLFAME analysis was scaled up from 0.5 g (usually sufficient) to 10 g and have concentrated the extract down to 30 microliters. The PLFAME peaks were only detected in the MS selective ion mode. The statistics indicated the results at this level were not quantitative. All fluorescent micrograph of the Ft. Lewis microbial community and PLFAME biomass number indicating that this was below a calculated detection limit. The PFLAME method worked well for a surface sediment with higher biomass (Figure 4.1.1a, WES sediment), and this showed little change with dithionite treatment.

The use of the live/dead stain and fluorescence detection to determine the biomass changes for dithionite treatment was not successful due to, apparently, low microbial biomass on the sediment and interference with sediment inorganic colloids. Initial tests of the live/dead stain were made with E. Coli cells (used as the standard reference) at 10^9 CFU/mL population. Two solutions were made (100% live cells, and 100% dead cells (killed with ethanol, then washed), which were then mixed to form standards (100% live, 90% live, 50% live, 10% live, and 0% live. Unfiltered and 5-micron filtered fluorescence were the same (Figures 4.1.7a and b), indicating the bacteria can easily pass through the 5-micron filter. The purpose of the filtration is to remove some of the inorganic colloids present in the sediment extractions. The live/dead stain measurement is the ratio of fluorescence at 510 to 540 nm to 620 to 650 nm (i.e., green/red fluorescence). Absorption areas are integrated in these two fluorescence windows and ratio calculated. The measurements after ~1 hour were different, which indicated that the live/dead stain deteriorates over time and/or in light. The standard phosphate buffered saline extraction method could not be used due to interference of phosphate with the live/dead stain. Measurement of microbial biomass by the live/dead stain using 0.85% NaCl extraction indicated a low

population. For experiments described below, the extracted population was grown with nutrient addition.

The influence of sodium dithionite alone, potassium carbonate alone, and sodium dithionite and potassium carbonate on the microbial biomass was measured in a series of batch experiments. A microbial population was extracted from the Ft. Lewis sediment and grown using trace nutrient addition. The maximum dithionite concentration used at the field scale is typically 0.03 mol/L sodium dithionite and 0.12 mol/L potassium carbonate (i.e., 4x the dithionite concentration), although laboratory experiments have used sodium dithionite concentrations as high as 0.1 mol/L. The sodium dithionite and

Figure 4.1.7. Live/dead stain standards for E. Coli that were: a) not filtered, and b) 5-micron filtered ($\pm15\%$).

concentrations used in these experiments was none, 0. 001, 0.01, 0.03, 0.06, 0.1, 0.3, and 0.6 mol/L (i.e., up to 6x greater than used for treating sediments. In one series of experiments, the mixture of sodium dithionite and potassium carbonate was used, similar to dithionite

treatment of sediment. The potassium carbonate concentration used in this experiment was 4x the dithionite concentration. The microbial biomass appeared to only slightly influenced by the 48 h dithionite/carbonate treatment (Figure 4.1.8), as there was some decrease in population, but in general, there was no difference in population as the dithionite concentration increased. The solution ionic strength was calculated (x-axis).

Figure 4.1.8. Influence of concentration of dithionite and potassium carbonate buffer on cell survival in 48 h ($\pm15\%$).

In a separate set of experiments, only sodium dithionite was reacted with the extracted microbial population for 48 h. Interestingly, there appeared to be a significant inverse correlation between dithionite concentration and the percentage of live microbes (Figure 4.1.9). At none or very low dithionite concentrations, the percentage of live cells was ~85%, but as the sodium dithionite (only)

28

concentration increased, the microbial population died. At the highest dithionite used in laboratory experiments (0.1 mol/L), 28% of the microbial population remained alive after 48 h. Because the ionic strength of this dithionite only solution was less than the dithionite/carbonate mixture (Figure 4.1.9), microbes appeared to tolerate the same dithionite concentration or higher concentration if potassium carbonate was present.

Figure 4.1.9. Influence of concentration of dithionite on cell survival in 48 h (±15%).

In a final set of experiments, only potassium carbonate was reacted with the microbial population for 48 h. In this case, there appeared to be little influence of the potassium carbonate concentration on the population (Figure 4.1.10). Therefore, it appears that the sodium dithionite concentration likely has the most influence on microbial death during dithionite

Figure 4.1.10. Influence of concentration of potassium carbonate buffer on cell survival in 48 h (±15%).

treatment of sediment, but the presence of the potassium carbonate buffer may allow the microbes to tolerate the dithionite (or sodium) concentration better.

4.1.1.4 Dithionite Exposure Time

Increased sediment/dithionite exposure time decreased the microbial survival. Very small dithionite concentrations (5E-4 mol/L) had little influence in microbial survival (as defined by acetate mineralization rate, see Appendix A), so exposure time had little influence. In contrast, high dithionite concentrations (0.05 mol/L, treatment #1, Figure 4.1.11) showed slower acetate mineralization for 1, 3, and 5 days, although little difference between 5 and 10 days of exposure. This indicates that dithionite itself kills some microbes (inferred from the decreased acetate mineralization rate) between 0 and 5 days, but because dithionite will complete disproportionate by 5 days to sulfate, the lack of difference in mineralization between 5 and 10 days appears to indicate that the sulfate (and carbonate) by products are not influencing the microbial population.

4.1.1.5 Energetic Mineralization in Reduced, then Oxic Systems

RDX mineralization in *reducing* environments as a function of the amount of dithionite treatment (without and with biostimulation) is described under Results Section 4.2. In this task, to assess the influence of dithionite exposure on the sediment microbial population (without having additional abiotic degradation caused by the reduced sediment), sediments were reduced

by dithionite, then oxidized. The influence on energetic mineralization should therefore be similar to acetate mineralization (which is not abiotically mineralized).

Comparison of RDX and TNT mineralization in untreated sediment to reduced/oxidized sediment (Figure 4.1.12a and b) show dithionite exposure apparently decreases the microbial population (i.e., similar to acetate mineralization results). For RDX and TNT there were five different treatments (differing dithionite concentration), and both RDX and TNT mineralization rate systematically decreased with increasing dithionite concentration. Both TNT and RDX mineralization in oxic sediments is very slow (i.e., only 1-3% mineralization after 400 h). Another energetic, CL-20, also showed similar results (Figure 4.1.12c), namely there was slower CL-20 mineralization with increasing dithionite treatment concentration (even though the sediments are oxidized). In this case, CL-20 mineralization is substantial (30% after 450 h), which is consistent with results in a previous CL-20 project study (SERDP ER-1255) in which other experiments show biomineralization in oxic systems is faster than in reducing systems. Again, these results were not meant to demonstrate the performance of reduced sediments for mineralizing energetics, which is substantially faster for RDX (and should be for TNT), as described in Task 2.2.
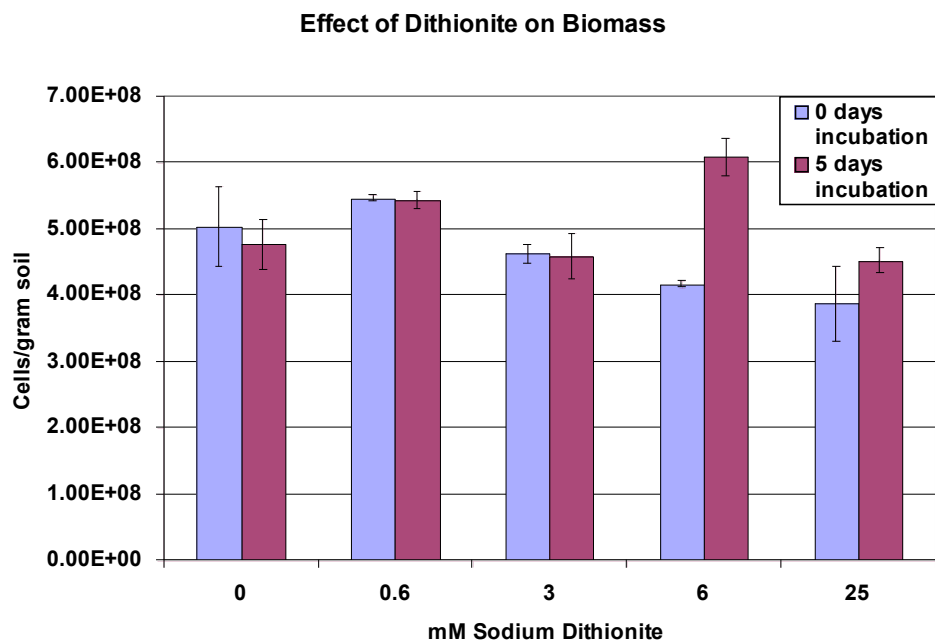
Figure 4.1.11. Effect of time and dithionite concentration on microbial biomass.
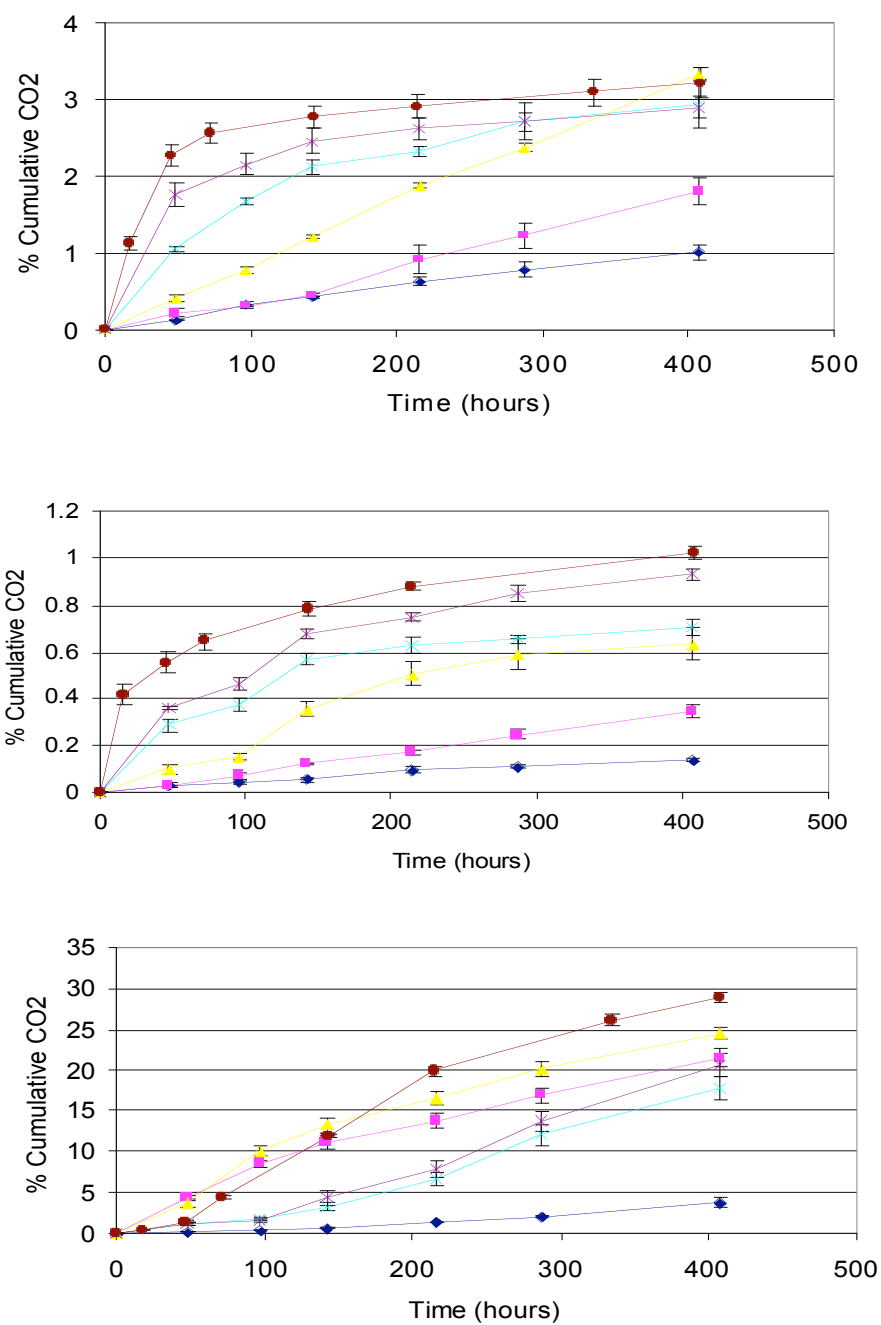
Figure 4.1.12. Energetic mineralization in sediments that are dithionite reduced (5 days), then oxidized: a) RDX, b) TNT, and c) CL-20

4.1.1.6 Energetic Mineralization in Reduced Systems

Experiments were conducted to determine the extent of mineralization of the explosives HMX and TNT in dithionite-treated soil under anaerobic conditions. Batch soil slurries were set up as above and consisted of 1 g of Ft. Lewis soil and 3 ml of a sodium dithionite/K_2CO_3 solution. There were three treatments in this experiment that consisted of different donor/ acceptor ratios where dithionite was the donor and iron in the soil was the acceptor. The ratios used were 29.68, 1.48, and 0.29, and dithionite and carbonate were kept at a ratio of 1:4. Controls contained soil and water without the addition of dithionite or carbonate. All treatments were incubated for 5 days under these conditions and were then washed twice with anaerobic pH 7 buffered water to remove excess dithionite and carbonate. Mineralization studies were carried out anaerobically by resuspending the washed soil in 6 ml of buffer containing the appropriate ^{14}C substrate (^{14}C-HMX, or ^{14}C-TNT). The concentration of HMX was 4 ppm and the concentration of TNT was 10 ppm, and both contained 7000 dpm/ml of radioactivity. To measure the mineralization of each compound, filter disks were dipped in a 1M barium hydroxide solution and inserted into the top of each test tube cap so that ^{14}C-CO_2 would be absorbed. At appropriate time points, the disks were removed and placed in scintillation cocktail to be counted. Fresh disks with barium hydroxide were then placed in each cap. These mineralization studies were carried out for 60 days and all experiments were done in duplicate.

Experiments were performed to address the ability of the soil microbial community to mineralize explosives under reduced conditions following treatment with various concentrations of dithionite. After soil was incubated with dithionite for 5 days under anaerobic conditions, mineralization studies were carried out with ^{14}C-HMX and ^{14}C-TNT. HMX mineralization was greatest when soil was amended with a moderate amount of dithionite (Figure 4.1.13a). At a donor/acceptor ratio (2*di/Fe) of 1.48, HMX mineralization was 47%. This is a much higher mineralization amount than in soil that was not exposed to dithionite, which mineralized only 14%. The highest dithionite concentration used in this study, 2*di/Fe = 29.68, resulted in 25% mineralization. These results are somewhat different from separate HMX mineralization studies (Results Section 4.2.3) in which higher dithionite exposure results in more rapid mineralization and a greater extend of mineralization. Again, the differences in result may reflect the batch dithionite treatment in this study washing out greater percentage of microbes (see Results Section 4.1.3).

Although mineralization values were much lower for TNT in general, the dithionite treatment of 2*di/Fe = 1.48 also resulted in the highest mineralization value, followed by the donor/ acceptor ratios of 29.68, 0.29, and 0. Results from these experiments indicate that a low dithionite treatment (0.018 M) increases explosive mineralization by microbes in the soil. When a much higher treatment is applied (0.09 M), mineralization values are almost half as great, although they remain higher than in the untreated control.

HMX Mineralization
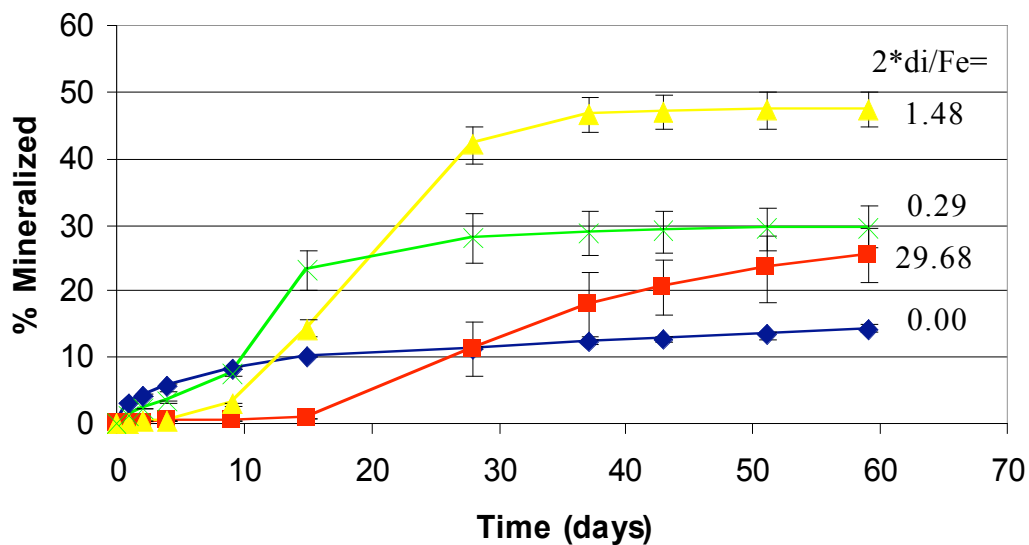
TNT Mineralization
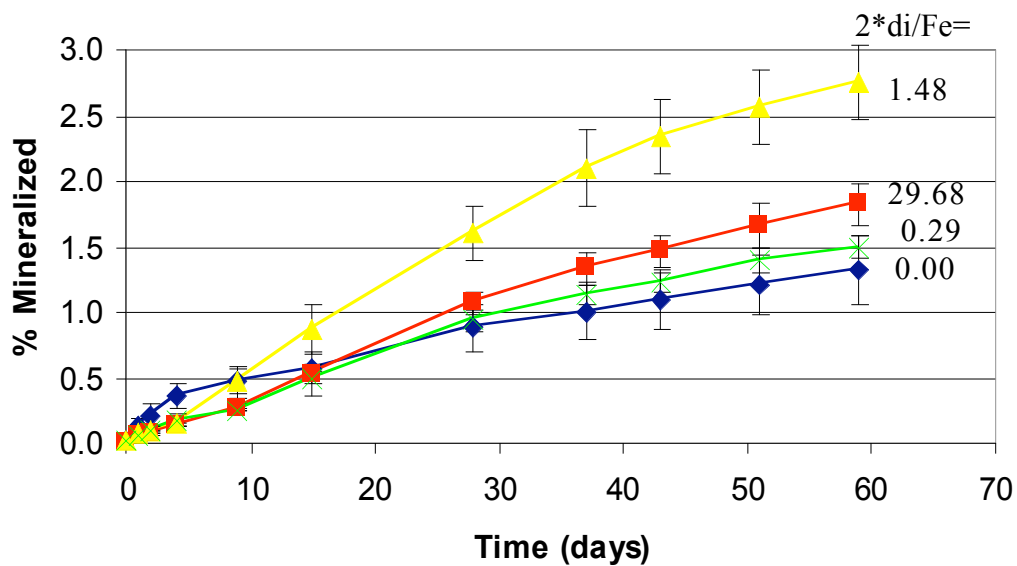
Figure 4.1.13. Anaerobic system ^{14}C-HMX and ^{14}C-TNT mineralization after exposure to various concentrations of dithionite for 5 days.

4.1.1.7 Energetic Mineralization in Reduced Sediment with Inhibitors

Experiments were set up to determine if a specific microbial population, such as sulfate-reducing bacteria or methanogens, is responsible for mineralizing explosives in dithionite-treated Ft. Lewis soil. Ammonium molybdate was used to inhibit sulfate-reducing bacteria (Oremland and Zehr 1986) and sodium 2-bromoethanesulfonate (BES) was used to inhibit methanogens (Zinder et al. 1984). Batch soil slurries were set up in test tubes in a Coy anaerobic glove bag using 1 g of Ft. Lewis soil and 3 ml of a dithionite/potassium carbonate solution. Sodium dithionite was added at a concentration of 0.09 M and potassium carbonate at a concentration of 0.36 M. The water in each tube was purged with ultra-pure nitrogen for 30 minutes before potassium carbonate and sodium dithionite were added. Ammonium molybdate was added at a concentration of 6 mM and BES at a concentration of 10 mM. The control in this experiment consisted of the reduced soil slurry without the addition of inhibitors. All treatments were incubated for 5 days under anaerobic conditions and were then washed twice with anaerobic pH 7 buffered water to remove residuals. Mineralization studies were carried out anaerobically by resuspending the washed soil in 6 ml of buffer containing the appropriate ^{14}C substrate (^{14}C-RDX, ^{14}C-HMX, or ^{14}C-TNT). RDX, HMX, and TNT were added at concentrations of 10 mg/L, 4 mg/L, and 10 mg/L, respectively, and each contained 5000 dpm/ml of radioactivity. To measure the mineralization of each compound, filter disks were dipped in a 1M barium hydroxide solution and inserted into the top of each test tube cap so that ^{14}C-CO_2 would be absorbed. At appropriate time points, the disks were removed and placed in scintillation cocktail to be counted. Fresh disks with barium hydroxide were then placed in each cap. These mineralization studies were carried out for 60 days and all experiments were done in duplicate.

Microcosm experiments were conducted using inhibitors to target certain microbial populations in soil. The purpose of this study was to determine if a specific group of bacteria is responsible for the mineralization of explosives in reduced soil. Ammonium molybdate was used to inhibit sulfate-reducers and sodium 2-bromoethanesulfonate to inhibit methanogens. There was a 69% decrease in RDX mineralization when sulfate-reducing bacteria were inhibited, but no effect when methanogens were inhibited (Figure 4.1.14a). With HMX, there was an 86% decrease in mineralization when sulfate-reducers were inhibited, but again no decrease when methanogens were inhibited (Figure 4.1.14b). TNT mineralization was not affected by either inhibitor (Figure 4.1.14c). These results indicate that sulfate-reducing bacteria play an important role in RDX and HMX mineralization in reduced soil and without their presence in the soil, the degradation of these explosives is greatly reduced.

Further experiments are needed to validate the accuracy of these results. The inhibitors were added to the soil at concentrations found in the literature and were not tested on the Ft. Lewis soil for optimal results prior to setting up this experiment. It is possible that methanogens were not inhibited due an insufficient amount of sodium 2-bromoethanesulfonate in the soil and not because they play an unimportant role in explosive degradation in this soil.

RDX Mineralization

HMX Mineralization

TNT Mineralization
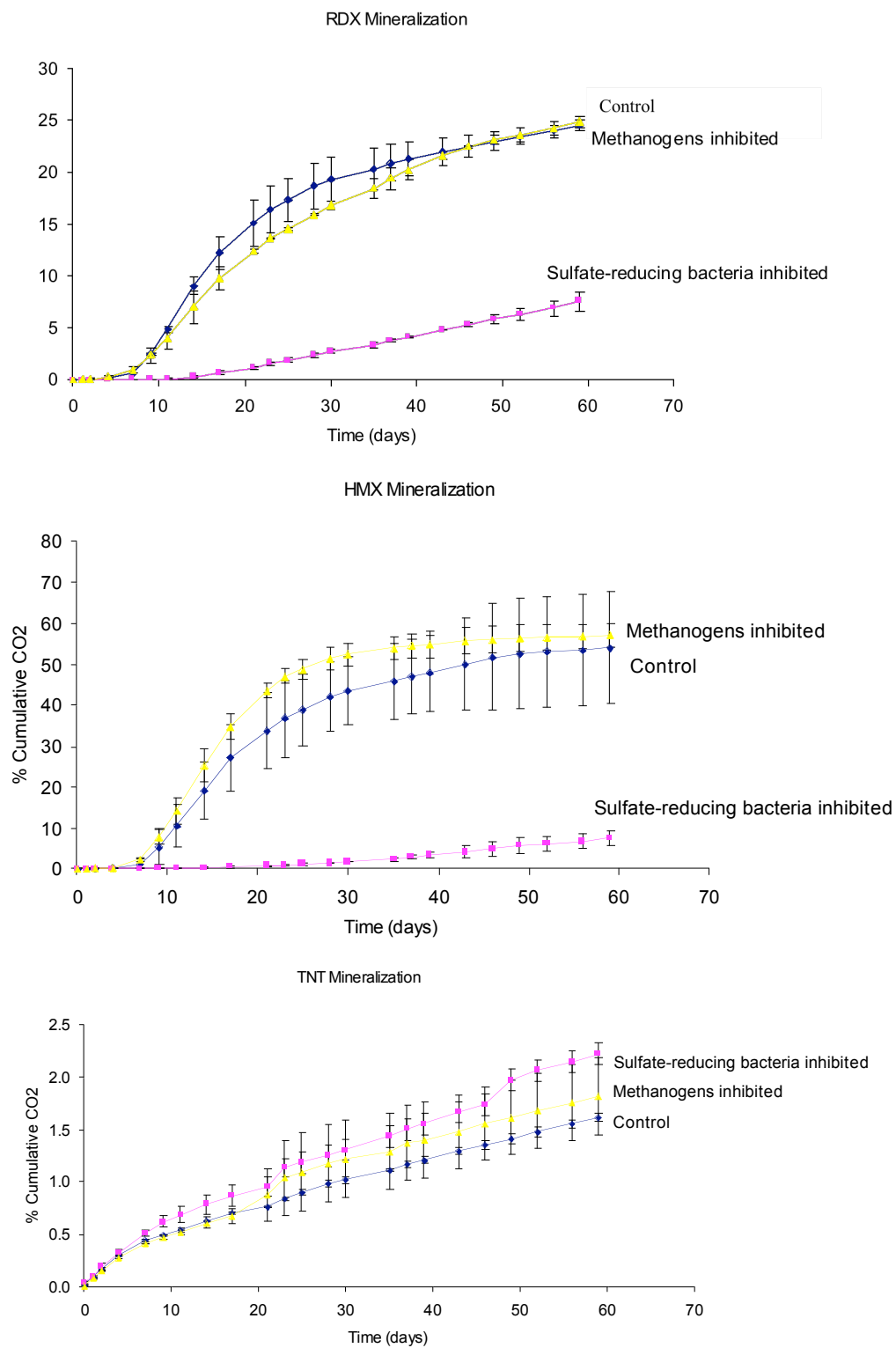
Figure 4.1.14. Mineralization of RDX (a), HMX (b), and TNT (c) after dithionite treatment with microbial inhibitors.

4.1.2 Biostimulation After Dithionite Treatment

In the previous section, preliminary mineralization data indicated that the microbial population decreases due to dithionite exposure (concentration and time). Although the population appears to decrease (based in the mineralization data), coupled RDX mineralization is significantly faster in the dithionite-reduced sediment (results under Task 2.2), indicating a substantial viable population. Experiments were conducted under this and Task 2.2 to stimulate growth of the microbial population with the addition of a carbon source (lactate) or trace nutrients. In this section, acetate mineralization with the addition of trace nutrients are reported.

Under Results Section 4.2, results of RDX mineralization with additional carbon or trace nutrients are reported.

Acetate mineralization with trace nutrient addition (parallels PNNL experiments without nutrients) showed some increase in acetate mineralization (Figure 4.1.15 versus Figure 4.1.4). Quantifying the acetate mineralization rates (Figure 4.1.16) clearly shows biostimulation increased the mineralization rate. However, low concentration dithionite treatments were most affected, as the high concentration data showed little difference between the addition (or not) of trace nutrients on the acetate mineralization rate. Additional data is needed, as the correlations are only fair. If correct, this data could indicate that because some microbes are killed by the dithionite treatment, those left are not as readily biostimulated.

4.1.3 Microbial Growth During RDX Mineralization: Carbon Mass Balance

A RDX degradation experiment was conducted in dithionite-reduced sediment with a set of five vials so that destructive sampling could be accomplished to determine the amount of carbon from RDX degradation was being incorporated into biomass. RDX mineralization in dithionite-reduced sediments has been
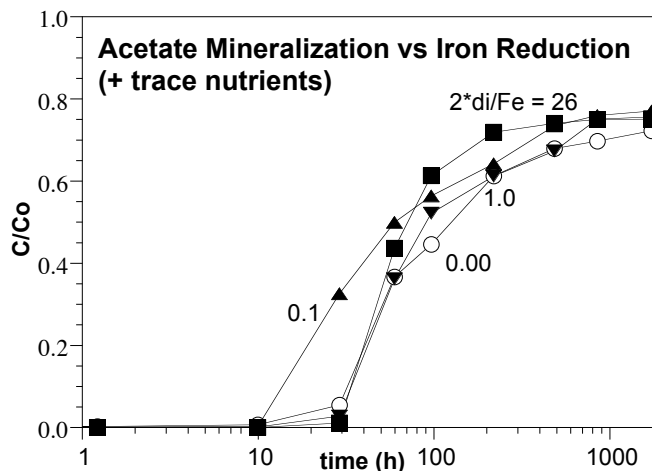
Figure 4.1.15. Acetate mineralization with added trace nutrients (data ± 2%, counting ± 0.2%).
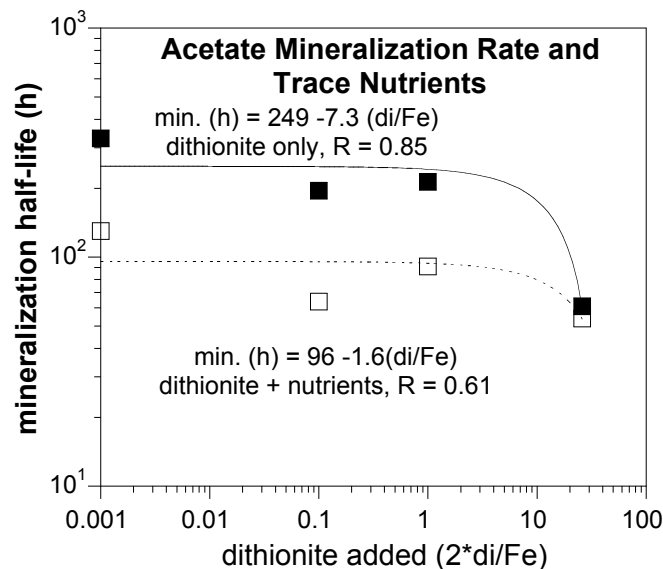
Figure 4.1.16. Acetate mineralization half-life with nutrient addition as a function of dithionite concentration (data ± 2%, counting ± 0.2%).

shown to mineralize as much as 78% of the carbon in RDX (results shown in Results Section 4.2.2). The question was hypothesized (at the 2005 IPR) that perhaps some carbon from RDX degradation was being incorporated into the microbes at early times, but by later times, microbial death may account for some of the final mineralization.

The amount of RDX incorporated into microbial biomass was determined in a set of batch experiments sequential extractions. A sediment with high dithionite reduction was used which previously showed a 200 h RDX mineralization half-life (30C) showed a slower RDX mineralization half-life (293 h; 29% CO_2 by 570 h) at 21C (Figure 7a), with 51% of the ^{14}C remaining in aqueous solution. The total amount of ^{14}C associated with biomass was 5 to 7%, as defined by several different extractions (Figure 4.1.17b and Table 2). The 1M NaOH (24 h), which was filtered minus the aqueous ^{14}C defined the total biomass associated ^{14}C from RDX. Time course data of this extraction ranged from 3.5% to 5.4%, and was relatively constant from 50 h to 576 h. Because the 1M NaOH may not fully dissolve the microbial biomass, the ^{14}C difference between unfiltered and 0.1 micron filtered amounts was also recorded (blue line Figure 4.1.17b), which was about 1 to 1.4% of the ^{14}C RDX total mass. Additional extractions were conducted at 576 h. A phosphate buffered saline solution extraction removed 6.75% of the ^{14}C from the biomass. A 10M NaOH solution was then added for 24 h, and ^{14}C measured in a CO_2 trap (1.4%) and aqueous associated with biomass (minus aqueous) of 5.4%, giving a total biomass associated percentage of 6.8%.

The RDX abiotic/biotic degradation pathway proposed for dithionite-reduced sediment (Results Section 4.2.2) shows several purely abiotic degradation reactions, one biotic and coupled abiotic/ biotic reaction (formate mineralization). Because all reactions are not biotic, there will not be as much carbon accumulation into microbes as with systems with only RDX biodegradation.
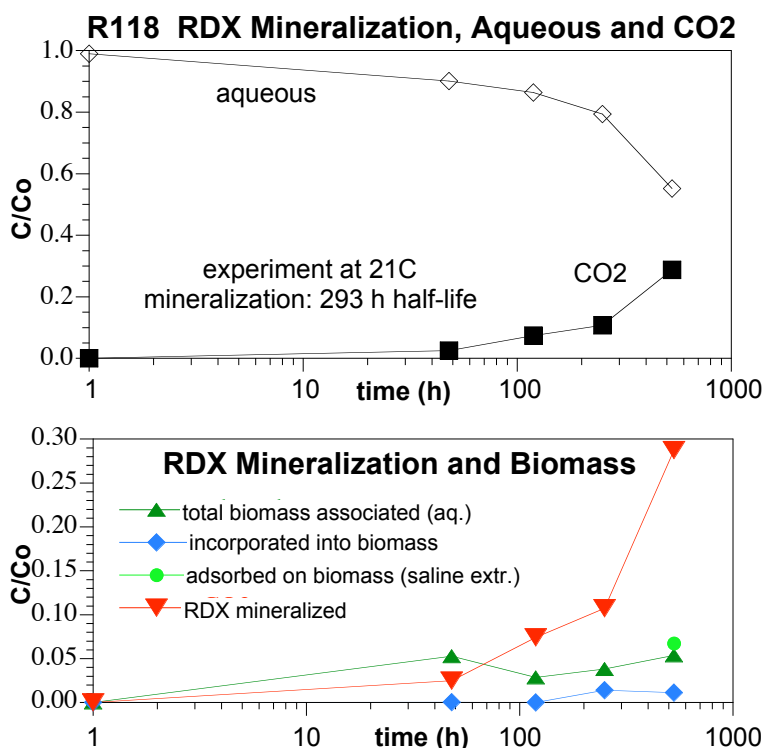
Figure 4.1.17. RDX mineralization and ^{14}C RDX mass balance of: a) aqueous and carbon dioxide, b) various microbial extracts. Data ±3% extraction error, counting error 0.2%.

The value of 5-7% carbon incorporation into biomass is similar to estimates in the range found for biodegradation of organic acids and glucose. Estimates of biomass yield can be made

using a generic cell formula of $C_5H_7O_2N$ and molecular weight of cells is 113 mg/mmole. RDX ($C_3H_6N_6O_6$, 222.26 g/mol) has a low percentage of carbon (as all energetics). In this experiment, 30 mL of 10 mg/L RDX are reacted with 5 g of reduced sediment (and associated microbes). Of the 1.35×10^{-6} mol RDX initially, 7% or 9.45×10^{-5} mmol were associated with biomass.

Citrate (C6 organic acid) biodegradation to formate and acetate yields 0.06 mmole-cells/mmole-citrate (0.04 mg-cells/mg-citrate, B. Moore and others, 2005), or 2.3% carbon associated with biomass. Lactate (C3 organic acid) biodegradation yields 0.063 mmole-cells/mmole-lactate (Bailey and Ollis 1986, Biochemical Engineering Fundamentals, p. 283), or 6.1% carbon associated with biomass. Glucose biodegradation yields 0.32 mmole-cells/mmole-glucose, or 3.6% carbon associated with biomass.

Table 4.1.3. Carbon from RDX incorporated into biomass during RDX mineralization.

| Treatment | Fraction 14C from RDX | | | | |
	50 h	119 h	250 h	576 h	phase
1. aqueous	0.9013			0.5520	aq. + soln microbe species
2. aqueous, 0.1 micron filtered	0.9104	0.8638	0.7935	0.5111	aqueous species
3. gas phase carbon dioxide trap	0.0250	0.07416	0.1075	0.2876	RDX mineralized
4. 1M NaOH (24 h), filtered - aqueous	0.0529	0.0288	0.0384	0.0319	total biomass associated
5. 1M NaOH (24 h), unfiltered - filtered	0.0035	-0.0145	0.0141		incorporated into microbes
6. 0.3M saline aq. extraction, unflitered - aq.				0.0675	aq. adsorbed on microbes
7. 10M NaOH (24 h), gas phase CO2 trap				0.0144	small MW biomass
8. 10M NaOH (24 h), filtered - aqueous				0.0539	total aq. biomass associated
9. 10M NaOH (24 h), unfiltered - filtered				0.0114	high MW biomass

4.1.4 Microbial Detachment with Dithionite Solution Addition

Measurements were made of microbial biomass in aqueous solution and on dithionite-reduced surfaces to determine the extent of microbial detachment. Over a range of dithionite-treated sediment, the microbial population, as defined by acrodyne orange direct counts, AODC, appeared to increase about 10x (Figure 4.1.18) even at the highest dithionite concentration, even though previous results (Figure 1) showed a similar increase in population with some dithionite treatment (by AODC), but a decrease in population at the highest dithionite concentration). Measurements of microbes in aqueous solution were made at the end of the dithionite reduction experiments, after the water was in equilibrium with the sediment for several months to calculate the microbial attachment, as
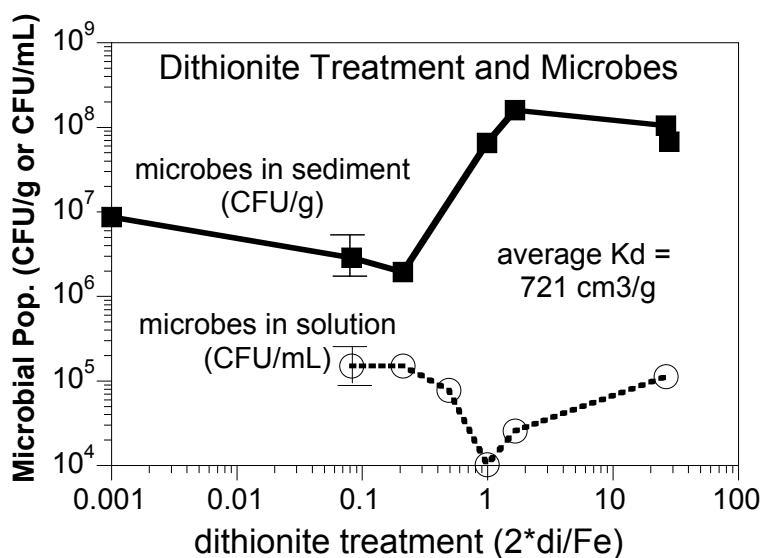
Figure 4.1.18. Microbial biomass on sediment surfaces and in solution by AODC (data ±15%).

defined by a distribution coefficient (K_d), which is the mass of microbes on the sediment (CFU/g) divided by the mass of microbes in solution (CFU/mL). The biomass in solution did not appear to change much over different dithionite treatments, indicating equilibrium in the low ionic strength groundwater was reached. The average K_d value for microbes was 721 cm³/g, which means approximately 3400x more microbes on the surface than in solution for a typical groundwater system (Rf = 1 + bulk density * K_d/porosity), where a bulk density of 1.8 g/cm³ is assumed and a porosity of 0.35 is assumed.

The apparent microbial attachment for microbes calculated as a K_d as a function of the dithionite concentration was shown to remain high for nearly all dithionite treatments (Figure 4.1.19) except for very high (0.1 mol/L) concentration. The calculated retardation factor for the highest dithionite treatment was 26 (K_d = 5.0 cm³/g), so a minimum of 26 pore volumes of water would be needed to advect the microbes out of this system. For laboratory experiments conducted at lower dithionite concentrations, the amount of biomass removal would be minimal (described in the following paragraph). At the field scale, there would likely be some biomass removal within a few feet around the injection well for high dithionite treatments, but this would be repopulated over time.

The microbial attachment/detachment that is likely to occur during dithionite treatment was calculated for different laboratory batch and column reduction treatments (Table 4.1.4). At high ionic strength, some microbes detach, and this effect is used, in fact to extract microbes from sediments using a phosphate buffered saline solution. For these calculations, a batch reduction consisted of four steps: a) dithionite reduction with 10 g of sediment and 120 mL of dithionite-laden water, b) centrifuge and resuspension in 120 mL of water (i.e., wash), c) centrifuge and resuspension in 120 mL of water (i.e., second wash), d) centrifuge and resuspension in 120 mL of water (i.e., third wash). A column reduction consists of: a) 24 pore volumes of dithionite solution injection over 5 days, then b) 30 pore volumes of water flush to remove residual dithionite solution. For all water flushes, the microbial K_d was assumed to be 721 cm³/g (measured value), or a lower value (100 cm³/g). For a "low" dithionite concentration reduction experiment, a K_d value equal to 1/10 the K_d value was used (i.e., lower adsorption in higher ionic strength water). For a high dithionite concentration reduction experiment, a K_d value equal to 1/20 the K_d value was used. The purpose of these calculations was to illustrate differences between batch and column reduction, and cases where much of the microbial population would be lost due to detachment.

Table 4.1.4. Calculated microbial detachment during reduction experiments.

process	low conc. reduction Kd assumed (cm3/g)	% microbes lost	high conc. reduction Kd assumed (cm3/g)	% microbes lost	low conc. reduction Kd assumed (cm3/g)	% microbes lost	high conc. reduction Kd assumed (cm3/g)	% microbes lost
batch reduction	72.1	14.3	36.1	25.0	10.0	54.5	5.0	70.6
centrifuge, wash	721	1.64	721	1.64	100	10.71	100	10.7
centrifuge, wash	721	1.64	721	1.64	100	10.71	100	10.7
centrifuge, wash	721	1.64	721	1.64	100	10.71	100	10.7
total		19.2		29.9		86.7		100.0
column reduction	72.1	6.46	36.1	12.88	10.0	45.78	5.0	89.8
water flush	721	0.65	721	0.65	100	4.66	100	4.66
total		7.1		13.5		50.4		94.5

For a system with a high K_d value (721 cm³/g), a low dithionite concentration experiment detaches few microbes in both batch and column systems (Table 4.1.4, first two columns of numbers). Microbes desorb from surfaces during the reduction process (i.e., higher ionic strength solution), whereas the water flush in both batch and column systems has little effect. For the same system with a high K_d value (721 cm³/g), a high dithionite concentration injection will remove more microbes from the system due to greater detachment at the higher ionic strength (third and fourth columns, Table 4.1.4).

If the microbes were more weakly attached to the sediment ($K_d = 100$), then there would be significant microbial detachment during the dithionite injection. For low dithionite concentration injection, the calculated microbial population loss is 87% for batch reduction and 50% for column reduction (Table 2, columns 5 and 6), whereas for a high dithionite injection, essentially all of the microbial population detaches and is flushed out of the system. While these calculations are not intended to reflect the exact detachment that would be observed, the important processes are illustrated, and implications to field scale dithionite reduction:

a) lower dithionite injection should result in less microbial detachment and removal from the sediment. At the field scale, dithionite reduction of sediment can be accomplished by a smaller volume, high dithionite concentration injection or similarly by a larger volume, lower dithionite concentration injection. If coupled abiotic/biotic remediation is desired, the lower dithionite concentration should be used to minimize biomass loss (from a detachment point of view illustrated here, but microbial death also results from high concentration injection, as described in Results Section 4.1.1).

b) microbial biomass that detaches into solution during dithionite injection could be measured at the field scale to quantify the amount of detachment. Sediment cores can be used to determine the microbial population on the sediment, so K_d values at field scale injections could be determined. At the field scale, even if microbes are flushed out of the dithionite treatment zone, over time, microbes will be advected into the system from upgradient locations.

c) At the laboratory scale, differences between batch and column reductions indicate some additional removal of microbes in batch systems,
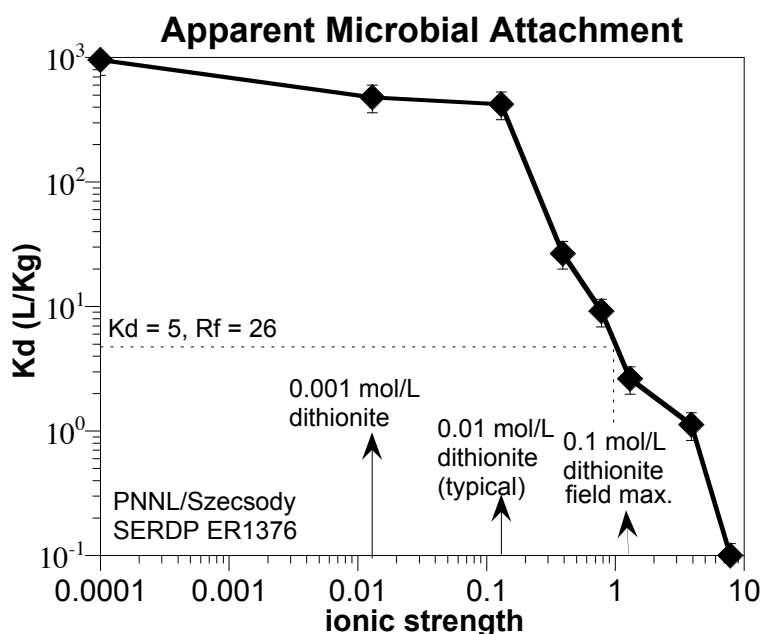
Figure 4.1.19. Microbial attachment calculated from microbial biomass aqueous and sediment extracted data (data ± 20%).

which should be more pronounced at higher dithionite concentrations. What may also be of significance are artifacts associated with the number of handling steps in batch systems (three different washes and resuspension after centrifugation), in which there could be some fine (reactive) sediment loss. Column systems appear to have less manual handling steps, so there may be fewer experimental artifacts. The higher sediment/water ratio in columns (similar to the field) versus batch systems is the main reason why there is less microbial detachment in columns.

4.2 Task 2 Chemical Reductant and Energetic Degradation

4.2.1 Geochemical Characterization of Dithionite Treatment of Sediment

4.2.1.1 Reductive Capacity, Iron Phases, and Eh

Abiotic and biotic experiments are conducted in this project using natural sediments that are treated with a mixture of sodium dithionite and potassium carbonate. In this task, differing techniques are used to quantify the influence of dithionite treatment on sediments. Results show that treatment with a large excess of dithionite to the reducible iron does not result in additional reductive capacity (Table 4.2.1), but other ferrous iron phases increased. The mass of reducible iron can be quantified by the reductive capacity measurement (oxidation of sediment in columns) or the 0.5M HCl ferrous iron extraction (1 h and 24 h extraction time), with similar results (Figure 4.2.1), although a different study found only a fair correlation (described below).   In addition, while iron extractions to not indicate greater capacity for high dithionite treatments, other evidence indicates there are changes in the ferrous surface phases (Section 4.3, Task 3.1), and these phases changes result in much more rapid RDX and HMX mineralization. Therefore, iron extractions and reductive capacity measurements are useful for quantifying low to moderate dithionite treatment (not high dithionite treatment), but additional characterization is needed to be able to predict energetic reactivity.

Ferric iron extractions (Table 4.2.1) did show some decrease with increasing dithionite treatment, but were less useful. Redox potential (Eh) aqueous measurement (i.e., assuming in equilibrium with reduced surface phases) qualitatively indicated reducing conditions (i.e., untreated, anoxic sediment 0 to -50 mV to dithionite-treated sediment was -460 mV). Iron phase extractions for the partially reduced sediment paralleled RDX and acetate results in other tasks indicate a systematic progression in reactivity with dithionite treatment.

Table 4.2.1. Quantification of iron phases in dithionite-reduced sediment.

treatment	exp.	ion exch. Fe^{II}	Fe^{II}	Fe^{II}	reductive capacity	amorphous Fe^{III} oxides	cryst+ am Fe^{III} oxides	total
2*dith/Fe	name	1M CaCl2 (μmol/g)	0.5M HCl, 24h (μmol/g)	0.5M HCl, 1 h (μmol/g)	(μmol/g)	am-oxalate (μmol/g)	DCB (μmol/g)	5M HCl (μmol/g)
26.8	R24	0.66	175.0	111.8	72.8	98.8	98.9	278
4.12	R31.1	1.24	105.4	74.1	67.1	102	59.5	211
1.12	R45	0.42	62.2	44.7	43.7	160	184	208
0.54	R47	0.33	27.9	28.6	27.6	150	170	194
0.237	R49	0.22	12.5	7.1	5.0	139	155	185
0.078	R51	0.05	7.1	11.7	5.0	155	146	180
0.000	untreated	0.05	4.7	10.0		150	509	253

(The header spans: "------ Fe^{II} phases ------" over the ion exch. Fe^{II}, Fe^{II}, Fe^{II}, and reductive capacity columns; "----- Fe^{III} phases -----" over amorphous Fe^{III} oxides and cryst+ am Fe^{III} oxides columns; "$Fe^{II}+Fe^{III}$" over the total column.)

Using exactly the mass of dithionite needed to react with sediment to 27 times more dithionite produced the same reducible iron concentration (Figures 4.2.1 and 4.2.2), whereas using a ratio of <1 resulted in less reducible iron, as measured by oxidation of the sediment in columns with air-saturated water. With a ratio of 0.5, the reductive capacity was reduced by roughly half. With a ratio of 0.2 and 0.05, the reductive capacity obtained was minimal. These results are consistent with previous results, which indicate the reductive capacity measurement (i.e., sediment oxidation in a column for several weeks) is a reliable, but time

Figure 4.2.1. Comparison of batch extraction technique (1 hour of 0.5M HCl extraction, precision ± 7%) to the 1-D column method of oxygen consumption (reductive capacity, precision ± 5%) for dithionite-reduced sediments.

consuming measurement. A more rapid measurement (0.5M HCl iron extraction, next section) was developed. Both batch-reduced and column-reduced sediments were treated with 0.5M HCl (1 h) to extract the "total Fe(II) phases," as defined by Heron and others (1994). There was a good correlation between the amount of dithionite treatment (redox capacity, Figure 4.2.1) and the 0.5M HCl extractable Fe(II) for this reduced Ft. Lewis sediment. However, in a separate study of Hanford sediments, a comparison of 78 redox capacity measurements to 200 iron extractions (1 h of 0.5M HCl) did not show a very good correlation. In that study, it was concluded that the short contact time did not access (or dissolve) the same iron oxides that a 2-3 week oxidation of sediment did (i.e., a significant amount of slow oxidation sites were not accounted for by the 1-hour 0.5M HCl extraction). In addition, that study found a 2-week 5M HCl extraction (at 80C) for total ferrous and ferric iron was correlated with the reductive capacity, also presumably indicating that the length of time of the experiment (i.e., ~2 weeks for both reductive capacity and total iron extractions) did allow for access to a similar number of reactive iron oxide/clay sites.

Figure 4.2.2. Reductive capacity (precision ± 5%) for differing dithionite treatments.

As sediment reacts with dithionite, resulting adsorbed ferrous iron (no color), siderite (grey), and FeS (black) change the color of the sediment. For a single sediment sample, the color can be used (Figure 4.2.3), but the observed color also

Figure 4.2.3. Dithionite treatment (% dithionite/Fe) and color.

changes with minerals present, grain size, and moisture content. Therefore, the color observed from pictures does not accurately reflect the reductive capacity, and is only qualitative.

While chemical reduction of sediments does not increase the reductive capacity with large excess of dithionite, there appear to be other chemical changes that take place. As described in other sections, the rate of RDX and HMX mineralization increases from sediment that is fully reduced with sufficient dithionite (i.e., dithionite/ferrous iron ratio of 1.5 to 3.0x) to a sediment that is fully reduced with excess dithionite (i.e., dithionite/ferrous iron ratio of 28x), which may indicate the presence of different ferrous iron phases on the sediment surface for highly reduced sediments. The redox potential of a solution in equilibrium with reduced sediments (Figure 4.2.4) changes significantly from untreated sediment to reduced sediment. There is a smaller change in the redox potential between sediments that are just fully reduced (i.e., dithionite/ferrous iron ratio of 1.5 to 3.0x) to sediments fully reduced with excess dithionite (i.e., dithionite/ferrous iron ratio of 28x), which may indicate changes in the specific ferrous iron phases present on the sediment surface. Iron extractions (Table 4.2.1) do not provide indication of changes between these two reduced sediments, although extractions are, unfortunately, not capable of determine the amount of ferrous iron present in 2:1 clays (i.e., dithionite will reduce some structural iron in 2:1 smectite clays).
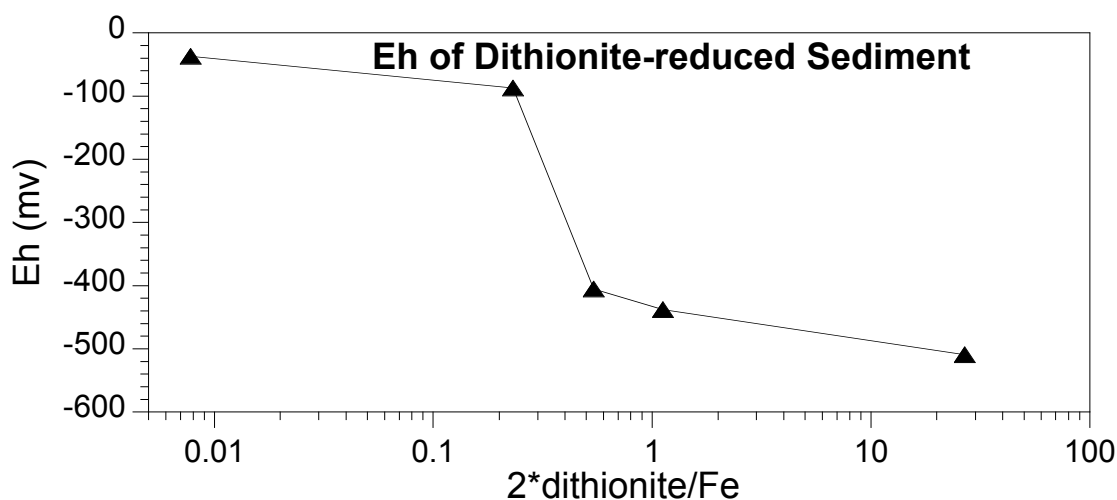
Figure 4.2.4. Solution redox potential of the dithionite-treated sediments (Eh ± 8%).

Because the sediment/water system contains microbes that are actively reducing energetics (and other carbon sources, if present), there are additional redox potential changes taking place. Three sediment water systems were considered: a) dithionite-reduced sediment with RDX, glucose and trace nutrient additions, b) untreated sediment with 0.4% zero valent iron, RDX, glucose, and trace nutrient additions, and c) untreated sediment with RDX, glucose, and trace nutrient additions. All three batch systems were initially anaerobic (oxygen removed) and pH/Eh measurements taken from hours to 2000 h. The dithionite-reduced sediment containing 80 μmol/g iron is equivalent to 0.4% ferrous iron, so the untreated sediment with the addition of 0.4% zero valent iron is roughly equivalent mass, although zero valent iron will eventually be more electronegative. The untreated sediment with only additions of RDX, glucose, and trace nutrients represents the biostimulation system that achieved the most rapid RDX mineralization rate (described in later sections). Results show that all systems become more reducing over time (Figure 4.2.5), but the dithionite-reduced sediment started at -0.2 v, whereas the two untreated sediment systems took some time to develop reducing conditions. The dithionite-reduced sediment achieved -0.5 v redox potential by 2000 h, whereas the zero-valent iron system reached this condition by 600 h. Pure zero valent iron systems (rather than the 0.4% zvi in this system) to achieve much more electronegative conditions. In a previous study on shallow soil remediation by mixing zero valent iron with the soil, researchers found that an Eh of -150 achieved the same RDX degradation rate as lower Eh values. The bioremediation system (green line, Figure 4.2.4) became only slightly electronegative (-0.05v) by 2000 h, which may be the reason why RDX
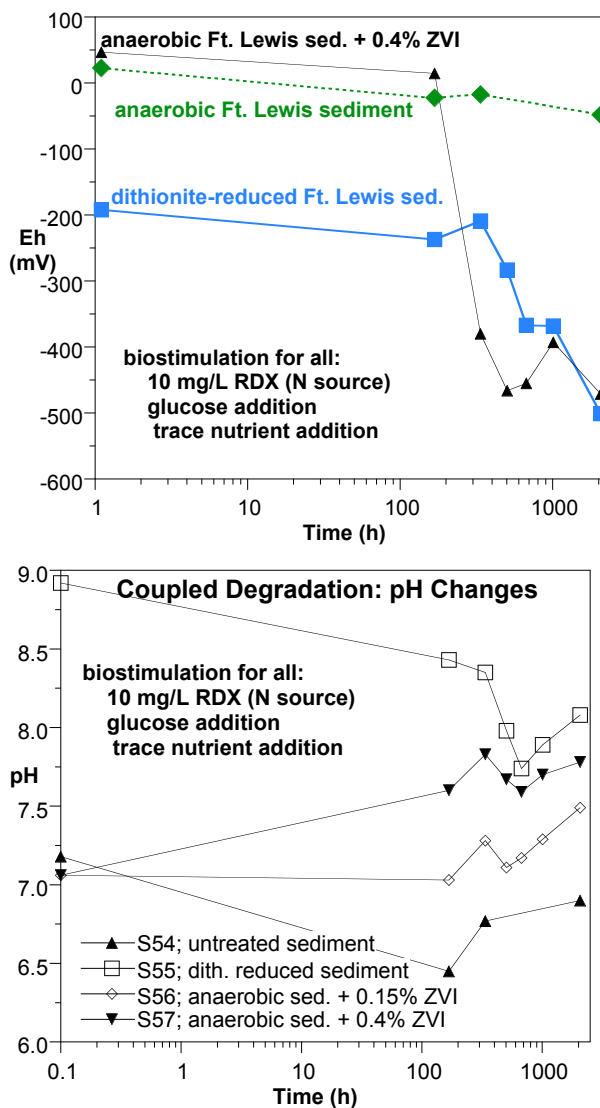
Figure 4.2.5. Redox potential (a) and pH changes (b) that occur during coupled abiotic/biotic degradation of RDX in: i) biostimulation system (i.e., untreated sediment with additions of glucose and trace nutrients), ii) dithionite-reduced sediment (0.4% Fe(II)) with glucose and trace nutrient additions, and iii) untreated sediment with addition of 0.4% zero valent iron and glucose and trace nutrients. Eh ± 8%, pH ± 3%.

degradation is so slow (i.e., first few steps are more rapid abiotically and this system is apparently not sufficiently electronegative to promote RDX degradation abiotically.

The ferrous iron, pH, and Eh was periodically monitored for 2000 h in a different system containing only anoxic water, reduced sediment, and 10 mg/L TNT (Figure 4.2.6, experiments X1-10). In both partially reduced sediment (experiments X1-5) and highly reduced sediment (experiments X6-10), the Eh remained relatively constant for the first 500 h (~-400 mV), then decreased (-600 mV) by 2000 h, possibly indicating some microbial activity degrading TNT. The pH was constant. The extractable ferrous iron (0.5M HCl for 1 h) decreased over time for both systems, although significantly for the partially reduced sediment, indicating some consumption of ferrous iron.

The pH of these systems generally increased slightly over 100s to 1000s of hours (Figure 4.2.4b). The dithionite-reduced system was initially at pH 8.8 just due to the carbonate pH buffer residue present during dithionite reduction. In the dilute soil/water system, the pH decreased to pH 7.7 by 400 h, then increased to pH 8.0 by 2000 h. Two sediment systems containing different amounts of zero valent iron (0.15% and 0.4%, Figure 4.2.4b) had an initial pH of 7.3, which increased to 7.6 (0.15% zvi) and 7.8 (0.4% zvi) by 2000 h. The pH of the bioremediation system initially at pH 7.3 increased to 7.4 by 2000 h.
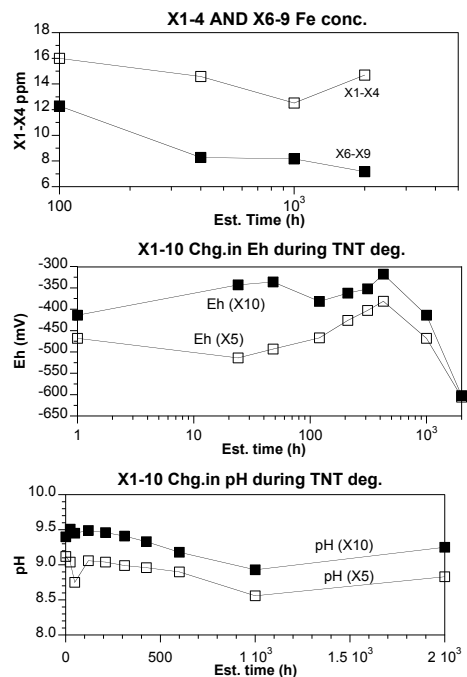
Figure 4.2.6. Fe^{II} (a), Eh (b), and pH (c) changes during TNT degradation.

4.2.1.2 Comparison of Iron Phases and Reductive Capacity

Abiotic and biotic experiments are conducted in this project using natural sediments that are treated with a mixture of sodium dithionite and potassium carbonate. All experiments used the potassium carbonate pH buffer at 4x the dithionite concentration. These dithionite-treated sediments were then characterized by: a) reductive capacity, b) adsorbed Fe(II) extraction (I M $CaCl_2$), c) total Fe(II) by 0.5M HCl, d) total Fe(II) by 5.0M HCl, e) amorphous Fe(III) oxides by NH2OH*HCl, and f) crystalline Fe(III) oxides by DCB minus the NH2OH*HCl. In the results section, the correlation (if any) between the dithionite treatment and the resulting iron phase measurement are shown.

These results indicate only the iron (II/III) phase measurements for dithionite treatment. Similar treatments were conducted with measurements of microbial activity (^{14}C acetate and ^{14}C RDX and HMX) in other sections. We hypothesized that high concentration of dithionite and pH buffer does increase the reducible iron concentration in the sediment, but decreases the microbial population (and subsequently the microbial activity).

4.2.1.3 Dithionite Treatment and Reductive Capacity

Using exactly the mass of dithionite needed to react with sediment to 27 times more dithionite produced the same reducible iron concentration (Figures 4.2.7a and 4.2.2), whereas using a ratio of <1 resulted in less reducible iron, as measured by oxidation of the sediment in columns with air-saturated water. With a ratio of 0.5, the reductive capacity was reduced by roughly half. With a ratio of 0.2 and 0.05, the reductive capacity obtained was minimal. These results are consistent with previous results, which indicate the reductive capacity measurement (i.e., sediment oxidation in a column for several weeks) is a reliable, but time consuming measurement. A more rapid measurement (0.5M HCl iron extraction, next section) was also developed).

4.2.1.4 Dithionite Treatment and Fe(II) Phase Measurement by 0.5M HCl Extraction

Both batch-reduced and column-reduced sediments were treated with 0.5M HCl (24 h) to extract the "total Fe(II) phases," as defined by Heron and others (1994). There was a positive correlation between the amount of dithionite treatment and the 0.5M HCl extractable Fe(II) (Figure 4.2.7b), although: a) the values were greater than the reductive capacity measurement, and b) it was unclear that with a dithionite/iron ratio >1, the ferrous iron concentration did not level off. In addition, column and batch reductions appeared to produce the same reducible iron concentration for the same dithionite/iron ratio in the treatment. These results indicate that the 0.5M HCl extraction is very useful, but a shorter contact time (i.e., <24 h) is needed to achieve similar results to the reductive capacity. This was investigated (Figure 4.2.8), and a contact time of 1 h and 24 h extractions were used (Table 4.2.1).
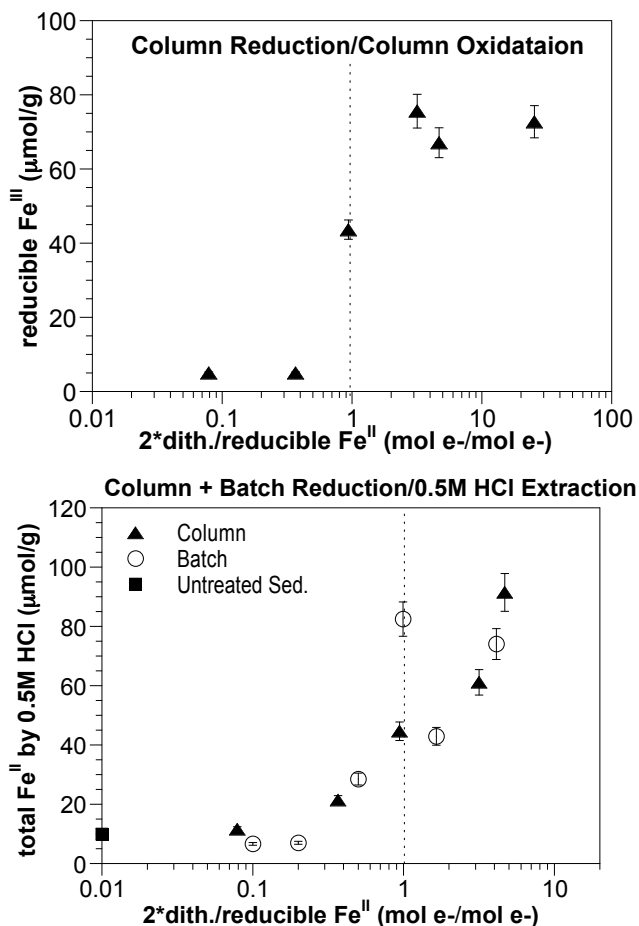
Figure 4.2.7. a) Sediment reductive capacity ±4%, and b) batch and column reduction and 24 h 0.5M HCl ferrous iron measurement (± 5%).
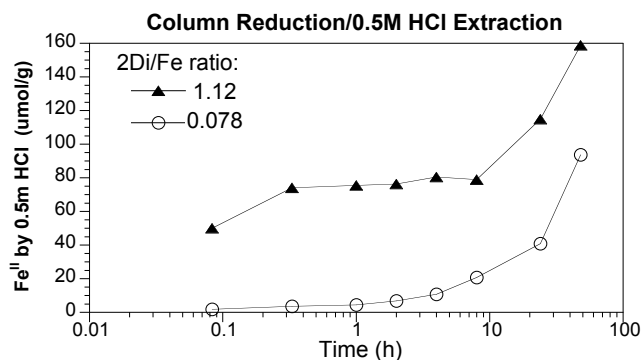
Figure 4.2.8. 0.5M HCl/sediment contact time during extraction (± 5%).

4.2.1.5 Dithionite Treatment and Total Fe(II) Phase by 5M HCl

Both batch-reduced and column-reduced sediments were treated with 5.0 M HCl (24 h) to extract the "total Fe(II) phases." In some studies, 21 days is used for this measurement. While the Heron and others (1994) paper defines which iron oxides are well dissolved by 5M HCl, little is said about dissolution of clays. These results show a well-defined correlation between the dithionite treatment and the 5M HCl extractable ferrous iron (Figure 4.2.9). The mass of ferrous iron extracted levels off at about 210 µmol/g (dithionite/iron >1) and decreases with less dithionite treatment. There is little difference between batch-treated and column-treated sediments. However, there is a significant problem with the 5M HCL extractable ferrous iron value for the untreated sediment, which should be low (but it is 250 µmol/g).

Column + Batch Reduction/5.0M HCl Extraction
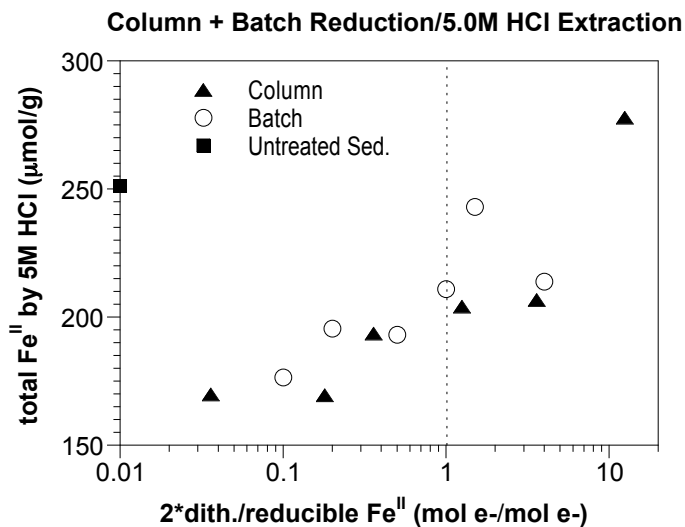
Figure 4.2.9. Batch and column reduction and 5M HCl ferrous iron extraction (±7%).

4.2.1.6 Dithionite Treatment and Adsorbed Fe(II)

Both batch-reduced and column-reduced sediments were treated with 1.0 M $CaCl_2$ ("ion-exchangeable ferrous iron) and the ferrous iron concentration in the extractant was measured. Historically, we have had considerable trouble with this measurement related to keeping the extractant solution oxygen-free so the aqueous ferrous iron is not oxidized. We may have done poorly in this set of experiments, or the extraction measurement indicates very small amount of adsorbed ferrous iron. Results (Figure 4.2.10a) in all cases indicate extremely small values (<0.04 µmol/g ferrous iron).

Laboratory artifacts associated with this adsorbed ferrous iron method were tested with a standard addition experiment. An anaerobic sediment in an anaerobic glove box with He bubbling (i.e., multiple methods to keep the system anaerobic) was divided into four vials and aqueous ferrous iron was added to each equivalent to 10, 20, 40, and 120 µmol/g of sediment. The ion exchangeable extraction method was then used on each, which recovered: 16.2, 31.8, 44.0, and 100.3 µmol/g of ferrous iron (average 83.5 ± 11% recovery, Figure 4.2.10b), and the untreated sediment itself had 13.4 µmol/g ferrous iron (average intercept). Some additional work is needed with this extraction to determine whether adsorbed ferrous iron is present in significant quantities in the reduced sediment.
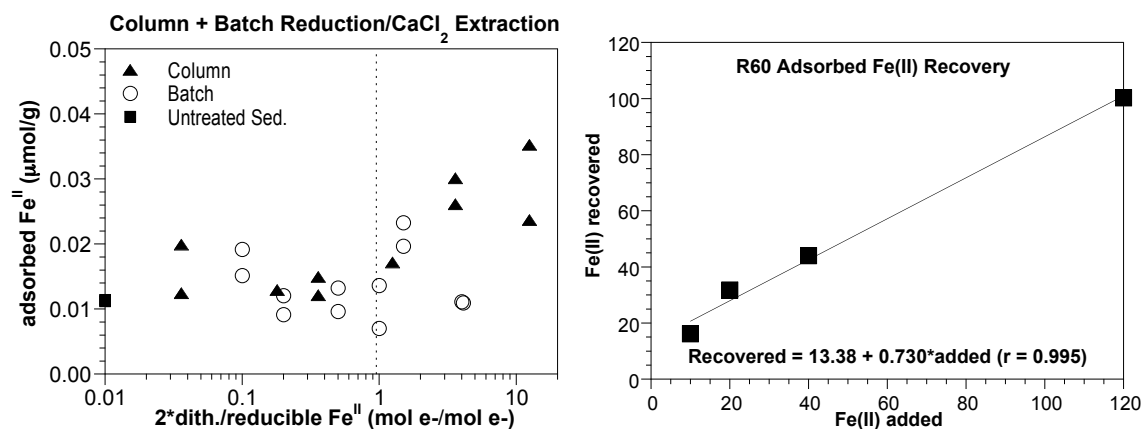
Figure 4.2.10. a) Batch and column reduction and 1M CaCl$_2$ ferrous iron extraction (±20%), and b) ion exchangeable ferrous iron recovered in test (±7%).

4.2.1.7 Dithionite Treatment and Ferric Iron Measurements

Both batch-reduced and column-reduced sediments were treated with DCB and NH2OH*HCl, which are used to extract crystalline and amorphous ferric phases (DCB) and amorphous ferric phases (NH2OH*HCl). Previous studies have shown that stronger dithionite treatment decreases the ferric phases, because crystalline and amorphous ferric oxides are dissolved and reduced. Both decreased with increasing dithionite treatment (Table 4.2.1 and Appendix P).

4.2.2 RDX Degradation/Mineralization in Abiotic/Biotic Treated Sediments

4.2.2.1 RDX Mineralization Rate in Reduced and Biostimulated Sediments

Previous studies of RDX biodegradation (McCormick and others 1981; Hawari 2000) have shown that there are multiple pathways with some intermediates that have never been positively identified (likely due to instability in aqueous solution). For the purpose of this study, abiotic, biotic, or coupled abiotic/biotic sediment systems are studied to determine conditions that produce the most rapid mineralization rate for energetics, as this has the greatest risk reduction of a subsurface spill. In this section, various influences on the RDX overall mineralization rate are described. In the following sections, individual degradation reactions are described. The initial four degradation steps of RDX (RDX to MNX to DNX to TNX to methylene dinitramine) are specific to RDX. However, both methylene dinitramine and formate are HMX and RDX intermediates.

Under iron reducing conditions in sediments tested (created by dithionite reduction of sediment or addition of zero valent iron) without and with biostimulation (carbon and/or trace nutrient addition), RDX is mineralized more rapidly as a direct function of the amount of dithionite added (i.e., ferrous iron present), as shown in Figure 4.2.11a. RDX was mineralized with a 31,000 h half-life (shown in Figure 4.2.11b) in untreated sediment, as compared to a 315 h half-life with high dithionite treatment (di/Fe = 26). This does not indicate abiotic reactions are

the only reactions involved in RDX mineralization. In fact, high dithionite treatment with a bactericide (gluteraldehyde) added (Figure 4.2.11b) showed essentially no mineralization, which clearly indicates microbes are necessary for RDX mineralization. As shown in Task 1 results, dithionite treatment has only a small effect on the microbial population, with a 10x decrease in population density at the highest dithionite concentration. Therefore, results shown in Figure 4.2.11b are abiotic treatment of sediment and much of the microbial population is still viable.

In comparison to the reduced sediment, the same Ft. Lewis sediment was augmented with just carbon and/or trace nutrient addition (Section 4.2.2.3). In all cases, biostimulation in an anaerobic environment produced more rapid RDX mineralization than in oxic systems, but all biostimulated systems were significantly slower than iron reduced systems. The most rapid

Figure 4.2.11. RDX mineralization rate in sediment/microbe/water systems with: a) dithionite addition only (microbes still alive), and b) dithionite and bactericide addition (data ± 2%).

biostimulation rate was glucose addition in an anoxic system (9900 h half-life). Additional biostimulation comparisons are made in Results Section 4.1 (biostimulation), with prestimulation (carbon addition) for a few weeks before ^{14}C-RDX is added.

Figure 4.2.12. RDX mineralization rate in sediment/microbe/water systems with dithionite reduction and biostimulation (carbon or trace nutrient addition) (data ± 2%).

The combination of both dithionite reduction and biostimulation (carbon or trace nutrient additions) produced the most rapid RDX mineralization rate observed (112 h half-life for trace nutrient addition, Figure 4.2.12). While this appears to indicate the most rapid increase in RDX mineralization is caused by iron reduction (i.e., apparent abiotic rate control on one or more reactions), there is a secondary contribution of necessary biotic (or coupled abiotic/biotic) reactions contributing to the overall observed RDX mineralization rate. To

50

determine the actual cause of this apparent abiotic and biotic control on RDX mineralization, individual degradation steps were examined, as described in this and following sections.

Additional comparison experiments were conducted in which RDX mineralization studies were conducted with: a) only dithionite reduction (partially or fully reduced), b dithionite reduction with the addition of trace nutrients. These results (Figure 4.2.13) showed that trace nutrients caused a significant increase in the RDX mineralization rate (for partially reduced sediment) and a smaller increase for fully reduced sediment. Trace nutrients (Table 4.2.2) consisted of metals needed for metabolic activity, amino acids, and vitamins.
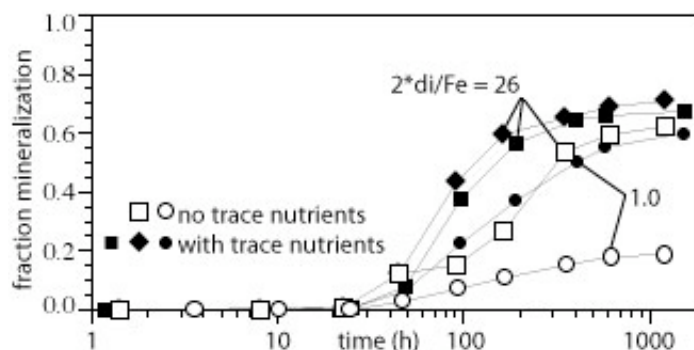
Figure 4.2.13. RDX mineralization rate in sediment/ microbe/water systems with dithionite reduction and trace nutrient additions (data ± 2%).

Table 4.2.2. Trace nutrients used in RDX mineralization experiments.

species	concentration
metals	**(mol/L)**
Fe+2	1.79843E-07
Mg+2	4.05731E-06
PO4	2.17391E-05
PO4	2.20442E-05
Mn+2	1.97059E-07
BO3-3	4.04334E-07
SeO3-2	1.44559E-07
MoO4-2	1.03327E-07
Co+2	2.07948E-07
Ni+2	9.51033E-08
Ca+2	1.83204E-07
Zn+2	1.54847E-07
amino acids	
L-Arginine	1.14811E-05
L-Serine	1.90295E-05
L-Glutamic Acid	1.35934E-05
vitamins	
*Biotin	8.18632E-09
*Folic Acid	4.53104E-09
*Pyridoxine HCl	4.86287E-08
*Riboflavin	2.65696E-10
*Thiamine	1.66218E-08
*Nicotinic Acid	4.06141E-08
*D-Pantothenic Acid	2.28061E-08
*Vitamin B12	3.689E-09
*P-Aminobenzoic Acid	3.64591E-08
*Thioctic Acid	2.4233E-08

RDX mineralization studies were conducted in reduced sediment with different carbon source additions (lactate, glucose), and showed mixed results. With the addition of a small amount of carbon (C/N ratio = 2.0), the addition of lactate had little effect on the RDX mineralization rate (Figure 4.2.14a compared with Figure 4.2.11a with no carbon addition). Similar results are shown with the addition of glucose (C/N ratio = 20, Figure 4.2.14b), with little immediate change in the RDX mineralization rate with the carbon source addition. In this case, experiments with and without glucose addition were conducted simultaneously at two different dithionite treatments to eliminate differences between experiments. Experiments are fairly reproducible (scintillation counting precision 0.2%; experiment reproducibility ±2% for mineralization), as shown in Figure 4.2.13 with duplicate experiments under the same conditions.

With a higher amount ratio of carbon to nitrogen (C/N = 100, Figure 4.2.14c), the addition of glucose had an immediate increase in the RDX mineralization rate. The mineralization rate increased from a 315 h half-life for dithionite only treatment to 112 h half-life for the same dithionite treatment and glucose addition (~3x increase). While this gives the appearance that carbon addition had little effect, it should be noted that the addition of carbon with immediate RDX mineralization (i.e., no time given to allow for microbial growth) simply means the microbes are not well acclimated to utilize RDX as the nitrogen source and the lactate or glucose as the carbon source. Acclimation time was examined to some extent, and it did provide up to a three times increase in the mineralization rate (Section 4.2.6). It should be noted, however, that prestimulation (with carbon and RDX addition, to increase metabolic pathways for RDX mineralization) is generally
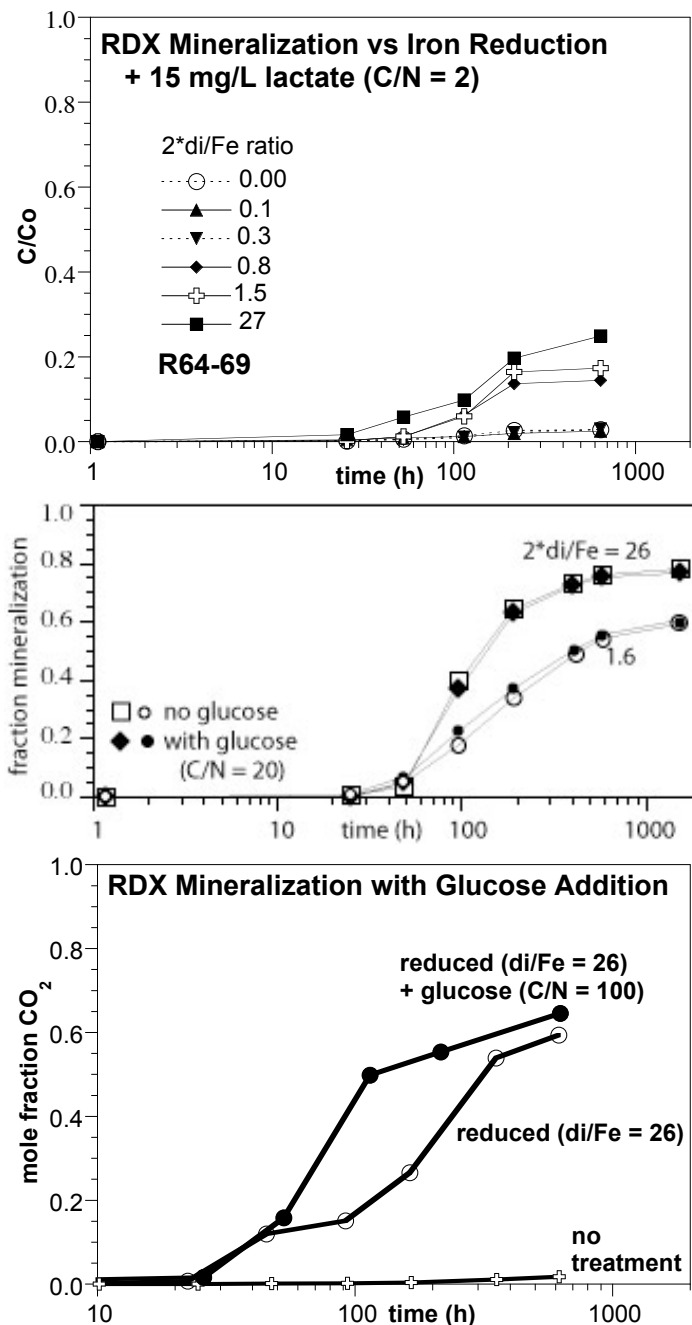
Figure 4.2.14. RDX mineralization rate in sediment/microbe/water systems with dithionite reduction and carbon additions: a) lactate, C/N = 2.0, b) glucose, C/N = 20, and c) glucose, C/N = 100 (data ± 2%).

accomplished by a few weeks of acclimation time (3 weeks or 504 h). If acclimation with the carbon addition was needed, what would be observed is similar RDX mineralization for cases with and without carbon addition at early times (<500 h, for example Figure 4.2.14b), then an increasingly more rapid mineralization rate for the carbon addition at later times (>500 h). This change in mineralization rate was not observed, indirectly indicating that over the time scale of 1500 h (9 weeks, 62 days), acclimation time with carbon addition did not influence the RDX mineralization rate.

Sequential RDX anaerobic biostimulation followed by oxic biostimulation was also investigated. TNT degradation was investigated in a system in which TNT and glucose have the same enzymatic degradation pathway (Section 4.2.4.2). This pathway degrades TNT to amino-intermediates that irreversibly sorb to sediment, so while TNT is not being mineralized, risk of the uncontrolled TNT release to the subsurface environment is being reduced as the mass is being immobilized. The same sediment treatment was investigated for RDX and HMX. The treatment involves biostimulation with a significant quantity of glucose (4000 mg/L) in anoxic/reduced systems, followed by oxidation. Because TNT cometabolic degradation to triaminotoluene (TAT) was most rapid in reduced sediments, we investigated HMX mineralization in slightly reduced sediments (dithionite/ferrous iron = 0.5) with and without 4000 mg/L glucose addition.
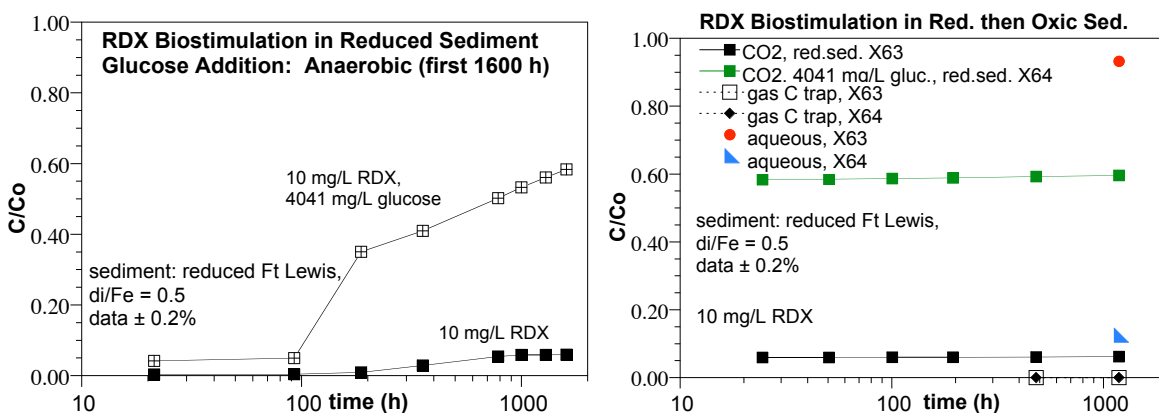
Figure 4.2.15. RDX mineralization rate in sequential anaerobic/oxic biostimulated sediments: a) anaerobic for the first 1600 h, b) oxic for the subsequent 1200 h (data ± 2%).

RDX mineralization in the sediment with low reduction was small (5.9%; Figure 4.2.15a) and consistent with previous results (Figure 4.2.13). The large amount of glucose addition greatly increased the RDX mineralization extent to 59.6% by 1600 h. Subsequent oxidation of both systems did not produce additional CO_2 (Figure 4.2.15b). In the system with just sediment reduction (no glucose). 93.2% of the ^{14}C RDX mass was still aqueous at 2800 with 5.9% mineralization (99.1% total). It is believed that methane is also produced, but gas phase carbon traps did not successfully capture the ^{14}C-methane (Figure 4.2.15b). This method is described in Section 4.2.4.1. Mass balance in the system with glucose addition was higher, with 12.5% aqueous at 2800 h and 59.6% mineralized (total 72.1%). Additional carbon mass is also associated with microbes, both sorbed and incorporated (see results Section 4.1.3).

One final treatment to reduced sediment involved the addition of sulfate in an attempt to simulate sulfate reducers. This could produce FeS and FeS_2, which would likely increase some abiotic steps in the RDX degradation pathway. Sulfate addition had no effect on RDX mineralization over the 1600 h experiments, at both low and high dithionite treatment of sediment (Figure 4.2.16). The importance of sulfate-reducing bacteria was investigated in

Task 1, with the addition of ammonium molybdate to some experiments, which inhibits sulfate reducers (Oremland and Zehr 1986). While over the time scale of the experiments shown sulfate reducers had no effect, driving an iron-reducing system (abiotically created) to a biotically controlled sulfate reducing environment (in a subsurface sediment system with a natural population of 10^6 CFU/g) would likely take additional time.
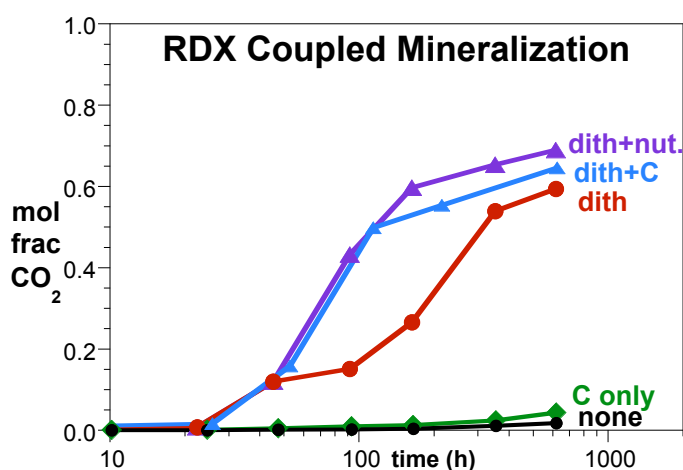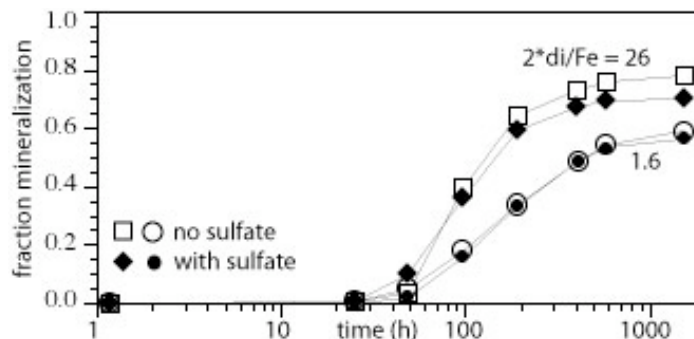

Figure 4.2.16. RDX mineralization rate in sediment/ microbe/water systems with dithionite reduction and sulfate additions (data ± 2%).

The overall RDX mineralization rate of RDX (to CO2) increases two orders of magnitude as a direct function of the amount of dithionite treatment. The dithionite treatment dissolves and reduces about 20% of ferric iron oxides to ferrous phases (Szecsody et al. 2005). The half-life of RDX mineralization decreases from 31,000 h for untreated sediment to 315 h for highly reduced sediment (Figure 4.2.17). Rates of individual reaction steps that are characterized in the following sections, are also plotted, and range in half-life from minutes to 100s of hours. The first four transformation steps (RDX -> MNX -> DNX -> TNX ->) are abiotic, and are fairly rapid (minutes, hours), so are not the rate limiting steps. These reaction rates increase significantly with sediment reduction, as ferrous iron surface phases (electron donor) increases.

Methylene dinitramine degradation has ~10 h half-life in untreated sediment and ~95 h half-life in highly reduced sediment, so is somewhat slow, but not the slowest reaction. Methylene dinitramine is degraded by acidic hydrolysis (i.e., abiotic reaction), so is more stable in the slightly more alkaline dithionite-treated sediment. So the apparent slowing of the methylene dinitramine degradation reaction with sediment reduction is only a function of the change in pH (not related to the reduced sediment, nor microbes). Formate degradation to carbon dioxide is the slowest reaction noted, with a 7400 h half-life in untreated sediment and a 60 h half-life in highly reduced
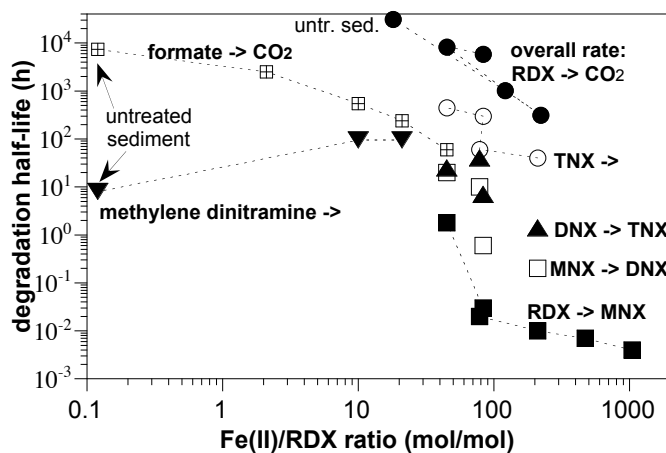
Figure 4.2.17. Transformation rates of RDX and intermediates in reduced sediments as a function of the ratio of ferrous iron to reactant (rates ± 25%).

sediment. This is the most likely rate limiting step for RDX mineralization. Formate mineralization appears to be a coupled abiotic/biotic reaction, requiring microbes and ferrous iron.

4.2.2.2 RDX Mineralization Rate in Sediment/Zero Valent Iron

For comparison, RDX mineralization studies were additionally conducted with anoxic, untreated sediment with small additional of zero valent iron. Researchers have previously noted that there can be some microbial activity near zero valent iron walls, so the possibility of sequential abiotic/biotic reactions can certainly occur. In addition, recent advances in injectable zero valent iron shows that small concentrations of 5-micron diameter zero valent iron can be injected relatively uniformly into porous media. Results of these laboratory experiments only extend over 1.3 meters, but do show a relatively uniform zero valent iron concentration of 0.5% at distance from the injection location. The zero valent iron is injected in a shear thinning fluid, which, under pressure, is easier to inject. Its gel-like consistency maintains the zero valent iron in suspension. The shear-thinning fluid should then dissolve, leaving the zero valent iron deposited within the porous media. While it is beyond the scope of this project to develop this injectable zero valent iron technology, the biogeochemical reactions associated with energetic degradation in mixed sediment/zero valent iron are within the scope of this study. The main purpose of this study is to develop a technology with the most rapid energetic mineralization rate using a modification of dithionite reduction of sediment and biostimulation. For comparison, mineralization rates in dithionite reduced sediments are compared to various biostimulation systems, and in this section, sediment/zero valent iron mixtures.

RDX can be mineralized in sediment with the addition of zero valent iron (Figure 4.2.18), whereas, zero valent iron alone cannot support mineralization, as some steps are biotic (or coupled, needing microbes). As described above, in natural aquifers, microbes advect to and grow in the reducing environment down gradient of many zero valent iron walls, so sequential abiotic/biotic reactions can occur. The RDX mineralization rates observed with small additions of zero valent iron (373 h to 550 h half-life) were only slightly slower than rates in reduced sediments (315 h half-life in highly reduced sediment). The hypothesized degradation pathway for RDX in reduced sediment (Figure 4.2.21) indicates the rate limiting coupled abiotic/biotic reaction (formate degradation). Because the coupled reaction involves both microbes and ferrous iron, either microbes are attached at sites of available abiotic electron transfer (i.e., microbes attached to some 2:1 smectite clays containing structurally reduced iron) or there is some electron transfer in aqueous solution. In the sediment/zero valent iron system, it is hypothesized that microbes are attached to sediment particles (due to electrostatic forces and high surface area). The relatively rapid RDX mineralization
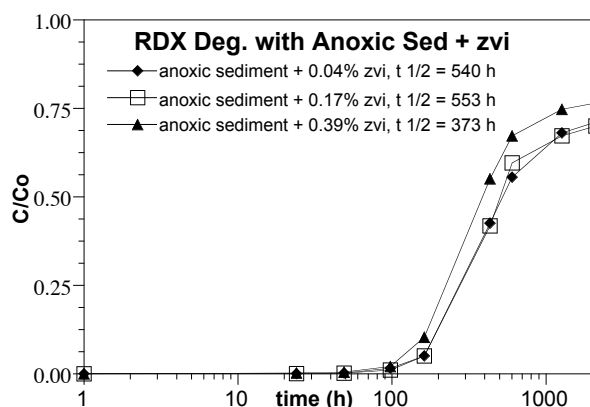
Figure 4.2.18. RDX mineralization anoxic sediment with small additions of 5-micron zero valent iron (data $\pm$ 2%).

rates observed in this sediment/zvi system imply some aqueous electron transfer, or completely separate sequential abiotic/biotic reactions rather than any coupled reactions.

4.2.2.3 RDX Mineralization Rate in Biostimulated Sediments

For comparison to dithionite-treated and zero-valent iron treated sediments, RDX mineralization was studied in various systems that received only biostimulation. The sediment biostimulation treatments included: a) oxic, no additions (oxic control), b) oxic, carbon (lactate) addition, c) oxic, trace nutrient additions, d) anoxic, no additions (anoxic control), e) anoxic, carbon (glucose) addition, f) anoxic, carbon (glucose) and sulfate addition), g) anoxic, RDX prestimulation (acclimation), h) anoxic, RDX prestimulation and carbon (glucose) addition), i) anoxic, RDX prestimulation and trace nutrient additions. An additional control experiment was anoxic untreated sediment with bactericide addition.

Experiments conducted in oxic and anoxic systems in show small amounts (2-5%) of mineralization and similar loss of aqueous components (20-40%). Magnification of the percentage of mineralization (Figure 4.2.19, scale only to 20% mineralized) shows that untreated sediment has some mineralization (2.7% mineralization in 1219 h; 31,000 h half-life), addition of trace nutrients more (5.7% mineralization in 1219 h; 14,400 h half-life), and addition of lactate the most rapid (2.9% mineralization in 644 h; 9900 h half-life). Compared with dithionite treatment alone (63% mineralization in 1219 h (315 h half-life) or dithionite treatment with trace nutrient addition (60% mineralization in 160 h, 73% by 1219 h, 112 h half-life), the coupled process (dithionite abiotic/biotic) is 100-300x more rapid RDX mineralization.
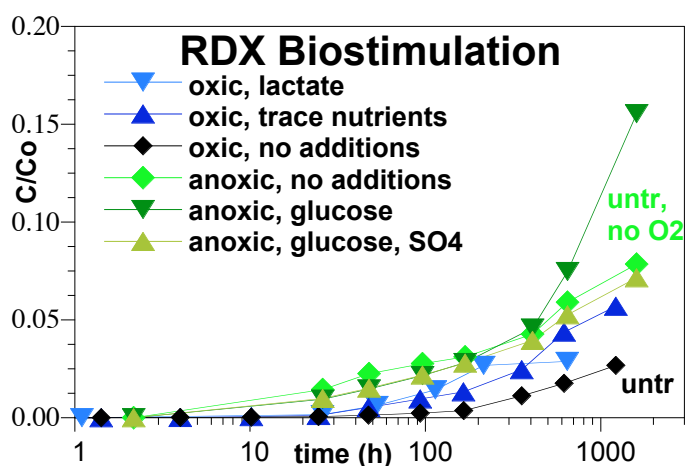
Figure 4.2.19. RDX mineralization rate in sediment/microbe/water systems with biostimulation only (carbon or trace nutrient addition; data ± 2%).

Additional anoxic biostimulation experiments were conducted that included RDX pretreatment for 200 h before 14C-labeled RDX was added (i.e., prestimulation to acclimate microbes to RDX). These prestimulation experiments produced the most rapid RDX mineralization rates, which were 2x to 3x faster than previous studies without RDX prestimulation (Figure 4.2.20). RDX mineralization rates were 4960 h half-life with just anoxic prestimulation (compared with 14,000 h half-life for anoxic biodeg.), 9170 h half-life for anoxic prestimulation with glucose addition (compared with 6400 h), and 5570 h half-life for anoxic prestimulation with trace nutrient addition. These biostimulation rates were still 100x to 300x slower than RDX mineralization in dithionite-treated sediments and zero-valent iron treated sediments (same % iron).
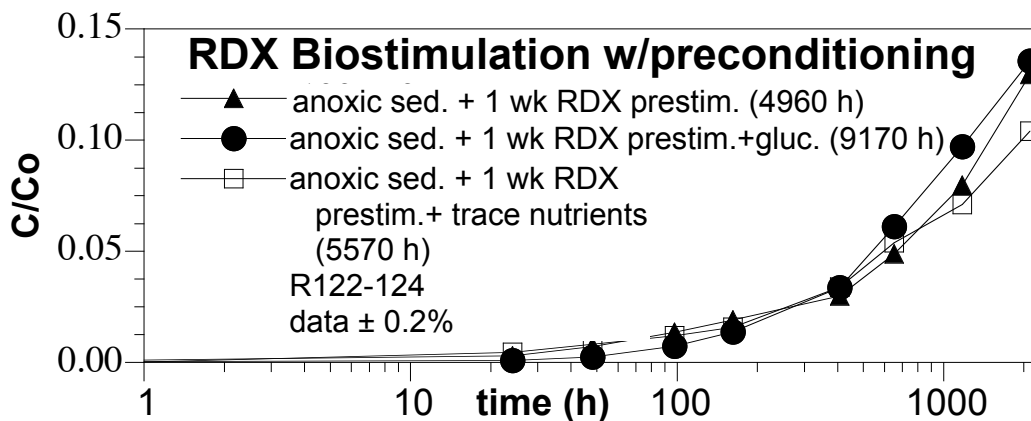
Figure 4.2.20. RDX biostimulation studies with RDX prestimulation (data ± 2%).

4.2.2.4 RDX Degradation Pathway

For RDX, the most rapid mineralization rate in dithionite-reduced sediment occurs in the sediment that has received the greatest amount of dithionite treatment (previous section). It has been previously hypothesized that RDX mineralization increases with sediment reduction because one or more rate-limiting steps is abiotic. Individual degradation steps of RDX and intermediates were investigated (following sections), which includes RDX, MNX, DNX, TNX, methylene dinitramine, and formate degradation (Figure 4.2.21). In most cases, experiments were conducted to determine if the reaction was purely abiotic or biotic or a coupled abiotic/biotic reaction. In addition, the degradation rate of each step was characterized in sediments that had a differing amount of reduction and compared with the overall RDX mineralization rate in order to determine if the rate of that specific reaction could be one of the rate-limiting steps. For example, the overall RDX mineralization rate in highly reduced sediments (half-life 315 h) was orders of magnitude slower than RDX degradation to MNX (half-life 1.8 minutes), so this step clearly could not be the rate limiting step even though the RDX -> MNX step was abiotic and increased orders of magnitude in rate with greater reduction of the sediment.

Methylene dinitramine degradation was initially hypothesized to be a biotic reaction (SERDP ER-1376 2004 annual report), as the degradation half-life was 100 h (in reduced sediment) and 9 h in untreated sediment. It was hypothesized that microbial death from the dithionite
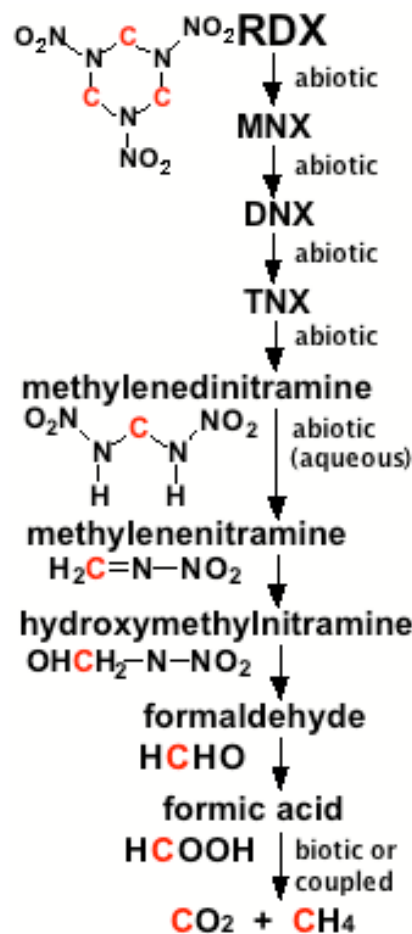
Figure 4.2.21. RDX degradation pathway in dithionite-reduced sediment with or without biostimulation.

57

treatment (which occurs, Section 4.1) accounted for slowing of the methylene dinitramine degradation rate. As described in a following section, this was not the case, methylene dinitramine degrades by acid hydrolysis in solution (more rapid under acid conditions), so it's degradation rate is unrelated to the presence of the sediment, but is related to the pH of the system.

The final step in RDX mineralization is degradation of formate to carbon dioxide, which can be a purely biotic reaction. However, in the reduced sediment system (shown in a following section), the formate mineralization rate increases orders of magnitude and is about the same rate as the overall RDX mineralization rate. Formate mineralization in reduced sediment is not an abiotic reaction, but still requires microbes in addition to the apparent use of ferrous iron as an electron donor. Therefore, in these reduced sediments, formate mineralization appears to be dominated by a coupled abiotic/biotic reaction, and this is the (or one of the) rate limiting steps in RDX mineralization.

4.2.2.5 RDX Degradation to MNX, DNX, and TNX

The initial transformation of RDX to MNX to DNX to TNX and to methylene dinitramine appear to be abiotic steps that occur fairly rapidly. To determine whether the initial RDX transformation steps are abiotic, parallel experiments of RDX degradation in reduced sediment without and with bactericides were compared. While the bactericide should not influence a purely abiotic reaction, it is also assumed that the bactericides do not oxidize the reduced sediment nor degrade/desorb the energetic compounds. A comparison of two RDX degradation experiments with dithionite-reduced sediment to dithionite-reduced sediment with four different bactericides (Figure 4.2.22a) showed that: a) gluteraldehyde and sodium 2-bromoethanesulfonate had no influence on the degradation rate, b) $HgCl_2$ slowed and stopped RDX degradation, and c) ammonium molybdate appeared to increase the RDX degradation rate. It was noted that $HgCl_2$ oxidized the sediment (black sediment turned grey). In a second series of experiments, gluteraldehyde addition to reduced sediment had no influence on RDX, MNX, DNX, and TNX transformation rates (Figure 4.2.22b). Therefore, it appears that these first four steps are abiotic.

The rate of transformation was quantified with a batch model (lines, Figure 4.2.23). The model, which incorporated each of these two electron transfer reactions (model 2) did fit the RDX degradation data slightly better than a single electron transfer (model 1). Although the simulated mass of MNX and DNX approximated the data, the timing of appearance/ disappearance of these intermediates lagged relative to simulated concentrations. In other words, data showed that disappearance of RDX did not immediately correspond to equal mass appearance of MNX, then DNX. Because sorption accounts for some RDX mass (and presumably degradation intermediates), a simulation was conducted with that incorporated sorption of RDX, MNX, DNX, and TNX (model 3), which did result in a time lag for the appearance of aqueous MNX and DNX that more closely approximates the data. Sorption parameters used were from an RDX sorption isotherm, which indicated that RDX sorption on this low organic carbon sediment was small and linear ($S = 0.26$ C, r = 0.99). Batch transformation rate parameters calculated from fitting degradation/sorption model to the data
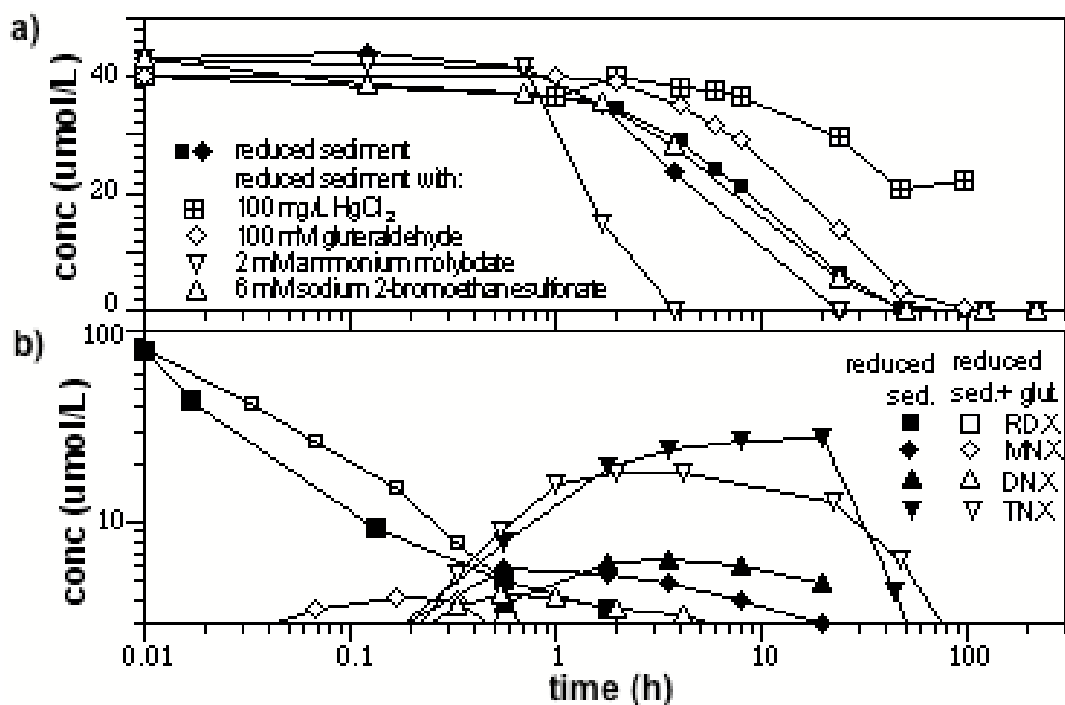
Figure 4.2.22. Effect of bactericides on the coupled RDX transformation in reduced sediment: a) RDX degradation rate only with addition of differing bactericides (sediment/water = 0.02 g/mL), and b) RDX, MNX, and DNX transformation rate with addition of gluteraldehyde (sediment/water = 0.2 g/mL). Data precision is ± 0.5% (RDX), ± 0.5% (MNX), ± 1.6% (DNX), and ± 0.5% (TNX).

(model 3) indicated that the first few transformation reactions are relatively rapid: a) RDX transformation half-life was 3.0 minutes, b) MNX transformation half-life was 30 minutes, c) DNX transformation half-life was 10 h, and d) TNX transformation half-life was 80 h (Table 4.2.3).

Table 4.2.3. RDX, MNX, DNX, and TNX transformation rates.

reaction	exp.	rate $(h^{-1} mol^{-1})$	half-life (h)
RDX -> MNX	6	1.3×10^{-5}	0.03
MNX -> DNX	3	1.8×10^{-6}	0.5
DNX -> TNX	3	3.0×10^{-6}	10
TNX ->	3	4.5×10^{-9}	80
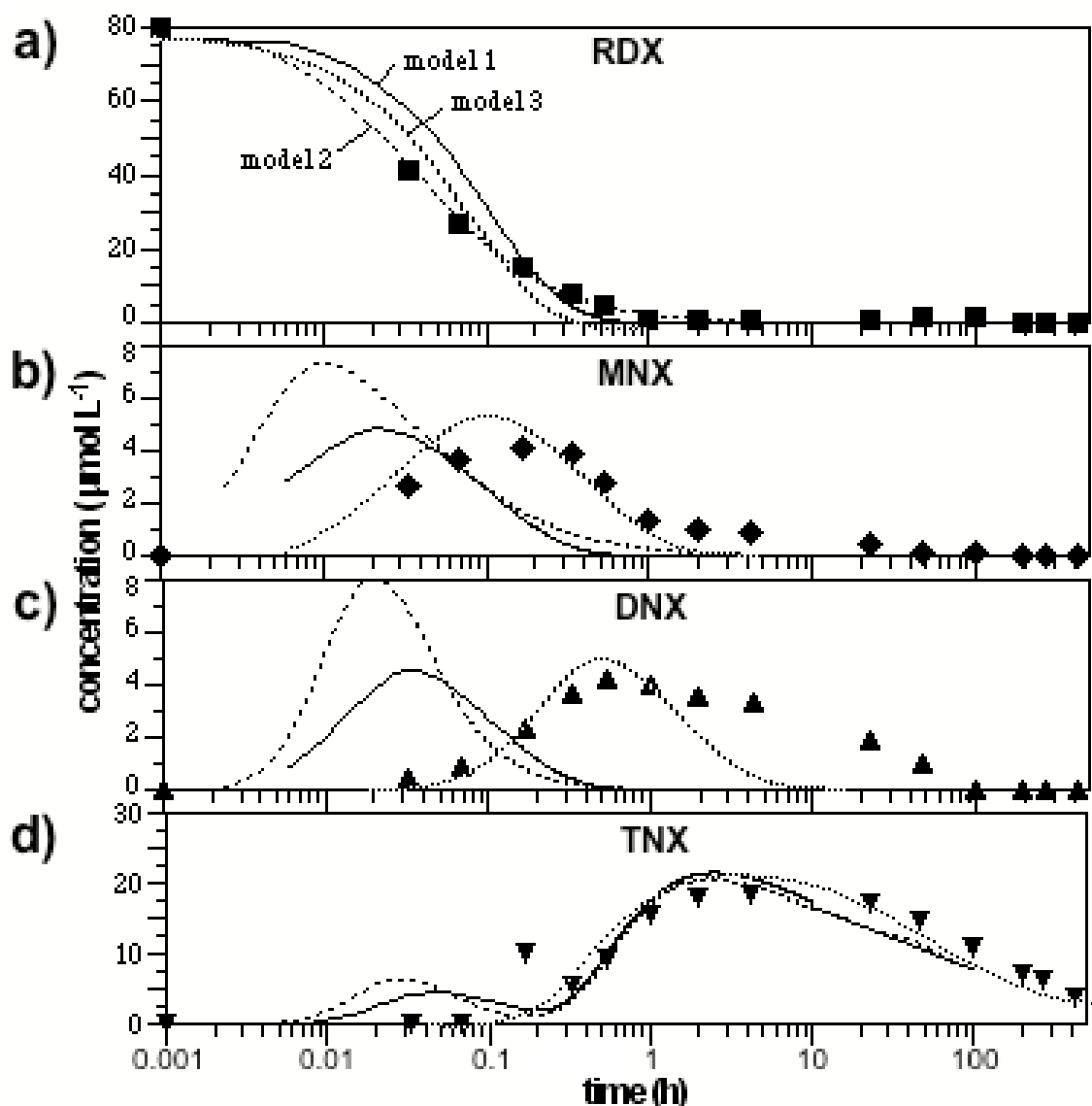
Figure 4.2.23. RDX degradation in a batch system with dithionite-reduced sediment (soil/water = 0.05 g/mL). Data and model simulations shown. Data precision is ± 0.5% (RDX), ± 0.5% (MNX), ± 1.6% (DNX), and ± 0.5% (TNX).

To determine whether the final transformation step of RDX intermediates to carbon dioxide is microbially or coupled controlled, RDX and acetate mineralization studies with and without a bactericide (gluteraldehyde) were compared (Figure 4.2.24). Because acetate cannot be abiotically mineralized, it was used as an indicator of microbial activity. Comparison of acetate mineralization in untreated to dithionite-reduced sediment (Figure 2.2.11) show little difference, so at least at the low dithionite treatment concentration (0.01 mol L-1) used here, the microbial population was not greatly influenced by the dithionite treatment. The addition of gluteraldehyde to the reduced sediment for 48 h before addition of acetate eliminated all mineralization (i.e., <0.6% after 1600 h), indicating acetate mineralization is entirely controlled by microbes. By comparison, RDX mineralization in dithionite-reduced sediment (half-life

60

315 h) was orders of magnitude more rapid than untreated sediment (half-life 31,000 h), but the addition of gluteraldehyde to reduced sediment also eliminated RDX mineralization. It is concluded that transformation of RDX intermediates to carbon dioxide requires microbes, but as shown in a following section, the individual reaction of formate degradation to carbon dioxide is dominated by a coupled abiotic/biotic reaction.

4.2.2.6 Methylene Dinitramine Degradation (RDX and HMX intermediate)

Initial studies at University of Nebraska, Lincoln (Figure 4.2.25) indicate that methylene dinitramine (MDNA) degrades rapidly in untreated sediment (half-life 9 h), but degradation is slower in reduced sediment (~95 h half-life for partially and fully reduced sediment). It was unclear from this data whether this is a biotic reaction or a coupled abiotic/biotic reaction (w/Fe^{III} phase), or abiotic reaction. It was hypothesized that the reaction is biotic, but experiments with bactericides were not successful. There are also difficulties with the stability of methylene dinitramine in aqueous solution.

Additional batch studies were conducted to determine: a) is MDNA degradation a biotic reaction, b) why is degradation

Figure 4.2.24. Influence of sediment reduction and bactericide on the mineralization rate of: a) RDX, and b) acetate (data $\pm 2\%$).
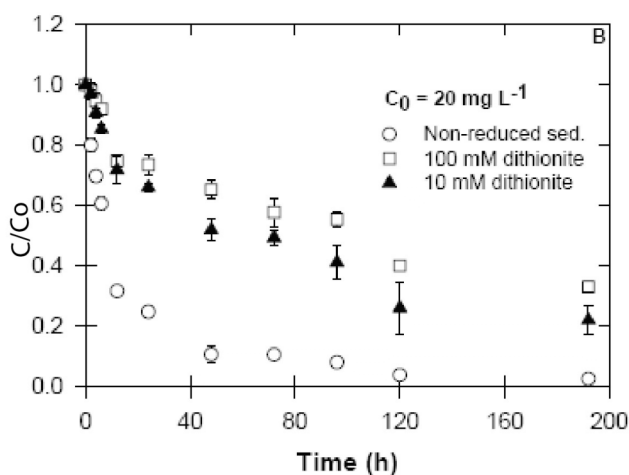
Figure 4.2.25. Degradation of methylene dinitramine in untreated and dithionite treated sediments (data $\pm 2\%$).

inversely related to sediment reduction. MDNA is stable under highly alkaline conditions (pH 11) for at least 50 h (Figure 4.2.26), and degrades more rapidly at lower pH. This is not unexpected, as methylene dinitramine hydrolysis is reported in anaerobic sludge (Hawari 1999). Alkaline stability is highly useful, as samples from an aqueous experiment can be made basic for HPLC analysis. This alkaline stability is the opposite of most energetics – RDX, HMX, and TNT are all stable under acidic conditions, and degrade at pH > 9.5 (TNT is stable to higher pH). Because dithionite-treated sediments tend to be alkaline (pH depends on the amount of washing and buffers), slower MDNA degradation in reduced sediment may be simply related to the pH. At pH 11, MDNA calibration on the HPLC is good to 50 mg/L, with a detection limit of 0.1 mg/L (Figure 4.2.27).

Figure 4.2.26. Degradation of methylene dinitramine in aqueous solution and pH.
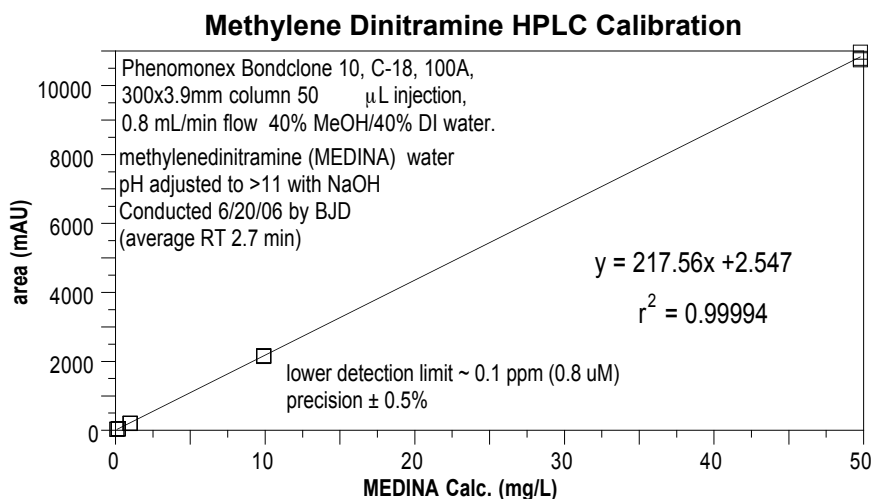
Figure 4.2.27. Methylene dinitramine HPLC calibration curve.

Because it was hypothesized that MDNA is degraded microbially, solutions of water/methanol (would not kill microbes) and water/acetonitrile (would kill microbes) were checked for stability. Neither was stable (Figure 4.2.28), which does not provide any evidence for microbial methylene dinitramine degradation or not.
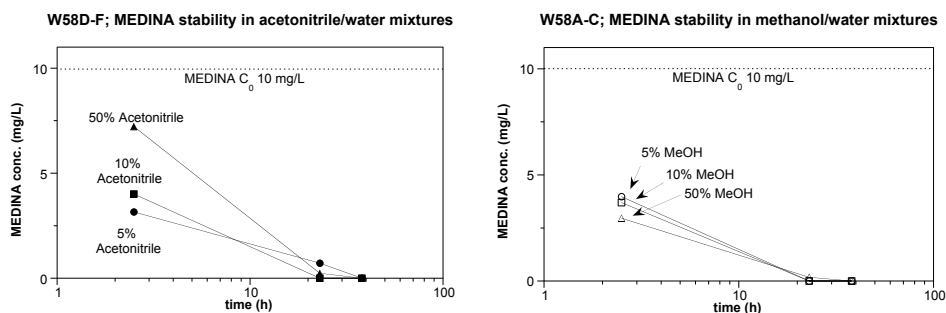
Figure 4.2.28. Degradation of methylene dinitramine in acetonitrile/water (a) and methanol/water (b) mixtures (data ± 2%).

Degradation of MDNA in oxic sediments (Figure 4.2.29) show the most rapid degradation in oxic water (no sediment, half-life about 0.5 h), with slower degradation in contact with oxic or anoxic sediment (with or without continuous UV light treatment). The pH of this untreated sediment is 7.2. Conclusions from this data are: a) methylene dinitramine is (abiotically) degraded in aqueous solution at neutral pH, b) presence or absence of oxygen in water has no influence on degradation, c) the reaction of abiotic as presence of UV light has no influence on the degradation rate (UV light present to kill the microbe), and d) presence of oxic sediment slows degradation; possibly due to adsorption.

Figure 4.2.29. Degradation of methylene dinitramine aqueous solution with or without oxygen or sediment (data ± 2%).

Because all experiments were conducted with filtered deionized water, there are likely few (possibly not zero) microbes in the aqueous solutions. The fact that the MEDINA degradation rate with only this oxic deionized water is fairly rapid appears to indicate that microbes are not degrading MEDINA.

Degradation of MDNA in reduced sediments (Figure 4.2.30) is occurring more slowly than in oxic sediments. The pH of these sediments varied from 8.2 to 9.6, which accounts for some of the alkaline stability (Figure 4.2.26). However, since methylene dinitramine stability is greater in the reduced sediment can be accounted for from just the alkaline conditions. Methylene dinitramine sorption to the sediment should be the same in oxic and reduced sediment, so cannot account for this increased stability.

Figure 4.2.30. Degradation of methylene dinitramine with reduced sediment.

Because methylene dinitramine is stable in reduced sediments, it could possibly build up in concentration, and therefore it's degradation could be the rate-controlling step in the overall RDX mineralization. An experiment was conducted in which RDX degradation is occurring in reduced sediment, and methylene dinitramine is specifically being analyzed for (Figure 4.2.31). RDX degraded with a half-life of 3 hours, with intermediates MNX, TNX, and DNX appearing from minutes to 40 h. Over the 300 h experiment, there was no measurable methylene dinitramine detected. The starting RDX concentration was high (22 mg/L or 0.1 mmol/L), and if all was degraded to methylene dinitramine (0.1 mmol/L or 13.7 mg/L) was well within the HPLC detection limits (Figure 4.2.27) of 0.1 mg/L methylene dinitramine. Therefore, methylene dinitramine is not building up during RDX degradation in reduced sediment, so it is not the rate-limiting step in RDX mineralization.
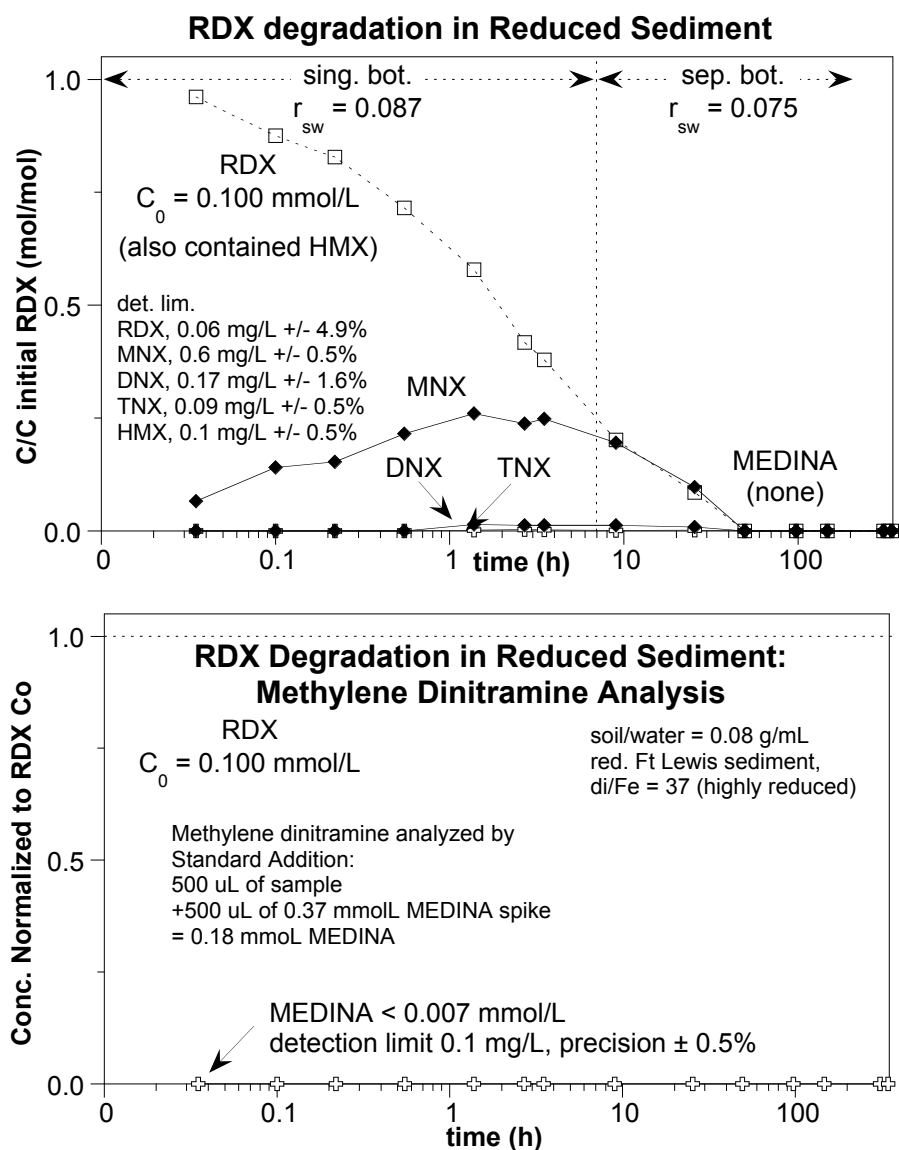
Figure 4.2.31. Degradation of RDX by reduced sediment: a) RDX, MNX, DNX, and TNX shown, and b) methylene dinitramine shown.

4.2.2.7 Formate Mineralization (RDX and HMX intermediate)

The mineralization rate of formate in untreated and dithionite reduced sediments was quantified to determine if it could be the (or one of the) rate limiting step in RDX and HMX mineralization. Acetate degrades in oxic sediment and reduction does not change the rate of degradation, implying sufficient microbes are able to mineralize the acetate (Results Section 4.1.1). Formate degradation in untreated sediment versus untreated sediment plus bactericide indeed indicated that formate mineralization requires microbes (i.e., no mineralization with the bactericide, Figure 4.2.32a). What is surprising is that the rate of formate mineralization increased significantly with the amount of sediment reduction (by two orders of magnitude, Figure 4.2.32b). Formate mineralization was quite rapid, showing 50% mineralization in 60 h for the highly reduced sediment. The formate mineralization rate was extremely slow in unreduced sediment (7400 h half-life), which was as rapid as a half-life of 60 h in highly reduced sediment. Therefore, the RDX mineralization rate of 100s of hours is most rate-limited by this formate to carbon dioxide transformation rate (i.e., this is the slowest rate of transformation rates observed, Figure 2.2.17). Transformation rates of RDX, MNX, DNX, and TNT were all much more rapid than format transformation. Because formate degradation is dependent on both the presence of microbes and highly dependent on some form of ferrous iron in the sediment, it is most likely a coupled abiotic/biotic reaction rather than a purely abiotic or purely biotic reaction.
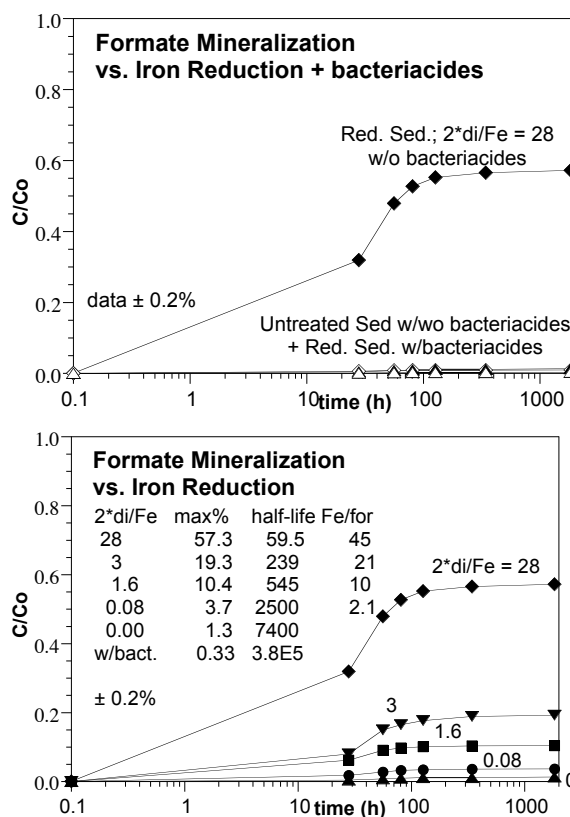
Figure 4.2.32. Formate mineralization: a) with and without bactericides, and b) in sediments with differing dithionite treatment (data $\pm$ 2%, counting error $\pm$ 0.2%).

4.2.3 HMX Degradation/Mineralization in Abiotic/Biotic Treated Sediment

4.2.3.1 HMX Degradation/Mineralization Rates in Dithionite-Reduced Sediment

Experiments were conducted to measure the rate of HMX degradation and mineralization and determine which steps were biotic or abiotic. The initial step of HMX degradation in dithionite-reduced sediment appears to be abiotic, based on parallel experiments in reduced sediment with and without gluteraldehyde (Figure 4.2.33a). In addition, the HMX degradation rate increased with increasing soil/water ratio (i.e., higher iron/HMX ratio, Figure 4.2.33b), so the HMX initial transformation rate appears to be an abiotic reaction.

Additional HMX degradation intermediates were identified, which includes methylene dinitramine (also an RDX degradation intermediate), as described in Results Section 4.3, and the degradation of methylene dinitramine in sediments is quantified in Results Section 4.2.2.7.

The mineralization rate of HMX was studied in untreated and dithionite-reduced sediments to determine the environment in which there is the most rapid mineralization rate and to determine which steps are abiotic or biotic. HMX mineralization does need microbes, as shown in parallel experiments with and without bactericides (three) for untreated sediment (Figure 4.2.34a) and dithionite-reduced sediment (Figure 4.2.34b). In untreated sediment, the HMX mineralization rate was very slow (half-life 7800 h) with 3.1% mineralization by 432 h, but there was essentially no mineralization in the presence of bactericides. These results indicate that HMX is slowly biodegraded in anoxic, untreated sediments. HMX was rapidly mineralized in dithionite-reduced sediments (162 h half-life), with 66.4% mineralization by 432 h. However, there is no mineralization in reduced sediment with the addition of bactericides (Figure 4.2.34b), indicating that biotic or coupled reactions occur.
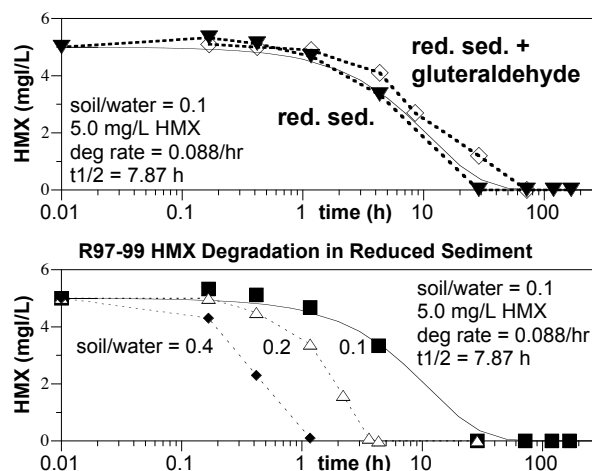
Figure 4.2.33. HMX degradation rate: a) with and without bactericide, and b) at different sediment/water ratios (data precision ± 0.5%)
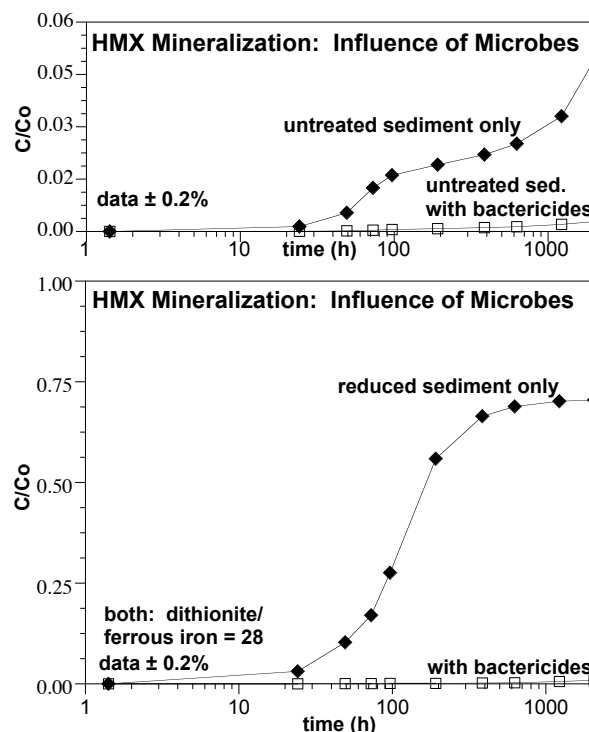
Figure 4.2.34. HMX mineralization rate with and without bactericides in: a) untreated sediment, and b) dithionite reduced sediment (data ± 2%, counting error ±0.2%).

HMX mineralization in reduced sediments was a direct function of the amount of sediment reduction (Figure 4.2.35a), similar to previous studies of RDX. Compared with RDX, HMX the mineralization rate was slightly (~2x) more rapid. In a separate study with the same sediment but batch reduced instead of column reduced sediment, a similar increase in HMX mineralization with sediment reduction was observed (Figures 4.2.35a and 4.2.36).
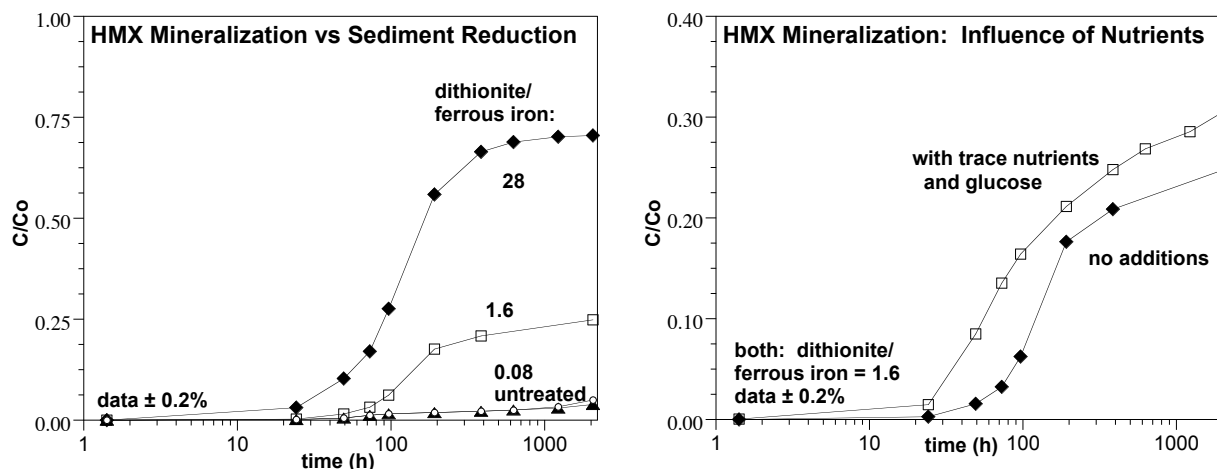
Figure 4.2.35. HMX mineralization rate in reduced sediments: a) as a function of the amount of reduction and b) with nutrients.
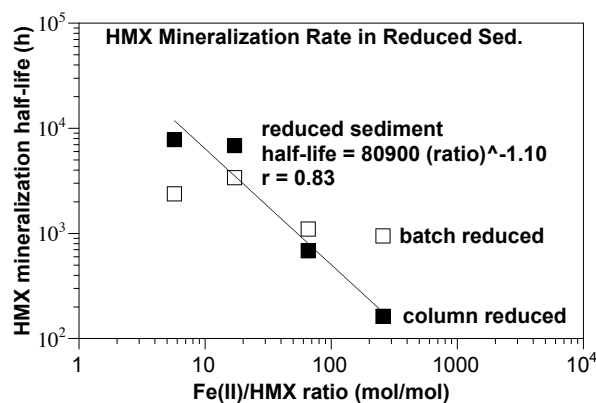
Figure 4.2.36. HMX mineralization rates observed in experiments as a function of the ferrous iron to HMX molar ratio (rates ± 25%).

The importance of biostimulation was shown by parallel experiments in partially reduced sediments with and without the addition of glucose and trace nutrients (Figure 4.2.35b). The HMX mineralization rate without nutrient addition (670 h half-life) was slightly faster with the addition of glucose and trace nutrients (560 h half-life).

67

4.2.3.2 HMX Degradation Pathway in Dithionite-Reduced Sediment

The first few HMX degradation intermediates were identified by Dr. Steve Comfort at University of Nebraska, Lincoln by LC/MS-MS, as described in Results Section 4.3, and followed a similar pathway to RDX in nitro-groups were transformed to nitroso-groups (Figure 4.2.37). Eventually the HMX cage was broken and methylene dinitramine was formed, as identified by LC/MS-MS.

The initial HMX degradation reaction in reduced sediment is believed to be an abiotic reaction, as parallel experiments with and without a bactericide showed similar degradation rate (Figure 4.2.34). Additional HMX degradation experiments were conducted in 1-D columns (Results Section 4.4), in which a more rapid HMX degradation rate was observed with greater sediment reduction (i.e., half-life decreased from 50 h in partially reduced sediment to 2.1 h in highly reduced sediment). It was also determined that the HMX degradation reaction was endothermic.

The degradation of mono-, di-, tri, and tetra-nitrosoHMX were not investigated further to determine of these degradation reactions were abiotic or biotic. As reported in Results Section 4.2.2.7, methylene dinitramine is degraded abiotically by acidic hydrolysis.

The overall HMX mineralization rate increased significantly (48x) with sediment reduction (7800 h half-life for untreated sediment, 162 h half-life for reduced sediment). The magnitude of the mineralization rate and change with sediment reduction was very similar to formate mineralization (reported in Results Section 4.2.2.7) in which unreduced sediment (7400 h half-life), which was as rapid as a half-life of 60 h in highly reduced sediment. Therefore, it is likely that the step controlling HMX mineralization in this reduced sediment is the formate mineralization step, which was determined to be a coupled abiotic/ biotic reaction. However, there could be other intermediates that exhibit slow reactions that were not identified in this study. Due to the similarity in structure, it is hypothesized (although not proven) that degradation of mono-, di-, tri, and tetra-nitrosoHMX are abiotic reactions, similar to the abiotic attach on RDX and the initial intermediates TNX, DNX, and MNX. The mechanism for breaking the heterocyclic HMX cage is unknown. Although structurally similar to RDX, HMX is somewhat more chemically stable (Hawari 1999), so is reported to be less amenable to biodegradation compared with RDX.
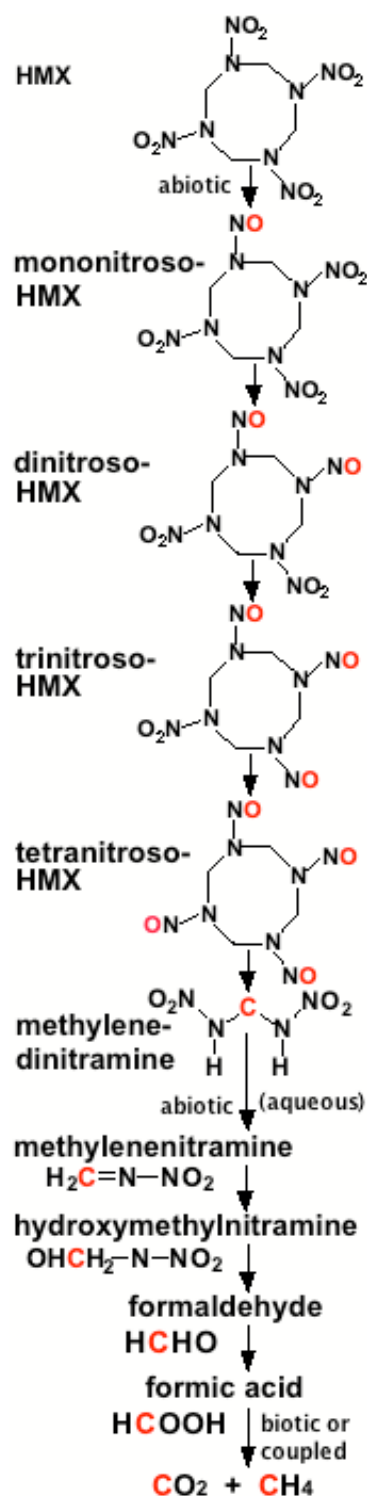
Figure 4.2.37. HMX degradation pathway in reduced sediments.

4.2.3.3 HMX Mineralization in Biostimulated/Reduced Sediments

TNT degradation was investigated in a system in which TNT and glucose have the same enzymatic degradation pathway (Section 4.2.4.2). This pathway degrades TNT to amino-intermediates that irreversibly sorb to sediment, so while TNT is not being mineralized, risk of the uncontrolled TNT release to the subsurface environment is being reduced as the mass is being immobilized. The same sediment treatment was investigated for RDX and HMX. The treatment involves biostimulation with a significant quantity of glucose (4000 mg/L). Because TNT cometabolic degradation to triaminotoluene (TAT) was most rapid in reduced sediments, we investigated HMX mineralization in slightly reduced sediments (dithionite/ferrous iron = 0.5) with and without 4000 mg/L glucose addition.

HMX mineralization in the sediment with low reduction was small (6.5%; Figure 4.2.38a) and consistent with previous results (Figure 4.2.35a). The large amount of glucose addition greatly increased the HMX mineralization extent to 45% by 1600 h. Subsequent oxidation of both systems did not produce additional CO_2 (Figure 4.2.38b). In the system with just sediment reduction (no glucose). 79.3% of the ^{14}C HMX mass was still aqueous at 2800 with 6.5% mineralization (85.8% total). It is believed that methane is

Figure 4.2.38. HMX mineralization rate in biostimulated sediments: a) anaerobic for the first 1600 h, b) oxic for the subsequent 1200 h.

also produced, but gas phase carbon traps did not successfully capture the ^{14}C-methane (Figure 4.2.44). This method is described in Section 4.2.4.1. Mass balance in the system with glucose addition was higher, with 13.5% aqueous at 2800 h and 47.2% mineralized (total 60.7%). Additional carbon mass is also associated with microbes, both sorbed and incorporated (see Results Section 4.1.3).

4.2.4 TNT Degradation/Mineralization in Abiotic/Biotic Treated Sediments

4.2.4.1 TNT Degradation and Mineralization in Dithionite-Reduced Sediment

Experiments were conducted to measure the rate of TNT degradation and mineralization and determine which steps were biotic or abiotic. Only a few TNT experiments have been done to date. Initial TNT degradation (25 mg/L) shows that the rate increases with increasing amount of ferrous iron (i.e., higher soil/water ratio, Figure 4.2.39), which indicates that there may be an abiotic component at least for the initial TNT degradation. As described in Results Section 4.3, different TNT degradation intermediates form with untreated sediment and dithionite-treated sediment (identified by LC-MS/MS). Additional TNT degradation experiments were conducted in 1-D columns with differing percentages of sediment reduction (Results Section 4.4), which also showed that TNT was degraded slightly more rapidly in more reduced sediment, but the correlation was weak.
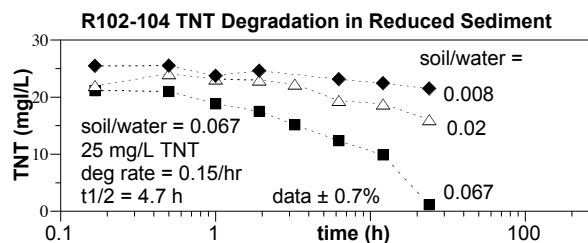
Figure 4.2.39. TNT degradation in reduced sediment at differing soil/water ratio ($\pm$ 0.7%).

Although the TNT degradation rate is relatively rapid, mineralization of TNT was very small in untreated or dithionite-reduced sediments, with a maximum mineralization of 1.3% observed for untreated sediment (1400 h) and 2.7% for dithionite-reduced sediment (1400 h, Figure 4.2.40). The TNT mineralization rates were about the same in untreated and in dithionite treated sediments (3 different treatments), with mineralization half-lives of 28,000 to 55,000 h. It was hypothesized that the most rapid TNT mineralization rate may occur by initial degradation in a reducing environment followed by oxic biodegradation of intermediates. The TNT data to date supports some of the hypothesis, namely that initial degradation of TNT is more rapid in a reducing environment. TNT mineralization in a reducing environment appears to be very slow, as is mineralization in an anoxic sediment/water environment (Figure 4.2.40, untreated sediment).
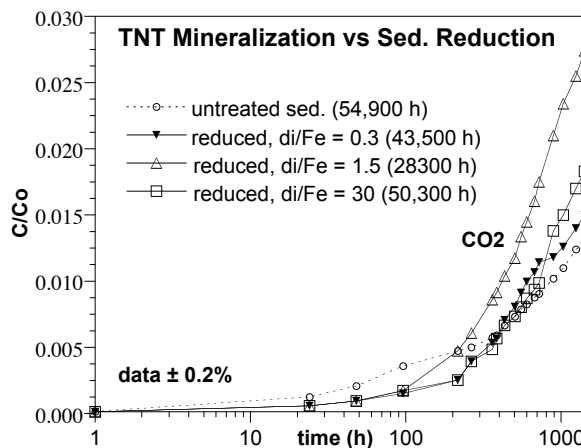
Figure 4.2.40. TNT mineralization in untreated and dithionite-reduced sediments (data $\pm$ 2%, counting error $\pm$0.2%).

Additional TNT mineralization studies were conducted in anoxic sediment, reduced sediment (differing amounts of reduction), and with the addition of carbon and trace nutrients. The mineralization extent for anoxic sediment (216,000 h half-life, Figure 4.2.41a) was extremely slow, and generally did not change with amount of sediment reduction. The addition of a carbon source (glucose) and trace nutrients (Table 4.2.2) increased the TNT mineralization about 10 fold, but the extent was still <1%. Subsequent oxidation of these bioreactors was conducted for an additional 1000 h to determine if TNT was degraded to intermediates in the reducing environment, then the intermediates could be degraded to CO_2 in an oxic system. There was essential no additional reactivity in all systems (Figure 4.2.41b), but there was a slight amount of additional mineralization in the biostimulated system (carbon and trace nutrient addition). This was still insignificant, as the total amount of TNT mineralization was <1%. While TNT mineralization was insignificant, TNT degradation to irreversibly sorbed amino-intermediates was significant. The highly reduced sediment with carbon addition (Figure 4.2.38b) had 44% aqueous ^{14}C compared with 73% to 83% in anoxic systems. This cometabolic process is described in detail in the following section.
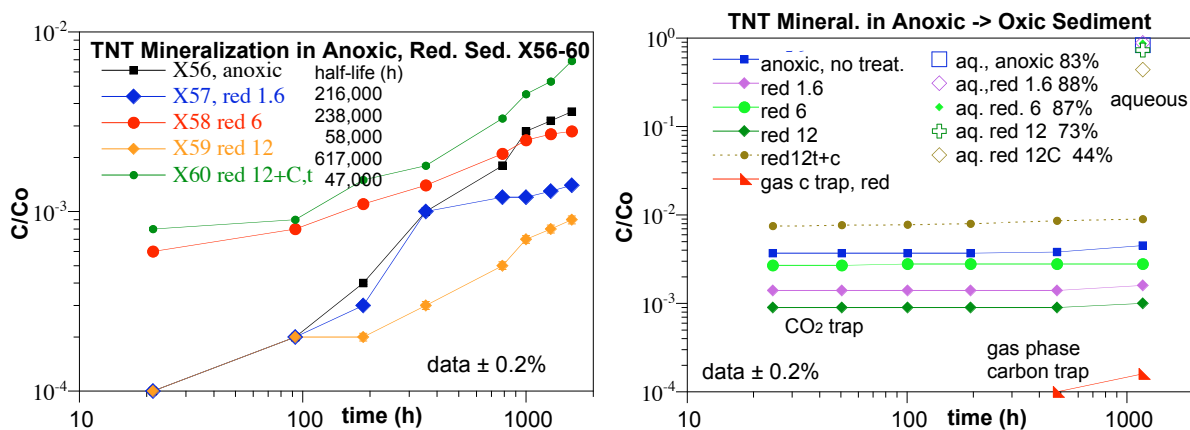
Figure 4.2.41. TNT mineralization in sequential reduced then oxic sediments (precision ± 0.2%), with: a) first 1600 h anoxic, and b) next 1000 h oxic.

4.2.4.2 TNT/Glucose Cometabolic Degradation

A series of experiments with TNT degradation products were initiated to investigate TNT remediation. Previous results with RDX and HMX have clearly demonstrated that highly reduced sediment will result in mineralization, where the amount of reduction is directly related to the rate of RDX or HMX mineralization (i.e., abiotic influence, and other data shows biotic influence as well). TNT behaves differently, and while sediment reduction results in a weak dependence on TNT degradation, TNT mineralization is extremely slow in oxic and reduced sediment. TNT has been previously shown (Daun et al. 1998; Lenke et al. 1998) to form amino-degradation products in bioreduced soil/sludge systems, which adsorb more strongly with the number of amino groups. This pathway has not been previously demonstrated to work in subsurface sediments, which only contain microbes, as opposed to the anaerobic stage, which ecotoxicological tests showed contained bacteria, daphnids, algae, cress plants, and earth worms;

Lenke et al. 1998). Glucose degrades to CO_2, where nitro- intermediates are reduced to nitroso, then ammonia intermediates (i.e., same functional group changes needed on TNT). The degradation pathway is TNT -> 2-aminodinitrotoluene, 4-aminodinitrotoluene -> 2,4-diaminonitrotoluene, 2,6-diaminonitrotoluene -> triaminotoluene (TAT, Figure 4.2.42). It has been previously hypothesized that the triaminotoluene polymerizes and forms irreversible bonds with clays in sediment. Therefore, while reducing conditions may not be able to mineralize TNT, if TAT is formed and it irreversibly binds (Achtnich et al. 1999), this would be a successful groundwater remediation technology. Sorption of TAT with humic matter in soils can also be irreversible (Daun et al. 1998), but this has little application to aquifer sediments, where the fraction organic carbon is very low (<0.05%). The previous studies were in sediments with organisms in addition to microbes. The system was a cometabolic process with glucose as the primary substrate. Subsequent aerobic treatment of the sediment can lead to further degradation of these amino-intermediates (Achtnich et al. 1999; Elovitz and Weber 1999; Weiss et al. 2004).

To test whether this cometabolic process would work for TNT, TNT, amino-, diamino-, and triaminotoluene intermediates were analyzed in long-term experiments (described in this section). In addition, sorption mass, rate, and reversibility experiments were conducted with 2-aminodinitrotoluene, 4-aminodinitrotoluene,

Figure 4.2.42. TNT cometabolic reduction pathway in the presence of glucose fermentation.

2,4-diaminonitrotoluene, and 2,6-diaminonitrotoluene, and triaminotoluene (described in the following section). TNT sorption is described in this section. Both 2-ADNT and 4-ADNT pathways occur, as confirmed by LC-MS (Figure 4.3.7).

A total of four long-term (2300 h, 96 days) experiments were conducted with glucose addition to Ft. Lewis sediment under: a) oxic conditions (untreated sediment), b) anoxic conditions (untreated sediment), c) iron reducing conditions, partially reduction (dithionite/iron = 11, and d) iron reducing conditions, high reduction (dithionite/iron = 27). TNT was degraded in biostimulated oxic sediment and anoxic sediment at slow rates, and low concentrations of aminotoluenes, diaminotoluenes, and triaminotoluene formed (Figure 4.2.43 and 4.2.44). Interestingly, TNT was degraded more rapidly in the oxic sediment (TNT loss half-life 240 h) than the anoxic sediment (TNT loss half-life 1700 h), even though the process should be

occurring under reducing conditions. Sorption of TNT and amino-intermediates was well characterized (following sections), and bar graphs (Figures 4.2.43 and 4.2.44) show the calculated sorption mass for each compound. At 2300 h, sorption was measured by solvent extraction of the sediment. It should be noted, however, that DANT and TAT sorption is not reversible (see following sections), so their mass is poorly (if any) extracted from the sediment. At the soil/water ratios in these experiments, the fraction of mass sorbed is relatively small, ranging from 26% for TNT and TAT to 11% for ADNT and DANT isomers. At the field scale, with ~20x higher soil/water ratio than these experiments (i.e., field sediment 5-6 g/mL versus 0.26 g/mL in these experiments), sorption is significantly greater. For example, TNT fraction sorbed would be 82% versus 26% in these batch studies. Biodegradation processes are generally slower in packed porous media compared with batch systems due to more limited mixing, and in addition, possibly due to sorption of the compounds may make microbial access somewhat more limited.

Figure 4.2.43. TNT/glucose cometabolic reduction in the presence of glucose fermentation in oxic Ft. Lewis sediment (initially). Sorbed concentrations in (b) calculated, based on separate experiments.

In both the oxic and anoxic sediment experiments, the mass balance of TNT and measured intermediates decreases from 100% to 60% (anoxic) or 25% (oxic) by 2300 h. This is a reflection of what TNT intermediates can be measured in the system. Previous studies indicate TAT is the final product in reduced systems (Daun et al. 1998), although our studies (described in the following section) show that TAT degrades rapidly in many sediment/water systems. It is hypothesized that the glucose/TNT cometabolic degradation is taking place in a reduced system. It is hypothesized that the (initially) oxic system may have had more rapid TNT degradation due to more rapid microbial growth with oxygen available as an electron acceptor. This could be confirmed by biomass measurements in future experiments. The (initially) oxic system (i.e., batch system with air headspace that was periodically shaken) is likely to be generally anoxic with high biomass concentrations, so was likely only initially oxic. Oxygen diffusion from the water/air interface would provide some oxygen during the long-term experiment (and the periodic mixing). Because oxygen saturation in water is so low (8.4 mg/L or 0.25 mmol/L at 25C), high biomass would readily consume any oxygen diffusing from the water/air interface. Continuous air sparging would be needed to insure the system stayed oxic at these (likely) high biomass concentrations. Photographs of the experimental systems at 1500 h (Figure 4.2.45)

Figure 4.2.44. TNT/glucose cometabolic reduction in the presence of glucose fermentation in anaerobic Ft. Lewis sediment. Sorbed concentrations in (b) calculated, based on separate experiments.

show a similar biomass color and turbidity associated with high biomass for the aerobic and anaerobic systems (X42 and X43), whereas reduced sediment experiments have a grey/green color of the reduced sediment and much lower turbidity (presumably lower biomass, X44 and X45).
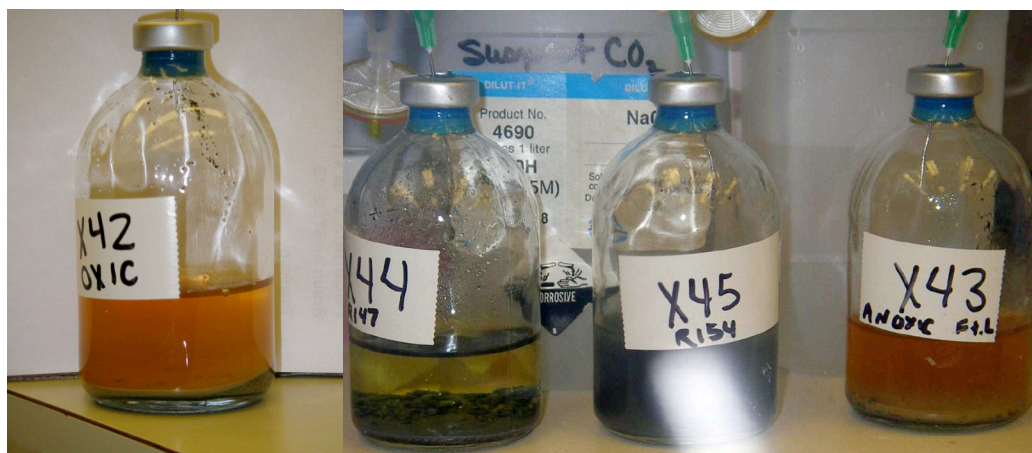
Figure 4.2.45. TNT/glucose cometabolic degradation experiments at 1500 h: a) oxic experiment X42, and b) anoxic (X43), and reduced sediment experiments (X44, X45).

Because this biostimulation system is purely biotic, it was not expected that reduced sediment would contribute to the rate of the reactions. However, both reduced sediments degraded TNT more rapidly and produced more significant quantities of the aminotoluene degradation products (Figure 4.2.46). In the oxic system, at 1000 h, about 0.38 mmol TNT was degraded and 0.14 mmol aminidinitrotoluene compounds were measured (about 1/3 the mass), with lesser amounts of diaminotoluene compounds and triaminotoluene. No TAT was recovered in the aerobic or anaerobic experiment, although at the pH at 2000 h was 5.52 (aerobic) and 7.23 (anaerobic), so TAT would likely be degraded. A sample of the biomass was also taken at
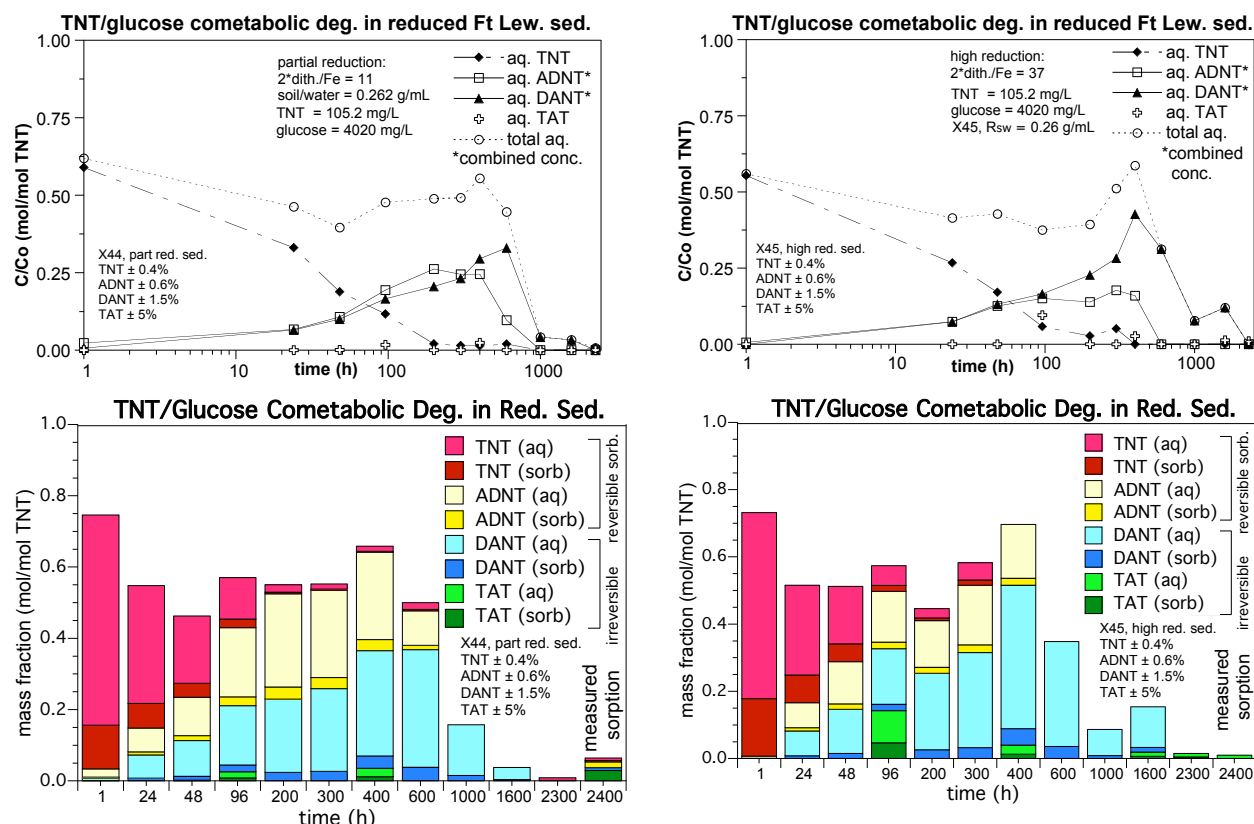
Figure 4.2.46. TNT/glucose cometabolic reduction in the presence of glucose fermentation in partially (a and c) and fully (b and d) reduced Ft. Lewis sediment. Sorbed concentrations in (b) calculated, based on separate experiments.

1000 h to determine how much TNT and degradation product mass was sorbed to the biomass (extracted with methanol). There were only small amounts of TNT, ADNT, and DANT sorbed on the microbes.

TNT at 105 mg/L (0.46 mmol/L) with 21 mmol/L glucose was degraded fairly rapidly in partially and fully reduced sediment. In fully reduced sediment (dithionite/iron = 37), the TNT degradation half-life was 18 h, and in partially reduced sediment (dithionite/iron = 11) was 26 h (Figure 4.2.46). This was 10 to 20 times more rapid than biodegradation alone (oxic sediment 240 h, anoxic sediment 1700 h). Combined aminodinitrotoluene compounds peaked in concentration at 200-500 h in both reduced sediments, accounting for 70% of the degraded TNT. The ADNT concentration in the fully reduced sediment was less than the partially reduced sediment. The diaminotoluene compound concentrations peaked at 700–1400 h, and accounted for 40-80% of the TNT mass. It should be noted that sorption of the ADNT and DANT compounds to the sediment surface would account for an additional 20% of the mass. At the end of these experiments, the solid phase was be extracted to try to recover any compounds (2400 h). As described earlier (shown in the following sections), most of these amino-intermediates are resistant to extraction by methanol. By 2000 h, the molar concentration of the DANT compounds was decreasing. Small quantities of TAT were measured during the course these experiments. At 2000 h, the pH of the partially reduced sediment was 6.23, and in the fully reduced sediment was 5.21. Under these conditions, TAT would not be stable due to acid

hydrolysis (described in the following section). Total mass recovery in both reduced systems (bar graphs, Figure 4.2.46c and d) show that by 500 h, 70% of the mass was TNT intermediates with no remaining TNT, and by 2400 h, <10% of the mass remained as measurable intermediates. Separate TAT experiments (following sections) showed that TAT degrades rapidly under acidic and neutral conditions (minutes, days), so given that these reduced systems were driven acidic presumably by microbial growth, it is likely that TAT was degraded.

If the TNT cometabolic pathway is dominated (entirely) by glucose biotic fermentation, then the absence of oxygen should increase the degradation rate. The experimental results that show the TNT/glucose system with slower degradation rates relative to the oxic system does not support the hypothesis that the absence of oxygen accelerates the fermentation process. Creation of iron reducing conditions (i.e., sediment reduction) may indirectly accelerate the TNT/glucose biodegradation rate by the low Eh conditions created, or directly because TNT and/or intermediates may be abiotically degraded more rapidly. Results in the previous section showed that sediment reduction does accelerate TNT degradation (presumed but not proven to be abiotic), so the clear possibility exists that the first step (TNT degradation) may be both abiotic and biotic.

TNT mineralization in parallel cometabolic TNT/glucose experiments (under the same oxic, anoxic, or reducing conditions) was also quantified in aerobic, anaerobic, and reducing systems. Reduced sediment systems quantified included partially reduced sediment (treated with dithionite with dithionite/iron ratios of 1.5, and 26), and the addition of trace nutrients (Table 4.2.2). For these systems, since it was shown that TAT is formed, and it irreversibly binds (next section), it is hypothesized that there will be little TNT mineralization. Experimental results in oxic, anaerobic, and reducing systems showed that there was less than 1% mineralization of TNT by 1600 h (Figure 4.2.47). There was essentially no statistical difference between experiments, although there was a slightly greater mineralization rate for the oxic system.
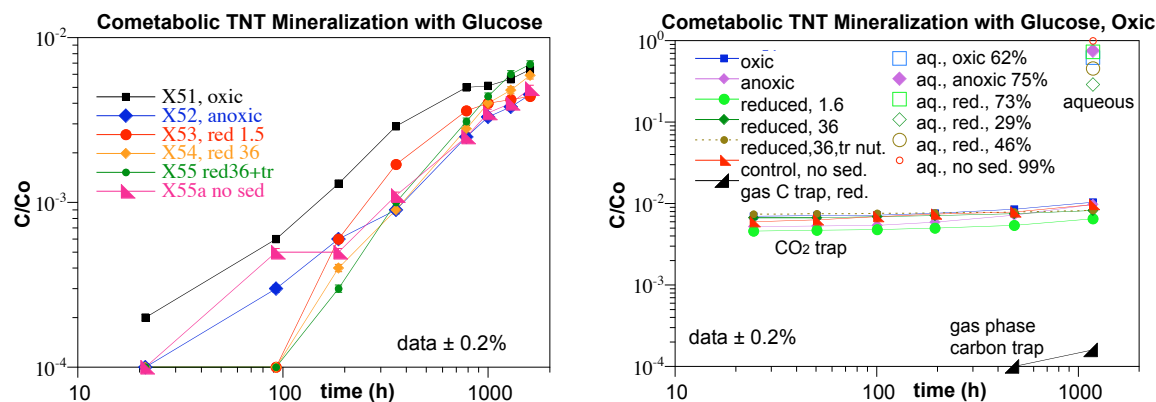
Figure 4.2.47. TNT/glucose mineralization in sequentially reduced, then oxic sediments: a) oxic, anaerobic, and reduced sediments, and b) subsequent oxidation after 1600 h (data ±2%, counting error ±0.2%)

The subsequent oxidation of all of these experimental systems should lead to greater mineralization for the reduced systems, assuming processes that occurred in sequential anaerobic/aerobic sludge (Achtnich et al. 1999; Elovitz and Weber 1999) would also occur in the subsurface sediment. Oxidation of these anaerobic and reduced experimental systems (Figure 4.2.47b) did not, in fact, show any additional mineralization in 1200 h of oxidation after the initial 1600 h of anaerobic or reducing conditions. In fact, the mineralization rate actually appeared to be slower. The total aqueous ^{14}C (TNT and other aqueous intermediates) after 1200 h of oxidation was 62% for the oxic system 75% for the anaerobic system, and 29% for the highly reduced system, clearly demonstrating the DANT and TAT irreversibly sorbed intermediates are being formed.

Measurement of TNT mineralization (and RDX and HMX mineralization) in batch and column experimental systems was accomplished by carbon dioxide traps in the headspace of the experimental vial or sealed effluent vials. At high pH, carbon dioxide partitions into the alkaline trap (1M NaOH). Because mineralization would also produce methane, an attempt was made to measure methane in the experiment headspace by placing a carbon trap (i.e., containing activated carbon with a surface area of 400 m^2/g). An extraction procedure (described below) was developed to extract organic compounds out of the activated carbon. Carbon measured in the headspace of TNT cometabolic degradation experiments was essentially zero (Figure 4.2.47b).

Simple measurement of the activated carbon in a scintillation vial was not effective due to light occlusion. Radioactive compounds are measured by scintillation counting, which requires nearly clear liquids to not occlude the light that occurs from fluorescence in the scintillation fluid from radioactive decay. Small amounts of light occlusion can be accounted for in counting efficiency, if constant. The addition of differing amounts of activated carbon, unfortunately, lead to increasing amounts of light occlusion, so the counting efficiency dropped from 95% (with no light occlusion) to 3% with 0.1 g of activated carbon (Figure 4.2.48). The occlusion would be less if the activated carbon would settle out of solution, but it did not settle in the viscous scintillation fluid. Activated carbon contains numerous polar functional groups (carboxylic), so solvent extraction of a sorbed organic compound would require both nonpolar and polar organic solvents. Testing six different organic solvents with differing polarity (Figure 4.2.49) showed that RDX was most efficiently removed with the more polar organic solvents (acetonitrile). For removal

Figure 4.2.48. RDX counting efficiency with the addition of differing mass of activated carbon.

of polar and nonpolar organic compounds, a procedure was developed where dichloromethane (nonpolar), methanol, then acetonitrile was sequentially used to remove organic compounds for scintillation counting.

77

4.2.4.3 TNT Aqueous Stability and Sediment Sorption

The TNT sorption rate is rapid (0.17 h to 0.28 h half-life, Figure 4.2.50a), with an average $K_d = 0.90 \pm 0.28$ cm^3/g for 5 experiments conducted at different soil/water ratios. TNT sorption was reversible, as an acetonitrile extraction removed 90-100% of the sorbed TNT (Table 4.2.4). TNT long-term interactions with even oxic sediment showed some degradation after about 24 h.

TNT is stable in most natural aquifer waters, but is degraded by alkaline hydrolysis at a pH > 10 (Figure 4.2.51). TNT was stable to 500 h at pH 10, but had a hydrolysis degradation half-life of 20 h at pH 11, and 5 h at pH 12.

The TNT degradation rate in reduced sediment varied with sediment reduction from 1 h to 800 h half-life, depending on the amount of sediment reduction. In oxic sediment, the degradation rate was slow – at pH 10, the degradation half-life was 50 h, and was related to the sediment and not the pH (Figure 4.2.50b).

TNT degradation rate was also a function of pH, and was degraded more rapidly by alkaline hydrolysis at pH 11 and 12 (half-life 18 h, 8 h respectively, Figure 4.2.51). TNT was degraded by sediment at pH 10, but pH 11 and 12, was degraded more rapidly by alkaline hydrolysis, as rates with and without the sediment were the same (Appendix G).

TNT degraded more rapidly in reduced sediment as a direct function of the amount of ferrous iron present (Figure 4.2.39, previous section). Additional TNT degradation experiments in reduced sediment were conducted in columns (Results Section 4.4).
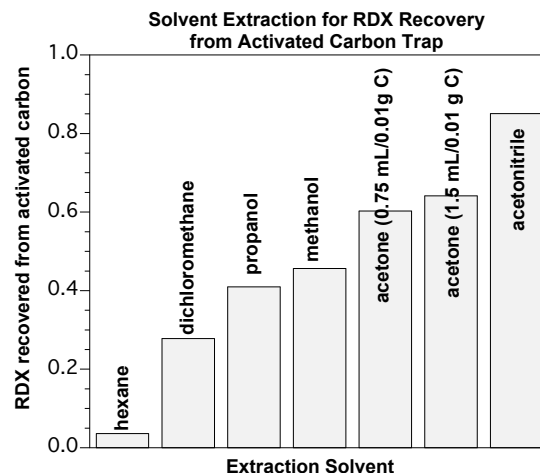
Figure 4.2.49. Organic solvent extraction efficiency for removing ^{14}C RDX from activated carbon (data ±0.3%).
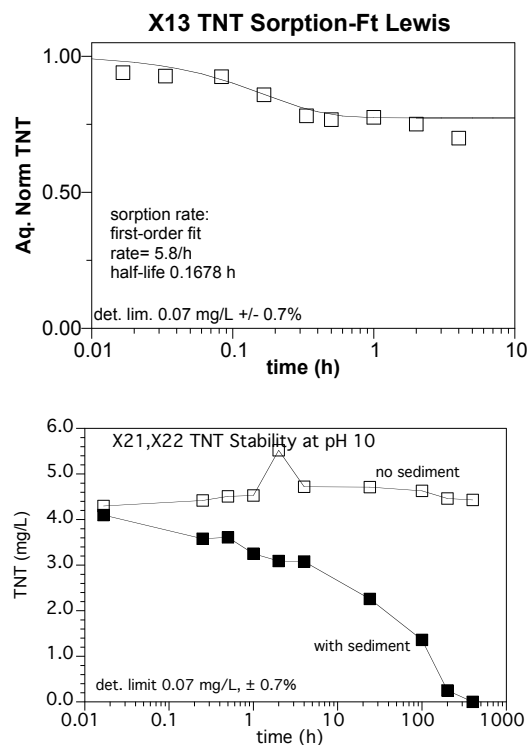
Figure 4.2.50. TNT sorption rate to oxic Ft. Lewis sediment (a) within hours, and slow degradation at pH 10 by sediment and not by alkaline hydrolysis (b).

78

Table 4.2.4. Sorption mass, rate, and reversibility for TNT and amino-intermediates.

compound	Kd	reversible*	rate (1/h)
TNT	0.900 ± 0.28	yes	0.24
2-ADNT	0.476 ± 0.22	partial	0.22
4-ADNT	0.393 ± 0.24	yes	0.16
2,4-DANT	0.301 ± 0.26	no	0.62
2.6-DANT	0.480 ± 0.16	no	0.31
TAT	1.25 ± 0.24	no	0.53

Figure 4.2.51. TNT alkaline hydrolysis at different pH.

4.2.4.4 2-Amino- and 4-Aminodinitrotoluene Sorption and Degradation

Sorption rate, sorption mass, and sorption reversibility experiments were conducted with 2-aminodinitrotoluene and 4-aminodinitrotoluene. The sorption rate of 2-aminodinitrotoluene (0.22/h) and 4-aminodinitrotoluene (0.16/h) was rapid (0.1 to 0.2 h half-life). The sorption mass of 2-ADNT (0.476 ± 0.22 cm^3/g) and 4-ADNT (0.393 ± 0.24 cm^3/g) was similar (Figure 4.2.52). Solvent extractions, however, showed that 100% of the 4-ADNT sorbed could be removed from the surface, but only 22-32% of the 2-ADNT could be removed from the surface, so 2-ADNT sorption was considered only partially reversible (Table 4.2.4). Sorption reversibility differed between 2-ADNT and 4-ADNT. 2-ADNT was resistant to desorption, as shown by a standard methanol extraction (w/sonication 24 h) recovering 22% to 32% of the sorbed mass, whereas 100% of the sorbed 4-ADNT was recovered by methanol extraction.

Figure 4.2.52. Sorption rate and mass for: a) 2-amino dinitrotoluene and b) 4-aminodinitrotoluene.

Both 2-ADNT and 4-ADNT degraded in reduced sediment that was a function of the amount of sediment reduction (Figure 4.2.53). With highly reduced sediment, the degradation half-life for 2-ADNT was 1.3 h and for 4-ADNT was 2.0 h. In partially reduced sediment, the degradation half-life for 2-ADNT was 110 h, and for 4-ADNT was 100 h. There was a very small degradation rate in unreduced sediment (>5000 h) for both compounds, as noted in experiments to 2000 h. This evidence supports the hypothesis that abiotic degradation of TNT and these initial intermediates (2-ADNT, 4-ADNT) in reduced sediment could be partially promoted by sediment reduction (i.e., Figure 4.2.42).

Figure 4.2.53. Degradation of:
a) 2-amino dinitrotoluene and
b) 4-aminodinitrotoluene.
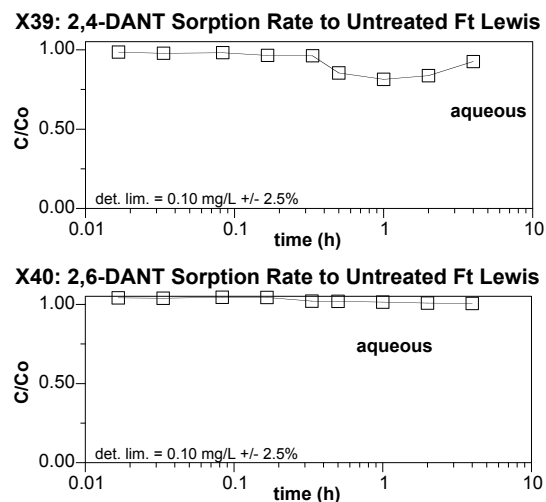
Figure 4.2.54. Sorption rate and mass for:
a) 2,4-diaminonitrotoluene and
b) 2,6-diaminonitrotoluene.

4.2.4.5 2,4-Diamino- and 2,6-Diaminodinitrotoluene Sorption and Degradation

2,4-DANT sorption mass averaged 0.301 ± 0.257 cm^3/g with a sorption rate of 0.62 h (half-life), whereas 2,6-DANT sorption mass averaged 0.480 ± 0.155 cm^3/g with a sorption rate of 0.31 h (half-life, Figure 4.2.54). Both 2,4-DANT and 2,6-DANT had ~0% recovery with a methanol extraction of sorbed mass, so sorption was not reversible (Table 4.2.4). A considerable amount of research has previously been conducted to understanding the binding of DANT compounds (Weiss et al. 2004). To many sediments tested, covalent bonds were formed with nearly all the DANT. These results are consistent with the hypothesis that the aminotoluenes irreversibly bind to one or more surfaces phases on the sediment as the number of amino groups increase.

Both 2,4-DNT and 2,6-DNT degraded in reduced sediment more rapidly as a function of the amount of sediment reduction (available ferrous iron, Figure 4.2.55). In fully reduced sediment, 2,4-DNT degradation half-life was 3.0 h and 2,6-DNT degradation half-life was 1.5 h. In partially reduced sediment, the 2,4-DNT degradation half-life was 100 h, and 2,6-DNT degradation half-life was 65 h. There was no degradation of 2,4-DNT or 2,6-DNT in unreduced sediments (data to 1500 h). While parallel experiments with bactericides were not conducted, it is believed that these rapid degradation rates are abiotic, considering the microbial population density in this subsurface sediment is low (10^6 CFU/g) in untreated and dithionite reduced sediments.
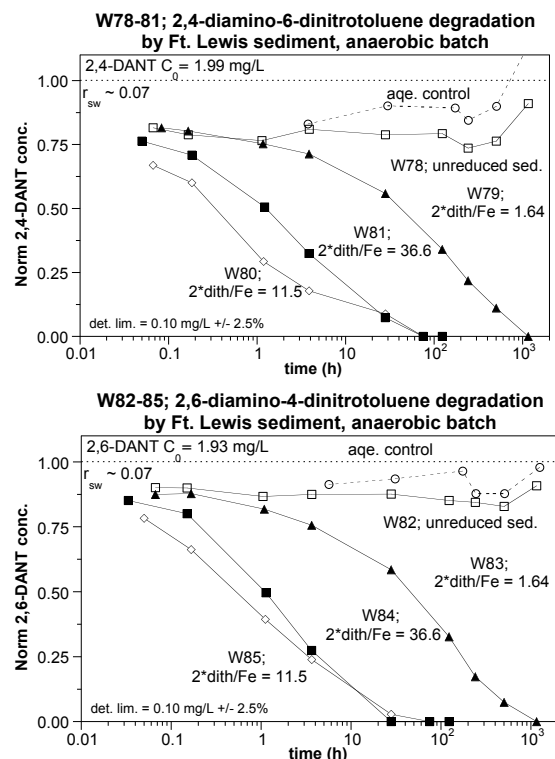
Figure 4.2.55. Degradation of:
a) 2,4-diaminonitrotoluene and
b) 2.6-diaminonitrotoluene.

4.2.4.6 Triaminotoluene Aqueous Stability

Figure 4.2.56. Aqueous stability of triaminotoluene (TAT) with: a) pH, b) dissolved oxygen, and c) UV light.

The aqueous stability of triaminotoluene (TAT) was investigated as a function of pH, dissolved oxygen, and UV light. Triaminotoluene is considered unstable in the presence of dissolved oxygen, so is purchased as a powder. Unfortunately, to be able to dissolve TAT in water, the rapid acidic hydrolysis (Figure 4.2.56). With no pH buffer, dissolving 100 mg/L TAT in deionized water gives a pH of 3.3, which has a degradation half-life of 6.4 h. At pH 2.5, the TAT degradation rate is more rapid (half-life 3.8 h), and at neutral pH, the TAT degradation rate is more slow (half-life 88 h), although still is not entirely stable. Under alkaline conditions, TAT is somewhat more stable, with a degradation half-life of 171 h at pH 8.8, and 306 h at pH 12. Samples taken for HPLC analysis were, therefore, brought to pH 12 for immediate analysis. Given this lack of aqueous stability over a wide pH range, TAT was most likely degraded in the TNT/glucose long-term experiments (Figure 4.2.43-46).

At pH 3.3, the presence of dissolved oxygen increased the TAT degradation rate to some extent. HPLC vials were kept anaerobic until analysis by helium bubbling during sample collection. Experiments were also conducted to determine if TAT was photosensitive. At pH 3.3, the introduction of UV light did not increase the degradation rate. It is possible that photodegradation is occurring, but at a rate slower than the acidic hydrolysis rate, so it could not be observed at pH 3.3.

4.3 Task 3 Coupled Abiotic and Biotic Processes

4.3.1 Identification of Abiotic or Biotic Reactions in Coupled Mineralization

The objective of this task is to quantify the relative importance of abiotic versus biotic processes in the mineralization of energetics.

Hypothesis 1. Coupled abiotic/biotic degradation of energetics is more rapid than biomineralization alone

Hypothesis 2. Initial energetic degradation steps are abiotic, and later steps are biotic.

4.3.1.1 Effect of Dithionite/Buffer Concentrations on HE Degradation

Using a dithionite-K_2CO_3 ratio at 1:2, 2 g of Pantex sediment was reduced with varying concentrations of dithionite and buffer. Increasing both dithionite and buffer concentrations during reduction significantly increased RDX destruction (Figure 4.3.1). Given that the sediment mass was fixed (2 g) and washed twice after reduction to remove entrained dithionite, the greater destruction observed with increased dithionite concentration can be attributed to a greater reduction of Fe^{III} to Fe^{II} (Table 4.3.1). Table 4.3.1 shows an increase in concentration of adsorbed Fe^{II} as well as total Fe^{II} with increasing dithionite concentration whereas the Fe^{III} content kept on decreasing. Monitoring the pH of the varying treatments revealed that the pH after 72 h was between 8.5 and 9.0. Although increasing the dithionite/buffer concentrations increased the rate and mass of RDX lost, none of

Figure 4.3.1. Transformation of RDX in a batch system containing 2 g Pantex sediment reduced with varying amounts of dithionite buffered with K_2CO_3. RDX $\pm 0.4\%$.

the dithionite/K_2CO_3 concentrations resulted in 100% removal (Figure 4.3.1). However, when the dithionite/K_2CO_3 ratio was increased from 1:2 to 1:4 (100 mM:400 mM), 2 g of reduced Pantex sediment completely removed the RDX (Figure 4.3.2). Likewise, when 4 g of sediment was reduced by this same treatment, rapid RDX destruction was observed (Figure 4.3.2). Increasing the amount of sediment exposed to dithionite reduced more Fe^{III} to Fe^{II} (Table 4.3.1) and thus increased RDX degradation.

The effect of dithionite/buffer ratios was further tested on all three HEs. The explosives RDX, HMX, and TNT were quickly degraded by the buffered, reduced sediments as compared to the unbuffered, reduced sediments (Figure 4.3.3). The pH of the reduced sediment buffered with K_2CO_3 ranged from 8.0 to 9.5 whereas in the absence of buffer, the pH was 7.2. All buffered sediments turned black, likely due to formation of magnetite (Fe_3O_4). Formation of iron sulfides (also black in color) should be considered but was unlikely because in the absence of buffer (pH = 7.2) the reduced sediment was light green. Total destruction of the three HEs after

Table 4.3.1. Iron phases during reduction of Pantex sediment with dithionite.

Dith. conc.	K$_2$CO$_3$ conc.	Solid: Solution ratio	Sorbed Fe^{II}	Fe^{II}CO3 or Fe^{II}S	Total Fe^{II}	Total Fe^{III}	Fe^{II} in super- natant
mM			μmol g^{-1}				mg L^{-1}
Untreated		1: 20	0.0 ± 0.0†	0.12 ± 0.0	24.2 ± 1.3	314 ± 11	0.0 ± 0.0
10	20	1: 20	6.3 ± 1.6	22.4 ± 0.9	57.7 ± 1.9	279 ± 9.2	0.1 ± 0.0
20	40	1: 20	9.9 ± 1.4	33.3 ± 1.2	91.5 ± 1.8	251 ± 8.2	0.3 ± 0.0
50	100	1: 20	11.8 ± 0.8	54.7 ± 1.7	107 ± 2.1	236 ± 5.1	0.4 ± 0.0
100	200	1: 20	14.3 ± 1.1	70.3 ± 1.2	126 ± 2.4	211 ± 12	1.2 ± 0.2
100	400	1: 20	13.3 ± 1.2	92.1 ± 1.1	167 ± 2.2	173 ± 5.7	0.0
100	400	1: 80	2.73 ± 0.4	21.1 ± 1.3	52.1 ± 1.1	171 ± 2.6	0.0
100	400	1: 40	5.1 ± 0.5	40.9 ± 1.8	89.7 ± 1.3	197 ± 4.9	0.0
100	400	1: 10	18.3 ± 2.7	102 ± 2.1	211 ± 2.9	202 ± 7.6	0.0
100	nil	1: 20	31.5 ± 3.8	30.2 ± 0.9	72.7 ± 1.9	263 ± 13	74.0 ± 3.2
100	C-B buffer	1: 20	11.6 ± 0.5	39.7 ± 1.2	110 ± 0.8	174 ± 2.1	74.2± 4.1

† Sample standard deviation of means ($n = 3$).
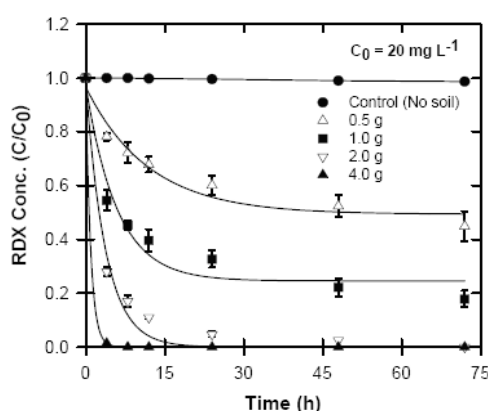
Figure 4.3.2. Transformation of RDX in a batch system containing varying amounts of reduced sediments. Sediments were reduced with 100 mM dithionite + 400 mM K$_2$CO$_3$. RDX ± 0.4%.

72 h of treatment increased from 10 to 50% by the addition of K$_2$CO$_3$ buffer (Figure 4.3.3). Differences in destruction rates between buffered and unbuffered treatments are likely due to mobilization and removal of some Fe^{II} in the supernatant at lower pH (Table 4.3.1). Szecsody et al. (2004) previously observed that using less buffer during dithionite reduction resulted in lower pH, which mobilized some iron and reduced less Fe^{III}. Similarly, Boparai et al. (2006a) observed significant alachlor transformation by reduced sediments in the presence of buffer but very limited transformation in the absence of buffer.

While studying the degradation of equimolar concentrations (10 μM) of explosives with reduced-sediment, the order of degradation was: TNT > RDX > HMX (Figure 4.3.4). The transformation products from reactions between explosives and reduced sediments were analyzed by LC/MS. The transformation of RDX by dithionite-reduced sediment resulted in the formation of nitroso products of RDX (MNX, DNX, TNX), which disappeared within a few hours of the reaction. As the reaction continued, a major product peak, eluting before the nitrosos and RDX, detected by HPLC, increased with time. This was further analyzed by LC/MS. The mass spectrum of this product is consistent with methylene dinitramine, with a molecular formula of CH$_4$N$_4$O$_4$ and nominal mass of 136, and in the negative
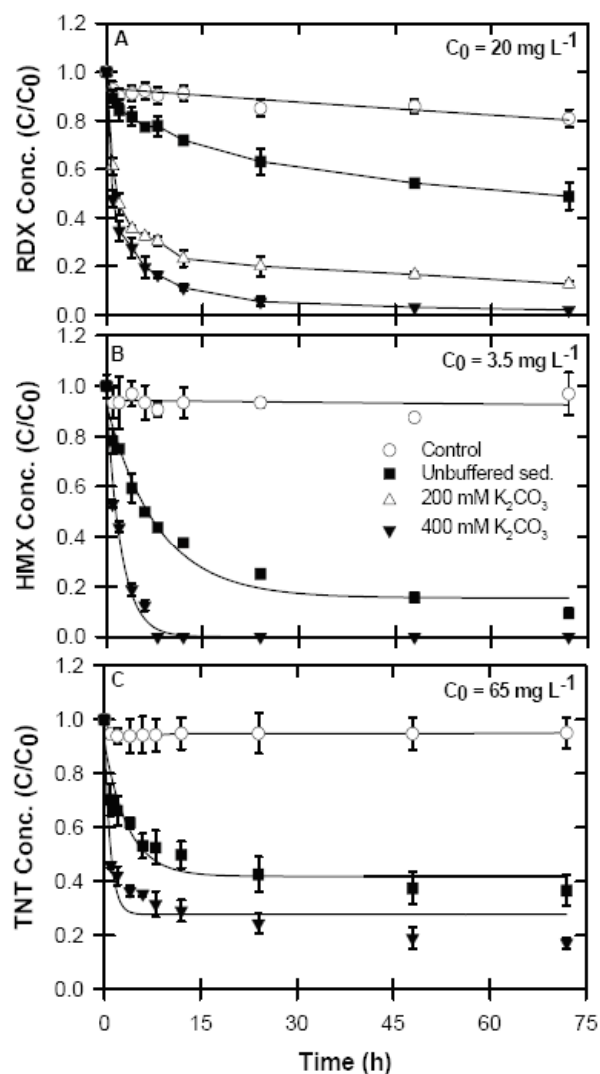
Figure 4.3.3. Transformation of (A) RDX (±0.4%), (B) HMX (± 0.4%), and (C) TNT (±0.7%) in unbuffered and K_2CO_3 (200 or 400 mM) buffered Pantex sediment + 100 mM dithionite.

Figure 4.3.4. Degradation of equimolar concentrations of explosives with reduced sediment (100 mM dithionite + 400 mM K_2CO_3). RDX, HMX ± 0.4%, TNT ± 0.7%.

ion mode this compound would lose a proton to give a formate adduct $[M-H+HCOO]^-$ ion at m/z 180 and as a dimer of methylene dinitramine at m/z 271 (Figure 4.3.5). Methylene dinitramine can be easily transformed biotically/abiotically (Halasz et al. 2002). While running the HMX treated with reduced sediment on LC/MS, the m/z 135 ion was the mass expected for the $[M-H]^-$ ion of methylene dinitramine (Figure 4.3.6) and its retention time also matched the chromatographic peak obtained from a standard solution of methylene dinitramine. Thus, methylene dinitramine was also observed during treatment of HMX with dithionite-reduced sediment. Likewise, the degradation products of TNT were 2-aminodinitro-toluene (2-ADNT) and 4-aminodinitrotoluene (4-ADNT), which were further degraded by the reduced sediments (Figure 4.3.7, Boparai et al. 2007). Some unidentified peaks were also detected.
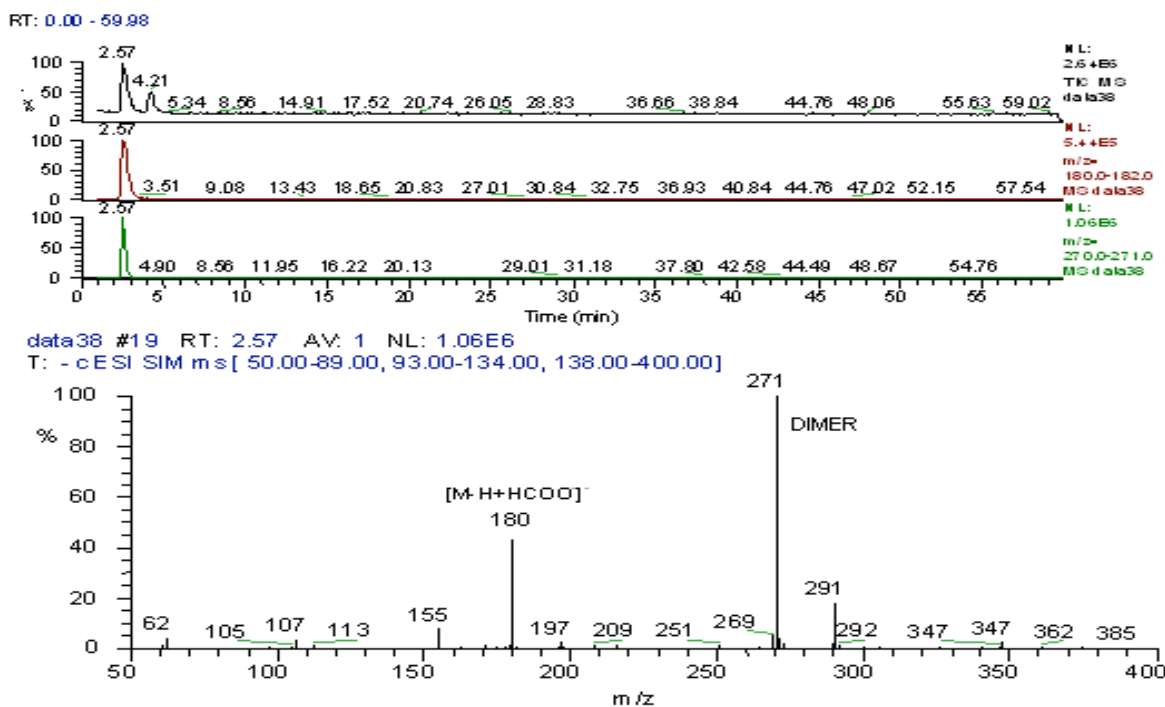
Figure 4.3.5. Negative mode total ion chromatograms and spectra showing methylene dinitramine (transformation product of reduced-sediment treated RDX).
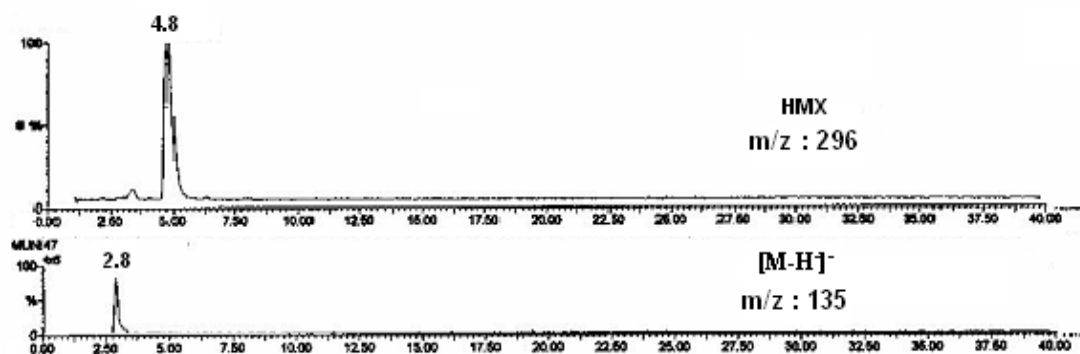
Figure 4.3.6. LC/MS analysis of HMX degradation in dithionite-treated sediment.
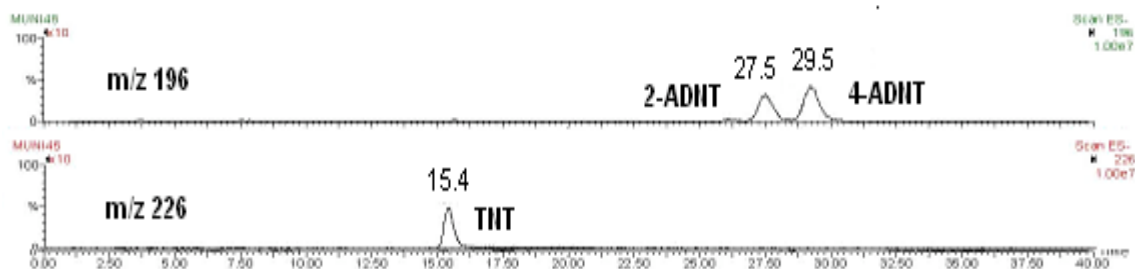
Figure 4.3.7. LC-MS/MS analysis of TNT degradation in dithionite-treated sediment.

4.3.1.2 Contribution of Sorbed Fe^{II} to Degradation Rates

When Pantex sediments treated with DCB were not washed with deionized H_2O, degradation rates were fast with total RDX removal observed within 6 h (Figure 4.3.8). By washing the

reduced sediments, degradation slowed considerably and only 60% of the RDX was transformed within 48 h. This is likely due to the high concentration of Fe^{II} present in the DCB extract (74 mg L^{-1}, Table 4.3.1). Considering that washing removed soluble iron species, we added Fe^{II} back into the system. When Fe^{II} was added to the washed sediment without adjusting pH (pH = 6.8), RDX destruction rates decreased further. However, when Fe^{II} was added and the pH maintained at 8.25 (pH observed in the unwashed treatment), destruction rates were greatly enhanced and approached destruction rates observed in the unwashed sediment (Figure 4.3.8). This indicates that the combination of (hydr)oxide surfaces, sorbed Fe^{II}, and alkaline pH were responsible for the enhanced destruction (Boparai et al. 2006a).
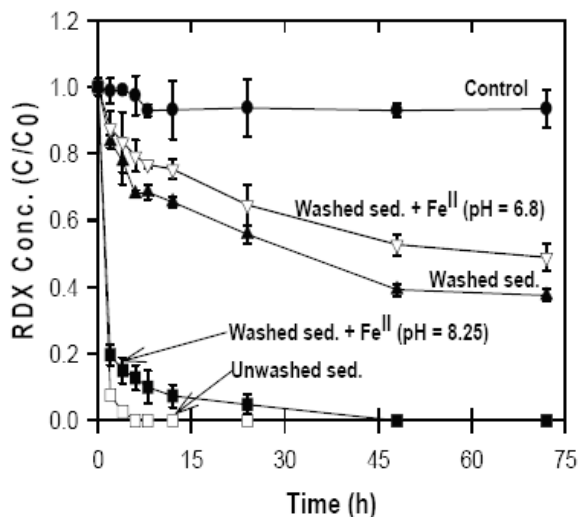
Figure 4.3.8. RDX degradation with washed and unwashed Pantex sediment reduced with 100 mM dithionite + DCB buffer. RDX ± 0.4%.

4.3.1.3 Reductive Capacity of Reduced Sediments to Degrade Energetics

The longevity of redox barriers will be dependent upon the redox capacity of the reduced sediment, volume or thickness of the redox zone, and the influx of dissolved oxygen and contaminants (i.e., electron acceptors). To determine the reductive capacity of a fixed mass of soil, RDX was repeatedly added to 2 g of sediment and changes in degradation rates observed. All RDX was lost from solution within 24 h of initial exposure to the reduced Pantex sediment but the transformation rate decreased with successive RDX reseedings (third, fourth, and fifth cycles) (Figure 4.3.9). When RDX was reseeded in the fifth cycle, RDX loss from solution was only 22% after 24 h.
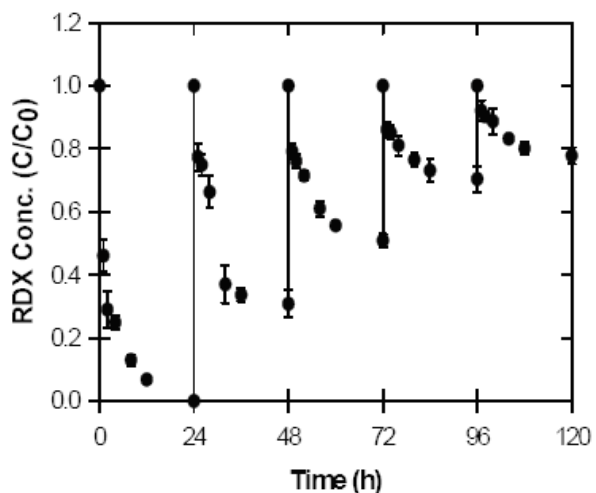
Figure 4.3.9. RDX destruction in solutions containing dithionite-reduced sediment and after reseeding RDX solution (20 mg L^{-1}). RDX ± 0.4%.

After losing its capacity to transform RDX, the reduced sediment could be regenerated by treating again with dithionite. Results from six cycles of successive reduction-oxidation showed that both RDX and TNT were effectively transformed with no change in degradation rates (data not shown). The stability of the sediment to transform explosives following regeneration (i.e., reduction) indicates little to no loss in reductive capacity. Such stability would be important if the aquifer sediment were to be used as a barrier to remediate contaminated water (Lee and Batchelor 2004). It is important to note that the HE concentrations used in the batch studies were approximately 10-fold larger than observed in the Pantex aquifer. Moreover, column rather than batch studies are more suited for determining pore volumes of groundwater that could be treated by in situ redox manipulation. Column studies by Szecsody et al. (2001) indicated that reduced Pantex sediment can treat several hundred pore volumes of groundwater, as shown in Results Section 4.2.1. Considering the hydrological characteristics of the Pantex site, it is estimated that the longevity of a redox barrier at Pantex could be 30 years or more (Aquifer Solutions, Inc., 2002) before the redox zone may need to be regenerated.

4.3.1.4 Evaluating Biodegradation as a Primary and Secondary Treatment for Removing RDX and TNT

Mineralization of RDX solutions exposed to dithionite-reduced Ft. Lewis sediment was initially greater than the control (parent RDX) (Figure 4.3.10A). For instance, at day 7, cumulative mineralization in the reduced sediment was nearly triple that of the control (11 versus 3.6%). With time, however, cumulative $^{14}CO_2$ production from the control eventually surpassed the reductive treatment after about 18 d (Figure 10A, Table 4.3.2). A similar trend was reported by Adam et al. (2005) for mineralization of RDX treated with dithionite-reduced Pantex sediment. ^{14}C-mass balance was >80% in all treatments, with the control containing slightly greater ^{14}C activity than the reduced sediment treatment (Table 4.3.2). Following exposure to dithionite-reduced solids, RDX transformation products were also mineralized (40% in 56 d). Biodegradation may be a secondary treatment for RDX degradates produced from in situ treatment with redox barriers. In contrast to RDX, very little mineralization of TNT occurred in the reduced sediment or the
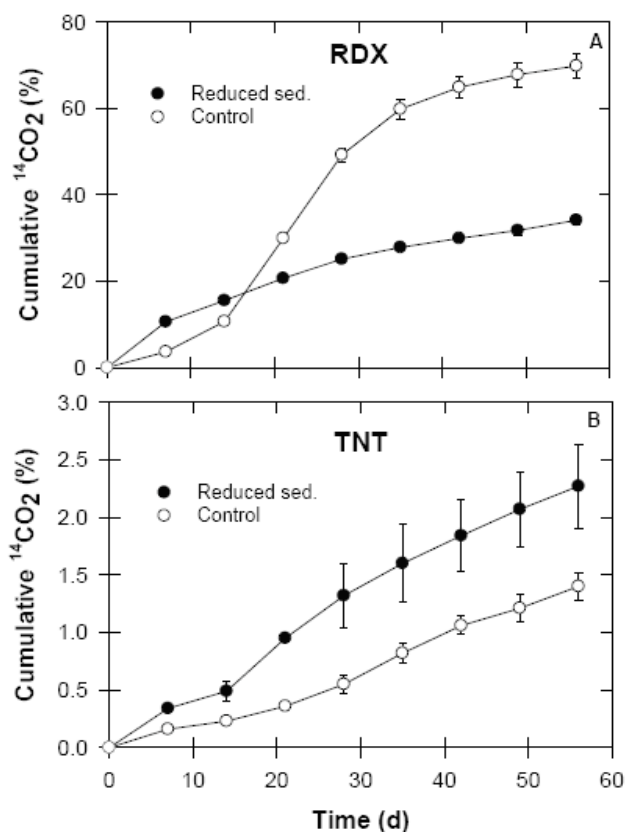
Figure 4.3.10. Cumulative $^{14}CO_2$ produced (% of initial ^{4}C) from aerobic aquifer microcosms incubated with (A) RDX spiked with ^{14}C-RDX (control) and chemically reduced RDX, and (B) TNT spiked with ^{14}C-TNT (control) and chemically reduced TNT. RDX ± 0.4%, TNT ± 0.7%.

control. After 8 weeks, the cumulative mineralization in the reduced sediment was only 2.3% and 1.4% in the control (Figure 4.3.10B, Table 4.3.2).

Table 4.3.2. ^{14}C-mass balances from dithionite-reduced sediment treated RDX and TNT.

Control/Treatment	Initial Activity Added (dpm)	Time (d)	Cumulative Trapped $^{14}CO_2$ (%)	Bound ^{14}C (%)	Total ^{14}C Recovered (%)
			RDX		
Control	149580	56	69.9 (2.9)	20.1 (5.2)	89.9 (8.1)
Dithionite-reduced sediment	149580	56	34.1 (1.0)	50.3 (10.5)	84.4 (11.5)
			TNT		
Control	113760	56	1.4 (0.1)	103 (5.0)	104 (4.9)
Dithionite-reduced sediment	113760	56	2.3 (0.4)	96.8 (18.7)	98.7 (19.6)

4.3.1.5 Methylene Dinitramine Transformation by Dithionite-Reduced Sediment

Methylene dinitramine (MDNA) was previously identified as a transformation product from treatment of RDX and HMX with both dithionite-reduced sediment and soluble/sorbed Fe^{II}. In the present study, a standard solution of MDNA was treated with reduced sediment. One set of experiments was conducted to determine MDNA fate in deionized water without any sediment. Methylene dinitramine (MDNA) was rapidly transformed in water both in the presence and absence of untreated sediment (Figure 4.3.8A). Halasz et al. (2002) found MDNA was unstable in water and spontaneously decomposed to give N_2O and HCHO in water. Interestingly, MDNA (20 mg L^{-1}) transformed much faster in water alone (>90%) than in the presence of non-reduced sediment (40-50%) after 10 h (Figure 4.3.11A). Halasz et al. (2002) similarly reported much faster MDNA decomposition in water alone than in sludge. There was no significant difference in MDNA transformation in non-reduced sediment under aerobic and anaerobic conditions (Figure 4.3.11A). Halasz et al. (2002) confirmed biodegradation of MDNA in the presence of sludge and biodegradation may similarly occur in the presence of sediment.
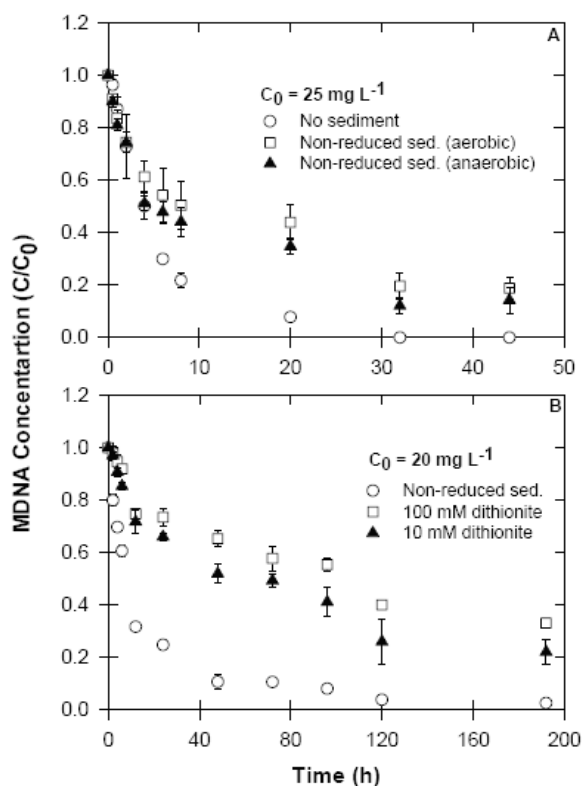
Figure 4.3.11. Degradation of MDNA (A) in water in the presence or absence of non-reduced sediment under aerobic or anaerobic conditions, (B) in partially reduced or highly reduced or untreated sediment. MDNA ± 0.5%.

MDNA transformation was compared in dithionite-reduced and non-reduced sediment. MDNA transformation was fast in non-reduced sediment (half-life = 8 h), whereas slower rates were observed in the partially reduced (10 mM dithionite) and highly reduced (100 mM dithionite) sediment (half-life = 95 h) (Figure 4.3.11B). These results may indicate that MDNA is not being degraded by ferrous iron (i.e. abiotically). This possibly signifies that MDNA degradation is a biotic process and the dithionite treatment adversely affects or kills the micro-organisms responsible for MDNA degradation (or they were washed out of the system). Batch experiments were conducted using differing bactericides to the sediment/water system. These biocides included 1% gluteraldehyde, 2 mM ammonium molybdate tetrahydrate, 6 mM sodium 2-bromoethanesulfonate, and $HgCl_2$. The purpose of the bactericides was to kill the microbes without influencing the abiotic reactions. Unfortunately, all the bactericides interfered with methylene dinitramine peak in the HPLC analysis and we could not verify the processes responsible for decreased methylene dinitramine degradation rates in the presence of reduced sediments. Experiments conducted at PNNL (Results Section 4.2.2.6) showed that methylene dinitramine is degraded rapidly by acidic hydrolysis (even at neutral pH). Methylene dinitramine is stable for 100s of hours in aqueous solution under alkaline conditions, and because dithionite reduction tends to create somewhat alkaline conditions in sediment, slower methylene dinitramine degradation rates in reduced sediments reflects the change in pH.

4.3.2 Influence of pH and Redox Conditions on Energetic Degradation

In situ redox manipulation is a technology involving injection of a chemical reductant (such as sodium dithionite buffered at high pH) into an aquifer. Because dithionite is a strong reductant, particularly in alkaline solutions (Eh^0= –1.12 V), it dissolves and abiotically reduces amorphous and some crystalline Fe^{III} oxides (Szecsody et al. 2004), leaving behind dissolved, structural, and adsorbed Fe^{II}. Hence, HE transformations similar to those observed in this study by Fe^{II} could occur in a permeable redox barrier designed for treatment of explosives in groundwater.

4.3.2.1 Degradation of RDX, HMX, and TNT by Fe^{II}

Degradation of RDX, HMX, and TNT by Fe^{II} was determined at pH 8.25 ± 0.1 under anaerobic conditions (Figure 4.3.12). As the initial concentration of solution Fe^{II} increased from 0.25 to 2.0 mM, degradation rates of RDX, HMX and TNT increased. Nearly complete degradation of all three explosives was observed when the Fe^{II} concentration was 2.0 mM, showing that Fe^{II} concentration is a critical factor affecting the degradation rates. At 1.0 and 2.0 mM Fe^{II}, TNT was most reactive followed by RDX and then HMX. The color of the precipitates changed from light brown to dark brown to dark green with increasing Fe^{II} concentration. Similarly, Maithreepala and Doong (2004) observed that the red-brown color of precipitates changed to green-brown as the concentration of Fe^{II} increased. Table 4.3.3 shows the concentrations of dissolved and sorbed Fe^{II} after treating 50 μM RDX with varying concentrations of Fe^{II} in the buffered solutions at pH 8.25. The sorbed Fe^{II} concentrations increased with increasing initial Fe^{II} concentration. The acid-extractable Fe^{II} concentrations were lower than the initial concentrations and likely a result of oxidation of Fe^{II} to Fe^{III} during RDX degradation. Fe^{III} was observed in all the reactors.
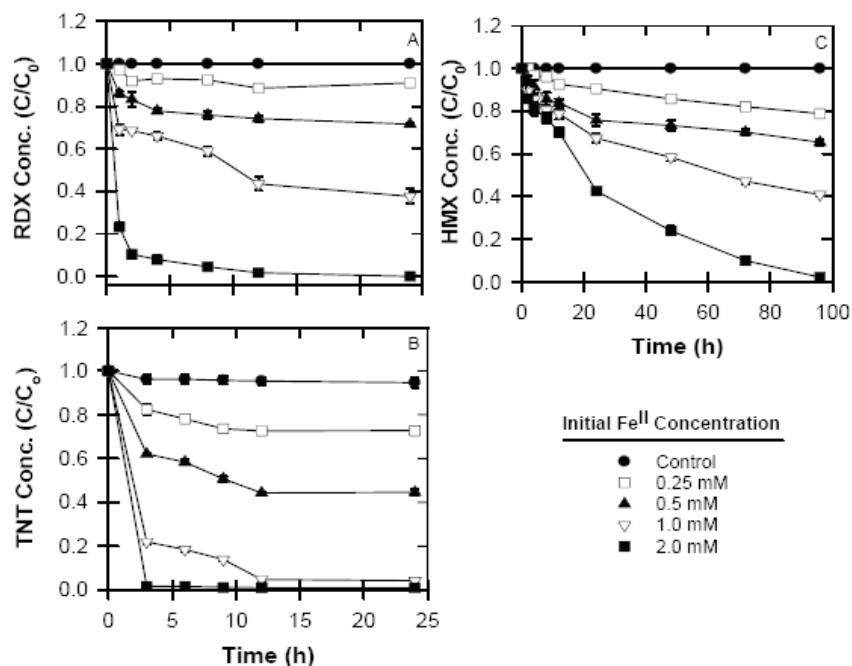
Figure 4.3.12. Effect of Fe^{II} concentration on the degradation of (A) RDX (50 μM), (B) HMX (10 μM), and (C) TNT (180 μM). The pH was maintained at 8.25 ± 0.1 using 50 mM EPPS buffer. RDX ± 0.4%, HMX ± 0.4%, and TNT ± 0.7%.

Table 4.3.3. Iron concentrations in dithionite-reduced sediments.

		Fe^{II} Concentrations (mM)			
pH	**Initial**	**Total Fe**	**Acid-Extractable**	**Dissolved**	**Adsorbed**
Control	2.0	2.02 ± .09	2.0 ± .04	1.99 ± .05	0.0
6.35	2.0	1.99 ± .06	1.93 ± .08	1.90 ± .06	0.03
6.85	2.0	1.99 ± .07	1.77 ± .04	1.70 ± .03	0.07
7.35	2.0	2.00 ± .09	1.54 ± .05	1.41 ± .03	0.13
7.85	2.0	2.01 ± .06	1.09 ± .06	0.88 ± .04	0.21
8.25	2.0	1.98 ± .08	0.65 ± .03	0.32 ± .02	0.33
8.55	2.0	2.00 ± .07	0.57 ± .04	0.04 ± 0.0	0.53
8.25	0.25	0.24 ± .06	0.15 ± .02	0.03 ± .01	0.12
8.25	0.50	0.49 ± .04	0.20 ± 0.02	0.06 ± .02	0.14
8.25	1.0	1.01 ± .05	0.30 ± .03	0.11 ± .03	0.19

The effect of pH on energetic degradation was determined at an initial Fe^{II} concentration of 2.0 mM (Figure 4.3.13). In the presence of Fe^{II}, no to slight changes in RDX Table 4.3.3. Concentrations of acid-extractable, eissolved and sorbed Fe^{II} in 50 μM RDX solution treated with varying Fe^{II} concentrations at different pHs after 24 h.

Concentrations were observed in the unbuffered control and pH 6.35 treatments (Figure 4.3.13A). Small changes in RDX concentration were observed at pH 6.85. As pH increased from 7.35 to 8.55, RDX was degraded more rapidly with 100% removal observed within 24 h (Figure 4.3.13A). HMX transformation by Fe^{II} was also sensitive to pH with responses similar to RDX but on a longer time scale (Figure 4.3.13B). Strathmann and Stone (2002) investigated carbamate degradation by Fe^{II} and reported a 10-fold increase in reaction rates for each unit increase in pH, which they attributed to a higher concentration of solution-phase hydroxo species. The sorbed Fe^{II} concentrations increased with increasing pH during degradation of RDX with 2 mM initial Fe^{II} (Table 4.3.3). The concentrations of acid-extractable Fe^{II} decreased after 24 h of reaction and reflects oxidation of Fe^{II} to Fe^{III} during degradation of RDX (Boparai et al. 2006b).
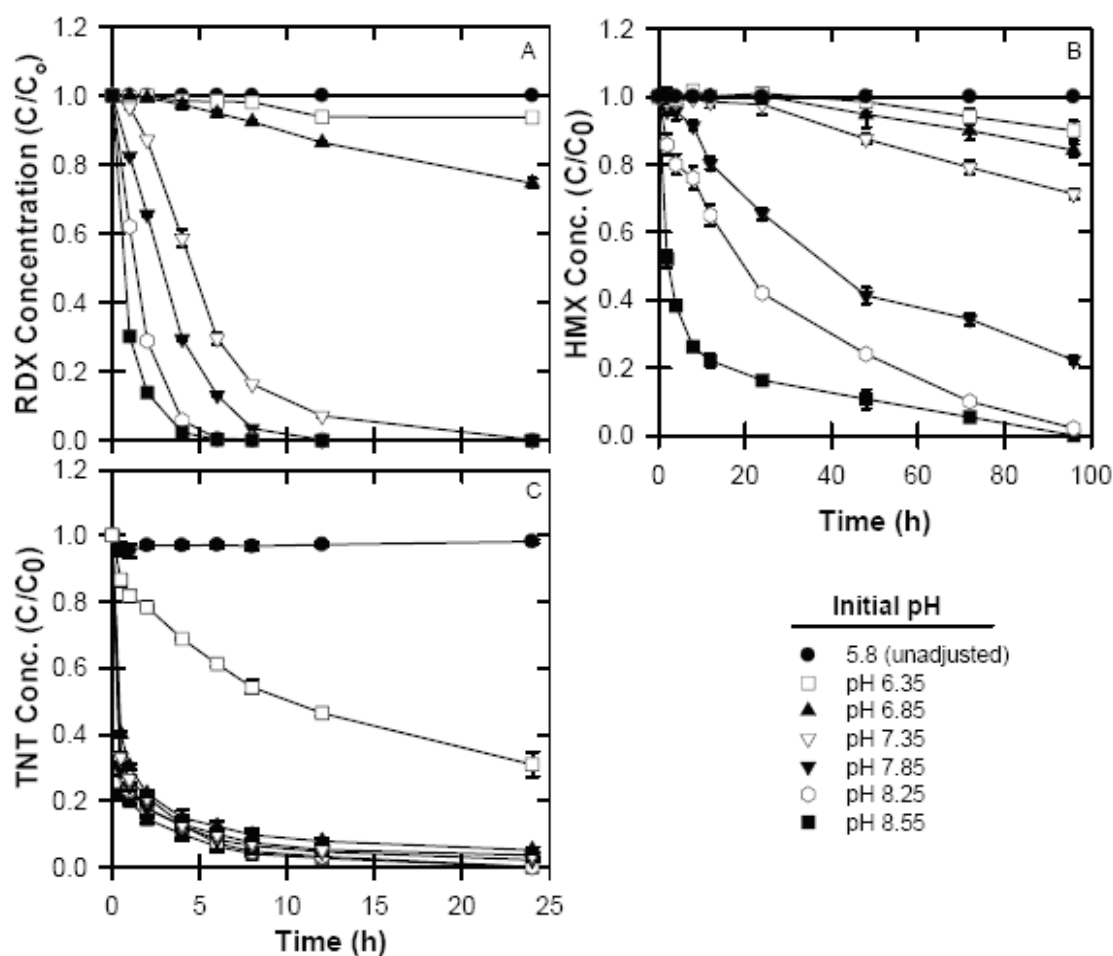
Figure 4.3.13. Effect of pH on the transformation of (A) 50 μM RDX, (B) HMX (10 μM) and (C) 180 μM TNT by 2 mM Fe^{II}. RDX ± 0.4%, HMX ± 0.4%, and TNT ± 0.7%.

During the pH experiments, no precipitates were observed in the solution at pH 6.35 and 6.85. Light green precipitates were observed at pH 7.35 and dark green precipitates at pH 7.85 to 8.55 that turned black with time. XRD analysis verified that the green precipitate was green rust (Figure 4.3.14A) and black precipitate was magnetite (Figure 4.3.14B). Strathmann and Stone (2002) also reported the Fe^{II} precipitate color changed from light gray to dark green with the change in solution pH. The green color is generally due to the formation of ferrous hydroxides or green rust, mixed Fe^{II}/Fe^{III} double hydroxides. While freshly prepared, "pure" $Fe(OH)_2$ is reported to be white, it turns green when traces of Fe^{III} are present (Strathmann and Stone 2002) or when it becomes oxidized (Leussing et al. 1953).
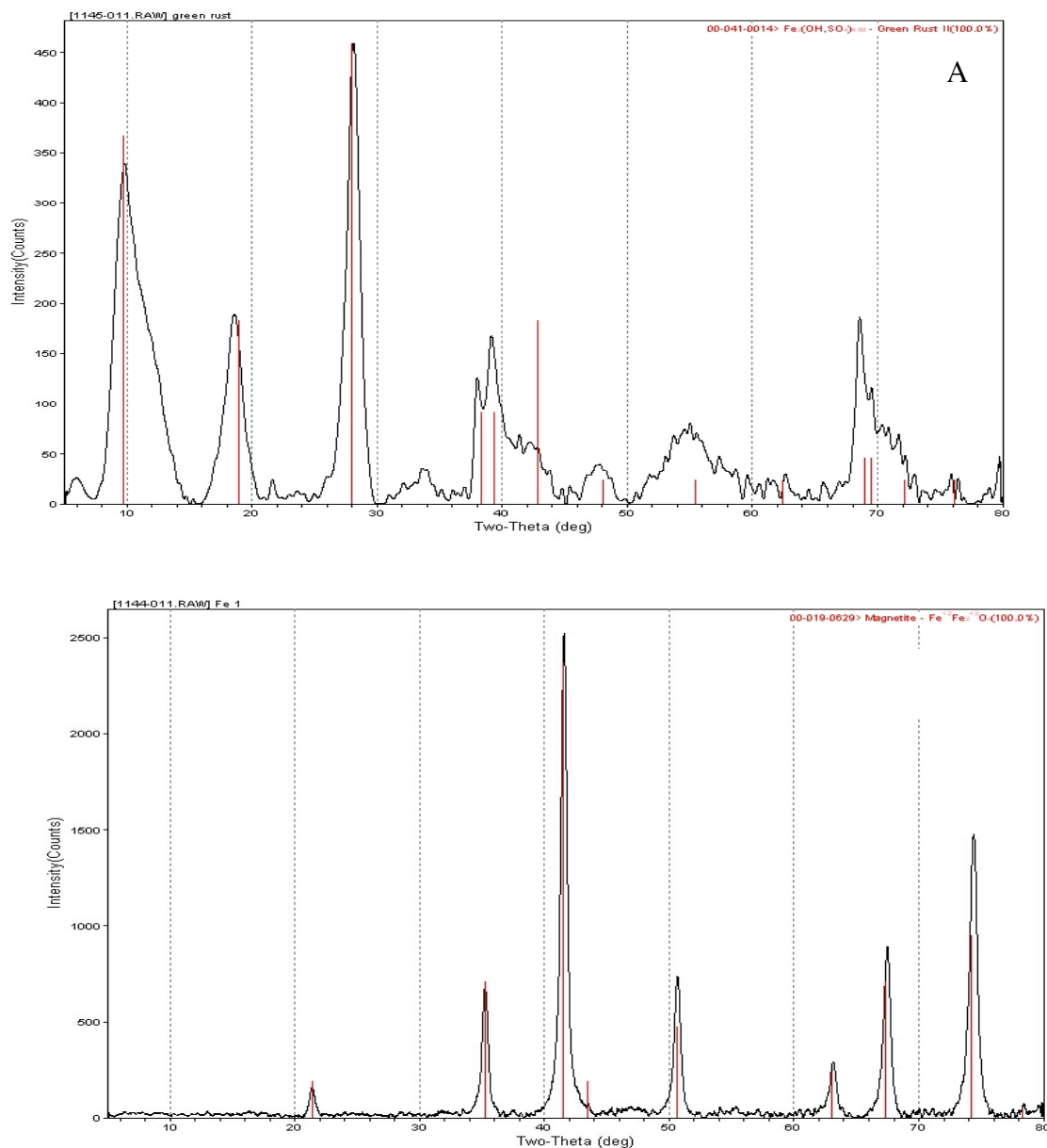
Figure 4.3.14. XRD patterns of (A) green rust and (B) magnetite after precipitation of Fe^{II} in the buffer solution at alkaline pH.

As the pH increased from 6.85 to 8.55, TNT was also degraded rapidly with 100% removal observed within 24 h (Figure 4.3.13C). Interestingly, there was no significant difference in TNT degradation kinetics within this pH range. Light green precipitates were observed at pH 7.35 and dark green precipitates at pH 7.85 to 8.55. With time, all treated TNT solutions turned yellow; this color change is likely due to the amino-degradation products (Vorbeck et al. 1998), which were observed during LC/MS analysis. The RDX degradation rate in the Ft. Lewis sediment (Figure 4.3.15) at pH 6, 7, 8, and 9 did not appreciably differ, indicating the significance of mineral phases produced.
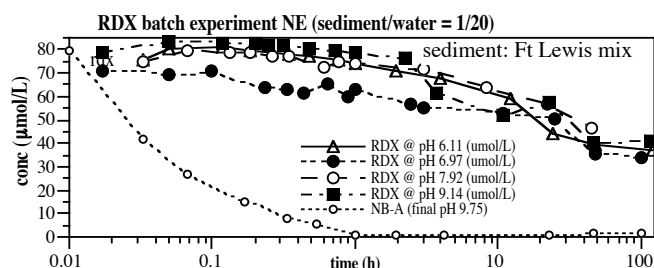
Figure 4.3.15. RDX degradation in reduced Ft. Lewis sediment at different pH (RDX ± 0.5%).

The removal of RDX by Fe^{II} (Figure 4.3.12A) differs from that reported by Gregory et al. (2004) who conducted similar experiments with 1.5 mM Fe^{II} (added as $FeCl_2$) and observed negligible RDX removal between pH 6 and 7.5 after 200 h. At pH 8.0, they reported the formation of a brown precipitate and RDX (72 μM) was removed within 10 d. The differences in RDX removal rates between the two studies may be due to experimental procedures. In the present study, $FeSO_4$ was used with EPPS buffer and we did not filter solutions prior to use. Gregory et al. (2004) used $FeCl_2$ with HEPES buffer and filtered all solutions through 0.02 μM filters. There were also differences in equilibration time following Fe^{II} addition to the buffers. These differences in experimental procedures were systematically investigated.

Filtering iron stock solutions (2 mM) prior to dilution into 50 mM EPPS or 50 mM HEPES did not result in a significant difference in RDX degradation (data not shown). The equilibration time of the iron-buffer solutions prior to addition of RDX (0, 12, or 24 h) also had no effect on RDX degradation rates (data not shown). Likewise, a comparison between $FeSO_4$ and $FeCl_2$ as Fe^{II} sources showed that both Fe^{II} salts resulted in the same RDX degradation rates (Figure 4.3.16A). Dark brown precipitates were observed with $FeCl_2$ and dark green precipitates with $FeSO_4$, both of which turned black with time. Strathmann and Stone (2002) investigated
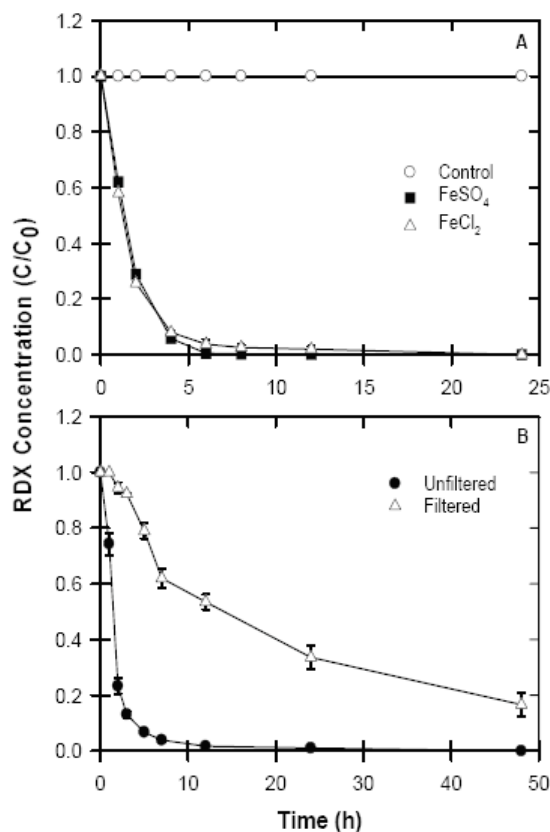
Figure 4.3.16. Comparison of (A) salts on RDX destruction following treatment with 2 mM Fe^{II}, (B) filtered and unfiltered buffer solutions containing 2.0 mM Fe^{II} in the presence of 50 mM EPPS at pH 8.25. RDX ± 0.4%.

the effects of various inorganic ligands on oxamyl reduction by Fe^{II} and found no discernible differences in reduction kinetics at chloride or sulfate concentrations of 0.001 to 0.1 M. They did, however, report a 1.6-fold increase in reduction kinetics when 0.5 M chloride was used.

The only experimental protocol that yielded significant differences in degradation rates was when the diluted Fe^{II} buffer solutions (EPPS buffer, pH 7.7, 2.0 mM Fe^{II} as $FeSO_4 \cdot 7H_2O$) were filtered immediately before adding the RDX. In this test, the filtered solution showed comparatively slower RDX degradation than the unfiltered solution (Figure 4.3.16B). Visual observation showed that filtering removed colloidal precipitates that were likely precursors to green rust or other iron oxides. However, even after filtration, there was still enough Fe^{II} to form Fe oxides again, resulting in the observed degradation.

4.3.2.2 Degradation Products

Treatment of RDX by Fe^{II} resulted in the formation of nitroso products of RDX (MNX, DNX, TNX), which disappeared within a few hours of the reaction (data not shown). As the reaction continued, a major product peak, eluting before the nitroso products of RDX increased with time. The mass spectrum of this product is consistent with methylene dinitramine and was confirmed with a standard. With time, methylene dinitramine was eventually degraded in the Fe^{II} treatment.

The transformation of HMX by Fe^{II} resulted in the formation of nitroso products of HMX (mono-through tetra-nitroso), with LC/MS analysis showing a consecutive loss of 16 amu (oxygen) from m/z=341 through 277. The nitroso derivatives were observed as formate adducts in the LC/MS analysis [M-H+HCOO$^-$] (Figure 4.3.17). A peak for the ion expected for the tetra-nitroso-HMX/formate adduct (m/z = 277) is seen in the chromatogram at 4.56 min. Smaller peaks for the ions expected for the tri-nitroso-HMX/formate adduct (m/z = 293) and the di-nitroso-HMX/formate adduct (309) are seen at retention times of 4.76 and 4.81 min, respectively. Peak from the ions expected for the mono-nitroso-HMX/formate adduct (m/z = 325) was observed at a retention time of 5.93 but the intensity of this peak was on the order of 10-20 times less intense than the previous ions' peaks. Treatment of TNT with Fe^{II} produced 2-aminodinitrotoluene (2-ADNT) and 4-aminodinitrotoluene (4-ADNT) as well as some unidentified peaks (data not shown). Using the AMTs as initial stock solutions, we also verified that 2-ADNT and 4-ADNT were further transformed in the presence of Fe^{II}.

4.3.2.3 Aerobic Versus Anaerobic Conditions

Treatments with zerovalent iron are generally implemented under anaerobic conditions because the presence of oxygen is expected to lower the efficiency of the process by competing with the target contaminants (Joo et al. 2004), accelerate iron aging (passivation), and cause loss of reactivity (Gaber et al. 2002). However, because many aquifers are oxic, the insertion of an iron barrier would result in some of the zerovalent iron being used to reduce O_2. Ironically, the destruction kinetics of certain contaminants by Fe^0 have been accelerated by exposure to air. Tratnyek et al. (1995) observed a higher rate of CCl_4 degradation by Fe^0 in an air-purged system
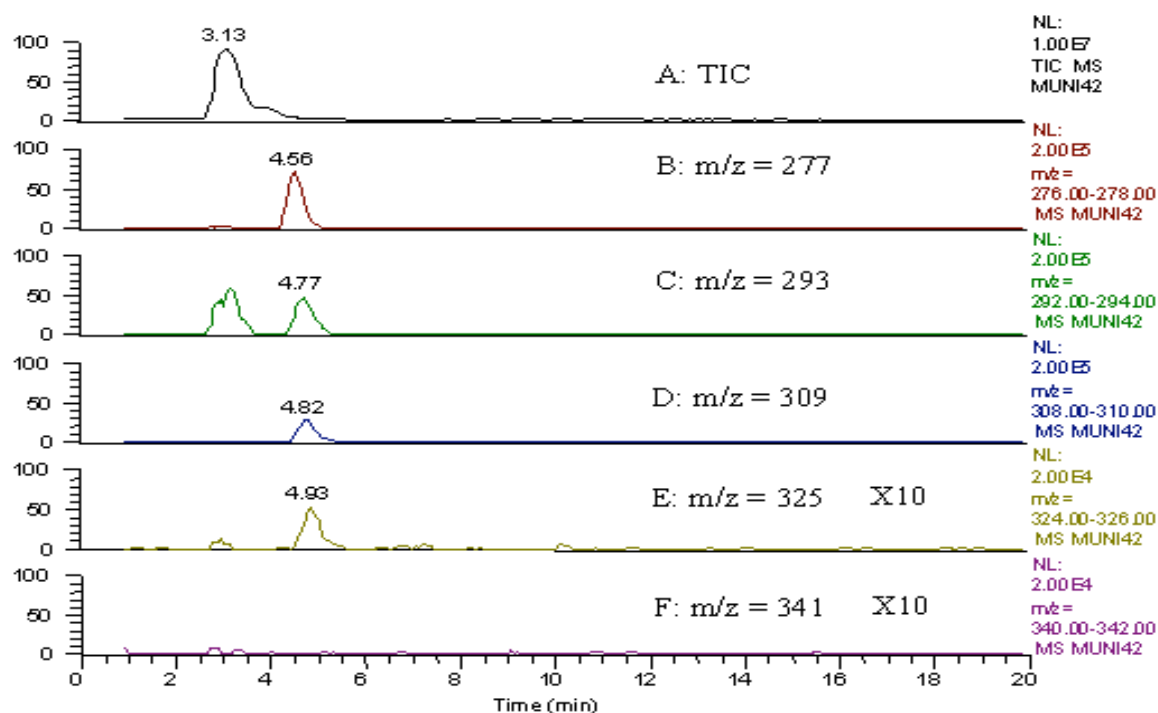
Figure 4.3.17. Total ion chromatographs (TIC) and selected ion chromatographs for HMX treated with 2 mM Fe^{II} at pH 8.25.

($t_{1/2}$ = 48 min) than in a nitrogen-purged ($t_{1/2}$ = 3.5 h) or oxygen-purged environment ($t_{1/2}$ = 111 Fe^0 in solution exposed to air than in solution purged with N_2. The Fe^0 present in a PRB would continue to consume incoming oxygen until completely passivated. Once passivated, ferrous iron would no longer be generated and its ability to transform contaminants severely limited. To illustrate this, a 50 μM RDX solution was equilibrated with Fe^{II} (2 mM) in a 50 mM EPPS buffer (pH 8.25 ± 0.1) inside and outside the anaerobic chamber. Dark green precipitates formed inside the chamber and resulted in RDX degradation. Yellow colored precipitates formed outside the chamber (identified as lepidocrocite by XRD) and no RDX degradation was observed (Figure 4.3.18). When green rust precipitates were allowed to form and the experimental unit was then removed from the anaerobic chamber (i.e., influx of dissolved oxygen), RDX

Figure 4.3.18. Changes in RDX concentration following treatment with 2 mM Fe^{II} at pH 8.25 ± 0.1 under aerobic and anaerobic conditions. Treatments show the effects of removing or keeping batch reactors under anaerobic conditions. RDX ± 0.4%.

transformation was completely halted (Figure 4.3.16). No further degradation occurred when Fe^{II} was added at 5 and 10 h to the reactors outside the chamber and pH maintained at 8.5.

Therefore, while zerovalent iron may facilitate transformations of contaminants in the presence of some dissolved oxygen, Fe^{II}-mediated transformations are less robust and more sensitive to dissolved oxygen concentrations. We recognize that the results from these batch experiments are not completely indicative to groundwater systems where dissolved oxygen concentrations would be much lower and soil-solution ratios much higher. During column studies, Szecsody et al. (2004) showed that low amounts of Fe^{II} (in various forms) could sustain a reducing environment for several hundred pore volumes.

4.3.2.4 RDX Degradation by Fe^{II} in the Presence of Aquifer Solids

In the absence of buffers, adding $FeSO_4$ to aqueous RDX solutions lowered the pH ≤ 6.0 and no degradation was observed. Aquifer solids obtained from the perched Pantex Aquifer (RDX-contaminated, Amarillo, Texas) were highly alkaline (pH 9) and it was hypothesized that these solids could buffer Fe^{II} additions and make RDX degradation possible. Thus, RDX degradation by 2.0 and 7.2 mM Fe^{II} in the presence of Pantex aquifer material was determined. The pH of the control treatment containing aquifer solids (RDX, no Fe^{II}) was 8.3 to 8.5 and little RDX degradation or adsorption occurred in this treatment (Figure 4.3.19A). Thus, Fe^{II} is required along with the desired pH to degrade RDX. When 7.2 mM Fe^{II} was added to the soil-water suspensions, the pH decreased to 6.7 to 6.9 and RDX degradation ($k = 0.552$ h^{-1}) was observed (Figure 4.3.19A). Similarly, when 2.0 mM Fe^{II} was added, RDX degradation occurred at almost the same rate ($k = 0.683$ h^{-1}) and the pH ranged between 7.65 and 7.85 (Figure 4.3.19A). In the latter case, although the Fe^{II} concentration was lower, the higher pH favored the reaction. Lee and Batchelor (2004) observed abiotic reductive dechlorination of chlorinated ethylenes by Fe^{II} in the presence of Silawa soil. Fe^{II} complexed to and/or associated with solid surfaces exhibits a very characteristic reactivity with respect to nitroaryl reduction (Hofstetter et al. 1999). The transformation of RDX in the presence of Fe^{II} and aquifer solids resulted in the production of MNX, DNX, and TNX (data not shown). As the reaction continued, these products also decreased with time.

For comparison, RDX degradation by Fe^{II} was determined in the presence of Ottawa sand (non-alkaline). When 2.0 mM Fe^{II} was added to the sand-water suspensions, the pH decreased to 6.2 and very little RDX degradation was observed (Figure 4.3.19B). However, RDX degradation occurred ($k = 0.312$ h^{-1}) when the pH of the RDX-Ottawa sand mixture was adjusted to 7.7 with buffer. This shows that the buffering capacity of Pantex sediment maintained the desired pH even after Fe^{II} additions and thus favored the RDX degradation whereas non-alkaline sand could not buffer the acidity of the Fe^{II} additions and hence, little RDX degradation occurred.

An additional experiment was conducted with 7.2 mM Fe^{II} at pH 6.85 (using EPPS) buffer without aquifer solids (Figure 4.3.19C). In this experiment, RDX transformation occurred within 75 h. Thus, destruction rates were much slower in the absence of soil indicating that the Pantex sediment facilitated degradation by either enhancing the precipitation of reactive iron oxides or providing surfaces for coordination of Fe^{II}, which subsequently reacted with RDX.

4.3.2.5 Fe^{III}-Facilitated Hydrolysis

Another consideration regarding the fate of RDX within a redox barrier involves its capacity to undergo hydrolysis. Iron corrosion increases the pH of surrounding pore water and several experiments have reported pH > 9 (Szecsody et al. 2004). Considering that oxidation of Fe^{II} will produce significant quantities of Fe^{III}, the effect of Fe^{III} on RDX transformation under alkaline pH was investigated. Results showed that RDX hydrolysis can occur at pH 10 under anaerobic conditions but when Fe^{III} was present, RDX removal was enhanced significantly (Figure 4.3.20). This synergistic effect is likely due to Fe^{III} serving as a Lewis acid and promoting RDX hydrolysis. Iron oxides in water can catalyze organic hydrolysis reactions, at least those known to be OH$^-$ catalyzed (Hoffman 1990). Although the OH$^-$ ion activity is greater at the positively charged oxide surface than in solution, coordination between structural Fe^{III} (Lewis acid) and the organic functional groups is the probable cause of decomposition (McBride 1994).
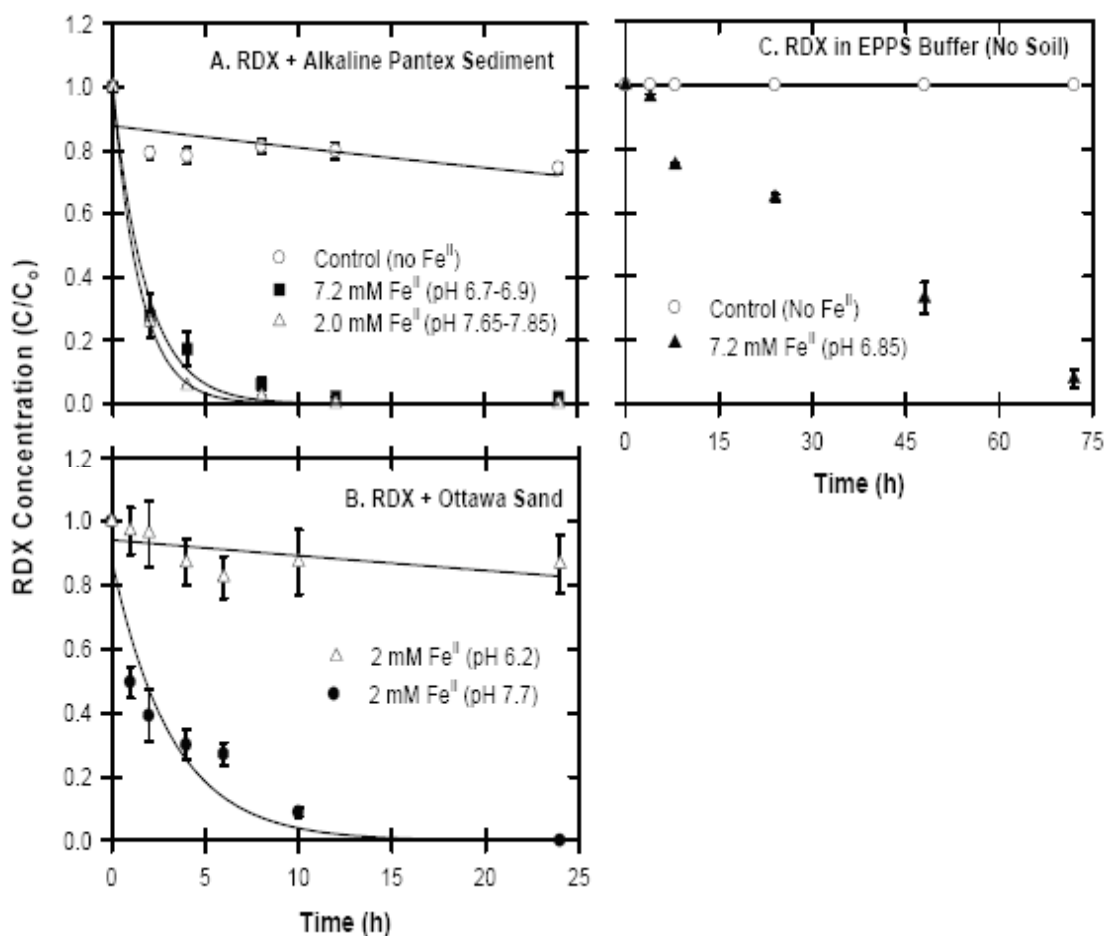
Figure 4.3.19. (A) Temporal changes in RDX concentration ($C_0 = 50$ μM RDX L^{-1}) following treatment with 2.0 and 7.2 mM Fe^{II} in the presence of Pantex aquifer material. (B) Changes in RDX concentration following treatment with 2.0 mM Fe^{II} in unbuffered pH (6.20) and buffered pH (7.7) solutions containing Ottawa Sand. (C) Changes in RDX concentration following treatment with 7.2 mM Fe^{II} at pH 6.85 (no soil). RDX ± 0.4%.

A known product of alkaline hydrolysis of RDX is 4-nitro-2,4-diaza-butanal (4-NADB) (Fournier et al. 2002). Mass spectra were consistent with 4-NADB (data not shown) but this product was in low concentration and not stable in the presence of Fe^{III}. To determine if Fe^{III} was facilitating transformation of 4-NADB, RDX was first transformed to 4-NADB under alkaline conditions and then Fe^{III} added to the solution (pH = 10). Once Fe^{III} was added, 4-NADB was further transformed to some unidentified products. These results indicate that Fe^{III} formation can aid in the degradation of RDX and 4-NADB.
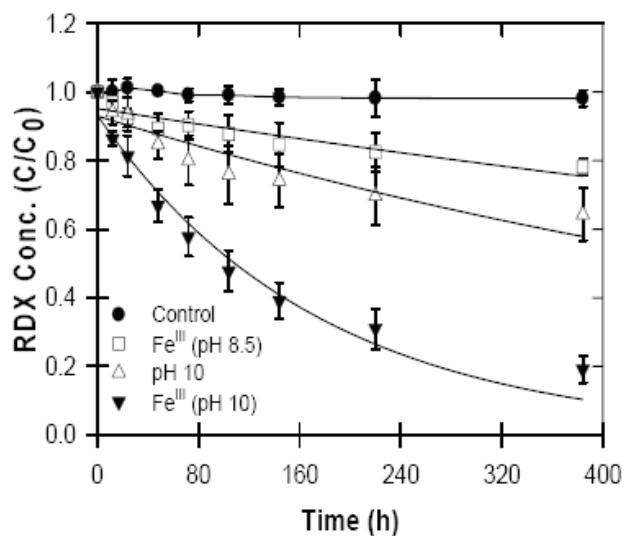
Figure 4.3.20. Facilitated hydrolysis of RDX by Fe^{III}. RDX ± 0.4%.

4.4 Task 4 Energetic Reactive Transport

4.4.1 RDX Reactive Transport in Reduced Sediments: Sorption and Degradation

Column experiments were conducted with Ft. Lewis sediment to assess RDX degradation and mineralization under some field–scale conditions. Small 1-D columns represent the soil/water ratio found in the field (i.e., packed porous media), but not natural cm or larger scale heterogeneities, as sediment is repacked (although natural mineralogical heterogeneities of iron oxides on grains are present). Three column experiments were conducted at laboratory temperatures (22°C), not field aquifer temperature (15-19°C) in the same 15 cm long column that was reduced by dithionite during flow. RDX was injected at three differing flow rates for a total of 950 h or 257 pore volumes. The reduced sediment column has 1.6×10^3 times greater ferrous iron than 10 mg/L RDX, so has a theoretical capacity to degrade 660 pore volumes of 10 mg/L RDX to mineralization (i.e., 24 electrons) or 2000 pore volumes to degrade 10 mg/L RDX to the fourth product (i.e., 8 electrons).

In two column experiments, RDX was injected into the dithionite-reduced sediment column at a flow rate to achieve a residence time of 4.4 h and 0.44 h in the column (i.e., reaction time), which is likely 1 to 2 orders of magnitude faster than would be found naturally in the Ft. Lewis aquifer. These high flow rates were necessary to collect degradation rate data. In the first experiment (residence time 4.4 h, Figure 4.4.1) the 10 mg/L RDX injected and the first three degradation products were completely degraded within the 4.4 hours (i.e., effluent concentrations of these 4 compounds were below detection limits). Methylene dinitramine was detected in all samples at ~4 μmol/L, with the first sample at a higher concentration. The detection limits for RDX is 0.05 mg/L, MNX 0.2 mg/L, DNX 0.16 mg/L, TNX 0.09 mg/L, and methylene dinitramine 0.11 mg/L. This experiment was run for 90 pore volumes (400 h), so there was no influence of dithionite remaining in the column initially. The first sample at 0.91 pore volumes (11 h) contained trace concentration of MNX. Plotted on a log concentration scale (Figure 4.4.1b), the effluent methylene dinitramine concentration is more clearly established as

RDX 1-D Transport in Reduced Sediment Column, 4.4 h/pv

RDX 1-D Transport in Reduced Sediment Column, 4.4 h/pv
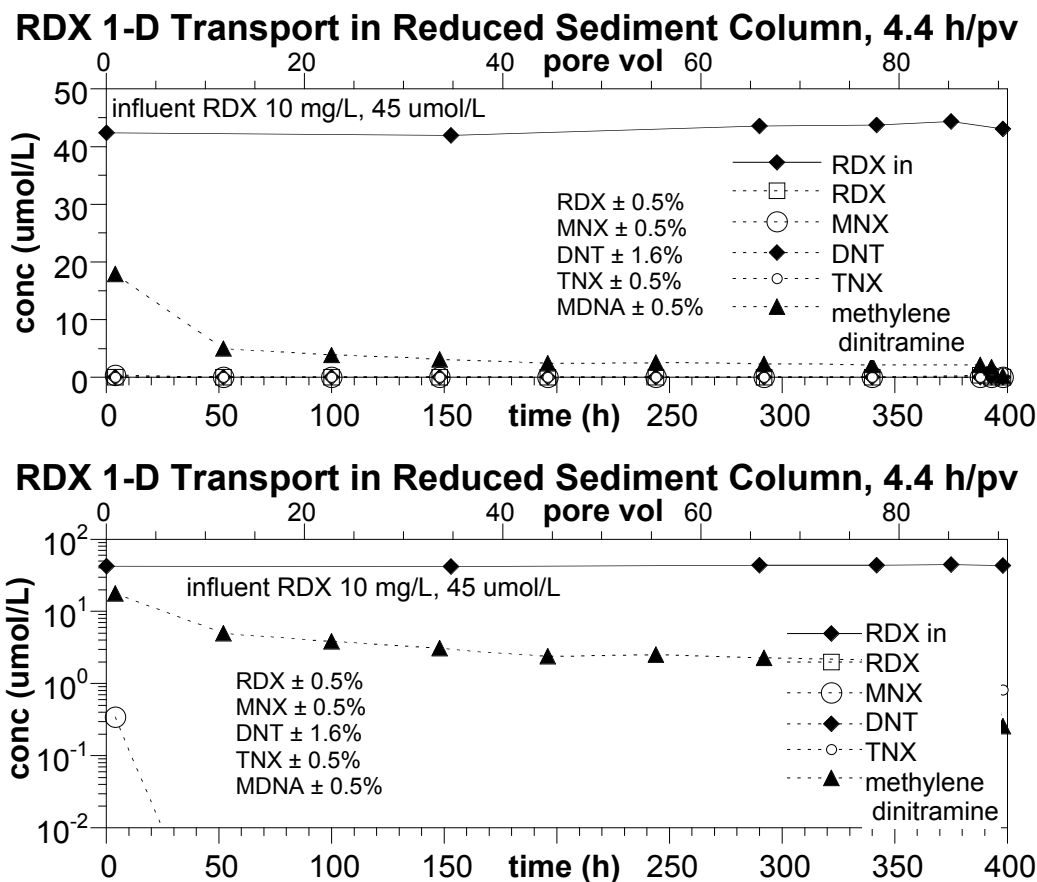
Figure 4.4.1. RDX degradation in 1-D columns with dithionite-reduced sediment (soil/water = 5.6 g/mL) at a flow rate of 4.4 h per pore volume (0 to 400 h).

constant, so a degradation rate can be determined. This rate is relatively slow compared with the first three degradation products (0.62/h or 1.1 h half-life), and consistent with batch results previously reported.

The second column was conducted with a 10-fold faster flow rate (0.44 h residence time) relative to the first column test. This column was run for an additional 110 pore volumes (i.e., from 400 h to 440 h or 93 pv to 203 pv, Figure 4.4.2). The effluent concentrations quickly leveled off with measurable concentrations of RDX (30% of influent), TNX (10% of RDX influent mass), DNX (2%), MNX (1.5%), and MDNA (0.3%). These effluent concentrations shown are more clearly separated on the log concentration scale (Figure 4.4.2b). While RDX and first three degradation product concentrations increased, the methylene dinitramine concentration decreased, as less was produced. Measurable effluent concentrations enabled calculation of a RDX removal rate (0.3 h), which is considerably slower than predicted from batch data (<1 second), although the next two products were below detection limits. The third degradation product (TNX) was being quickly degraded (0.17 h half-life, or faster than predicted from batch data). Sorption in columns, removing 77% of the aqueous mass, would have some influence on slowing the RDX degradation rate initially (until sorption equilibrium was reached), so may account for some of the observed effect. In addition, all aqueous/surface reaction rates

RDX 1-D Transport in Reduced Sediment Column, 0.44 h/pv
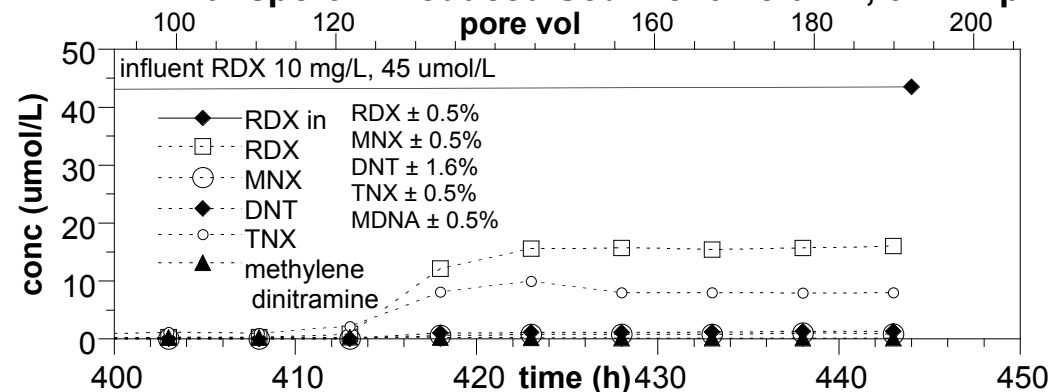
RDX 1-D Transport in Reduced Sediment Column, 0.44 h/pv
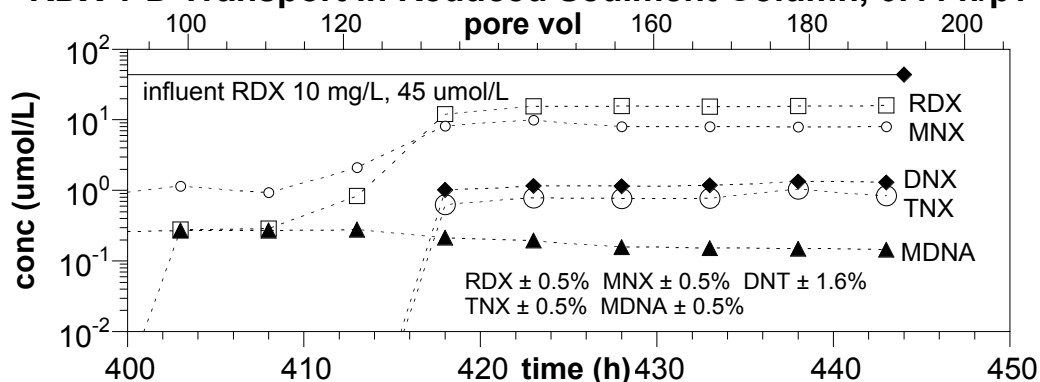
Figure 4.4.2. RDX degradation in 1-D columns with dithionite-reduced sediment (soil/water = 5.6 g/mL) at a flow rate of 0.44 h per pore volume (400 to 440 h).

are limited by the diffusion rate in aqueous solution. These fairly fast rates show that RDX degradation by dithionite-reduced sediment is a viable technology. A reduced sediment wall needs to be constructed to achieve a residence time of only a few hours to degrade RDX.

Three RDX column experiments were conducted to compare the rate of mineralization to batch studies. In the first two experiments, new, highly reduced Ft. Lewis sediment was used. In the third experiment, reduced, then oxidized sediment (for 220 pore volumes, of an estimated 250 pore volume capacity) was used. For the first 220 pore volumes, this experiment was degrading RDX (Figures 4.4.1 and 4.4.2). It is expected that as the sediment is oxidized, due to less ferrous iron sites available for abiotic and coupled reactions, the RDX mineralization rate would decrease.

In the first RDX mineralization column (Figure 4.4.3a) with an 89 h residence time, aqueous measurements of the effluent showed 8% and 20% mass loss of aqueous species initially (diamonds, Figure 4.4.3a), which increased to 42% by 500 h. Mineralization initially was very small for the first 200 h, then increased to 43% by 500 h. The final mineralization rate was more rapid than observed in batch systems (115 h half-life, versus 315 h half-life observed in batch systems, Figure 4.2.11). This column system had a sediment/water ratio of 5.6 g/mL compared

with 0.2 g/mL in the batch experiment. If the RDX mineralization process was purely abiotic, then scaling the rate would be purely a function of the ferrous iron mass (i.e., reactant), or the column experiment should have a rate 28x greater than the batch experiment, based on 28x greater ferrous iron present per mole of RDX. However, some of the sequential RDX mineralization reactions are dependent on microbes directly for biotic and coupled abiotic/biotic reactions (i.e., formate mineralization is a coupled reaction). Microbial reactions tend to occur more slowly in column systems due to inadequate mixing and nutrient transport limitations.
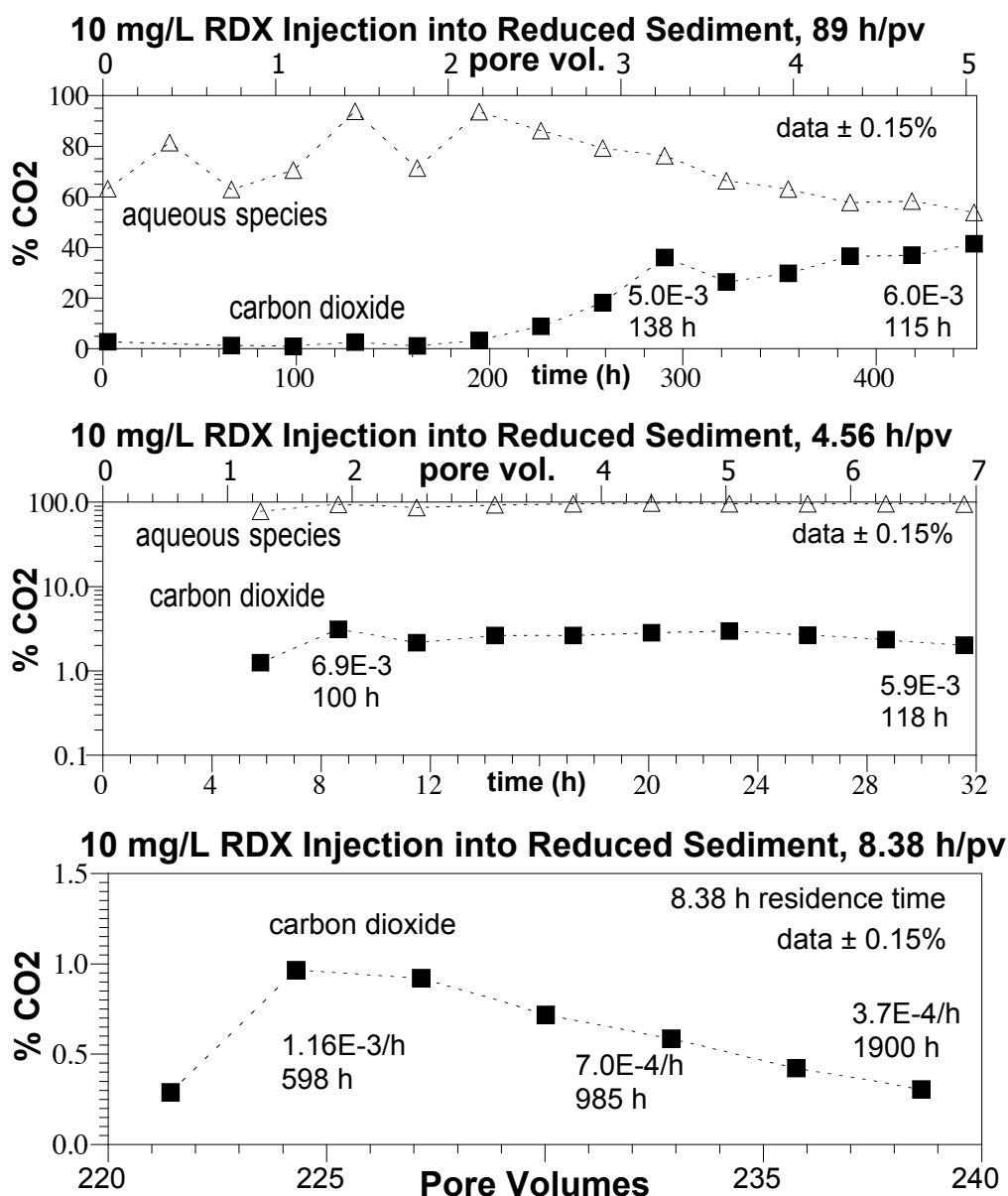
Figure 4.4.3. RDX mineralization in 1-D columns with dithionite-reduced sediment at a residence time of: a) 89 h, b) 4.56 h, and c) 8.38 h residence time.

The lag of initial mineralization for >200 h is indicative of time required for sufficient biomass growth before mineralization would occur in appreciable quantities. The leveling off of the RDX mineralization may be caused by a balance of how much RDX could be mineralized in the 89 h residence time in the column.

The second RDX mineralization column (Figure 4.4.3b) with a 4.56 h residence time was the same sediment column in Figure 4.4.3a (i.e., microbes already mineralizing RDX).

There was no mineralization lag observed, and by 10 h, a steady state ~3% mineralization remained constant for the next 32 h. The calculated mineralization rate was nearly the same as the previous experiment at 100 h to 118 h half-life. During this short amount of time, there was little chance for additional microbial growth, which would (possibly) alter the mineralization rate, so this experiment at a different RDX influx rate simply demonstrates that the ~115 h half-life for RDX is a robust mineralization rate that applies at different flow rates.

In the third RDX mineralization experiment 220 pore volumes of oxygen-saturated water (8.4 mg/L or 0.256 mmol/L) and RDX (10 mg/L or 0.05 mmol/L) was injected through the column before this mineralization experiment (i.e., Figures 4.4.1 and 4.4.2). It was hypothesized that RDX mineralization would be slower in this column, as many of the ferrous iron sites would have been oxidized. Experimental results (Figure 4.4.3c) indeed showed that RDX mineralization was ~6x slower than in highly reduced Ft. Lewis sediment. RDX mineralization half-lives for this partially reduced sediment were 600 h (225 pv) to >1000 h (at >240 pv). The highly reduced Ft. Lewis sediment has a total ferrous iron mass of about 73 μmol/g (Table 4.2.1), which is equivalent to 270 pore volumes of oxygen-saturated water (4 moles of iron are oxidized per mole of O_2 reduced).

RDX sorption would produce a slight lag before appearance in the effluent. Given the RDX sorption (Figure 4.4.4), with $K_d = 0.26$ cm^3/g, the RDX retardation factor should be 2.1, so RDX sorption equilibrium would have been reached by 2 pore volumes after injection in 1-D column experiments shown, so calculation of degradation products would not be influenced, as all data is taken >2 pore volumes.
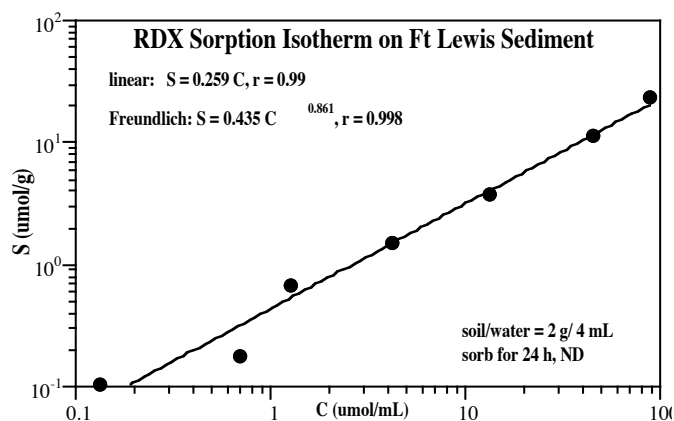
Figure 4.4.4. RDX sorption isotherm on oxic Ft. Lewis sediment (Szecsody et al. 2001). RDX ± 0.5%.

4.4.2 HMX Reactive Transport in Reduced Sediments: Sorption and Degradation

A series of 24 1-D column experiments were conducted with energetic (TNT, HMX) injection into sediment columns with differing amounts of reduction at 10°C, 22°C, 35°C, 49°C, and 62°C. The purpose of this study is to: a) determine accurate energetic degradation rates under field-scale aquifer conditions of high soil/water ratio and temperature, b) determine the

longevity of a reduced sediment zone to degrade energetics, and c) determine the activation energy of energetic degradation by ferrous iron in the sediment. HMX degrades more rapidly with greater ferrous iron present, as shown in batch experiments (Figure 4.2.31), and in 1-D columns (Figure 4.4.5). This initial reaction was shown to be an abiotic reaction (Figure 4.2.31). At the high sediment/water ratios in columns (and in aquifers), the HMX degradation half-life was fairly rapid, with 2.1 h in highly reduced sediment. The HMX degradation half-life increased with lower reduction to 50 h with partially reduced sediment (Figure 4.4.5b). Sorption of HMX to the sediment was calculated from the initial breakthrough, and averaged 0.095 ± 0.013 cm^3/g, or an average retardation factor of 1.4. At colder temperature, the HMX degradation rates (at the same amount of reduction) were more rapid (Figure 4.4.5a, 10°C), and at elevated temperature, the HMX degradation rates were slower (Figure 4.4.5c, 35°C), so the reaction was exothermic. The HMX degradation rates, even in partially reduced sediment (i.e., slowest 1.8 h half-life) were very viable to consider this technology at field scale.

Calculation of the intrinsic HMX degradation rate for all experiments over the 10-62°C temperature range enabled determination the activation energy of the reaction and how this may change with sediment reduction. First, the first-order half-life for each experiment was calculated from the steady state concentration reached during HMX breakthrough. As shown in Figure 4.4.5b, initial HMX breakthrough involves a slight lag due to the solute simply being transported into the column and some lag associated with sorption. Therefore, the steady state concentration was reached by later pore volumes as the process(es) degrading HMX in the reduced sediment reached a state of equilibrium. The first-order degradation rate was calculated from this steady state relative concentration (i.e., 0.70 for the red diamond data in Figure 4.4.5b) and the solute residence time in the column (1.37 h in this case). For this example, the pseudo-first order rate was 0.229/h. Given that the HMX degradation reaction is an electron transfer reaction involving both HMX (electron acceptor) and one or more ferrous iron surface phases (electron donor), the first step in HMX degradation to mononitroso-HMX (Figure 4.2.35) has a second-order rate coefficient. This actual (intrinsic) rate coefficient can be calculated by dividing the pseudo-first order rate coefficient by the number of moles of iron and HMX in the system (6.5E-4 µmol Fe^{II} and 1.27E-7 µmol HMX in this example). The calculated intrinsic rate for this example is 0.00277 [h^{-1} µmol^{-2}]. It should be noted that the ratio of Fe^{II}/HMX is quite large (5100), so degradation of HMX causes an insignificant decrease in the ferrous iron concentration, so another interpretation of the intrinsic rate just considers the Fe^{II} concentration constant. However, because HMX degradation experiments varying the HMX concentration and sediment reduction (i.e., mass of ferrous iron) are being considered, this Fe^{II}/HMX ratio is considerably smaller in the partially reduced sediment. The activation energy is calculated from the change in this intrinsic degradation rate with temperature.

The activation energy for HMX degradation by dithionite-reduced sediment was calculated to be 37.5 kJ/mol, based on moderate and highly reduced sediment experiments (Figure 4.4.6). The amount of ferrous iron in dithionite reduced sediment with a dithionite/iron ratio of 4.1/1 and 22/1 is 70-73 µmol/g (Table 4.2.1), although, as stated earlier, while this reductive capacity is the same (based on dissolved oxygen consumption), there are changes in the actual surface species for highly reduced sediment, which causes more rapid energetic degradation. In
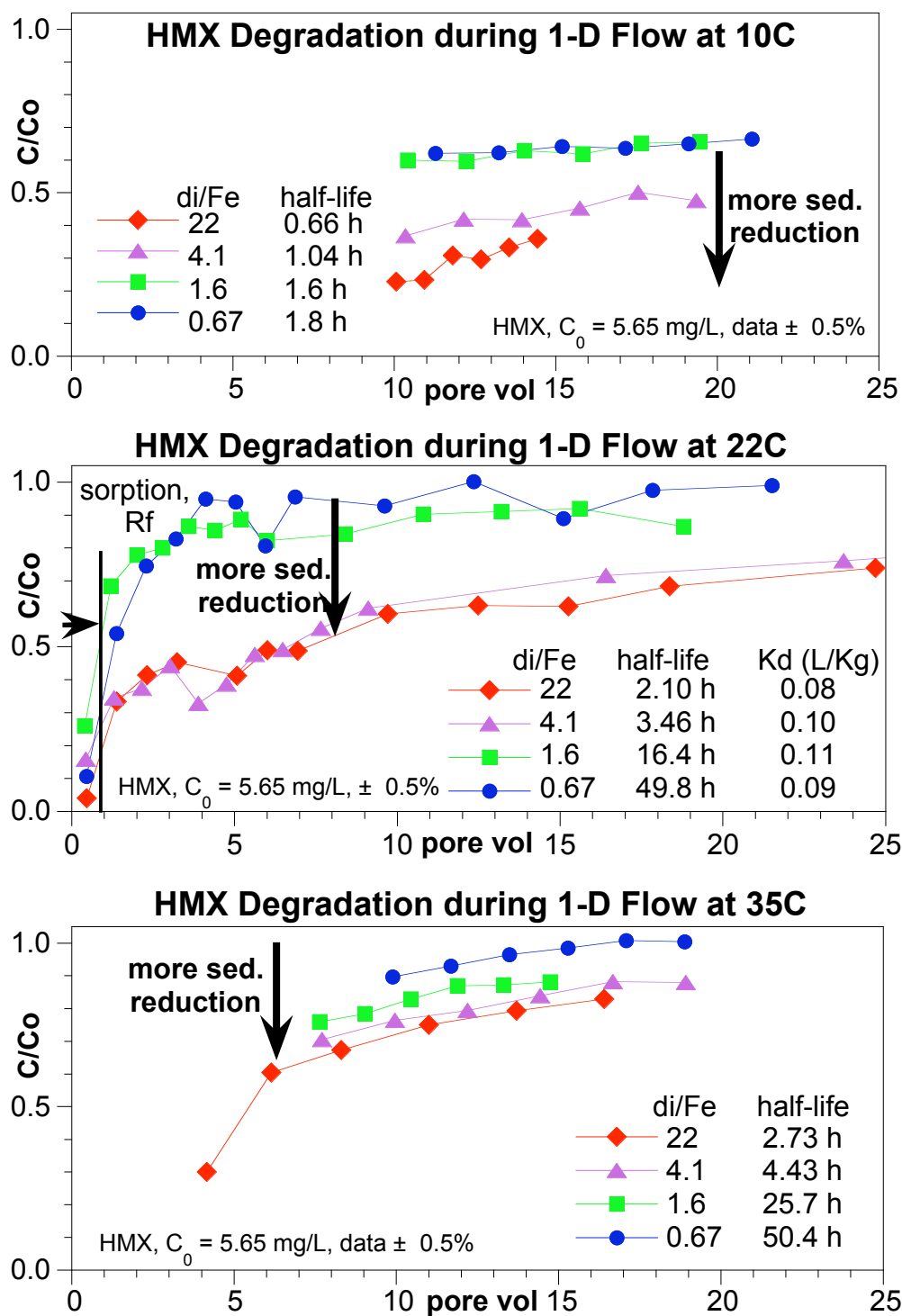
Figure 4.4.5. HMX sorption and degradation in 1-D columns at differing amounts of sediment reduction at: a) 10ºC, b) 22ºC, and c) 35ºC.

sediments with low reduction (i.e., dithionite/iron = 0.67, Figure 4.4.6), the activation energy is nearly zero, likely indicating multiple ferrous iron surface phases (and possibly microbes) are slowly degrading HMX, whereas at high reduction, a single ferrous iron surface phase is degrading HMX (and this exothermic reaction is responding to the temperature change). This 37.5 kJ/mol activation energy is large enough (>10 kJ/mol) that it is most likely a chemically-controlled rate and not a diffusion controlled rate (<10 kJ/mol).

4.4.3 TNT Reactive Transport in Reduced Sediments: Sorption and Degradation

Figure 4.4.6. HMX activation energy in partially to highly reduced sediment, based on column studies (rates ± 20%).

Trinitrotoluene injection into 24 reduced sediment columns at different TNT concentration, sediment reduction, and temperature ($10^{o}C$ to $62^{o}C$) showed roughly results as HMX, with observed sorption and degradation rate increasing with sediment reduction and decreasing temperature (Figure 4.4.7). At 22C TNT sorption was considerable greater than HMX, with a calculated K_d of 1.55 ± 0.67 cm^3/g or an average retardation factor of 8.0 (Figure 4.4.7b). Because mainly the steady state TNT concentration reflecting the degradation rate was desired, in some experiments, effluent sampling was then not conducted for the first 10 pore volumes of the experiment. The TNT degradation rate at $22^{o}C$ was a weak function of the amount of sediment reduction. However, at $10^{o}C$, sediment reduction had a considerable effect on the TNT degradation rate, with a 37x more rapid rate for highly reduced sediment (Figure 4.4.7a) compared with partially reduced sediment. At $35^{o}C$, the TNT degradation rate change with temperature was much smaller (5x) between highly reduced and partially reduced sediment (Figure 4.4.7c). At $49^{o}C$, the TNT degradation rate change between highly and partially reduced sediment was also small (4.3x, in Appendix E). Finally, at $62^{o}C$, the TNT degradation rate change between highly and partially reduced sediment was again small (2.8x). Therefore, this exothermic reaction (i.e., more reactive at colder temperature) appears be considerably less effective at higher temperature.

The exothermic TNT degradation reaction over the entire $10^{o}C$ to $62^{o}C$ temperature range did not show a consistent trend with either temperature or sediment reduction (Figure 4.4.8). The two lowest reductions showed essentially no change in TNT degradation rate over the $52^{o}C$ temperature change (although HMX did not show a change for the lowest reduction, Figure 4.4.6). The two highest reductions showed no change in the TNT degradation rate from $35^{o}C$ to $62^{o}C$, but did show an increase in rate as the temperature decreased from $35^{o}C$ to $10^{o}C$. This lack of consistent trend could reflect experimental artifacts (i.e., one or more set of column experiments contained errors) or it could reflect multiple processes behaving differently over
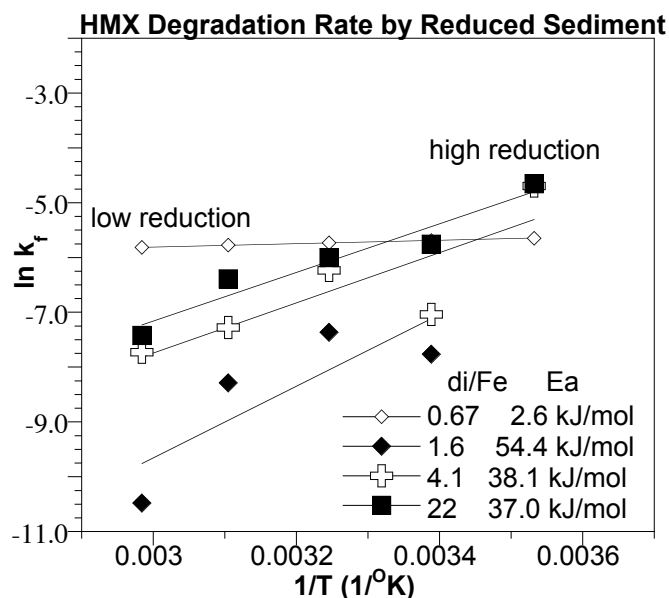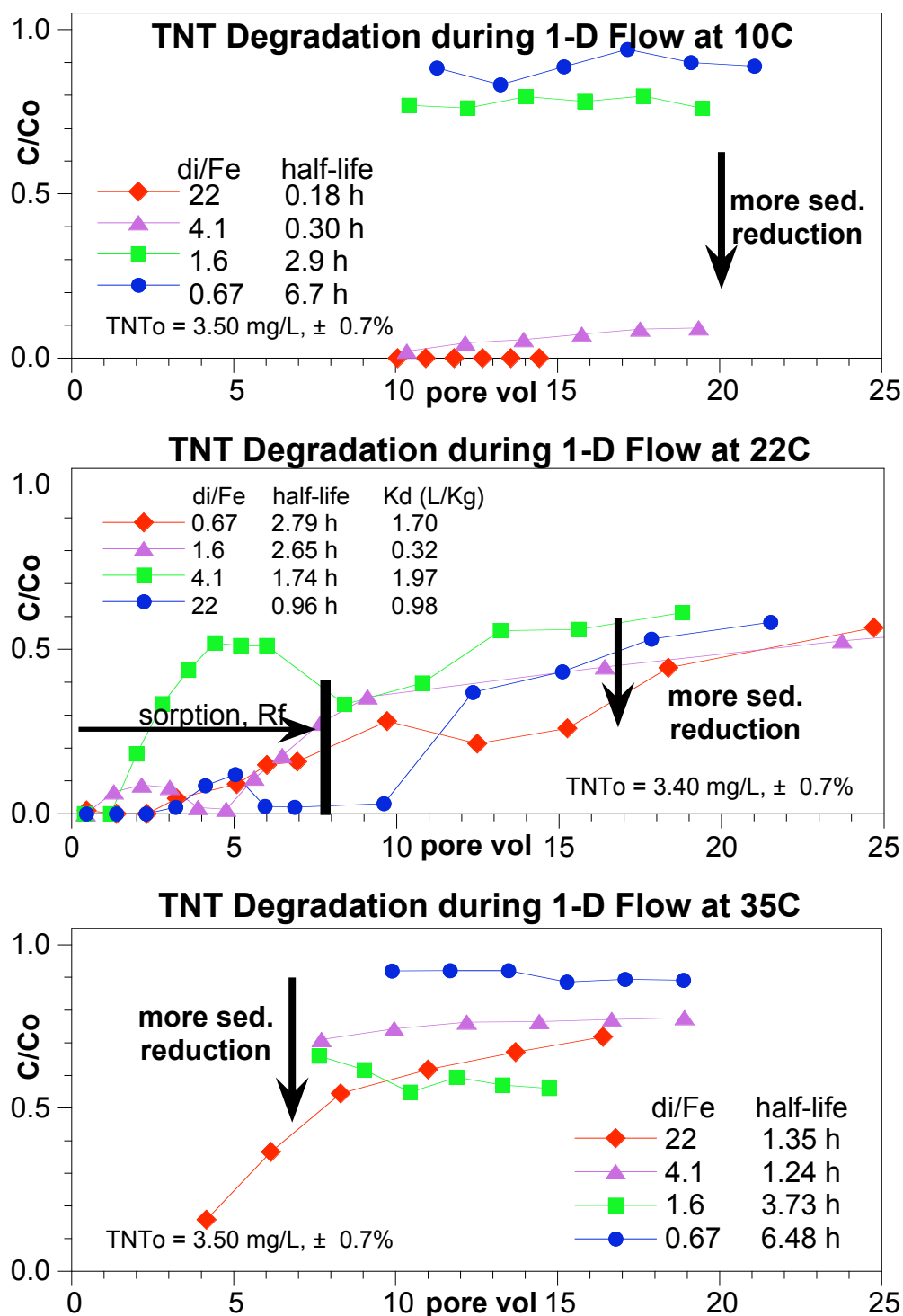
Figure 4.4.7. TNT sorption and degradation in 1-D columns at differing amounts of sediment reduction at: a) 10ºC, b) 22ºC, and c) 35ºC.

the temperature range. Because both HMX and TNT were simultaneously injected in these 24 sediment columns, and the HMX experimental results showed consistent change in the HMX degradation rate over the entire temperature range for the moderate to highly reduced sediment (Figure 4.4.6), this suggests that there were not experimental artifacts in these experiments. Therefore, the inconsistent change in the TNT degradation rate with temperature are likely accurate observations (Figure 4.4.8), but the cause it unknown.

Figure 4.4.8. TNT activation energy in partially to highly reduced sediment, based on column studies (rates ± 20%).

The relative contributions of abiotic and biotic degradation for the initial TNT degradation were not determined in this study, although experimental data shows that both abiotic and biotic processes can rapidly degrade TNT (i.e., Figure 4.2.36 abiotic, Figure 4.2.39 biotic). While no additional nutrients were added to these column experiments, higher temperatures are expected to facilitate more rapid microbial activity. One possible explanation of the observed temperature trends is that lower temperature experiments are dominated by abiotic processes and trends observed in higher temperature experiments are dominated by biotic processes. Between 10°C and 35°C, the two highest reduction data sets were used to calculate an activation energy. This 48.3 to 65 kJ/mol activation energy (chemical control) may, therefore reflect the exothermic reaction of abiotic degradation of TNT. It should be noted that this is an unproven hypothesis, and parallel reduced sediment with and without bactericides could be used to address the relative biotic contribution to the observed trends.

4.5 Energetic Oxidation by Persulfate

In collaboration with ER-1489, energetic degradation (oxidation) experiments were conducted with CL-20 (2,4,6,8,10,12-Hexanitro-2,4,6,8,10,12-Hexaazaisowurzitane, CAS 135285-90-4). CL-20 was the subject of a previous SERDP project (ER-1255), and it is not widely available. These experiments consisted of reacting 3.5 mg/L C-20 in aqueous solution with persulfate at a molar ratio (persulfate/CL-20) at 10:1 and 100:1. These experiments were conducted at 25°C, 30°C, 40°C, 50°C, 60°C, and 70°C. At each temperature, there was an additional vial containing no persulfate, as CL-20 is known to degrade in water. In addition, RDX and HMX persulfate oxidation experiments were conducted at 40°C, for a total of 21 experiments. CL-20 is degraded in aqueous solution in glass vials and at high pH, so polycarbonate vials were used, which was previously demonstrated not to cause CL-20 degradation (Szecsody et al. 2004).
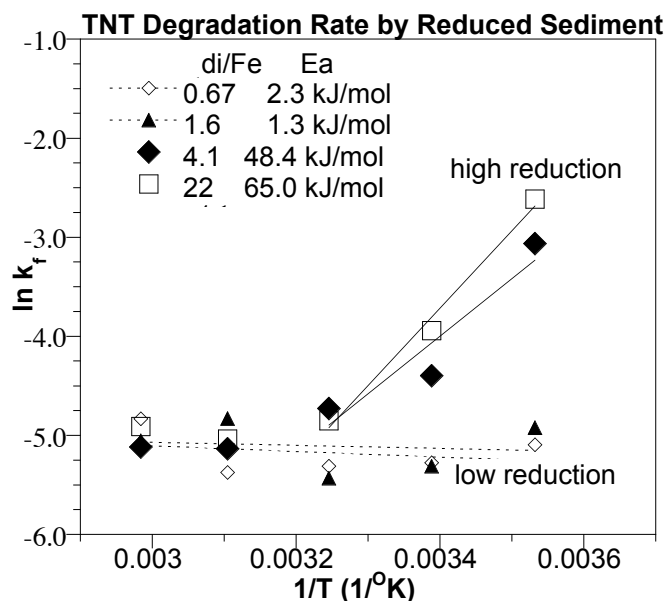
The CL-20 aqueous stability experiments at different temperature (Figure 4.5.1) showed that CL-20 degradation is more rapid at increasing temperature. The half-life at 70°C was 25 h versus 1000 h for 40°C.

CL-20 Aqueous Stability
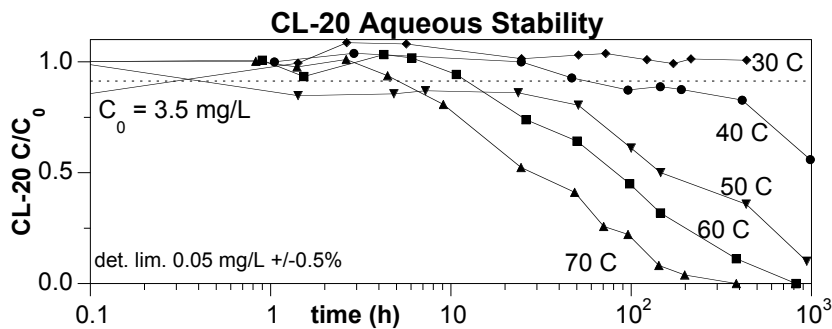
Figure 4.5.1. CL-20 degradation in aqueous solution.

CL-20 reactivity with aqueous persulfate is limited. At 50°C, 60°C, and 70°C, experiments with 10x or 100x (mol/mol) persulfate/CL-20 (Figure 4.5.2) show less degradation than just deionized water. At 30°C and 40°C, the degradation rate in the presence of persulfate is the same as in deionized water. Therefore, it appears that persulfate oxidation would not be a viable subsurface remediation technology for CL-20.

Additional experiments were conducted with RDX and HMX at 40°C and 22°C. In contrast to CL-20, persulfate did degrade RDX and HMX at low concentrations (3.5 mg/L RDX), but did degrade RDX at high concentrations (31 mg/L RDX). Rates were slow; 800 h and 1600 h half-life for RDX with a 4.2 and 11x persulfate/RDX ratio, but more rapid at higher RDX concentration (578 h half life at 31 mg/L RDX, 64x persulfate/RDX ratio. For HMX, at a persulfate/HMX ratio of 71, the degradation half-life was 3200 h, and at a ratio of 140 h, the degradation half-life was 2000 h. The difference in low and high concentration of explosives may reflect degradation of the persulfate at low concentrations in aqueous solution, rendering it much less reactive with the energetic.
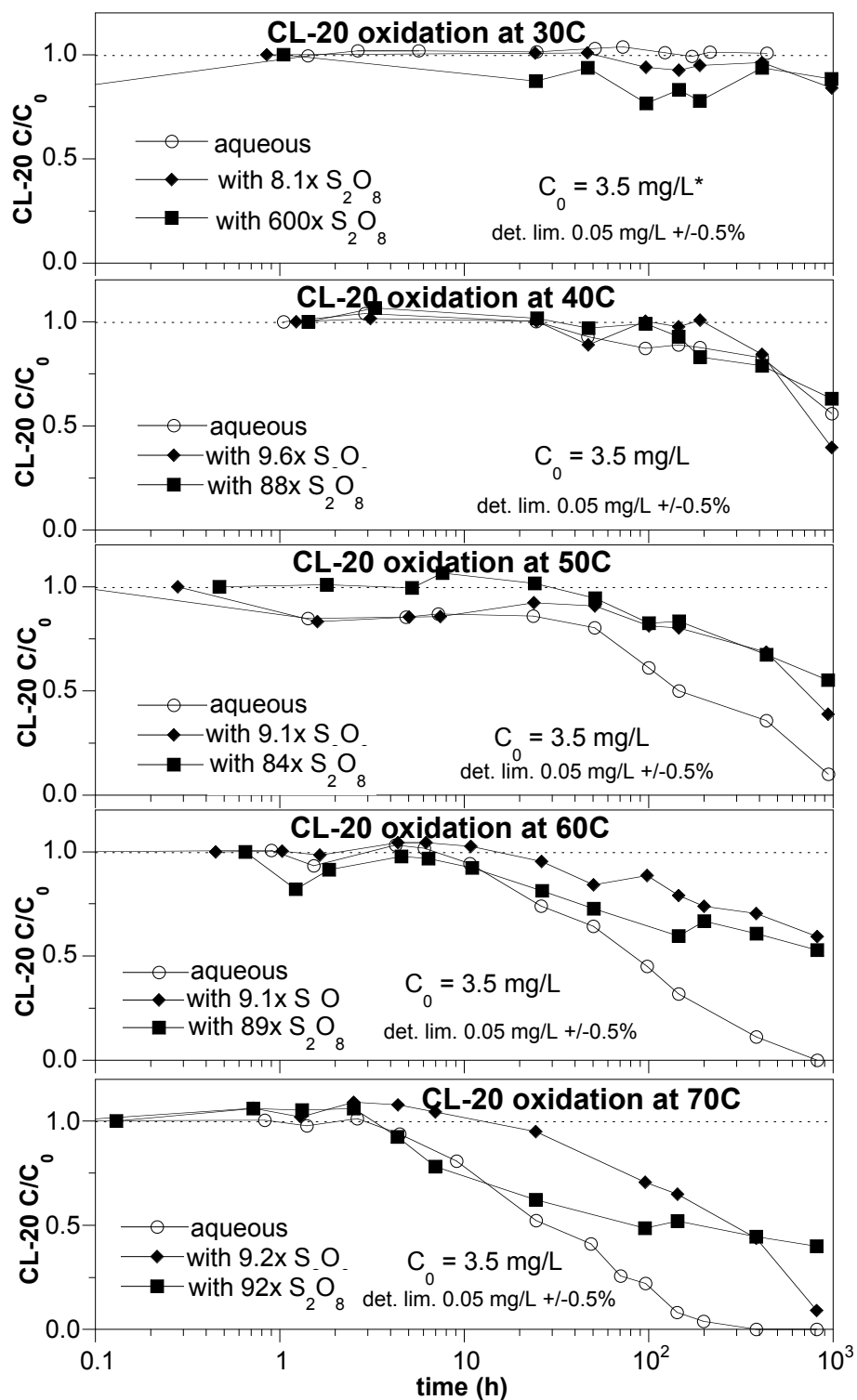
Figure 4.5.2. CL-20 degradation in the presence of aqueous persulfate.

3.5 mg/L RDX oxidation by persulfate at 40C

31 mg/L RDX oxidation by persulfate at 22C

HMX oxidation by persulfate at 40C
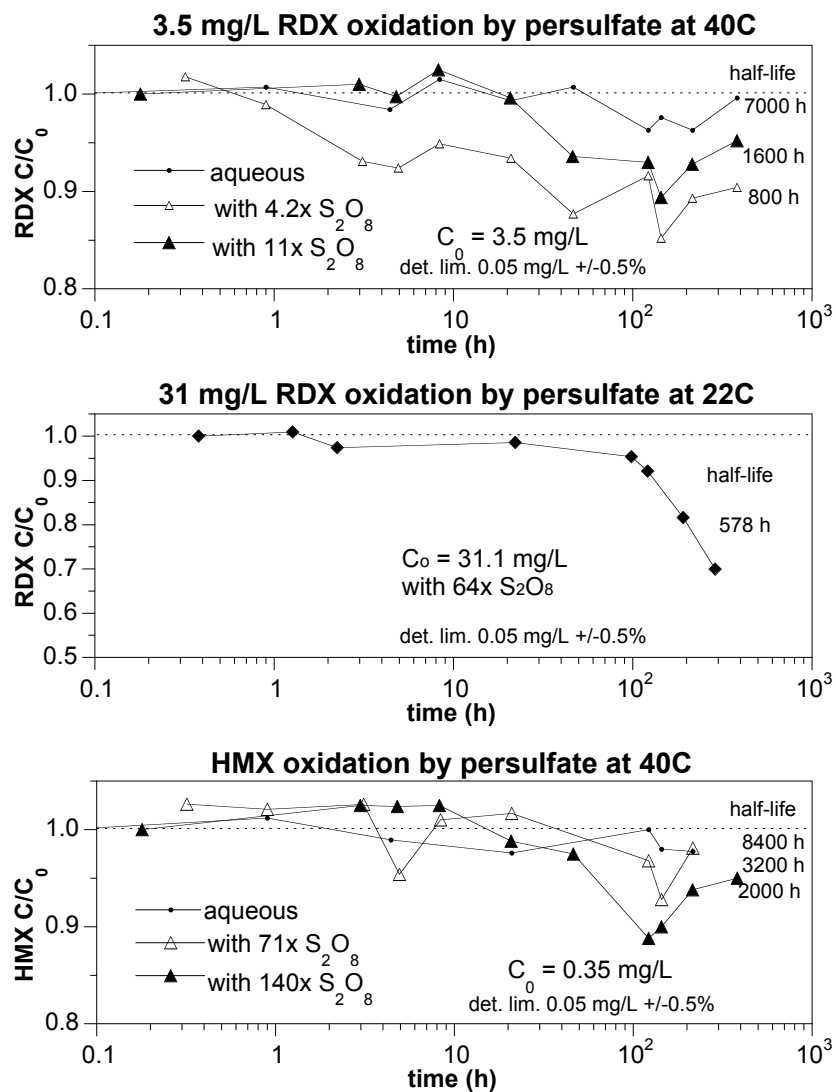
Figure 4.5.3. Persulfate oxidation of a) 3.5 mg/L RDX, b) 31 mg/L RDX, and b) HMX.

5. Summary

This project was initiated by SERDP to quantify processes and determine the effectiveness of abiotic/biotic mineralization of energetics (RDX, HMX, TNT) in aquifer sediments by combinations of biostimulation (carbon, trace nutrient additions) and chemical reduction of sediment to create a reducing environment. Initially it was hypothesized that a balance of chemical reduction of sediment and biostimulation would increase the RDX, HMX, and TNT mineralization rate significantly so that this method could be used for groundwater remediation of energetics. Because both abiotic and biotic processes are involved in energetic mineralization in sediments, it was further hypothesized that consideration for both abiotic reduction *and* microbial growth was need to optimize the sediment system for the most rapid mineralization rate. Results of the numerous experiments within this project do show that there are separate optimal abiotic/biostimulation sediment treatments for RDX/HMX and for TNT. Optimal sediment treatment for RDX and HMX, which have chemical similarities and similar degradation pathways, is mainly chemical reduction of sediment, which increases the RDX/HMX *mineralization* rate 100-150x (relative to untreated sediment), with additional carbon or trace nutrient addition also increasing the RDX/HMX mineralization rate an additional 3-4x. In contrast, the optimal sediment treatment for TNT involves mainly biostimulation (glucose addition), which stimulates a TNT/glucose cometabolic degradation pathway, degrading TNT to amino-intermediates that irreversibly sorb (i.e., end product is not CO_2). TNT mass migration risk is minimized by these transformation reactions, as the triaminotoluene and 2,4- and 2,6-diaminonitrotoluene products produces are irreversibly sorbed to sediment. These transformation rates are increased further by chemical reduction of sediment. So summarizing the optimal aquifer sediment treatment for energetics studied:

Table 5.1. Sediment primary and secondary treatment and energetic degradation.

energetic	untreated sed. mineralization half-life (h)	primary treatment	treated sed. mineralization half-life (h)	secondary treatment	treated sed. mineralization half-life (h)
RDX	31,000	dithionite reduction of sediment	315	carbon addition trace nutrients	140 112
HMX	7,800	dithionite reduction of sediment	162	carbon, trace nutrients	135
TNT*	55,000 (to TAT)	glucose addition (product = TAT)	8030	dithionite reduction of sediment	610

The details of the treatment processes and energetic pathway for each energetic are described in the following sections. In addition the effect of dithionite reduction of sediment on the microbial population survival, growth, and detachment is also described.

5.1 RDX Mineralization Pathway and Rate in Reduced/Biostimulated Sediments

The influence of chemical reduction of sediment on the energetic degradation/ mineralization rate is significant for RDX and HMX (Figure 5.1), but not as significant for TNT (following section). Comparisons of dithionite-reduced sediment to 7 different biostimulation systems (same sediment) and zero valent iron/sediment mixtures show that RDX mineralization rate and extent is the highest for dithionite-reduced sediment, but zero valent iron/sediment mixture is as good a treatment technology (Table 5.2). HMX is mineralized more rapidly than RDX in reduced sediment and the HMX mineralization extent is nearly as high. Given that HMX and RDX degradation steps are similar (nitroso-groups first attacked), it is not surprising that these sequential abiotic/biotic reactions in reduced sediment show similar results.

RDX mineralization increases significantly with dithionite treatment, and indicates subsurface sediment remediation by in situ chemical reduction of sediment should be highly effective. The influence of dithionite treatment in promoting RDX mineralization was far greater than biostimulation alone (i.e., either a carbon source or trace nutrients added, or with prestimulation). More specifically,

Figure 5.1. RDX mineralization rate in sediment/microbe/water systems with dithionite reduction and biostimulation (carbon or trace nutrient addition). Data ± 2%.

RDX mineralization with untreated sediment had a 31,000 h half-life, whereas anoxic biostimulation with lactate addition had a half-life of 9900 h, and biostimulation with trace nutrient addition had a half-life of 14,400 h, and anoxic prestimulation with trace nutrient and carbon source addition (5600 h half-life; Table 5.2). All oxic biostimulation studies showed slower RDX mineralization rates compared with anoxic systems. In contrast, RDX mineralization with dithionite treatment (315 h half-life) or dithionite treatment with trace nutrients (112 h half-life) were 50x to 300x more rapid. Additions of 5-micron zero valent iron (0.04% to 0.4% - same weight percentage as ferrous iron in dithionite-reduced sediment) to sediment achieved nearly the same RDX mineralization rates (373 h to 540 h half-life) as dithionite treated sediment.

The degradation pathway for RDX transformation to carbon dioxide in reduced sediment was determined experimentally (some steps). The first for transformation steps (RDX -> MNX -> DNX -> TNX -> methylene dinitramine) were determined to be abiotic, as the addition of a bactericide to the reduced sediment did not slow the transformation rates. These abiotic transformation steps are rapid (5 minute to 4.5 h half-life, Table 5.3), so not rate limiting in the

Table 5.2. Energetic mineralization rate: comparison of treatments

energetic or intermediate system		CO$_2$ (%)	mineralization time (h)	half-life (h)	rate (1/h)	correlation with reductant	#	R	min. rate (mol g^{-1} d^{-1})
RDX	**no treatment**								
	oxic, no treatment	2.7	1219	31,000	2.24E-05				6.05E-11
	anoxic, no treatment	7.7	1605	14,000	4.95E-05				1.34E-10
	biostimulation								
	oxic biostim: trace nutrients	5.6	1219	14,400	4.81E-05				1.30E-10
	oxic biostim: lactate	3.0	642	14,600	4.75E-05				1.28E-10
	anoxic biostim: glucose	16	1605	6,400	1.08E-04				2.92E-10
	anoxic biostim: glucose, SO$_4$	7.0	1605	15,000	4.62E-05				1.25E-10
	anoxic, prestimulation	1.4	97	4,960	1.40E-04				3.78E-10
	anoxic, prestim. + glucose	0.7	97	9,170	7.56E-05				2.04E-10
	anoxic, prestim. + tr. nutrients	1.2	97	5,570	1.24E-04				3.35E-10
	chemical reduction + biostimulation								
	dithionite addition (di/Fe = 28)	63	1219	315	2.70E-03	$t_{1/2} = 150\ di^{-0.48}$	4	0.78	7.30E-09
	1-D column, dithionite treated sed.	42	89	113.2	6.12E-03				3.31E-08
	1-D column, dithionite treated sed.	2.7	4.5	114.0	6.08E-03				3.29E-08
	1-D column, reduced/oxidized	1.1	8.38	525.1	1.32E-03				7.13E-09
	dithionite + trace nutrients	78.1	1533	112	6.19E-03	$t_{1/2} = 51 di^{-0.55}$	3	0.97	1.67E-08
	dithionite + lactate	26	640	682	1.02E-03	$t_{1/2} = 205\ di^{-0.42}$	6	0.98	2.76E-09
	dithionite + glucose	76.5	1533	140	4.95E-03	$t_{1/2} = 5.5\ di^{-1.2}$	3	0.99	1.34E-08
	zero valent iron addition								
	100% zero valent iron	0.0							0.00E+00
	0.04% zvi + anoxic sediment	42.6	432	540	1.28E-03				3.47E-09
	0.17% zvi + anoxic sediment	41.8	432	553	1.25E-03				3.39E-09
	0.4% zvi + anoxic sediment	55.1	432	373	1.86E-03	$t_{1/2} = 63 zvi^{-0.363}$	3	0.90	5.02E-09
	controls								
	no treatment + bactericides	1.3	1650	87,000	7.97E-06				2.15E-11
	reduced sediment + bactericides	1.1	1650	100,000	6.93E-06				1.87E-11
	0.4% zvi + sediment + bactericides	0.15	170	78,000	8.89E-06				2.40E-11
HMX	**no treatment**								
	anoxic, no treatment	3.1	432	7,800	8.89E-05				1.80E-10
	chemical reduction								
	dithionite addition (high reduction)	66.4	432	162.5	4.27E-03	$t_{1/2} = 9.5\ di^{-1.10}$	4	0.83	8.65E-09
	dithionite addition (low reduction)	20.8	432	670	1.03E-03				2.10E-09
	dithionite (low red.) + glucose + tr. n	24.8	432	560	1.24E-03	(lower % reduction)			2.51E-09
	controls								
	no treatment + bactericides	0.08	192	170,000	4.08E-06				8.26E-12
	reduced sediment + bactericides	0.13	192	100,000	6.93E-06				1.41E-11
TNT	**no treatment**								
	anoxic, no treatment	1.3	1416	54,900	1.26E-05				3.34E-11
	chemical reduction								
	dithionite addition (low reduction)	2.7	1416	28300	2.45E-05				6.47E-11
	dithionite addition (high reduction)	1.8	1416	50300	1.38E-05	$t_{1/2} = 14\ di^{-0.273}$	3	0.99	3.64E-11
	dithionite (low red.) + glucose + tr. n	0.9	1800	47,000	1.47E-05				2.99E-11
	cometabolic TNT/glucose degradation								
	untreated sediment, anoxic	0.80	2400	207000	3.35E-06				8.85E-12
	reduced sediment	0.75	2400	223000	3.14E-06				8.29E-12
	sequential reduced, then oxic sed.	0.71	2400	231000	3.0E-06				7.85E-12
formate	**chemical reduction**								
	dithionite addition (low reduction)	10.4	1700	545	1.27E-03				3.36E-09
	dithionite addition (high reduction)	57.3	1700	59.5	1.16E-02	$t_{1/2} = 190\ di^{-0.48}$	4	0.99	3.08E-08
	controls								
	no treatment	1.3	1700	7400	7.70E-06				1.56E-11
	no treatment + bactericides	0.33	1700	360000	1.94E-06				3.94E-12
	reduced sediment + bactericides	0.25	1700	470000	1.47E-06				2.98E-12

overall RDX to CO$_2$ transformation which increases from a half-life of 31,000 h to 315 h half-life with sediment reduction (Table 5.2). The average RDX to MNX degradation rate (i.e., average of all batch/column experiments) was $1.47 \pm 1.47 \times 10^{-5}$ mol g^{-1} day^{-1} (average half-life 4.8 minutes). The average MNX to DNX degradation rate was $7.42 \pm 9.77 \times 10^{-6}$ mol g^{-1} day^{-1}

(average half-life 32 minutes). The average DNX to TNX degradation rate was 7.28 ± 11.0 x 10^{-6} mol g^{-1} day^{-1} (average half-life 1.8 h). Finally, the average TNX to MDNA degradation rate was 4.48 ± 6.32 x 10^{-6} mol g^{-1} day^{-1} (average half-life 4.5 h). These rates were quantified by a sequential reaction fit to batch data.

Methylene dinitramine (MDNA) transformation in reduced sediments was most rapid by acid hydrolysis (i.e., aqueous degradation reaction) with an average transformation rate of 8.91 ± 2.42 x 10^{-6} mol g^{-1} day^{-1} (average half-life 55 hours). MDNA transformation was slower in reduced sediment relative to untreated sediment, which was initially hypothesized possibly as a biotic reaction (i.e., if the dithionite treatment killed a significant fraction of the population). However, the cause of slower MDNA transformation in reduced sediments is more alkaline pH (8.5 to 9.2) in reduced sediments. The MDNA concentration does not buildup in batch experiments of RDX degradation in dithionite-reduced sediments, but was measured in some 1-D column experiments at low to moderate concentrations. This observation is consistent with aqueous MDNA degradation, as the ~100x lower soil/water ratio in batch experiments leads to greater MDNA degradation. Therefore, given that the range of observed MDNA degradation rates observed in this study only varied between 0.5 h and 250 h (half-life), it is not the rate-limiting step in RDX mineralization, where the half-life decreases from 31,000 h to 315 h upon increasing sediment reduction. However, the slowest MDNA degradation rates were observed in column studies (high soil/water ratios), so it is likely that at the field scale MDNA degradation could be slowing the overall RDX mineralization rate. This can be confirmed by any MDNA buildup over time.

The final RDX mineralization step is the transformation of formate to carbon dioxide. This reaction can occur biotically, but in dithionite-reduced sediments experiments demonstrated that this is a coupled abiotic/biotic reaction. The presence of a bactericide stopped mineralization (i.e., microbes are involved mineralizing formate), and increasing amounts of sediment reduction increased the formate mineralization rate (i.e., abiotic component of the reaction). Formate mineralization was quite slow in untreated sediment (7400 h half-life) with similarity to RDX mineralization (31,000 h half-life), and rapid in reduced sediment (60 h half-life) again with similarity to RDX mineralization (315 h half-life). It is likely that this reaction is the rate-limiting step in RDX mineralization in dithionite-reduced sediments. Therefore, the apparent strong abiotic control of RDX mineralization (i.e., the 270x increase in rate in direct proportion to the amount of dithionite treatment to produce ferrous iron surface phases, Figure 5.2) is actually not abiotic control but increasing the rate of this coupled formate mineralization reaction (which also requires microbes).
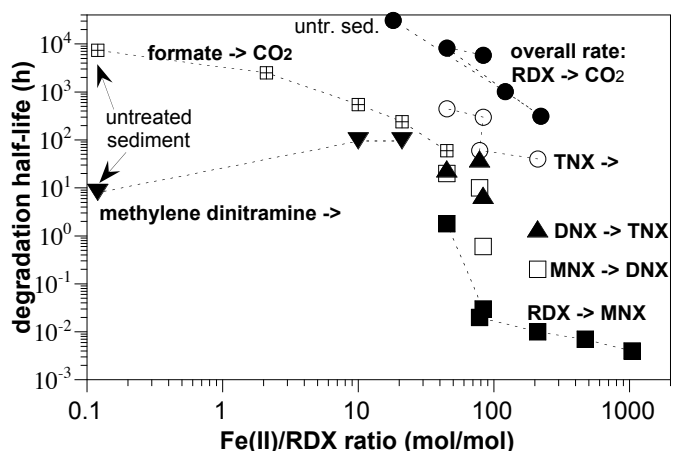
Figure 5.2. Transformation rates of RDX and intermediates in reduced sediments as a function of the ratio of ferrous iron to reactant (rates $\pm 20\%$).

Table 5.3. Degradation rates of RDX and intermediates by reduced sediment/biostimulation.

Solute	sediment (di/Fe = **)	T°C	C/Co	residence time (h)	rate (1/h)	solute conc (mg/L)	r_{sw} (g/mL)	half-life (h)	intrinsic rate (h^{-1} $umol^{-2}$)	degradation rate (mol g^{-1} d^{-1})
RDX	Ft Lewis, di/Fe = 22, W41	22			46.210	10	0.5	0.015	1.12E+00	2.807E-05
	Ft Lewis, di/Fe = 22, W41	22			69.315	10	0.25	0.01	3.37E+00	4.210E-05
	Ft Lewis, di/Fe = 22, W41	22			69.315	10	0.13	0.01	6.75E+00	4.210E-05
	Ft Lewis, di/Fe = 22, W41	22			23.105	10	0.05	0.03	5.62E+00	1.403E-05
	Ft Lewis, di/Fe = 22, W41	22			17.329	10	0.05	0.04	4.22E+00	1.052E-05
	Ft Lewis, di/Fe = 22, W41	22			1.386	10	0.03	0.5	6.75E-01	8.420E-07
	Ft Lewis, di/Fe = 22, W41, pH = 6.1	22			17.329	10	0.05	0.04	4.22E+00	1.052E-05
	Ft Lewis, di/Fe = 22, W41, pH = 7.0	22			5.776	10	0.05	0.12	1.41E+00	3.508E-06
	Ft Lewis, di/Fe = 22, W41, pH = 7.9	22			11.552	10	0.05	0.06	2.81E+00	7.016E-06
	Ft Lewis, di/Fe = 22, W41, pH = 9.1	22			17.329	10	0.05	0.04	4.22E+00	1.052E-05
	Ft Lewis, di/Fe = 22, W41	22			11.552	10	4.5	0.06	3.12E-02	7.016E-06
	Ft Lewis, di/Fe = 22, W41	22	0.3	4.4	0.081	10	4.5	8.55	2.19E-04	4.923E-08
MNX	Ft Lewis, di/Fe = 22, W41	22			34.657	10	0.5	0.02	7.82E-01	2.268E-05
	Ft Lewis, di/Fe = 22, W41	22			34.657	10	0.25	0.02	1.56E+00	2.268E-05
	Ft Lewis, di/Fe = 22, W41	22			6.931	10	0.13	0.1	6.26E-01	4.537E-06
	Ft Lewis, di/Fe = 22, W41	22			1.155	10	0.05	0.6	2.61E-01	7.561E-07
	Ft Lewis, di/Fe = 22, W41	22			1.386	10	0.05	0.5	3.13E-01	9.074E-07
	Ft Lewis, di/Fe = 22, W41	22			0.277	10	0.03	2.5	1.25E-01	1.815E-07
	Ft Lewis, di/Fe = 22, W41	22			11.552	10	4.5	0.06	2.90E-02	7.561E-06
	Ft Lewis, di/Fe = 22, W41	22	0.1	4.4	0.024	10	4.5	28.95	6.01E-05	1.567E-08
DNX	Ft Lewis, di/Fe = 22, W41	22			34.657	10	0.5	0.02	7.22E-01	2.459E-05
	Ft Lewis, di/Fe = 22, W41	22			34.657	10	0.25	0.02	1.44E+00	2.459E-05
	Ft Lewis, di/Fe = 22, W41	22			0.578	10	0.13	1.2	4.81E-02	4.099E-07
	Ft Lewis, di/Fe = 22, W41	22			0.204	10	0.05	3.4	4.24E-02	1.447E-07
	Ft Lewis, di/Fe = 22, W41	22			0.315	10	0.05	2.2	6.56E-02	2.236E-07
	Ft Lewis, di/Fe = 22, W41	22			0.124	10	0.03	5.6	5.15E-02	8.784E-08
	Ft Lewis, di/Fe = 22, W41	22			11.552	10	4.5	0.06	2.67E-02	8.198E-06
	Ft Lewis, di/Fe = 22, W41	22	0.02	4.4	0.005	10	4.5	150.96	1.06E-05	3.258E-09
TNX	Ft Lewis, di/Fe = 22, W41	22			17.329	10	0.5	0.04	3.30E-01	1.343E-05
	Ft Lewis, di/Fe = 22, W41	22			17.329	10	0.25	0.04	6.61E-01	1.343E-05
	Ft Lewis, di/Fe = 22, W41	22			0.020	10	0.13	35	1.51E-03	1.535E-08
	Ft Lewis, di/Fe = 22, W41	22			0.013	10	0.05	52	2.54E-03	1.033E-08
	Ft Lewis, di/Fe = 22, W41	22			0.011	10	0.05	65	2.03E-03	8.263E-09
	Ft Lewis, di/Fe = 22, W41	22			0.004	10	0.03	160	1.65E-03	3.357E-09
	Ft Lewis, di/Fe = 22, W41	22			11.552	10	4.5	0.06	2.45E-02	8.952E-06
	Ft Lewis, di/Fe = 22, W41	22	0.015	4.4	0.003	10	4.5	202	7.28E-06	2.662E-09
MDNA	Ft Lewis, di/Fe = 22, W41	22			1.386	10		0.5	#DIV/0!	1.374E-06
	Ft Lewis, di/Fe = 22, W41	22			69.315	10	0.25	0.01	2.07E+00	6.872E-05
	Ft Lewis, di/Fe = 22, W41	22			0.069	10	0.13	10	4.13E-03	6.872E-08
	Ft Lewis, di/Fe = 22, W41	22			0.017	10	0.05	40	2.58E-03	1.718E-08
	Ft Lewis, di/Fe = 22, W41	22			0.008	10	0.05	90	1.15E-03	7.635E-09
	Ft Lewis, di/Fe = 22, W41	22			0.003	10	0.03	250	8.26E-04	2.749E-09
	Ft Lewis, di/Fe = 22, W41	22			1.118	10	4.5	0.62	1.85E-03	1.108E-06
	Ft Lewis, di/Fe = 22, W41	22	0.003	4.4	0.001	10	4.5	1015.09	1.13E-06	6.770E-10

5.2 HMX Mineralization Pathway and Rate in Reduced/Biostimulated Sediments

HMX mineralization in reduced sediments was predominantly a function of the amount of sediment reduction (Figure 5.3a), with a smaller function of biostimulation (trace nutrient or carbon addition, Figure 5.3b), similar to previous studies of RDX. In untreated sediment, the HMX mineralization rate was very slow (half-life 7800 h), whereas in dithionite-reduced sediments, HMX mineralization was 48x more rapid (162 h half-life). Mineralization extent in reduced sediments was as much as 66.4%.

The HMX degradation pathway in reduced sediment is very similar to RDX with initial attack of the nitroso- groups, then ring cleavage forming methylene dinitramine (Figure 4.2.35). The first five degradation products were identified by LC-MS (Dr. Steve Comfort, UNL) as mono-, di-, tri, and tetra-nitrosoHMX and methylene dinitramine. The initial degradation reaction of HMX to mononitrosoHMX is an abiotic reaction, as the addition of a bactericide did not slow HMX degradation in reduced sediment. In addition, greater sediment reduction (more ferrous iron) increased the rate of this initial reaction. The activation energy for this initial HMX degradation reaction by dithionite-reduced sediment was calculated to be 37.5 kJ/mol, based on moderate and highly reduced sediment 1-D column experiments (Figure 4.4.6). This reaction is actually exothermic, so is more rapid at colder temperatures.

Figure 5.3. HMX mineralization rate in reduced sediments: a) as a function of the amount of reduction and b) with nutrients (data ± 2%).

The average HMX transformation rate is 1.6×10^{-6} mol g^{-1} day^{-1} (average half-life 48 minutes) at 22°C in packed porous media (high soil/water ratio of 1-D columns and aquifers, Table 5.4). This rate is still two to three orders of magnitude more rapid than the overall HMX mineralization rate, so not rate limiting. Although fewer HMX intermediates were investigated, previously described degradation of methylene dinitramine (half-life 8 h in reduced sediment) indicates that it is also not the rate limiting step. The coupled mineralization of formate, which is very slow in untreated sediment (7400 h half-life) and rapid in reduced sediment (60 h half-life) could be the rate-limiting step for HMX mineralization, where the mineralization half-life changes from 7800 h in untreated sediment to 162 h in reduced sediment.

Table 5.4. Degradation rates of HMX by reduced sediment/biostimulation.

sediment (di/Fe = **)	T°C	C/Co	residence time (h)	rate (1/h)	solute conc (mg/L)	r_{sw} (g/mL)	half-life (h)	intrinsic rate (h^{-1} $umol^{-2}$)	degradation rate (mol g^{-1} d^{-1})
Ft Lewis, di/Fe = 0.67, W46	10	0.64	1.14	0.391	5.0	4.5	1.77	2.17E-02	8.916E-08
Ft Lewis, di/Fe = 1.6, W47	10	0.62	1.11	0.431	5.0	4.5	1.61	1.22E-02	9.809E-08
Ft Lewis, di/Fe = 4.1, W48	10	0.48	1.10	0.667	5.0	4.5	1.039	1.27E-02	1.520E-07
Ft Lewis, di/Fe = 22, W49	10	0.34	1.02	1.058	5.0	4.5	0.655	1.93E-02	2.409E-07
Ft Lewis, di/Fe = 0.67, W28	22	0.86	1.01	0.149	0.6	4.5	4.64	6.90E-02	4.081E-09
Ft Lewis, di/Fe = 1.6, W27	22	0.78	1.03	0.241	0.6	4.5	2.87	5.69E-02	6.593E-09
Ft Lewis, di/Fe = 4.1, W26	22	0.61	0.73	0.677	0.6	4.5	1.024	1.07E-01	1.851E-08
Ft Lewis, di/Fe = 22, W25	22	0.73	0.58	0.543	0.6	4.5	1.277	8.24E-02	1.483E-08
Ft Lewis, di/Fe = 0.67, W31	22	0.975	2.19	0.012	5.65	4.5	59.96	5.67E-04	2.975E-09
Ft Lewis, di/Fe = 1.6, W32	22	0.89	2.50	0.047	5.65	4.5	14.87	1.17E-03	1.200E-08
Ft Lewis, di/Fe = 4.1, W30	22	0.71	1.37	0.250	5.65	4.5	2.773	4.20E-03	6.434E-08
Ft Lewis, di/Fe = 22, W29	22	0.61	2.16	0.229	5.65	4.5	3.029	3.69E-03	5.890E-08
Ft Lewis, di/Fe = 0.67, W36	35	0.985	1.10	0.014	4.5	4.5	50.45	8.46E-04	2.816E-09
Ft Lewis, di/Fe = 1.6, W35	35	0.89	1.40	0.083	4.5	4.5	8.33	2.62E-03	1.706E-08
Ft Lewis, di/Fe = 4.1, W34	35	0.87	0.89	0.156	4.5	4.5	4.430	3.30E-03	3.207E-08
Ft Lewis, di/Fe = 22, W33	35	0.81	0.83	0.254	4.5	4.5	2.730	5.14E-03	5.204E-08
Ft Lewis, di/Fe = 0.67, W40	49	0.995	1.00	0.005	4.13	4.5	138.28	3.36E-04	9.430E-10
Ft Lewis, di/Fe = 1.6, W39	49	0.98	0.75	0.027	4.13	4.5	25.73	9.23E-04	5.068E-09
Ft Lewis, di/Fe = 4.1, W38	49	0.925	0.80	0.097	4.13	4.5	7.113	2.24E-03	1.833E-08
Ft Lewis, di/Fe = 22, W37	49	0.89	0.75	0.155	4.13	4.5	4.461	3.43E-03	2.923E-08
Ft Lewis, di/Fe = 0.67, W44	62	0.995	7.25	0.001	5.14	4.5	1002.55	3.73E-05	1.619E-10
Ft Lewis, di/Fe = 1.6, W43	62	0.84	8.19	0.021	5.14	4.5	32.56	5.86E-04	4.984E-09
Ft Lewis, di/Fe = 4.1, W42	62	0.755	6.51	0.043	5.14	4.5	16.056	7.98E-04	1.011E-08
Ft Lewis, di/Fe = 22, W41	62	0.685	4.56	0.083	5.14	4.5	8.354	1.47E-03	1.943E-08
Ft Lewis, di/Fe = 22, batch	22	0.5	7.87	0.088	5.00	0.5	7.870	2.86E-02	2.006E-08
Ft Lewis, di/Fe = 22, batch	22	0.5	8.40	0.083	5.00	0.5	8.400	2.68E-02	1.879E-08
Ft Lewis, di/Fe = 22, batch	22	0.5	2.70	0.257	5.00	0.25	2.700	4.16E-02	5.847E-08
Ft Lewis, di/Fe = 22, batch	22	0.5	0.42	1.650	5.00	0.13	0.420	1.34E-01	3.759E-07

5.3 TNT Degradation Pathway and Rate in Biostimulated/Reduced Sediments

Trinitrotoluene is degraded to triaminotoluene (TAT) and possibly further by a cometabolic process at a moderate rate with glucose addition (primary treatment) and sediment reduction (secondary treatment). Degradation of TNT to triaminotoluene in untreated sediment had a half-life of 55,000 h, which was 7x more rapid in glucose-amended sediment (half-life 8050 h, Figure 5.4a), and an additional 13x more rapid in dithionite-reduced sediment that was glucose amended (half-life 610 h, Figure 5.4b, Table 5.6). The final product (triaminotoluene) is difficult to measure due to irreversible sorption and rapid aqueous degradation, so it may be degraded further. This cometabolic process was previously reported (Daun et al. 1998; Achtnich et al. 1999; Elovitz and Weber 1999; Weiss et al. 2004) for treatment of surface soils, which contained bacteria, daphnids, algae, cress plants, and earthworms, but has not been reported in a subsurface sediment containing only bacteria. This amino-degradation pathway is a viable subsurface remediation technology as it produces dinitroaminotoluene and triaminotoluene products that irreversibly sorb, which was demonstrated in this project. A number of experiments were conducted in this study to prove that this TNT amino-degradation pathway was a viable subsurface remediation technology. These included sorption mass, rate, and reversibility experiments for TNT, 2-aminodinitrotoluene, 4-aminodinitrotoluene, 2,4-diaminonitrotoluene, 2,6-diaminonitrotoluene, and triaminotoluene. In addition, degradation rate experiments were conducted with TNT and these intermediates with oxic and reduced subsurface sediments. While sorption of TNT and the initial degradation products 2-ADNT and 4-ADNT was

reversible, sorption of the further degradation products 2,4-DANT, 2,6-DANT, and TAT was not reversible (Table 5.5). Sorption reversibility was characterized with a methanol extraction for 18 h with sonication. Previous research (Weiss et al. 2004) demonstrated that DANT compounds form covalent bonds with sediment components.

Both 2-ADNT and 4-ADNT degraded in reduced sediment that was a function of the amount of sediment reduction. With *highly* reduced sediment, the degradation half-life for 2-ADNT was 1.3 h and for 4-ADNT was 2.0 h. In partially reduced sediment, the degradation half-life for 2-ADNT was 110 h, and for 4-ADNT was 100 h. Both 2,4-DANT and 2,6-DANT degraded in reduced sediment more rapidly with the amount of sediment reduction (available ferrous iron, Figure 4.2.51). In *highly* reduced sediment, 2,4-DANT degradation half-life was 3.0 h and 2,6-DANT degradation half-life was 1.5 h. In partially reduced sediment, the 2,4-DANT degradation half-life was 100 h, and 2,6-DNT degradation half-life was 65 h. There was no degradation of 2,4-DANT or 2,6-DANT in unreduced sediments (data to 1500 h). The aqueous stability of triaminotoluene (TAT) was investigated as a function of pH, dissolved oxygen, UV light, presence of sediment, and amount of sediment reduction.

Triaminotoluene degraded rapidly by acid hydrolysis. At pH 2.5, the TAT degradation rate is more rapid (half-life 3.8 h), and at neutral pH, the TAT

Figure 5.4. TNT/glucose cometabolic degradation in a) untreated, and b) reduced sediment. TNT (red) and ADNT (yellow) are mobile (reversibly sorb), whereas DANT (blue) and TAT (green) irreversibly sorb.

Table 5.5. Sorption mass, rate, and reversibility for TNT and amino-intermediates.

compound	Kd (L/Kg)	reversible	rate (1/h)
TNT	0.900 ± 0.28	yes	0.24
2-ADNT	0.476 ± 0.22	partial	0.22
4-ADNT	0.393 ± 0.24	yes	0.16
2,4-DANT	0.301 ± 0.26	no	0.62
2.6-DANT	0.480 ± 0.16	no	0.31
TAT	1.25 ± 0.24	no	0.53

degradation rate is more slow (half-life 88 h), although still is not entirely stable. Under alkaline conditions, TAT is somewhat more stable, with a degradation half-life of 171 h at pH 8.8, and 306 h at pH 12. Therefore, TAT was likely degraded in oxic and reduced sediments, but more slowly in reduced sediments due to the increase in pH. Sediment interactions were difficult to

conduct with TAT due to the lack of sorption reversibility (i.e., it was not possible to determine if TAT was irreversibly sorbed or degraded).

Degradation rates were quantified for TNT and intermediates along this cometabolic pathway (i.e., with glucose addition) in oxic, anoxic, partially-reduced, and fully-reduced sediment (Table 5.6). The most rapid degradation occurred in reduced sediments (with glucose addition). In reduced sediment, the TNT degradation rate was 2.4×10^{-7} mol g^{-1} day^{-1} (half-life 18 h), the 2-ADNT degradation rate was 9.7×10^{-7} mol g^{-1} day^{-1} (half-life 0.31 h), the 4-ADNT degradation rate was 4.6×10^{-7} mol g^{-1} day^{-1} (half-life 0.65 h), the 2,6-DANT degradation rate was 3.1×10^{-7} mol g^{-1} day^{-1} (half-life 1.0 h), the 2,4-DANT degradation rate was 6.6×10^{-7} mol g^{-1} day^{-1} (half-life 0.46 h), and the TAT degradation rate was 1.1×10^{-8} mol g^{-1} day^{-1} (half-life 381 h).

The subsequent oxidation of all of these experimental systems should lead to greater mineralization for the reduced systems, assuming processes that occurred in sequential anaerobic/aerobic sludge (Achtnich et al. 1999; Elovitz and Weber 1999) would also occur in the subsurface sediment. Oxidation of these anaerobic and reduced experimental systems did not, in fact, show any additional mineralization in 1000 h of oxidation after the initial 1600 h of anaerobic or reducing conditions. The mineralization extent in the first 1600 h or anaerobic or reducing conditions and in the subsequent 1000 h of oxidation were all <1% and rates were extremely slow ($<3 \times 10^{-11}$ mol g^{-1} day^{-1}).

The extent to which abiotic versus biotic reactions control the TNT/glucose cometabolic degradation to TAT has only been partially determined. Clearly, the major influence on TNT degradation along this pathway is microbial enzymatic degradation. However, individual degradation experiments with TNT and amino-intermediates (Table 5.6) have demonstrated increased degradation in the same sediment with greater sediment reduction. It is therefore clear that abiotic (or coupled abiotic/biotic) reactions are therefore increasing the rate of this amino-degradation pathway. Abiotic contribution to the rate is approximately equal to biotic contribution as glucose addition alone increased the TNT -> TAT rate 6.8x, whereas additional dithionite treatment increased the rate an additional 13x, for a total of 90x increase in rate, compared to untreated sediment.

TNT mineralization in dithionite-reduced sediments (*without* glucose cometabolic degradation) behaves very differently than RDX and HMX (Table 5.7 for TNT versus Table 5.3 for RDX and Table 5.4 for HMX). The TNT initial transformation rate does increase with increasing amount of ferrous iron (indicating abiotic control, Table 5.7). However, TNT mineralization was very small in untreated and reduced sediments (<2.7% in 1400 h, Table 5.2) and showed no trend in rate with increasing dithionite treatment of sediment. Therefore, TNT degradation in this subsurface sediment appears to be greatly enhanced by predominantly biostimulation (cometabolic degradatioin with glucose), which produces irreversibly sorbed triaminotoluene. Dithionite reduction of sediment greatly accelerated this biostimulation process (by about 11x), but abiotic reactions appeared secondary to the primarily biotic degradation process. TNT mineralization was small in both biostimulated and/or dithionite-reduced sediments, TNT degradation to triaminotoluene is a viable subsurface remediation technology, due to the irreversible sorption of TAT (i.e., it is no longer mobile in the subsurface environment).

Table 5.6. Degradation rates of TNT and amino-intermediates by biostimulation (cometabolic degradation w/glucose) with or without sediment reduction.

Solute	sediment (di/Fe = **)	T°C	C/Co	residence time (h)	rate (1/h)	solute conc (mg/L)	r_{sw} (g/mL)	half-life (h)	intrinsic rate (h^{-1} $umol^{-z}$)	degradation rate (mol g^{-1} d^{-1})
TNT	oxic Ft Lewis sediment	22		2300	2.89E-03	105	0.23	240	1.08E-03	1.801E-08
	anaerobic Ft Lewis sediment			2300	4.08E-04	105	0.23	1700	1.53E-04	2.543E-09
	reduced Ft Lewis sed. (di/Fe = 11)			2300	2.67E-02	105	0.23	26	1.43E-04	1.663E-07
	reduced Ft Lewis sed. (di/Fe = 37)			2300	3.85E-02	105	0.23	18	1.97E-04	2.402E-07
2-ADNT	oxic Ft Lewis sediment	22		2300	6.30E-04	105	0.23	1100	2.36E-04	3.930E-09
	anaerobic Ft Lewis sediment			2300	1.78E-05	105	0.23	39000	6.65E-06	1.108E-10
	reduced Ft Lewis sed. (di/Fe = 4)			2300	2.86E-03	105	0.23	242	1.53E-05	1.786E-08
	reduced Ft Lewis sed. (di/Fe = 22)			2300	3.77E-03	105	0.23	184	1.93E-05	2.349E-08
	reduced Ft Lewis sed. (di/Fe = 1.8)				6.80E-03	7.33	0.07	102	2.80E-03	2.959E-09
	reduced Ft Lewis sed. (di/Fe = 11)				2.17E+00	7.33	0.07	0.32	5.25E-01	9.431E-07
	reduced Ft Lewis sed. (di/Fe = 37)				2.24E+00	7.33	0.07	0.31	5.42E-01	9.735E-07
4-ADNT	oxic Ft Lewis sediment	22		2300	6.30E-04	105	0.23	1100	2.36E-04	3.930E-09
	anaerobic Ft Lewis sediment			2300	1.78E-05	105	0.23	39000	6.65E-06	1.108E-10
	reduced Ft Lewis sed. (di/Fe = 4)			2300	2.86E-03	105	0.23	242	1.53E-05	1.786E-08
	reduced Ft Lewis sed. (di/Fe = 22)			2300	3.77E-03	105	0.23	184	1.93E-05	2.349E-08
	reduced Ft Lewis sed. (di/Fe = 1.8)				8.15E-03	7.33	0.07	85	3.36E-03	3.550E-09
	reduced Ft Lewis sed. (di/Fe = 11)				8.35E-01	7.33	0.07	0.83	2.02E-01	3.636E-07
	reduced Ft Lewis sed. (di/Fe = 37)				1.07E+00	7.33	0.07	0.65	2.59E-01	4.643E-07
2,6-DANT	oxic Ft Lewis sediment	22		2300	8.63E-05	105	0.23	8030	3.23E-05	5.383E-10
	anaerobic Ft Lewis sediment			2300	6.30E-05	105	0.23	11000	2.36E-05	3.930E-10
	reduced Ft Lewis sed. (di/Fe = 4)			2300	7.97E-04	105	0.23	870	4.26E-06	4.969E-09
	reduced Ft Lewis sed. (di/Fe = 22)			2300	1.14E-03	105	0.23	610	5.83E-06	7.087E-09
	reduced Ft Lewis sed. (di/Fe = 1.8)				7.37E-03	7.33	0.07	94	3.03E-03	3.210E-09
	reduced Ft Lewis sed. (di/Fe = 11)				3.01E-01	7.33	0.07	2.30	7.31E-02	1.312E-07
	reduced Ft Lewis sed. (di/Fe = 37)				7.15E-01	7.33	0.07	0.97	1.73E-01	3.111E-07
2,4-DANT	oxic Ft Lewis sediment	22		2300	8.63E-05	105	0.23	8030	3.23E-05	5.383E-10
	anaerobic Ft Lewis sediment			2300	6.30E-06	105	0.23	110000	2.36E-06	3.930E-11
	reduced Ft Lewis sed. (di/Fe = 4)			2300	7.97E-04	105	0.23	870	4.26E-06	4.969E-09
	reduced Ft Lewis sed. (di/Fe = 22)			2300	1.14E-03	105	0.23	610	5.83E-06	7.087E-09
	reduced Ft Lewis sed. (di/Fe = 1.8)				8.06E-03	7.33	0.07	86	3.32E-03	3.509E-09
	reduced Ft Lewis sed. (di/Fe = 11)				5.33E-01	7.33	0.07	1.30	1.29E-01	2.321E-07
	reduced Ft Lewis sed. (di/Fe = 37)				1.51E+00	7.33	0.07	0.46	3.65E-01	6.561E-07
TAT	oxic Ft Lewis sediment	22		2300	1.73E-05	105	0.23	40000	6.49E-06	1.081E-10
	anaerobic Ft Lewis sediment			2300	3.47E-06	105	0.23	200000	1.30E-06	2.161E-11
	reduced Ft Lewis sed. (di/Fe = 4)			2300	3.15E-04	105	0.23	2200	1.68E-06	1.965E-09
	reduced Ft Lewis sed. (di/Fe = 22)			2300	1.82E-03	105	0.23	381	9.33E-06	1.135E-08
	aqueous, pH 3.3 (no sediment)				1.58E-01	105	0.23	4.4	5.90E-02	9.825E-07
	aqueous, pH 7.1 (no sediment)				5.55E-03	105	0.23	125	2.08E-03	3.458E-08
	aqueous, pH 8.8 (no sediment)				2.10E-03	105	0.23	330	1.12E-05	1.310E-08
	aqueous, pH 12 (no sediment)				1.05E-03	105	0.23	660	5.39E-06	6.550E-09
CO2	oxic Ft Lewis sediment	22		2300	0.00E+00	105	0.23	198000	0.00E+00	0.000E+00
	anaerobic Ft Lewis sediment			2300	0.00E+00	105	0.23	234000	0.00E+00	0.000E+00
	reduced Ft Lewis sed. (di/Fe = 4)			2300	0.00E+00	105	0.23	212000	0.00E+00	0.000E+00
	reduced Ft Lewis sed. (di/Fe = 22)			2300	0.00E+00	105	0.23	224000	0.00E+00	0.000E+00

Table 5.7. Degradation rates of TNT by reduced sediment.

sediment (di/Fe = **)	T°C	C/Co	residence time (h)	rate (1/h)	solute conc (mg/L)	r_{sw} (g/mL)	half-life (h)	intrinsic rate (h^{-1} $umol^{-2}$)	degradation rate (mol g^{-1} d^{-1})
Ft Lewis, di/Fe = 0.67, W46	10	0.889	1.14	0.103	3.5	4.5	6.72	6.27E-03	2.146E-08
Ft Lewis, di/Fe = 1.6, W47	10	0.766	1.11	0.240	3.5	4.5	2.89	7.45E-03	4.993E-08
Ft Lewis, di/Fe = 4.1, W48	10	0.08	1.10	2.294	3.5	4.5	0.302	4.78E-02	4.769E-07
Ft Lewis, di/Fe = 22, W49	10	0.022	1.02	3.742	3.5	4.5	0.185	7.47E-02	7.779E-07
Ft Lewis, di/Fe = 0.67, W28	22	0.786	1.01	0.238	0.39	4.5	2.91	1.30E-01	5.523E-09
Ft Lewis, di/Fe = 1.6, W27	22	0.532	1.03	0.613	0.39	4.5	1.13	1.71E-01	1.419E-08
Ft Lewis, di/Fe = 4.1, W26	22	0.358	0.73	1.407	0.39	4.5	0.493	2.63E-01	3.260E-08
Ft Lewis, di/Fe = 22, W25	22	0.627	0.58	0.805	0.39	4.5	0.861	1.44E-01	1.864E-08
Ft Lewis, di/Fe = 0.67, W31	22	0.438	2.19	0.377	5.65	4.5	1.84	1.42E-02	1.267E-07
Ft Lewis, di/Fe = 1.6, W32	22	0.518	2.50	0.263	5.65	4.5	2.63	5.05E-03	8.830E-08
Ft Lewis, di/Fe = 4.1, W30	22	0.612	1.37	0.358	5.65	4.5	1.934	4.62E-03	1.203E-07
Ft Lewis, di/Fe = 22, W29	22	0.28	2.16	0.589	5.65	4.5	1.176	7.29E-03	1.978E-07
Ft Lewis, di/Fe = 0.67, W36	35	0.889	1.10	0.107	4.5	4.5	6.48	5.05E-03	2.859E-08
Ft Lewis, di/Fe = 1.6, W35	35	0.771	1.40	0.186	4.5	4.5	3.73	4.48E-03	4.965E-08
Ft Lewis, di/Fe = 4.1, W34	35	0.609	0.89	0.557	4.5	4.5	1.244	9.02E-03	1.489E-07
Ft Lewis, di/Fe = 22, W33	35	0.653	0.83	0.513	4.5	4.5	1.350	7.97E-03	1.372E-07
Ft Lewis, di/Fe = 0.67, W40	49	0.912	1.00	0.092	4.13	4.5	7.52	4.74E-03	2.260E-08
Ft Lewis, di/Fe = 1.6, W39	49	0.792	0.75	0.311	4.13	4.5	2.23	8.17E-03	7.627E-08
Ft Lewis, di/Fe = 4.1, W38	49	0.761	0.80	0.341	4.13	4.5	2.030	6.02E-03	8.375E-08
Ft Lewis, di/Fe = 22, W37	49	0.745	0.75	0.392	4.13	4.5	1.766	6.64E-03	9.628E-08
Ft Lewis, di/Fe = 0.67, W44	62	0.24	7.25	0.197	5.14	4.5	3.52	8.14E-03	6.010E-08
Ft Lewis, di/Fe = 1.6, W43	62	0.08	8.19	0.308	5.14	4.5	2.25	6.51E-03	9.415E-08
Ft Lewis, di/Fe = 4.1, W42	62	0.06	6.51	0.432	5.14	4.5	1.604	6.13E-03	1.319E-07
Ft Lewis, di/Fe = 22, W41	62	0.08	4.56	0.554	5.14	4.5	1.251	7.53E-03	1.691E-07
Ft Lewis, di/Fe = 22, batch	22	0.5	4.70	0.147	5.00	0.5	4.70	5.56E-02	4.380E-08
Ft Lewis, di/Fe = 22, batch	22	0.5	72.00	0.010	5.00	0.25	72.0	1.20E-01	2.859E-09
Ft Lewis, di/Fe = 22, batch	22	0.5	350.00	0.002	5.00	0.13	350.0	8.21E-02	5.882E-10

5.4 Sediment Microbial Changes with Dithionite and Biostimulation Treatment

The microbial population, in general, appears to be little affected by low to moderate dithionite/carbonate concentrations used to reduce sediment. High dithionite concentrations (0.1 mol/L) do appear to cause high microbial death (90% death, as defined by PCR/DNA and AODC biomass and acetate mineralization half-life, Figure 5.5a, b). However, it should be noted that high (>0.03 mol/L) dithionite concentrations lead to microbial detachment from sediment (Figure 5.5c), so some biomass decrease observed may, in fact, be washout. The remaining population is well able to mineralize RDX and HMX intermediates, as mineralization rates are most rapid for RDX and HMX in highly reduced sediments that received the high dithionite concentration treatment. The live-dead stain was used to further define microbial population death during dithionite treatment. In separate sets of experiments, the microbial population decreased the most with separate dithionite exposure (i.e., no potassium carbonate), but the microbial population showed little relationship between carbonate concentration and death when exposed to only the carbonate buffer. The combined exposure to sodium dithionite and potassium carbonate showed less death than exposure to dithionite alone, indicating the carbonate buffer appears to allow microbes to tolerate dithionite exposure.

The amount of RDX incorporated into microbial biomass (up to 7%) during RDX mineralization by reduced sediment was determined by several different extraction methods in experiments. In this coupled degradation experiment, RDX was degraded so that only 51% aqueous species remained by 576 h and 29% was mineralized. At 560 h, 6.8% of the carbon from RDX was associated with microbial biomass, as determined by: a) phosphate-buffered saline extraction, b) 1 M NaOH dissolution of biomass, and c) 10 M NaOH dissolution of biomass. This amount of carbon incorporation was similar to reported yields of citrate biodegradation (2.3% citrate carbon mass associated with microbes), lactate (6.1%), and glucose (3.6%). The amount of carbon mass associated with biomass was relatively constant from 50 h to 576 h, although the adsorbed RDX mass may have been greater at early times and carbon mass incorporated with microbes may be greater at later times. During the 10M NaOH dissolution of biomass, about 1.4% of the ^{14}C from RDX was released as carbon dioxide. Based on these results, microbial death at later (>1000 h) time periods in other RDX mineralization studies may have contributed as much as 5 to 7% of the mineralization observed.

5.5 Sediment Abiotic Changes with Dithionite and Biostimulation Treatment

Abiotic and biotic experiments conducted in this project used natural sediments that are treated with a mixture of sodium dithionite and potassium carbonate. Results show that increasing dithionite treatment (at low concentrations) increases the resulting ferrous iron, but treatment with a large excess of dithionite does not result in additional reductive capacity (Table 5.8), but other ferrous iron phase changes do occur. A comparison of the reductive capacity (oxidation of sediment in columns) to the 0.5M HCl ferrous iron extraction (1 h extraction time) showed similar results (Figure 5.6a), although a different study found only a fair correlation (Szecsody et al. 2005a). It is believed that the reductive capacity more accurately reflects field scale conditions, as this oxygen consumption measurement occurs over a relatively
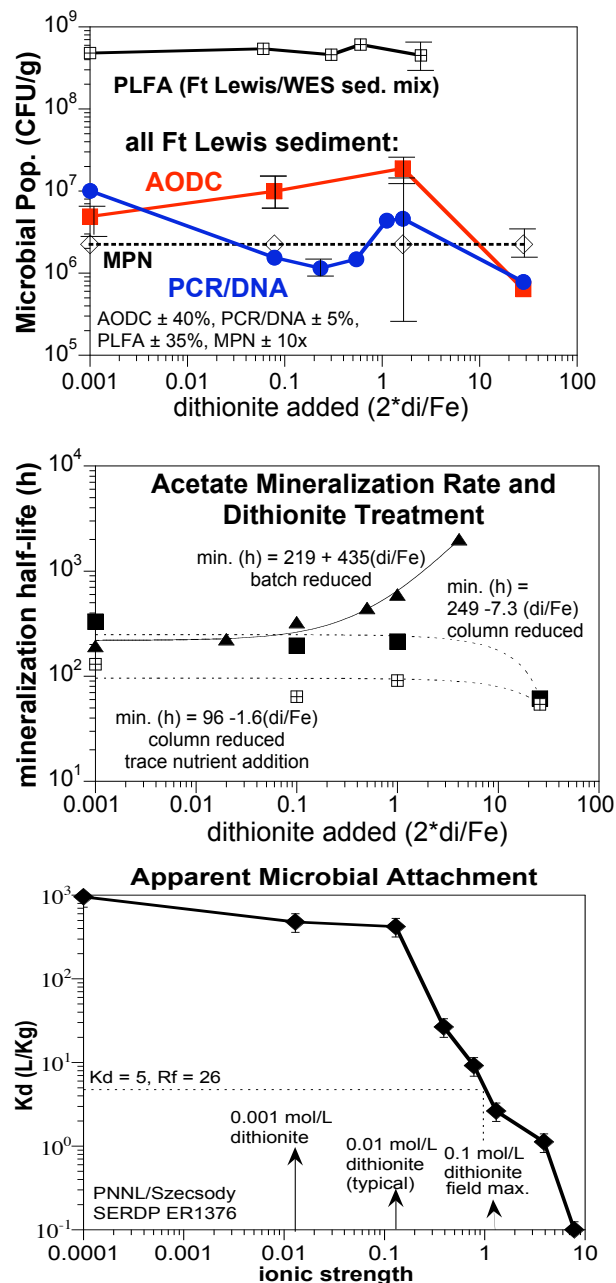
Figure 5.5. Dithionite treatment: a) biomass change, and b) acetate mineralization change, c) microbial detachment.

long time period (1 to 3 weeks), to accesses differing ferrous surfaces phases, some of which react slowly. In contrast, the 0.5 M HCl extraction (1 h) only accesses easy to dissolve ferrous surface phases.

While reductive capacity does not indicate greater capacity for high dithionite treatments, there are clearly differences in ferrous surface phases (Table 5.8), and RDX and HMX mineralization rates are much more rapid in highly reduced sediment (Figures 5.1a, 5.3a). Therefore, iron extractions and reductive capacity measurements are useful for quantifying low to moderate dithionite treatment, and additional characterization is needed to be able to predict energetic reactivity. The sediment/water system is a more reducing environment with greater sediment reduction (Figure 5.6b). There is a smaller change in the redox potential between sediments that are just fully reduced (i.e., dithionite/ferrous iron ratio of 1.5 to 3.0x) to sediments fully reduced with excess dithionite (i.e., dithionite/ferrous iron ratio of 28x), which may indicate changes in the specific ferrous iron phases present on the sediment surface. Iron extractions (Table 5.8) do not provide indication of changes between these two reduced sediments. While iron extractions reasonably well characterize ferrous oxide phases (and adsorbed ferrous iron), they do not account for structurally reduced iron in 2:1 smectite clays (Szecsody et al. 2004), which can account for a significant amount of the reductive capacity.
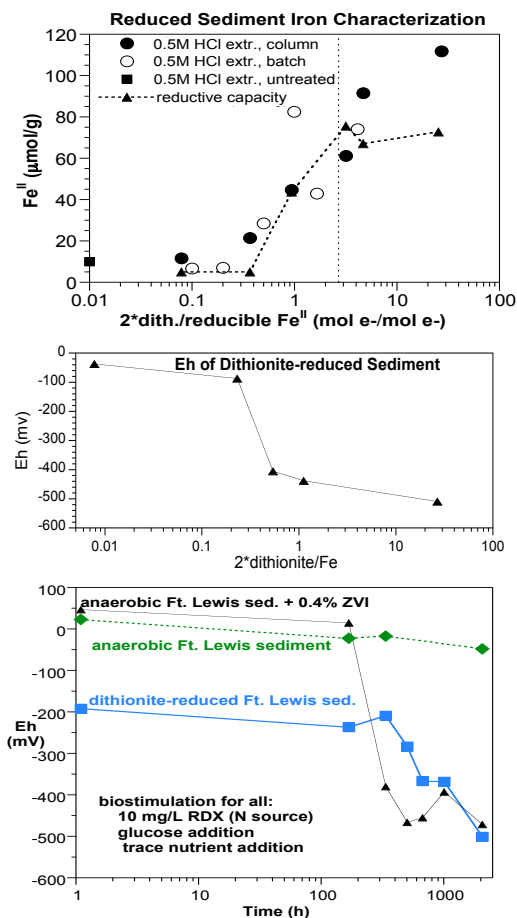
Figure 5.6. Abiotic changes in sediment: a) reductive capacity and ferrous iron, b) Eh both with differing dithionite treatment, and c) Eh change over time with microbial activity by RDX biodegradation.

Table 5.8. Sediment iron phase changes during differing dithionite treatment.

treatment	exp.	ion exch. Fe^{II}	Fe^{II}	Fe^{II}	reductive capacity	amorphous Fe^{III} oxides	cryst+ am Fe^{III} oxides	total
		1M CaCl2	0.5M HCl, 24h	0.5M HCl, 1 h		am-oxalate	DCB	5M HCl
2*dith/Fe	name	(µmol/g)	(µmol/g)	(µmol/g)	(µmol/g)	(µmol/g)	(µmol/g)	(µmol/g)
26.8	R24	0.66	175.0	111.8	72.8	98.8	98.9	278
4.12	R31.1	1.24	105.4	74.1	67.1	102	59.5	211
1.12	R45	0.42	62.2	44.7	43.7	160	184	208
0.54	R47	0.33	27.9	28.6	27.6	150	170	194
0.237	R49	0.22	12.5	7.1	5.0	139	155	185
0.078	R51	0.05	7.1	11.7	5.0	155	146	180
0.000	untreated	0.05	4.7	10.0		150	509	253

Additional redox potential changes take place over time in the reduced/biostimulated sediments because the sediment/water system contains microbes that are actively reducing energetics (and other carbon sources, if present). In a biostimulated system (i.e., anaerobic, no dithionite reduction, Figure 5.6c, green line), the redox potential slowly decreased from near zero to -70 mV over 2000 h of RDX biodegradation. In contrast, the dithionte-reduced sediment started at a lower redox potential (-200 mV), which decreased further to -500 mV by 2000 h (Figure 5.6c, blue line). An anaerobic sediment with 0.4% zero valent iron also achieved -500 mV by 2000 h. Therefore, both abiotic reduction of sediment (shown by initial Eh) and biotic degradation of various carbon sources (shown by greater redox potential over time) contribute to the overall redox state of the system. In a separate set of experiments, the ferrous iron, pH, and Eh was periodically monitored for 2000 h in a system containing only anoxic water, reduced sediment, and 10 mg/L TNT (Figure 4.2.6). In both partially- and highly-reduced sediment, the Eh remained relatively constant for the first 500 h ($\sim$-400 mV), then decreased (-600 mV) by 2000 h, possibly indicating some microbial activity degrading TNT. The pH was constant. The extractable ferrous iron (0.5M HCl for 1 h) decreased over time for both systems, although significantly for the partially reduced sediment, indicating some consumption of ferrous iron. The pH of the reduced sediment can have a significant influence on energetic degradation, but it is dependent on the nature of the ferrous iron surface phases. For the Ft. Lewis (Washington) aquifer sediment, in which there is minimal adsorbed Fe(II) created, the energetic degradation rate was about the same between pH 6 and 9. In contrast, a Pantex (Texas) aquifer sediment, which when reduced contains significant adsorbed Fe(II), did show a significant different in the energetic degradation rate between pH 5.8 and 8.5. Some of this behavior can be explained by the pH adsorption edge for Fe(II) is about 6.5, so significant desorption occurs at lower pH. Finally, a Puchack (NJ) aquifer sediment showed no difference in chromate degradation kinetics at a pH of 4.5 to 6.5, as much of the reductive capacity was structural iron in clays (Vermeul et al. 2006).

5.6 Implications for Field Scale Subsurface Remediation of Energetics

Uncontrolled release of energetics RDX, HMX, and TNT to the surface and subsurface environment can occur through munition manufacture, storage, and deployment (UXO and partial detonations). RDX and HMX are common groundwater contaminants due to slow aerobic degradation in soils and vadose zone sediments and minimal sorption. In contrast, TNT is a common soil/shallow sediment contaminant with limited TNT migration because of aerobic (Boopathy et al. 1994) and anaerobic (Funk et al. 1993) degradation in soils as well as significantly greater sorption. For the Ft. Lewis aquifer sediment used in this study (i.e., 60-90 ft depth, fraction organic carbon <0.05%), RDX sorption [$K_{d, RDX}$] averaged 0.26 ± 0.07 cm^3/g, HMX sorption [$K_{d, HMX}$] averaged 0.095 ± 0.013 cm^3/g, and TNT sorption [$K_{d, TNT}$] averaged 1.55 ± 0.67 cm^3/g. Therefore, the average retardation factor (R_f) for these three energetics are: 2.2 (RDX), 1.4 (HMX), and 8.0 (TNT) for this sediment. TNT groundwater contamination does occur, however, typically at sites with subsurface burial of UXO.

For groundwater contamination of RDX and HMX, results of this study have shown that dithionite reduction of sediment exerts the greatest impact on mineralization. Additional biostimulation (carbon or trace nutrient addition) increases the mineralization rate a small amount (in addition to dithionite treatment). For RDX, the mineralization rate in

dithionite-reduced sediment was 98x more rapid than untreated sediment (31,000 h half-life), and dithionite-reduced sediment with biostimulation was 277x more rapid than untreated sediment (112 h half-life Table 5.1). For HMX, the mineralization rate in dithionite-reduced sediment was 48x more rapid than untreated sediment (7800 h half-life), and dithionite-reduced sediment with biostimulation was 58x (162 h half-life) more rapid than untreated sediment. Comparisons were made with some other treatments. Addition of 0.4% zero valent iron was nearly as effective, with almost as high mineralization rates (Figure 5.5), but 60% mineralization extent compared with 78% mineralization extent for dithionite-reduced sediments. It is considerably more difficult to inject nanoscale zero valent iron uniformly into subsurface sediments (although trench/fill with zero valent iron for <50 ft deep applications is very effective). Many different biostimulation sediment treatments were compared to dithionite reduction of sediment. All biostimulation treatment experiments showed much slower RDX mineralization compared with the dithionite reduction of sediment with some carbon or trace nutrient addition. It is believed that biostimulation treatment of this subsurface sediment with very low microbial population (10^6 CFU/g) would take a few weeks (in the lab) to a few months (in the field, colder aquifer temperature) for the microbial population to grow sufficiently to achieve high mineralization rates. Therefore the short time scale experiments of this study (40 day to 90 day) may bias results toward the abiotic treatment, as weeks to months of preconditioning may be needed for biostimulation alone. Microbes were clearly necessary for RDX and HMX mineralization, as addition of bactericides stops both RDX and HMX mineralization. In addition, the rate limiting step for both RDX and HMX mineralization appears to be the coupled abiotic/biotic mineralization of formate, which is 12x more rapid in reduced sediments (half-life 60 h, compared to untreated sediment with a half-life of 7400 h), yet also requires microbes.

Subsurface contamination of TNT would best be treated with glucose addition, to stimulate the cometabolic TNT/glucose degradation amino-degradation pathway, producing 2-aminodi-nitrotoluene (2-ADNT), 4-aminodinitrotoluene (4-ADNT) -> 2,4-diaminonitrotoluene (2,4-DANT), 2,6-diaminonitrotoluene (2,6-DANT) -> triaminotoluene (TAT). While the initial monoamino- products are more toxic than TNT, both diamino- and triamino-toluene irreversibly sorb, are immobilized in the subsurface environment (demonstrated). Interestingly, TNT cometabolic degradation is most rapid in dithionite-reduced sediment (half-life 610 h, producing TAT), compared with just glucose addition (half-life 8030 h; untreated sediment 55,000 h). Therefore glucose addition alone increased the TAT production rate by 6.8x, whereas glucose addition and dithionite reduction increased the TAT production rate 90x. The 610 h half-life for TNT degradation to triaminotoluene is still somewhat slow for a viable groundwater remediation technology. Typically a reaction half-life of 100 h or faster is needed to have sufficient resi-dence time in a subsurface treatment zone to achieve full degradation. These TNT/glucose cometabolic experiments were conducted in batch systems at low sediment/water ratios, and additional experimentation at high sediment/water ratios would be needed to determine how rapid the TAT production rate would be under field-scale conditions of these high sediment/water ratios (and temperature) in aquifers. It is believed that the contribution of abiotic degrada-tion to TNT degradation would increase at the higher sediment/water ratios, but the microbial population would be much slower to grow to the same population density in packed porous media compared to mixed batch systems. Therefore, it is difficult to predict the resulting TNT cometabolic degradation rate in aquifers from these low sediment/water ratio experiments due to the multiple biotic, abiotic, and possibly coupled reactions that occur.

125

Optimal delivery of remediation reactants for the energetics in this study involves creating a reduced zone (with chemical reduction of sediment or zero valent iron addition), carbon and/or trace nutrient addition, and consideration of the effect of these treatments on the subsurface microbial population. Delivery of the reactants to an aquifer requires consideration of: a) access, b) kinetic formation, and c) persistence. Injection of the aqueous reductant (sodium dithionite with potassium carbonate pH buffer) has no depth limitation. Because the sediment reduction half-life with sediment (Szecsody et al. 2004) is 4 to 7 h in different sediments, and dithionite disproportionates (degrades) in aqueous solution with a 27 h half-life, optimal injection rates need to deliver the dithionite to the aquifer within a day, then allowing a week for reduction. RDX and HMX are most rapidly mineralized in highly reduced zones, but dithionite concentrations higher than 0.03 mol/L mobilize much of the microbial population. Therefore, creation of a highly reduced zone would best be accomplished by multiple injections of 0.03 mol/L dithionite. The longevity of the reduced zone is dependent on the mass of reducible iron in the aquifer sediments (i.e., immobile electron donor mass reservoir) and the flux of electron acceptors (i.e., energetics, dissolved oxygen, other electron acceptors) through that reduced aquifer zone. Observed dithionite-reduced barrier longevity range from 2 to 13 years. Oxidized sediment can be re-reduced with little loss in reductive capacity. An alternative to dithionite reduction of sediment is zero valent iron addition. At implementation depths of 50 ft or less, trench and fill methods have been extensively used to emplace a solid zero valent iron barrier. It is not clear whether this type of zero valent iron barrier (i.e., not mixed with sediment, so fewer iron –microbe interactions) would be as effective for mineralization of energetics. Addition of zero valent iron mixed with sediment has been implemented at field scale through augers to a depth of ~100 ft. Experiments in this study have shown that sediment/zero valent iron mixtures are almost as effective for RDX mineralization (with abiotic and coupled abiotic/biotic steps). Deeper emplacement is possible using nanoscale zero valent iron injected with a gel or shear-thinning fluid, although this technology is still in development. While zero valent iron barriers theoretically have enormous capacity (i.e., longevity), emplaced zvi barriers have significantly shorter longevity due to metal oxide buildup on the upgradient edge of the barrier, both coating the barrier and causing flow bypass. These problems are significantly worse in aquifers with elevated ions. Subsurface delivery of carbon is straightforward, but aqueous reagents are not persistent (sorb little), so would need to be periodically pulsed into the aquifer over long periods of time. Alternatively, solid phase compounds that slowly release carbon have been developed and successfully used at the field scale.

In conclusion, dithionite reduction of sediment results in a mixture of ferrous iron phases and does result in some microbial population death at high concentration (10x death at 0.1 mol/L dithionite), but the mineralization of RDX and HMX increases directly with the amount of dithionite treatment (Figure 5.7a, b) most likely due to the rate-limiting step (formate mineralization), which is a coupled reaction requiring both ferrous iron surface phases and viable microbes. TNT *mineralization* was not accelerated significantly in any combination of biostimulation and/or dithionite reduction of sediment (Figure 5.7c). However, TNT degradation to triamino-toluene was 90x more rapid in biostimulated (glucose addition) sediments that were also dithionite reduced (Figure 5.7d). Degradation to triaminotoluene in reducing soils (and subsequent mineralization under oxic conditions) has been previously used in surface soils, which contained bacteria, daphnids, algae, cress plants, and earth worms (Daun et al. 1998; Achtnich et al. 1999; Elovitz and Weber 1999; Weiss et al. 2004), but has not been previously reported in

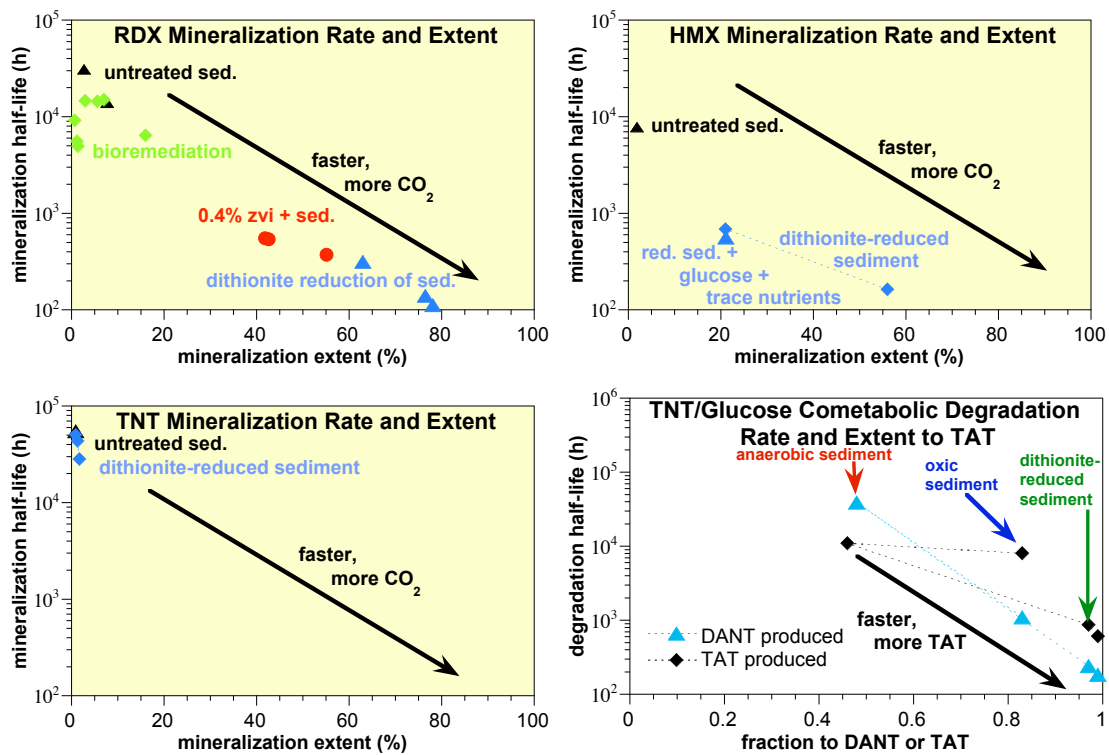**Figure 5.7**. Energetic mineralization rate (half-life) and extent for different remediation technologies on the same sediment: a) RDX, b) HMX, c) TNT. d) TNT cometabolic degradation rate and extent to DANT (blue) or TAT (black).

a subsurface sediment containing only bacteria. Subsequent oxic TNT mineralization of the reduced/ biostimulated subsurface sediments in this study did not produce significant mineralization (< 1%).

6. References

Achtnich C, U Sieglen, H Knackmuss, and H Lenke. 1999. "Irreversible binding of biologically reduced 2,4,6-trinitrotoluene to soil." *Env. Toxicology and Chemistry* 18(11):2416-2423.

Adam M, S Comfort, T Zhang, and M Morley. 2005. "Evaluating biodegradation as a primary and secondary treatment for removing RDX from a perched aquifer." *J. Hazardous Materials* 9(1):9-19.

Aquifer Solutions, Inc. 2002. *Conceptual deployment scenarios for in situ remediation of the southeast perched aquifer plume Pantex Plant, Amarillo, Texas*. Aquifer Solutions Inc., Evergreen, Colorado.

Agrawal A and P Tratnyek. 1996. "Reduction of nitroaromatic compounds by zero-valent iron metal." *Environmental Science and Technology* 30:153-160.

Amonette J, D Workman, D Kennedy, J Fruchter, and Y Gorby. 2000. "Dechlorination of carbon tetrachloride by Fe(II) associated with goethite." *Environmental Science and Technology* 34:4606-4613.

Binks PR, S Nicklin, and NC Bruce. 1995. "Degradation of Hexahydro-1,3,5-trinitro-1,3,5-triazine (RDX) by Stenotrophomonas maltophilia PB1." *Applied and Environmental Microbiology* 61:1318-132l.

Boopathy R, CF Kulpa, J Manning, and CD Montemagno. 1994. "Biotransformation of 2,4,6-trinitrotoluene (tnt) by co-metabolism with various co-substrates: A laboratory-scale study." *Bioresource Technology* 47:205-208.

Boopathy R and JF Manning. 2000. "Laboratory Treatability Study on Hexahydro-1,3,5-Trinitro-1,3,5-Triazine (RDX) Contaminated Soil from the Iowa Army Ammunition Plant, Burlington, IA." *Water Env. Res.* 72:238-242.

Boparai H, P Shea, S Comfort, and D Snow. 2006a. "Dechlorinating chloroacetanilide herbicides by dithionite-treated aquifer sediment and surface soil." *Environmental Science and Technology* 40(6):3043-3049.

Boparai H, S Comfort, P Shea, T Satapanajaru, and J Szecsody. 2006b. "Degradation of High Explosives with Aqueous Fe(II) and Freshly Precipitated Iron Minerals." *Environmental Science and Technology*, submitted June 2006.

Boparai H, S Comfort, and J Szecsody. 2007. "Degradation of RDX, TNT, and HMX by dithionite-treated aquifer sediment and surface soil." *Environmental Science and Technology*, in preparation.

Brannon JM, DD Adrian, and JC Pennington. 1992. *Slow Release of PCB, TNT, and RDX from Soils and Sediments, Vicksburg, MS*. U.S. Army Engineer Research and Development Center, Waterways Experiment Station.

Bruns-Nagel D, O Drzyzga, K Steinbach, TC Schmidt, EV Low, T Gorontzy, KH Blotevogel, and D Gemsa. 1998. "Anaerobic/aerobic composting of 2,4,6-trinitrotoluene-contaminated soil in a reactor system." *Environmental Science and Technology* 32:1676-1679.

Comfort SD, PJ Shea, LS Hundal, Z Li, BL Woodbury, JL Martin, and WL Powers. 1995. "TNT transport and fate in contaminated soil." *J. Environ. Qual.* 24:1174-1182.

Crocker F, K Thompson, J Szecsody, and H Fredrickson. 2005. "Biotic and abiotic degradation of hexanitrohexaazaisowurtzitane (CL-20) and hexahydro-1,3,5-trinitro-1,3,5-triazine (RDX) in Soils." *Journal of Environmental Quality* 34:2208-2216.

Daun G, H Lenke, M Ruess, and H Knackmuss. 1998. "Biological treatment of TNT-contaminated soil. 1. anaerobic cometabolic reduction and interaction of TNT and metabolites with soil components." *Environmental Science and Technology* 32:1956-1963.

Elovitz M and E Webber. DATE. "Sediment-mediated reduction of 2,4,6-trinitrotoluene and fate of the resulting aromatic (poly)amines." *Environmental Science and Technology* 33:2617-2625.

Esteve-Nunez A and JL Ramos. 1998. "Metabolism of 2,4,6-Trinitrotoluene by Pseudomonas sp. JLR11." *Environmental Science and Technology* 32:3802-3808.

Fournier D, A Halasz, J Spain, P Fiurasek, and J Hawari. 2002. "Determination of key metabolites during biodegradation of hexa-hydro-1,3,5-triazine with Rhodococcus sp-strain DN22." *Appl. Environ. Microbiol.* 68:166-172.

Freedman D and K Sutherland. 1998. "Biodegradation of RDX under nitrate-reducing conditions." *Water Science Technology* 38:33-40.

Fruchter J, V Vermeul, M Williams, and J Szecsody. 2000. "Creation of a Subsurface Permeable Treatment Barrier Using In Situ Redox Manipulation." *Ground Water Monitoring Review* 1:66-77.

Funk S, D Roberts, D Crawford, and R Crawford. 1993. "Initial-phase optimization for bioremediation of munition compound-contaminated soils." *Applied and Env. Microbiology* 59(7):2171-2177.

Gaber HM, SD Comfort, PJ Shea, and TA Machacek. 2002. "Metolachlor dechlorination by zerovalent iron during unsaturated transport." *J. Environ. Qual.* 31:962-969.

Gregory KB, P Larese-Casanova, GF Parkin, and MM Scherer. 2004. "Abiotic transformation of hexahydro-1,3,5-trinitro-1,3,5-triazine by FeFe[II] bound to magnetite." *Environ. Sci. Technol.* 38:1408-1414.

Halasz A, J Spain, L Paquet, C Beaulieu, and J Hawari. 2002. "Insights into the formation and degradation mechanisms of methylenedinitramine during the incubation of RDX with anaerobic sludge." *Environ. Sci. Technol.* 36:633-638.

Hawari J, S Beaudet, A Halasz, S Thiboutot, and G Ampleman. 2000. "Microbial degradation of explosives: biotransformation versus mineralization." *Appl. Microbiol. Biotechnol.* 54:605-618.

Hawari J. 1999. "Biodegradation of RDX and HMX: From Basic Research to Field Application." *In* JC Spain, JB Hughes, and H Knackmuss, eds., *Biodegradation of Nitroaromatic Compounds and Explosives: Boca Raton, Florida*. Lewis Publishers, p. 277-310.

Heijman CG, E Grieder, C Holliger, and RP Schwarzenbach. 1995. "Reduction of nitroaromatic compounds coupled to microbial iron reduction in laboratory aquifer columns." *Environmental Science and Technology* 29:775-783.

Heron G, C Crouzet, AC Bourg, and TH Christensen. 1994. "Speciation of Fe(II) and Fe(III) in contaminated aquifer sediments using chemical extraction techniques." *Environmental Science and Technology* 28:1698-1705.

Heron G, TH Christensen, and JC Yell. 1994. "Oxidation capacity of aquifer sediments." *Environ. Sci. Technol.* 28:153-158.

Hoffman MR. 1990. "Catalysis in Aquatic Environments." In *Aquatic Chemical Kinetics*; W. Stumm, ed.; John Wiley and Sons, New York. p 71-111.

Hofstetter TB, CG Heijman, SB Haderlein, C Holliger, and RP Schwarzenbach. 1999. "Complete reduction of TNT and other (poly)nitroaromatic compounds under iron reducing subsurface conditions." *Environ. Sci. Technol.* 33:1479-1487.

Hundal LS, J Singh, EL Bier, PJ Shea, SD Comfort, and WL Powers. 1997. "Removal of TNT and RDX from water and soil using iron metal." *Environmental Pollution* 97:55-64.

Joo SH, AJ Feitz, and TD Waite. 2004. "Oxidative degradation of the carbothioate herbicide, molinate, using nanoscale zero-valent iron." *Environ. Sci. Technol.* 38:2242-2247.

Lee W and B Batchelor. 2004. "Abiotic reductive dechlorination of chlorinated ethylenes by soil." *Chemosphere* 55:705-713.

Lenke H, J Warrelmann, G Daun, K Hund, U Sieglen, U Walter, and H Knackmuss. 1998, "Biological treatment of TNT-contaminated soil. 2. biologically induced immobilization of the contaminants and full-scale application." *Environmental Science and Technology* 32:1964-1971.

Leussing DL and IM Kolthoff. 1953. "The solubility product of ferrous hydroxide and the ionization of aquo-ferrous ion." *J. Am. Chem. Soc.* 75:2476-2479.

Maithreepala RA and RA Doong. 2004. "Synergistic effect of copper ion on the reductive dechlorination of carbon tetrachloride by surface-bound Fe^{II} associated with goethite." *Environ. Sci. Technol.* 38:260-268.

McCormick NG, FE Feeherry, and HS Levinson. 1976. "Microbial transformation of 2,4,6-tirnitrotoluene and other nitroaromatic compounds." *Applied and Environmental Microbiology* 31:949-958.

McCormick NG, JH Cornell, and AM Kaplan. 1981. "Biodegradation of hexahydro-1,3,5-trinitro-1,3,5-triazine." *Applied and Environmental Microbiology* 42:817-823.

Mcbride MB. 1994. *Environmental Chemistry of Soils*. Oxford University Press, New York.

Oremland R and J Zehr. 1986. "Formation of methane and carbon dioxide from dimethylselenide in anoxic sediments and by a methanogenic bacterium." *Appl. Environ. Microbiol* 552(5):1031-1036.

Pecher K, S Haderlein, and R Schwartzenback. 2000. "Reduction of polyhalogenated methanes by surface-bound Fe^{II} in aqueous suspension of iron-oxides." *Environmental Science and Technology* 36:1734-1741.

Ronen Z, A Brenner, and A Abeliovich. 1998. "Biodegradation of RDX-contaminated wastes in a nitrogen-deficient environment." *Water Science Technology* 38:9-22.

SERDP. 1993. *An approach to estimation of volumes of contaminated soil and groundwater for selected army installations*. Labat-Anderson Inc., Prepared for the Executive Director, Strategic Environmental Research and Development Program.

Sheremata T and J Hawari. 2000. "Mineralization of RDX by the white rot fungus Phanerochaete chrysosporium to carbon dioxide and nitrous oxide." *Environmental Science and Technology* 34:3384-3388.

Singh J, S Comfort, L Hundal, and P Shea. 1998a. "Long-term RDX sorption and fate in soil." *Journal of Environmental Quality* 27:572-577.

Singh J, S Comfort, and P Shea. 1998b. "Remediating RDX-contaminated water and soil using zero-valent iron." *Journal of Environmental Quality* 27:1240-1245.

Singh J, S Comfort, and P Shea. 1999. "Iron-mediated remediation of RDX-contaminated water and soil under controlled Eh/pH." *Environmental Science and Technology* 33:1488-1494.

Stookey LL. 1970. "Ferrozine - A new spectrophotometric reagent for iron." *Anal. Chem.* 42:779-781.

Strathmann TJ and AT Stone. 2002. "Reduction of the pesticides oxamyl and methomyl by Fe^{II}: Effect of pH and inorganic ligands." *Environ. Sci. Technol.* 36:653-661.

Szecsody JE, FJ Brockman, GP Streile, and MJ Truex. 1993. "Transport and Biodegradation of Quinoline in Horizontally Stratified Porous Media." *J. Contaminant Hydrology* 15:277-304.

Szecsody JE, J Fruchter, MA McKinley, CT Resch, and T Gilmore. 2001. *Feasibility of in situ redox manipulation of subsurface sediments for RDX remediation at Pantex*. Pacific Northwest National Laboratory, Richland, Washington.

Szecsody JE, JS Fruchter, MD Williams, VR Vermuel, and D Sklarew. 2004. "In situ chemical reduction of aquifer sediment: Enhancement of reactive iron phases and TCE dechlorination." *Environ. Sci. Technol.* 38:4656-4663.

Szecsody J. 2004. *Automated Fluid Analysis Apparatus and Techniques*. Patent 6,706,527.

Szecsody J, M Williams, and V Vermeul. 2002. *Flow through Electrode with Automated Calibration*. U.S. Patent 6,438,501.

Szecsody J, V Vermeul, J Fruchter, M Williams, B Devary, J Phillips, M Rockhold, and Y Liu. 2005a. *Effect of geochemical and physical heterogeneity on the Hanford 100D area in situ redox manipulation barrier longevity*. PNNL-15499, Pacific Northwest National Laboratory, Richland, Washington.

Szecsody J, J Phillips, V Vermeul, J Fruchter, and M Williams. 2005b. *Influence of nitrate on the Hanford 100D area In Situ Redox Manipulation barrier longevity*. PNNL-15262, Pacific Northwest National Laboratory, Richland, Washington.

Tratnyek PG, TL Johnson, and A Schattauer. 1995. *Interfacial phenomena affecting contaminant remediation with zero-valent iron metal*. Emerging Technologies in Hazardous Waste Management VII. Atlanta, Georgia. American Chemical Society; p. 589-592.

Vorbeck C, H Lenke, P Fischer, JC Spain, and H-J Knackmuss. 1998. "Initial reductive reactions in aerobic microbial metabolism of 2,4,6-trinitrotoluene." *Appl. Environ. Microbiol.* 64:246-252.

Vermeul V, J Fruchter, M Williams, and J. Szecsody. 2002. "Creation of a Subsurface Permeable Reactive Barrier." In: G Winkle (ed), *Groundwater Remediation of Trace Metals*. Academic Press.

Vermeul V, M Williams, J Evans, J Szecsody, B Bjornstad, and T Liikala. 2000. *In Situ Redox Manipulation Proof-of-Principle Test at the Ft. Lewis Logistics Center*. PNNL-13357, Pacific Northwest National Laboratory, Richland, Washington.

Vermeul V, JE Szecsody, MJ Truex, CA Burns, DC Girvin, JL Phillips, BD Devary, A Fischer, and S-M W Li. 2006. *Treatability Study of In Situ Technologies for Remediation of Hexavalent Chromium in Groundwater at the Puchack Well Field Superfund Site, New Jersey*. PNNL –16194, Pacific Northwest National Laboratory, Richland, Washington.

Waisner SA, H Fredrickson, L Hansen, M Zappi, G Myrick, and S Banerji. 2000. *Removal of RDX from a Contaminated Groundwater by In-Situ Bioremediation*. U.S. Army Research and Development Center, Waterways Experiment Station, Vicksburg, Mississippi.

Waisner S, L Hansen, H Fredrickson, C Nestler, M Zappi, S Banerji, and R Bajpai. 2002. "Biodegradation of RDX within soil-water slurries using a combination of differing redox incubation conditions." *J. Haz. Materials* 95(1-2):91-106.

Weiss J, A McKay, C Derito, C Watanabe, K Thorn, and E Madsen. "Development and application of pyrolysis gas chromatography/mass spectrometry for the analysis of bound trinitrotoluene residues in soil." *Environmental Science and Technology* 38:2167-2174.

Wildman MJ and P Alvarez. 2001. "RDX degradation using an integrated Fe(0)-microbial treatment approach." *Wat. Sci. Technol.* 43:25-33.

Attachment 1: Publications and Presentations

Publications
fully funded by this project unless otherwise noted
* partially funded by this project SERDP ER-1376, partially by SERDP ER-1255
** partially funded by this project

Adam M, S Comfort, T Zhang and M Morley. 2005. "Evaluating biodegradation as a primary and secondary treatment for removing RDX from a perched aquifer." *J. Hazardous Materials* 9(1):9-19.**

Boparai H, S Comfort, P Shea, T Satapanajaru, and J Szecsody. 2006. "Degradation of High Explosives with Aqueous Fe(II) and Freshly Precipitated Iron Minerals." *Environmental Science and Technology*, submitted June 2006.

Boparai, H., Comfort, S., and J. Szecsody, 2007, Degradation of RDX, TNT, and HMX by dithionite-treated aquifer sediment and surface soil, Environmental Science and Technology, in preparation.

Boparai H, P Shea, S Comfort, and D Snow. 2006. "Dechlorinating chloroacetanilide herbicides by dithionite-treated aquifer sediment and surface soil." *Environmental Science and Technology* 40(6):3043-3049.

Comfort S. 2006. "Remediating RDX and HMX Contaminated Soil and Water." In *Bioremdiation of Aquatic and Terrestrial EcoSystems*, editors, M Fingerman and R Nagabhushanam, Science Publishers, Inc., Enfield, New Hampshire.

Crocker F, K Indest, and H Fredrickson. 2006. "Biodegradation of the cyclic nitramine explosives RDX, HMX, and CL-20." *Applied Microbiology and Biotechnology*, submitted.

Crocker F, J Szecsody, and H Fredrickson. 2005. "Biodegradation of hexanitrohexaazaiso-wurtzitane (CL-20) under anaerobic conditions." *Applied Environmental Microbiology* 34:2208-2216.*

Crocker F, K Thompson, J Szecsody, and H Fredrickson. 2005. "Biotic and abiotic degradation of CL-20 and RDX in soils." *Journal of Environmental Quality* 34:2208-2216.*

Szecsody JD Kennedy, and D Girvin. 2007. "Enhancement of CL-20 degradation in sediment suspensions by the iron reducing bacteria Shewanella putrefaciens (strain CN32)." *Environmental Science and Technology*, submitted.*

Szecsody J, J McKinley, J Fruchter, M Williams, V Vermeul, H Fredrickson, and K Thompson. 2006. *In situ chemical reduction of sediments for TCE, energetics, and NDMA remediation, Remediation of Chlorinated and Recalcitrant Compounds*, Monterey, California.**

Szecsody J, J Fruchter, VR Vermeul, M Williams, and B Devary. 2005. "In Situ Reduction of Aquifer Sediments to Create a Permeable Reactive Barrier to Remediate Chromate: Bench-Scale Tests to Determine Barrier Longevity." Chapter 9, J Jacobs, ed., *Groundwater Remediation of Chromate*, CRC Press.**

Szecsody J, M Williams, J Fruchter, V Vermeul, and D Sklarew. 2004. "In Situ Reduction of Aquifer Sediments: Enhancement of Reactive Iron Phases and TCE Dechlorination." *Environmental Science and Technology* 38:4656-4663.**

Thompson K, F Crocker, and H Fredrickson. 2005. "Mineralization of the cyclic nitramine explosive hexahydro-1,3,5-trinitro-1,3,5-triazine (RDX) by Gordonia and Williamsia sp." *Applied and Environmental Microbiology* 71(12):8265-8272.

Szecsody J, C Ainsworth, B Devary, A Fischer, H Fredrickson, K Thompson, S Comfort, and H Boparai. 2004. *Enhancement of In Situ Bioremediation of Energetic Compounds by Coupled Abiotic/Biotic Processes: Annual Report for 2004*. SERDP, Washington, D.C.

Szecsody J, D Girvin, B Devary, C Resch, A Fischer, H Fredrickson, K Thompson, S Comfort, and H Boparai. *Enhancement of In Situ Bioremediation of Energetic Compounds by Coupled Abiotic/Biotic Processes: Annual Report for 2005*. SERDP, Washington, D.C.

Presentations

Boparai H, S Comfort, T Satapanajaru, and J Szecsody. 2005. Degradation kinetics of energetic compounds by Fe(O) corrosion products, SERDP Annual Meeting, December 2005, Washington, D.C.

Boparai H, S Comfort, and J Szecsody. 2006. Evaluating In Situ Redox Manipulation for Remediating Explosive-Contaminated Groundwater, SERDP Annual Meeting, December 2006, Washington, D.C.

Durkin L, J Szecsody, and B Devary. 2007. Explosives in Our Environment: The Problem of TNT Contamination, American Chemical Society, Cleveland Section Meeting, Notre Dame College, March 7, 2007.

Szecsody J, S Comfort, and H Boparai. 2004. Abiotic/Biotic Remediation of Energetic Compounds by Coupled Processes, SERDP Annual Conference, November 29-December 2, 2004, Washington, D.C.

Szecsody J, D Girvin, B Devary, M Qasim, F Crocker, and H Fredrickson. 2004. Transport and Degradation of the Explosives CL-20 and RDX in Subsurface Sediments, Fourth Annual Society of Environmental Toxicology and Chemistry (SETAC) World Congress, Portland, Oregon, November 18, 2004.*

Szecsody J, J McKinley, A Fischer, H Booparai, S Comfort, K Thompson, and H Fredrickson. 2005. Subsurface remediation of RDX and other energetics by coupled abiotic and biotic processes, SERDP Annual Meeting, December 2005, Washington, D.C.

Szecsody J, J McKinley, J Fruchter, M Williams, V Vermeul, H Fredrickson, and K Thompson. 2006. In situ chemical reduction of sediments for TCE, energetics, and NDMA remediation, Remediation of Chlorinated and Recalcitrant Compounds, Monterey, California, May 2006.

Szecsody J, J Phillips, B Devary, L Durkin, H Boparai, S Comfort, K Thompson, and H Fredrickson. 2006. Differences in Coupled Abiotic/Biotic Degradation of RDX, HMX, and TNT in Subsurface Sediments, SERDP Annual Meeting, December 2006, Washington, D.C.

Szecsody J, E Murphy, T Resch, J Phillips, and M Williams. 2005. Microbial transport mechanisms in subsurface sediments, American Geophysical Union, Annual Fall Meeting, San Francisco, California, December 2005 (invited speaker).**

Attachment 2: Students

Boparai, Hardiljeet. PhD student (graduated) worked for Dr. Steve Comfort, University of Nebraska, Lincoln, 2004-2006.

Devary, Brooks. Chemical Engineering undergraduate, worked Dr. Jim Szecsody, Pacific Northwest National Laboratories, 2004-2006.

Durkin, Lisa. Chemistry undergraduate, worked for Dr. Jim Szecsody, Pacific Northwest National Laboratories, summer 2006.

Fisher, Ashley. Post-B.S. Chemistry student, worked for Dr. Jim Szecsody, Pacific Northwest National Laboratories, summers 2005-2006.

Liu, Ying. Physical Sciences undergraduate, worked for Dr. Jim Szecsody, Pacific Northwest National Laboratories, summer 2005.

Appendix A: RDX Degradation by Coupled Abiotic/Biotic Processes

R91: RDX Degradation by Red. Sediment + gluteraldehyde

Ft. Lewis Sed. Reduced
2*di/Fe=28, r_{sw} = 0.1

+ 100 mM gluteraldehyde

C_0 = 10mg/L

Det. Lim. 0.15mg/L
+/- 0.5%
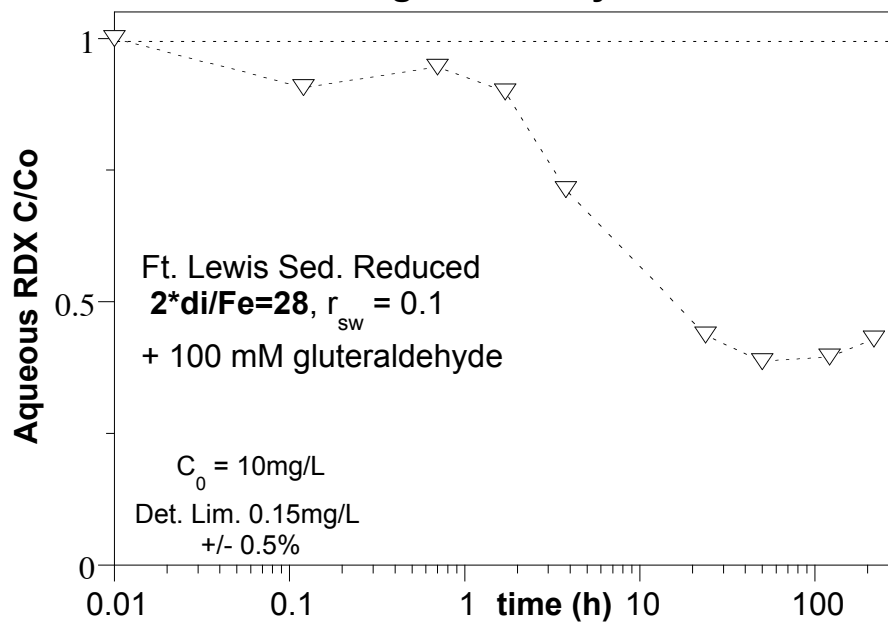
R92: RDX Degradation by Red. Sediment + ammonium molybdate tetrahydrate
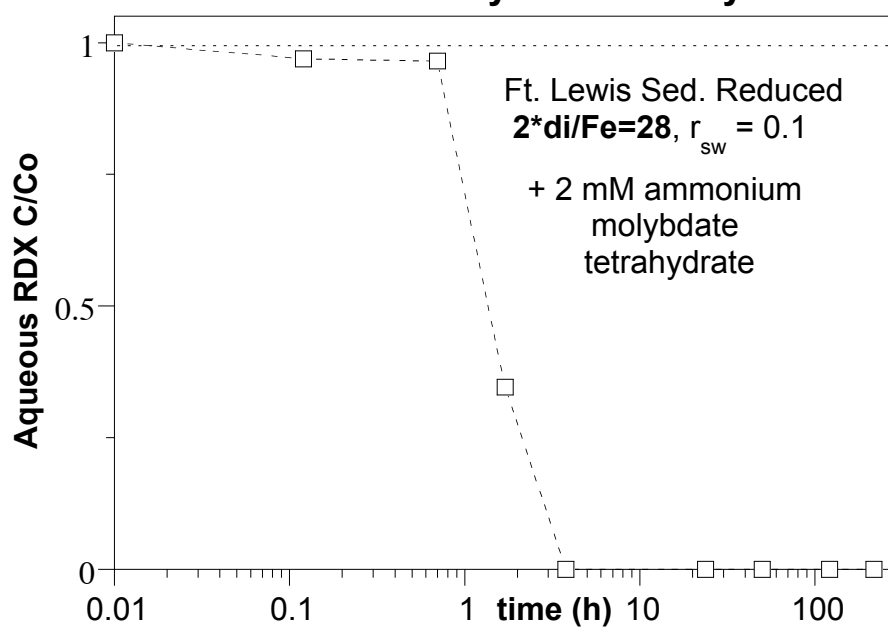
Ft. Lewis Sed. Reduced
2*di/Fe=28, r_{sw} = 0.1

+ 2 mM ammonium
molybdate
tetrahydrate

A.1

R93: RDX Degradation by Red. Sediment
+ sodium 2-bormoethanesulfonate

Aqueous RDX C/Co

Ft. Lewis Sed. Reduced
2*di/Fe=28, r_{sw} = 0.1

+ 6 mM sodium
2-bromoethanesulfonate

C_0 = 10mg/L

Det. Lim. 0.15mg/L
+/- 0.5%

time (h)

RDX Degradation by Red. Sediment
+ Bactericides

Aqueous RDX C/Co

+ 6 mM sodium
2-bromoethanesulfonate

Controls
(solid points)

Ft. Lewis Sed. Reduced
2*di/Fe=28, r_{sw} = 0.1

C_0 = 10mg/L

Det. Lim. 0.15mg/L
+/- 0.5%

+ 2 mM
ammonium
molybdate
tetrahydrate

+ 100 mg/L
HgCl$_2$

+ 100 mM
gluteralehyde

time (h)

A.2

**R93: RDX Degradation by Red. Sediment
+ sodium 2-bormoethanesulfonate**

Aqueous RDX C/Co

Ft. Lewis Sed. Reduced
2*di/Fe=28, r_{sw} = 0.1

+ 6 mM sodium
2-bromoethanesulfonate

C_0 = 10mg/L
Det. Lim. 0.15mg/L
+/- 0.5%

0.01   0.1   1   **time (h)** 10   100

A.3

A.4

RDX

NB-A, sed/water = 1/20
Ft Lewis sediment

model 1
$RDX + 2 Fe^{2+} \rightarrow MNX + 2 Fe^{3+} + 2OH^-$

$RDX + Fe^{2+} \rightarrow MNX + Fe^{3+} + OH^-$
model 2

MNX

$MNX + 2 Fe^{2+} \rightarrow DNX + 2 Fe^{3+} + 2OH^-$

$MNX + Fe^{2+} \rightarrow DNX + Fe^{3+} + OH^-$

NB-A, sed/water = 1/20

DNX

$DNX + 2 Fe^{2+} \rightarrow TNX + 2 Fe^{3+} + 2OH^-$

TNX

$TNX + 2 Fe^{2+} \rightarrow UN1 + 2 Fe^{3+} + 2OH^-$

RDX

NB-A, sed/water = 1/20

final

tnx

unknown 1

mnx   **dnx**

surface Fe2+   NB-A, sed/water = 1/20

surface Fe3+, also (OH)- generated

A.5

A.7
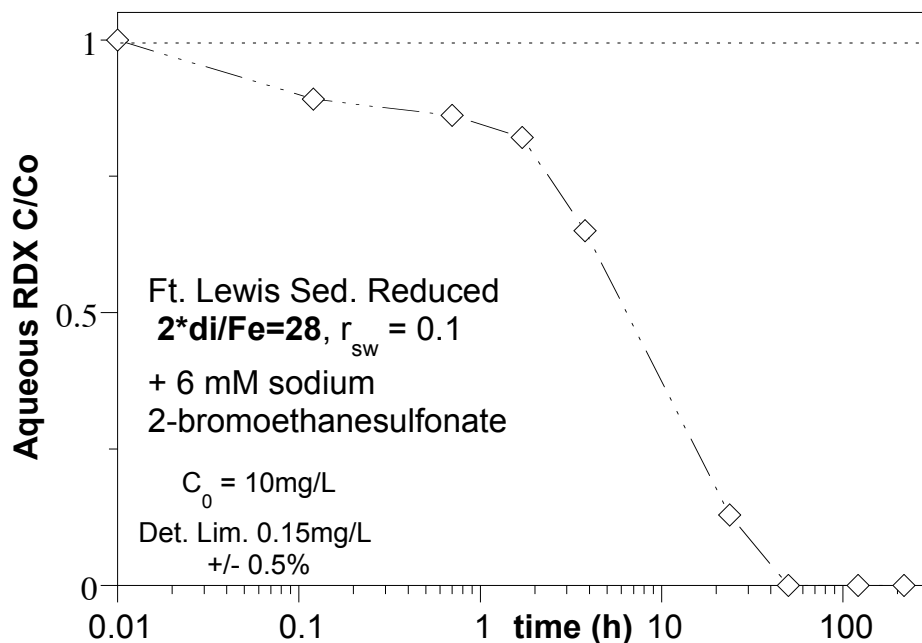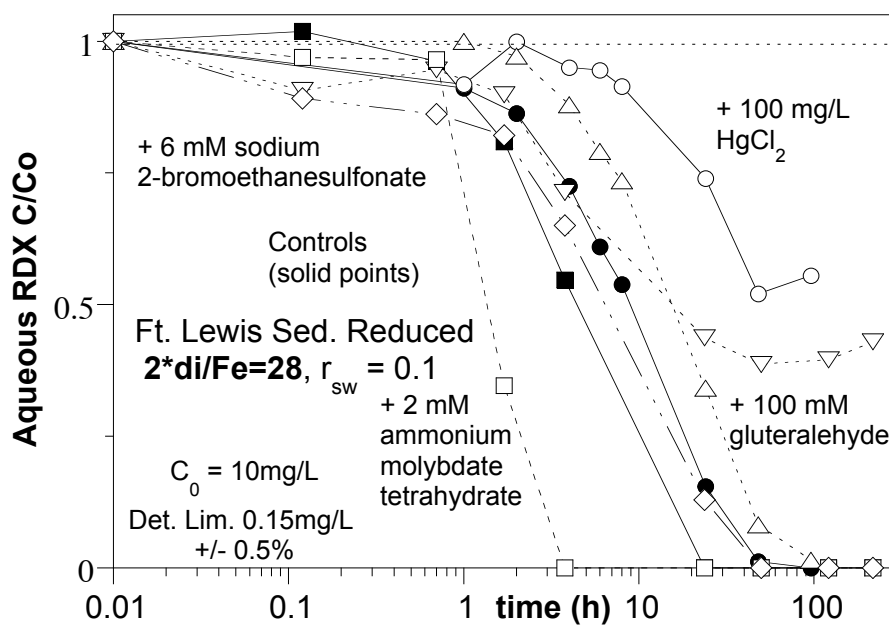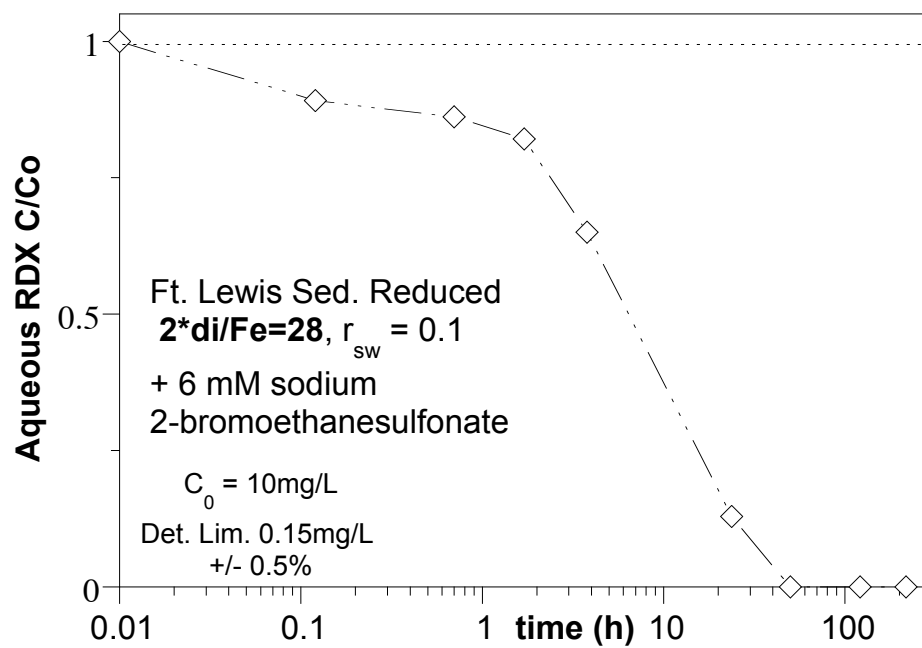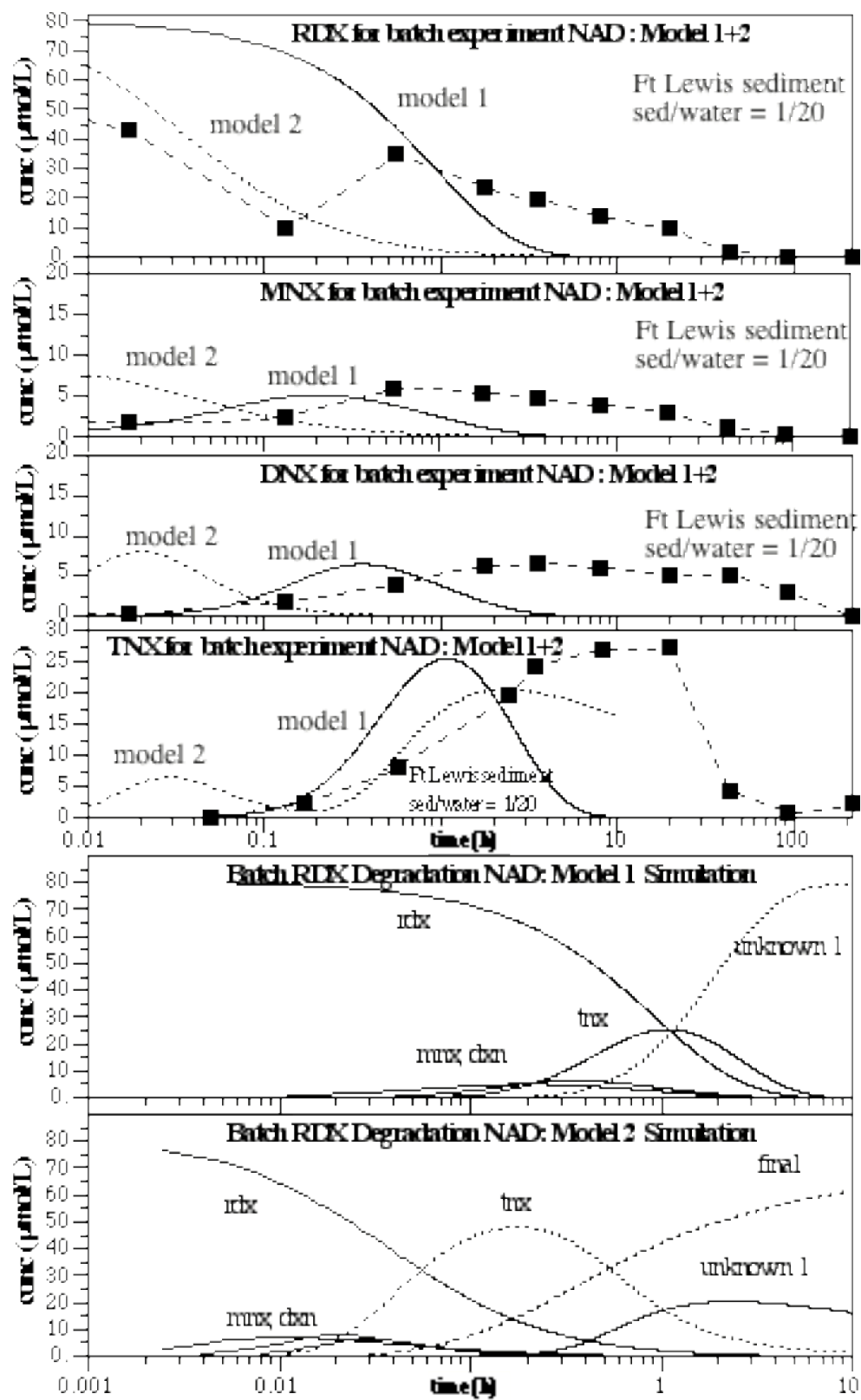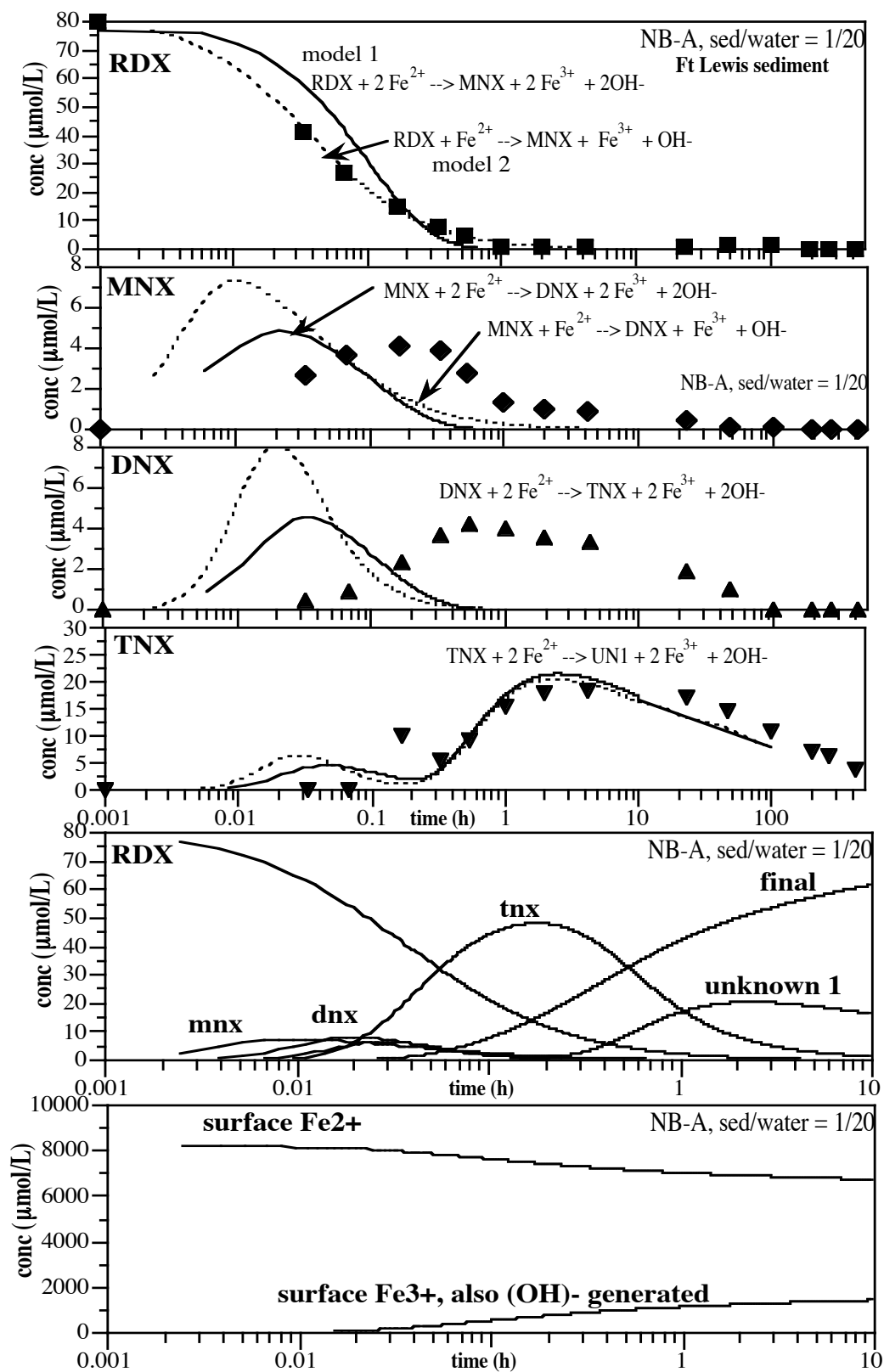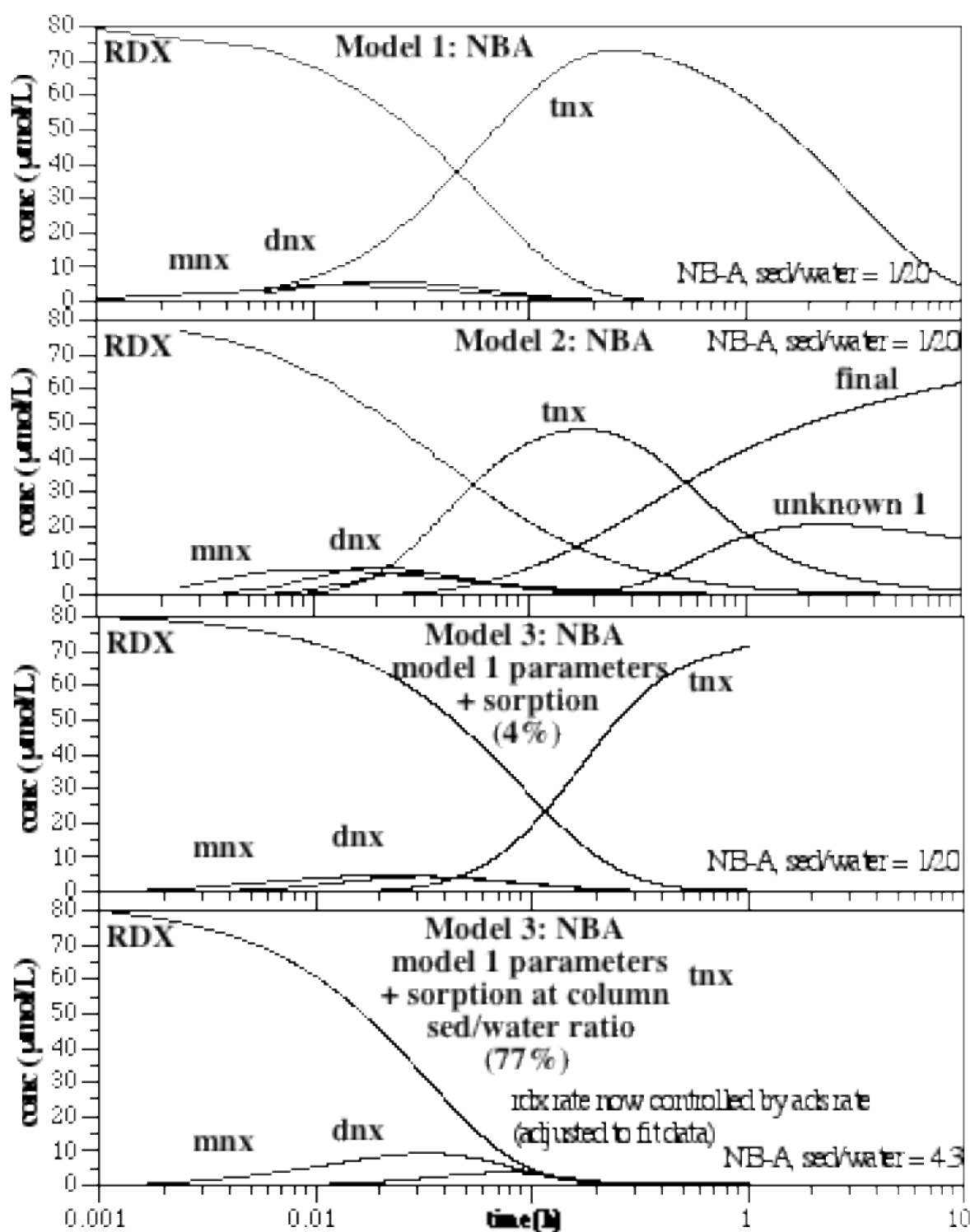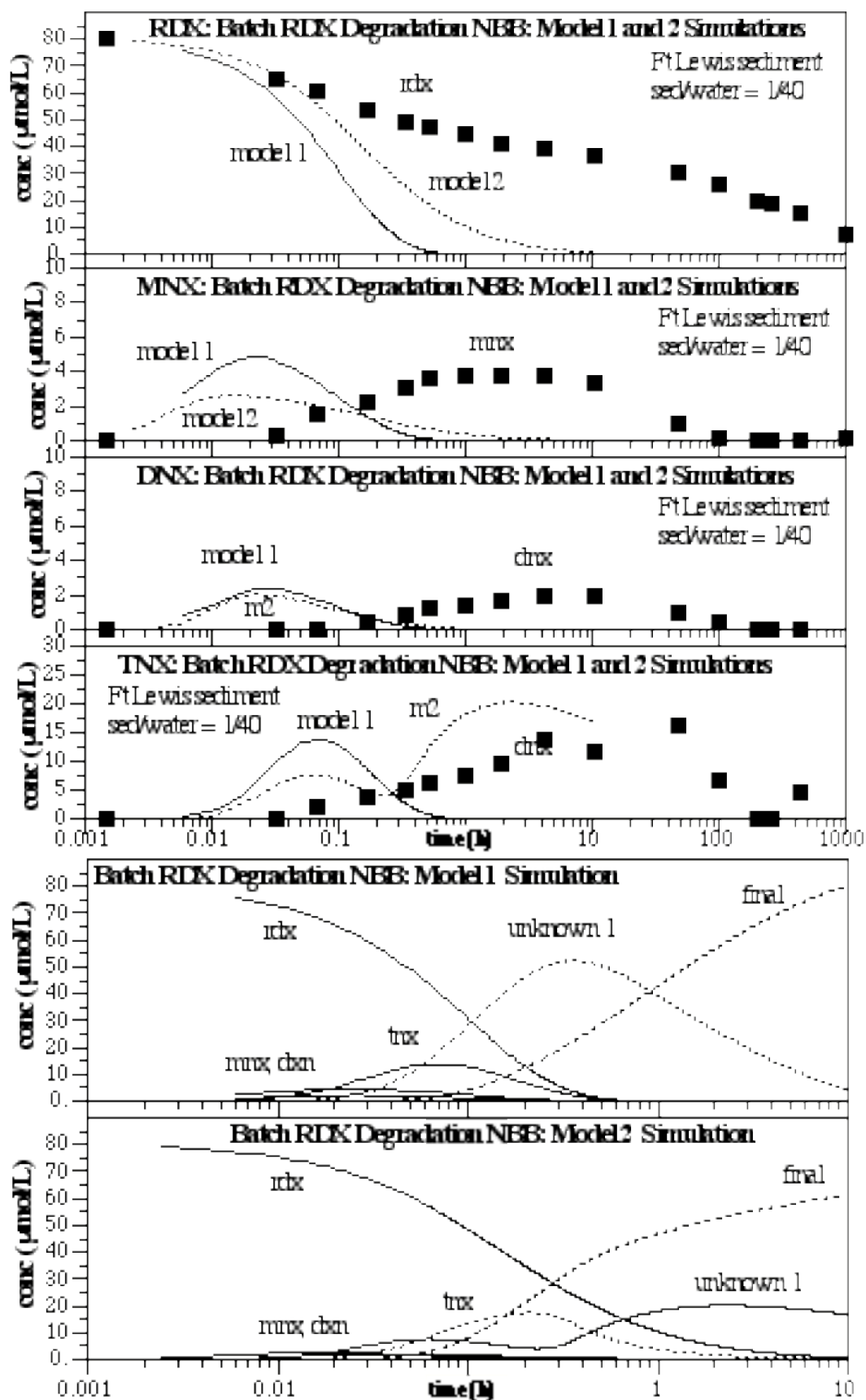
W45; RDX->MEDINA degradation by red. Ft. Lewis
2*dith./Fe = 37, batch r_{sw} = 0.087-0.075
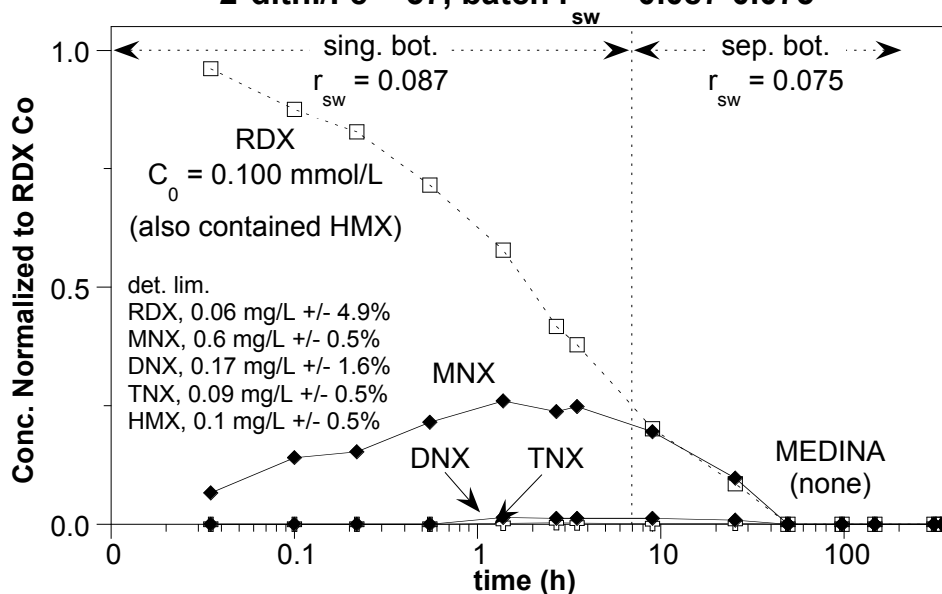
W45; RDX->MEDINA degradation by red. Ft. Lewis
2*dith./Fe = 37, batch r_{sw} = 0.087-0.075
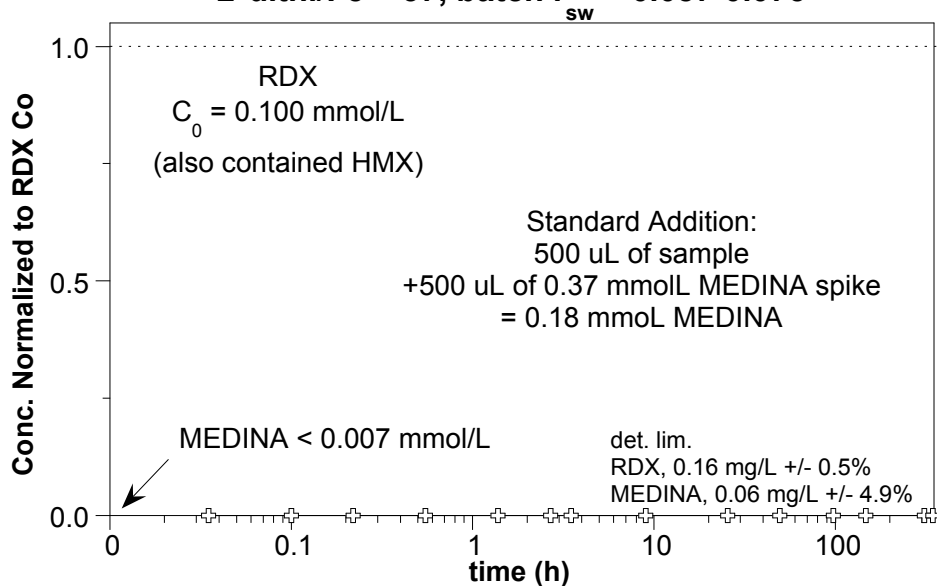
**W45; RDX->MEDINA degradation by red. Ft. Lewis
MEDINA Standard Additions**
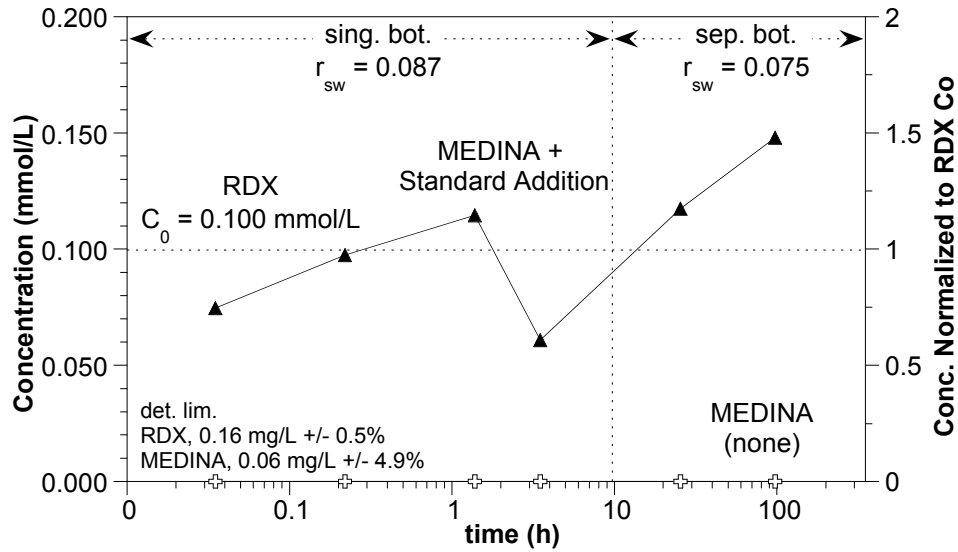
**W45; RDX->MEDINA degradation by red. Ft. Lewis
2*dith./Fe = 37, batch r_{sw} = 0.087-0.075**

W51; MEDINA batch deg. by oxic, anaerobic Ft. Lewis comp.

MEDINA C_0 < 10 mg/L

oxic sed., He bubbled
r_{sw} = 0.168

Samples analyzed
~ 3.5h after collection

det. lim. 0.06 mg/L +/- 4.9%
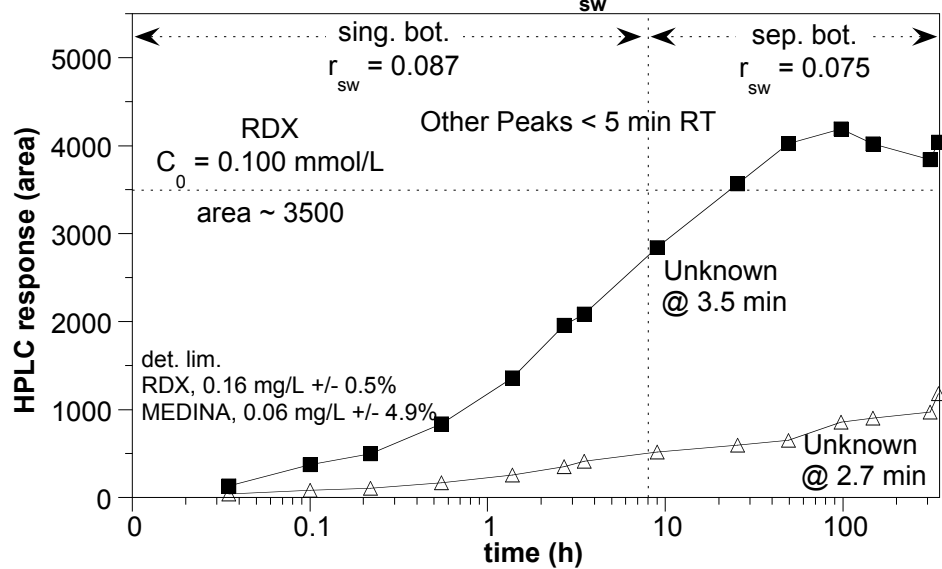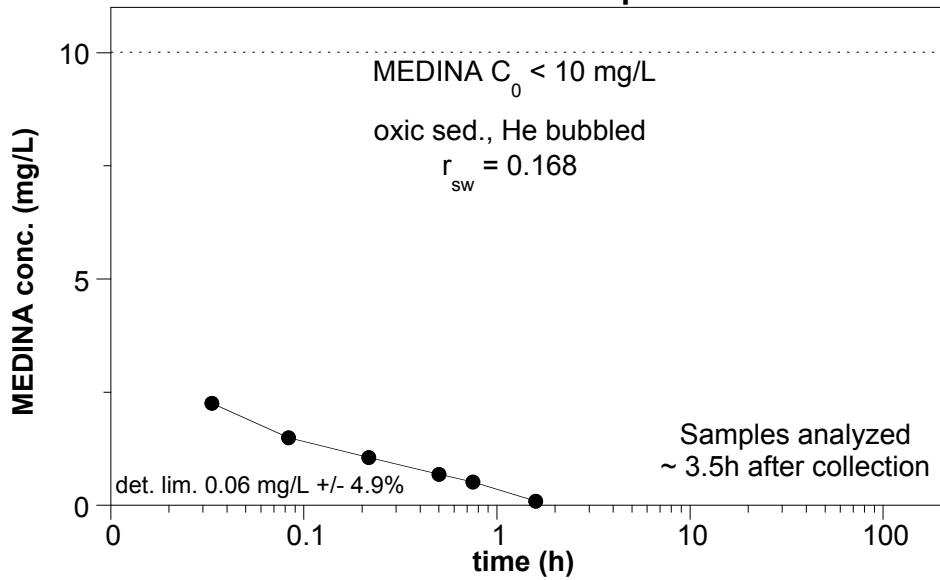
W52; MEDINA batch deg. by red., anaerobic Ft. Lewis comp. 2*dith/Fe = 0.53
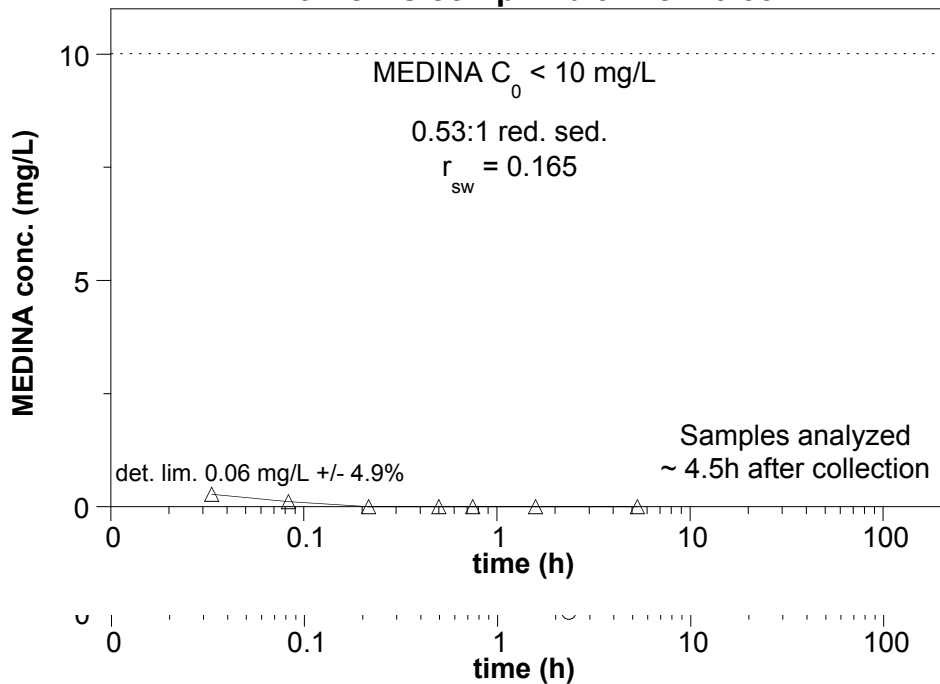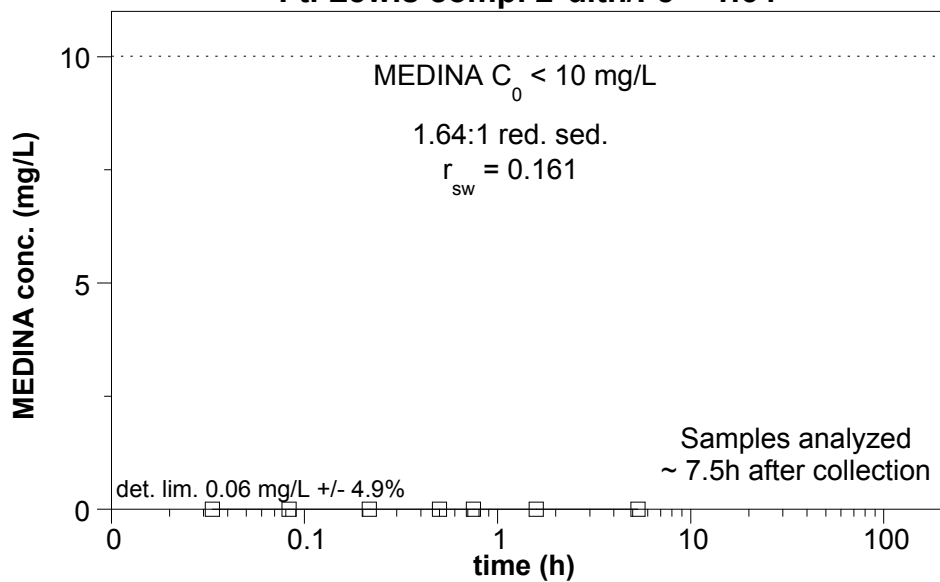
MEDINA C_0 < 10 mg/L

0.53:1 red. sed.
r_{sw} = 0.165

Samples analyzed
~ 4.5h after collection

det. lim. 0.06 mg/L +/- 4.9%

B.3

W53; MEDINA batch deg. by red., anaerobic
Ft. Lewis comp. 2*dith/Fe = 1.64

MEDINA C_0 < 10 mg/L

1.64:1 red. sed.
r_{sw} = 0.161

Samples analyzed
~ 7.5h after collection

det. lim. 0.06 mg/L +/- 4.9%

MEDINA conc. (mg/L)

time (h)

W54; MEDINA batch deg. by red., anaerobic
Ft. Lewis comp. 2*dith/Fe = 21.9

MEDINA C_0 < 10 mg/L

21.9:1 red. sed.
r_{sw} = 0.157

Samples analyzed
~ 7.5h after collection

det. lim. 0.06 mg/L +/- 4.9%

MEDINA conc. (mg/L)

time (h)

B.4

W50-54; MEDINA batch deg. by oxic and red.
Ft. Lewis comp.

MEDINA C_0 < 10 mg/L

r_{sw} ~ 0.16

W50: oxic sed.

W51: oxic sed + He bubble

W53: 1.64:1 red. sed

W54: 21.9:1 red. sed

W52: 0.53:1
red. sed

MEDINA conc. (mg/L)

time (h)

det. lim. 0.06 mg/L +/- 4.9%
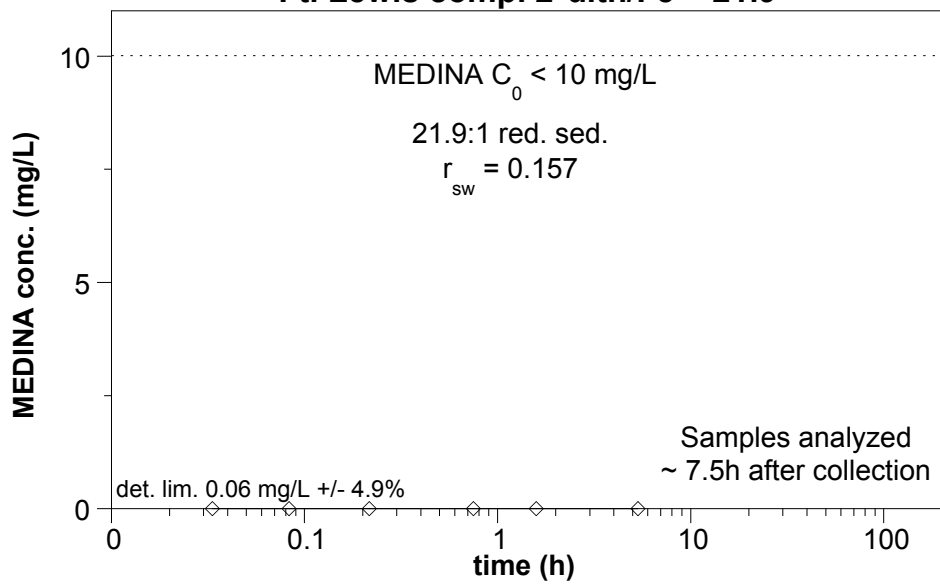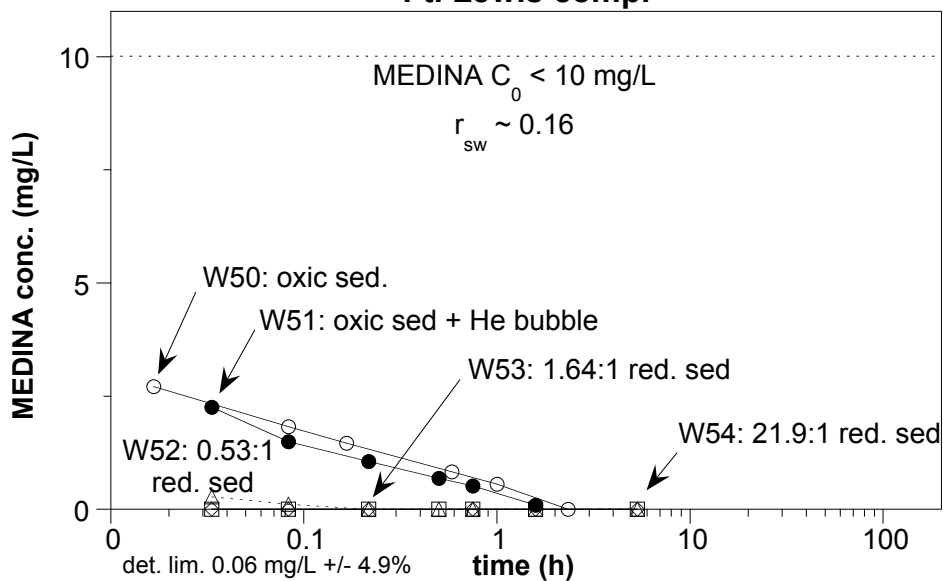
W55; MEDINA batch deg. by oxic, anaerobic
Ft. Lewis comp. + UV light treatment

MEDINA C_0 ~ 20 mg/L

(started with spike)

oxic sed., He bubbled +UV light

r_{sw} = 0.142

Samples analyzed
~ 6h after collection

MEDINA conc. (mg/L)

time (h)

det. lim. 0.06 mg/L +/- 4.9%

B.5
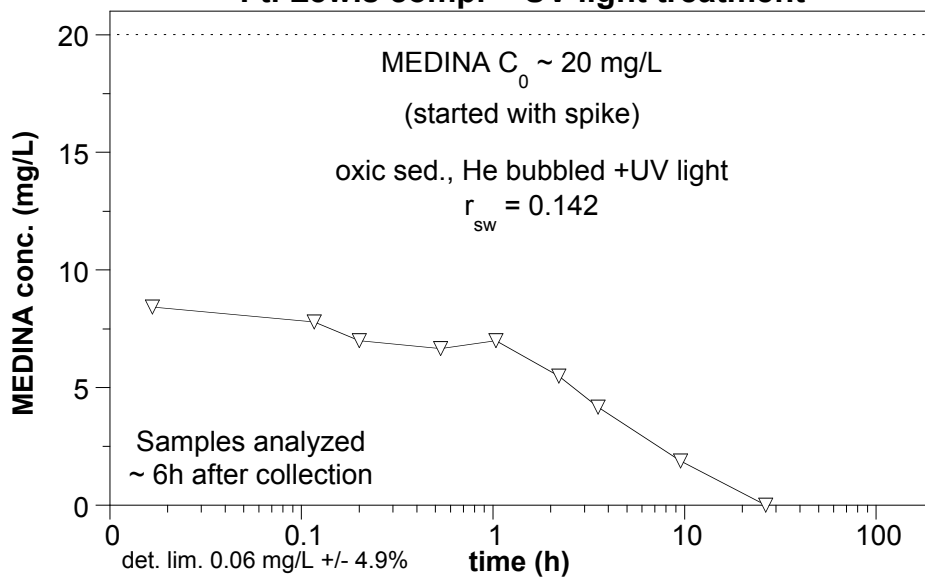
W56; MEDINA batch deg. by red., anaerobic
Ft. Lewis comp. 2*dith/Fe=1.64 + UV light treatment

MEDINA C_0 ~ 20 mg/L

(started with spike)

1.64:1 red. sed +UV light

r_{sw} = 0.157

Samples analyzed
0-7h after collection

det. lim. 0.06 mg/L +/- 4.9%   **time (h)**

MEDINA conc. (mg/L)
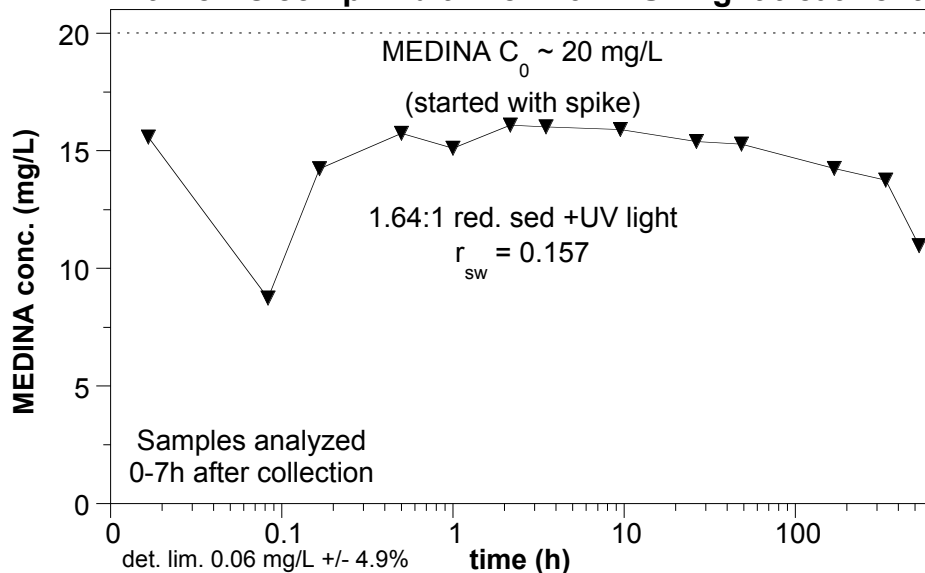
W55-56; MEDINA batch deg. by oxic and red.
Ft. Lewis comp. + UV light treatment

MEDINA C_0 ~ 20 mg/L

W56: 1.64:1
red. sed

(started with spike)

r_{sw} ~ 0.16

W55: oxic sed.

det. lim. 0.06 mg/L +/- 4.9%   **time (h)**

MEDINA conc. (mg/L)

B.6
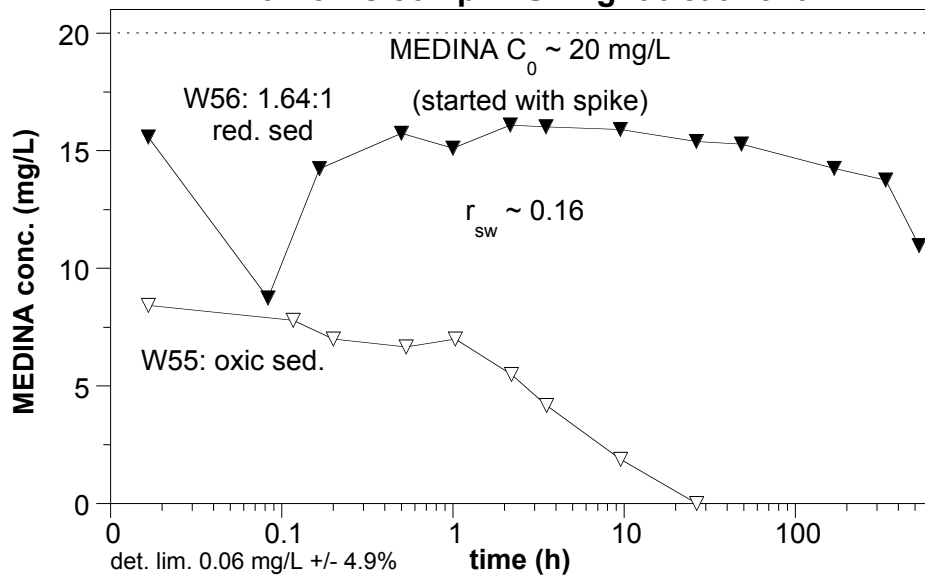
Appendix C: Formate Mineralization (RDX, HMX Intermediate)

R105; Formate Mineralization vs. Iron Reduction

R66 Col. Red. Sed.
$2*di/Fe = 28$, $r_{sw} = 0.15$

rem. AQ fraction

R106; Formate Mineralization vs. Iron Reduction + glucose + trace nutrients

R66 Col. Red. Sed.
$2*di/Fe = 28$, $r_{sw} = 0.12$

rem. AQ fraction

R107; Formate Mineralization vs. Iron Reduction

R20-21 Col. Red. Sed.
$2*di/Fe = 3$, $r_{sw} = 0.04$

rem. AQ
fraction

R108; Formate Mineralization vs. Iron Reduction

R67 Col. Red. Sed.
$2*di/Fe = 1.6$, $r_{sw} = 0.13$

mineralized

AQ frac.

C.2

R109; Formate Mineralization vs. Iron Reduction

R51 Col. Red. Sed.
$2*di/Fe = 0.08$, $r_{sw} = 0.13$

mineralized

AQ frac.

C/Co

time (h)

R110; Formate Mineralization vs. Iron Reduction

Untreated Ft. Lewis Sed.
$r_{sw} = 0.13$

AQ frac.

mineralized

C/Co

time (h)

C.3

R111; Formate Mineralization vs. Iron Reduction + bactericides

R66 Col. Red. Sed.
$2*di/Fe = 28$, $r_{sw} = 0.13$

AQ frac.

mineralized

C/Co

time (h)

R112; Formate Mineralization vs. Iron Reduction + bactericides

Untreated Ft. Lewis Sed.
$r_{sw} = 0.13$

AQ frac.

mineralized

C/Co

time (h)

Formate Mineralization vs. Iron Reduction

Formate Mineralization vs. Iron Reduction + bactericides or trace nutrients + glucose

Formate Mineralization vs. Iron Reduction + bactericides

Red. Sed.; 2*di/Fe = 28 w/o bactericides

Untreated Sed w/wo bactericides + Red. Sed. w/bactericides

C/Co

time (h)

C.6

Appendix D: RDX Mineralization by Coupled Abiotic/Biotic Process

RDX Mineralization – exposed to dithionite for 1 day, then oxidized
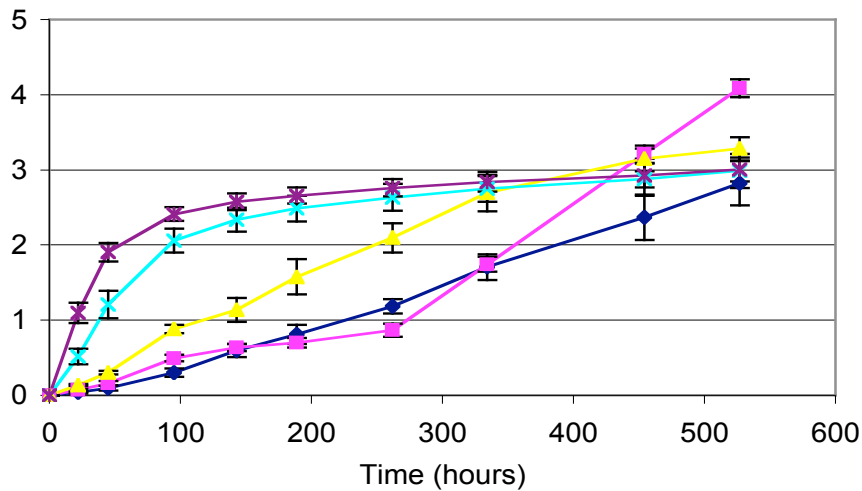
RDX Mineralization – exposed to dithionite for 3 days, then oxidized

◆ Treatment 1	■ Treatment 2	▲ Treatment 3
✕ Treatment 4	✱ Treatment 5	● Control-No treatment

treatment	2* di/Fe
1	4.0
2	1.0
3	0.5
4	0.1
5	0.02

RDX Mineralization – exposed to dithionite for 5 days, then oxidized

RDX Mineralization – exposed to dithionite for 10 days, then oxidized

D.2

R44, RDX min., untreated sed., anoxic

total aqueous

C_0 = 10mg/L

Det. Lim. 0.15mg/L
+/- 0.5%

mineralized

R45, RDX min., untreated sed.+ nutr., anoxic

total aqueous

C_0 = 10mg/L

Det. Lim. 0.15mg/L
+/- 0.5%

mineralized

R46, RDX min., R30 sed.(0.08), anoxic

total aqueous

C_0 = 10mg/L

Det. Lim. 0.15mg/L
+/- 0.5%

mineralized

R47, RDX min., R30 sed. (0.08)+ nutr., anoxic

total aqueous

C_0 = 10mg/L

Det. Lim. 0.15mg/L
+/- 0.5%

mineralized

D.3

R48, RDX mineralization, R26 sed.(1.0), anoxic

total aqueous

$C_0 = 10mg/L$

Det. Lim. 0.15mg/L

+/- 0.5%

mineralized

R49, RDX min., R26 sed. (1.0)+ nutr., anoxic

total aqueous

failed: NaOH dripped into sediment

$C_0 = 10mg/L$

Det. Lim. 0.15mg/L

+/- 0.5%

mineralized

R50, RDX mineralization, R23 sed.(25), anoxic

total aqueous

mineralized

$C_0 = 10mg/L$

Det. Lim. 0.15mg/L

+/- 0.5%

R51, RDX min., R23 sed. (25)+ nutr., anoxic

total aqueous

mineralized

$C_0 = 10mg/L$

Det. Lim. 0.15mg/L

+/- 0.5%

D.4

RDX Mineralization vs Iron Reduction

hypothesis: RDX mineralization is a measure
of abiotic + biotic response. Definitely need
bugs, so expect partially reduced is fastest
results: most reduced is fastest RDX min.
-> very resistant bugs?

2*di/Fe = 26

1.0

0.00 0.08

C_0 = 10mg/L

Det. Lim. 0.15mg/L
+/- 0.5%

C/Co

time (h)

RDX Mineralization vs Iron Reduction + Nutrients

hypothesis: RDX mineralization is a measure
of abiotic + biotic response. Definitely need
bugs, so expect partially reduced is fastest.
Added nutrients should increase rate.
results: rate increased with nutrients:

2di/Fe	half-life no nutr	half-life w/nutr
26	323	112

(others slower)

2*di/Fe = 26

0.00 0.08

C_0 = 10mg/L

Det. Lim. 0.15mg/L
+/- 0.5%

C/Co

time (h)

D.5

RDX Mineralization + Lactate vs Iron Reduction

R64-69

2*di/Fe ratio
- 0.00
- 0.1
- 0.3
- 0.8
- 1.5
- 27

C_0 = 10mg/L

Det. Lim. 0.15mg/L
+/- 0.5%

C/Co

time (h)

R64, RDX min., untreated sed. + lactate

total aqueous

C_0 = 10mg/L

Det. Lim. 0.15mg/L
+/- 0.5%

mineralized

C/Co

time (h)

R65, RDX min., R51 sed (0.1). + lactate

total aqueous

C_0 = 10mg/L

Det. Lim. 0.15mg/L
+/- 0.5%

mineralized

C/Co

time (h)

D.6

R66, RDX min.+ lactate, R49 sed (0.3)

total aqueous

C_0 = 10mg/L

Det. Lim. 0.15mg/L

+/- 0.5%

mineralized

C/Co

time (h)

R67, RDX min.+ lactate, R47 sed (0.8)

total aqueous

C_0 = 10mg/L

Det. Lim. 0.15mg/L

+/- 0.5%

mineralized

C/Co

time (h)

R68, RDX min.+ lactate, R45 sed (1.5)

total aqueous

C_0 = 10mg/L

Det. Lim. 0.15mg/L

+/- 0.5%

mineralized

C/Co

time (h)

R69, RDX min.+ lactate, R24 sed (27)

total aqueous

C_0 = 10mg/L

Det. Lim. 0.15mg/L

+/- 0.5%

mineralized

C/Co

time (h)

D.7

R78: RDX Biostimulation by oxic, unt. sed, + tr. nutr.

Ft. Lewis Sed. Untreated, r_{sw} = 0.167

In oxic environment
10mg/L 14C-RDX + 8.0 mM PIPES
+ 3 mL nutrient solution

Det. Lim. 0.15mg/L
+/- 0.5%

Mineralized C/Co

time (h)

R79: RDX Biostimulation by anoxic, unt. sed, + glucose

Ft. Lewis Sed. Untreated, r_{sw} = 0.167

In anaerobic environment
10 mg/L 14C-RDX+ 8.0 mM PIPES
+ 0.16 mg/L glucose

Det. Lim. 0.15mg/L
+/- 0.5%

Mineralized C/Co

time (h)
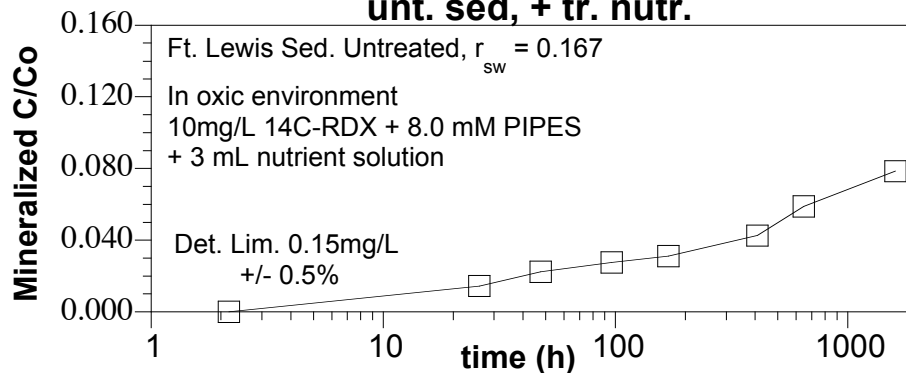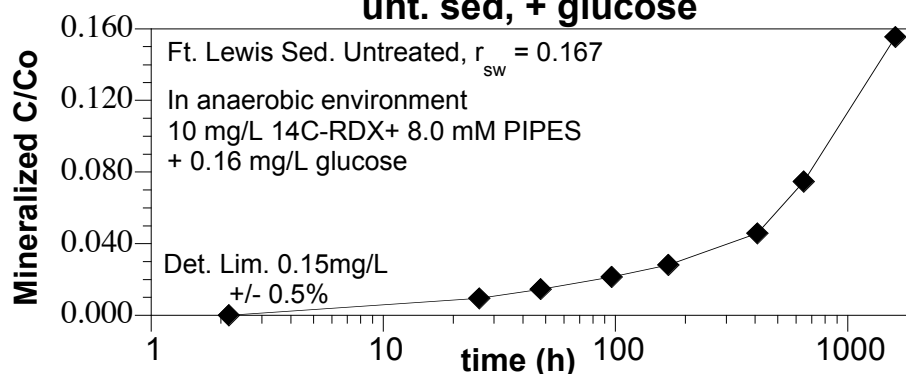
R80: RDX Biostimulation by anoxic, unt. sed, + glucose + sulfate

Ft. Lewis Sed. Untreated, r_{sw} = 0.167

In anaerobic environment
10 mg/L RDX + 8.0 mM PIPES
+ 0.16 mg/L glucose + 1.0 mM sulfate

Det. Lim. 0.15mg/L
+/- 0.5%

Mineralized C/Co

time (h)

RDX Biostimulation:
R78 Oxic, untr.sed., tr. nutr
R79 Anoxic, untr. + glucose
R80 Anoxic, untr. + glucose+SO4

Det. Lim. 0.15mg/L
+/- 0.5%

mineralized

RDX Biostimulation
oxic, lactate
oxic, trace nutrients
oxic, no additions
anoxic, no additions
anoxic, glucose
anoxic, glucose, SO4

C_0 = 10mg/L
Det. Lim. 0.15mg/L
+/- 0.5%

untr,
no O2

untr

R81: RDX Mineralization by Red. Sediment

Ft. Lewis Sed. Reduced **2*di/Fe=28**, r_{sw} = 0.167

In anaerobic environment
10 mg/L 14C-RDX + 0.01 M PIPES

Det. Lim. 0.15mg/L
+/- 0.5%

R82: RDX Mineralization by Red. Sediment + tr. nutr.

Ft. Lewis Sed. Reduced **2*di/Fe=28**, r_{sw} = 0.167

In anaerobic environment
10 mg/L 14C-RDX + 0.01 M PIPES
+ 3mL nutrient solution

Det. Lim. 0.15mg/L
+/- 0.5%

R83: RDX Mineralization by Red. Sediment + glucose

Ft. Lewis Sed. Reduced **2*di/Fe=28**, r_{sw} = 0.167

In anaerobic environment
10 mg/L 14C-RDX + 0.01 M PIPES
+ 0.16 mg/L glucose (C/N = 20)

Mineralized RDX C/Co

Det. Lim. 0.15mg/L
+/- 0.5%

time (h)

R84: RDX Mineralization by Red. Sediment + glucose + sulfate + tr. nutr.

Ft. Lewis Sed. Reduced **2*di/Fe=28**, r_{sw} = 0.167

In anaerobic environment
10 mg/L 14C-RDX + 0.01 M PIPES
+ 0.16 mg/L glucose (C/N = 20)
+ 1 mM sulfate + 3mL nutrient sol.

Mineralized RDX C/Co

Det. Lim. 0.15mg/L
+/- 0.5%

time (h)

D.11

R85: RDX Mineralization by Red. Sediment

Ft. Lewis Sed. Reduced **2*di/Fe=3.0**, r_{sw} = 0.167

In anaerobic environment
10 mg/L 14C-RDX + 0.01 M PIPES

Det. Lim. 0.15mg/L
+/- 0.5%

R86: RDX Mineralization by Red. Sediment + trace nutrients

Ft. Lewis Sed. Reduced **2*di/Fe=1.6**, r_{sw} = 0.167

In anaerobic environment
10 mg/L 14C-RDX + 0.01 M PIPES
+ 3mL nutrient solution

Det. Lim. 0.15mg/L
+/- 0.5%

R87: RDX Mineralization by Red. Sediment + glucose

Ft. Lewis Sed. Reduced **2*di/Fe=1.6**, r_{sw} = 0.167

In anaerobic environment
10 mg/L 14C-RDX + 0.01 M PIPES
+ 0.16 mg/L glucose (C/N = 20)

Det. Lim. 0.15mg/L
+/- 0.5%

Mineralized RDX C/Co

time (h)

R88: RDX Mineralization by Red. Sediment + glucose + sulfate + tr. nutr.

Ft. Lewis Sed. Reduced **2*di/Fe=1.6**, r_{sw} = 0.167

In anaerobic environment
10 mg/L 14C-RDX + 0.01 M PIPES
+ 0.16 mg/L glucose (C/N = 20)
+ 1mM sulfate + 3 mL nutrient sol.

Det. Lim. 0.15mg/L
+/- 0.5%

Mineralized RDX C/Co

time (h)

RDX Mineralization vs Iron Reduction
+ Trace Nutrients

C_0 = 10mg/L
Det. Lim. 0.15mg/L
+/- 0.5%

R45-51,R82, R86

2*di/Fe = 28
26
1.6
0.00   0.08

C/Co

time (h)

RDX Mineralization vs Iron Reduction:
+ 0.16 mg/L Glucose Addition (C/N = 20)

2*di/Fe = 26

1.6

□ no glucose, R81
◆ w/glucose, R83
○ no glucose, R86
● w/glucose, R87

C_0 = 10mg/L
Det. Lim. 0.15mg/L
+/- 0.5%

C/Co

time (h)

D.14

RDX Mineralization vs Iron Reduction: Sulfate Addition

2*di/Fe = 26

□ no sulfate, R83
◆ w/sulfate, R84
○ no sulfate, R87
● w/sulfate, R88

1.6

C_0 = 10mg/L

Det. Lim. 0.15mg/L
+/- 0.5%

C/Co

time (h)

R118 RDX Mineralization, Aqueous and CO2

aqueous

experiment at 21C
mineralization: 293 h half-life

CO2

R118 RDX Mineralization, Biomass

adsorbed on biomass (saline extr.)

adsorbed on biomass
(NaOH extr.)

incorporated into biomass

RDX Deg. with Anoxic Sed + zvi
- anoxic sediment + 0.04% zvi, t 1/2 = 540 h
- anoxic sediment + 0.17% zvi, t 1/2 = 553 h
- anoxic sediment + 0.39% zvi, t 1/2 = 373 h

R119-121 RDX Deg. with Anoxic Sed + zvi

119 aq

119 co2

anoxic sediment + 0.04% zvi, t 1/2 = 540 h

C/Co

time (h)

R119-121 RDX Deg. with Anoxic Sed + zvi

120 aq

120 co2

anoxic sediment + 0.17% zvi, t 1/2 = 553 h

C/Co

time (h)

R119-121 RDX Deg. with Anoxic Sed + zvi

121 aq

121 co2

anoxic sediment + 0.39% zvi, t 1/2 = 373 h

C/Co

time (h)

R122 RDX Anoxic Biodeg w/prestimulation

aqueous

122 aq

122 co2

CO2

R123 RDX Anoxic Biodeg w/prestim + glucose

aqueous

123 aq

123 co2

CO2

R124 RDX Anoxic Biodeg w/prestim + tr.nutr.

aqueous

124 aq

124 co2

CO2

R122-124 RDX Biostimulation

anoxic sed. + 1 wk RDX prestim. (4960 h)

anoxic sed. + 1 wk RDX prestim.+gluc. (9170 h)

anoxic sed. + 1 wk RDX prestim.+ trace nutrients (5570 h)

D.18

RDX mineralization half-life (h)

10^5

reduced sediment

10^4

zvi in sediment

10^3

reduced sediment in column

10^2

10   100   1000   10^4

Fe(0 or II)/RDX ratio (mol/mol)

R76: RDX Mineralization by Reduced Sediment + Bacteriacides

Mineralized RDX C/Co

1.0

Ft. Lewis Sed. Reduced 2*di/Fe=28, r$_{sw}$ = 0.167

In anaerobic environment
10mg/L 14C-RDX + 0.17 mL 0.5M PIPES
+ 0.1mL/5mL 25% gluteraldehyde
+ 2mM molbdate tetrahydrate
+ 6mM sodium 2-bromoethanesulfonate

0.5

0.0

1   10   100   1000

time (h)

RDX Counting Efficiency with Activated Carbon

14C RDX = 7405 dpm/mL

Conclusions:
1. need 0.01 g carbon in experiments
2. counting with activated carbon inefficient < 15%
3. need solvent extraction (acetone better than dichloromethane)

acetone extraction

dichloromethane extraction

Y-axis: **14C RDX/14C RDX (std)**
X-axis: **activated carbon (g)**

Solvent Extraction for RDX Recovery from Activated Carbon Trap

Y-axis: **RDX recovered from activated carbon**
X-axis: **Extraction Solvent**

Bars: hexane, dichloromethane, propanol, methanol, acetone (0.75 mL/0.01g C), acetone (1.5 mL/0.01 g C), acetonitrile

Appendix E: CL-20 Mineralization in Reduced/Oxidized Sediment
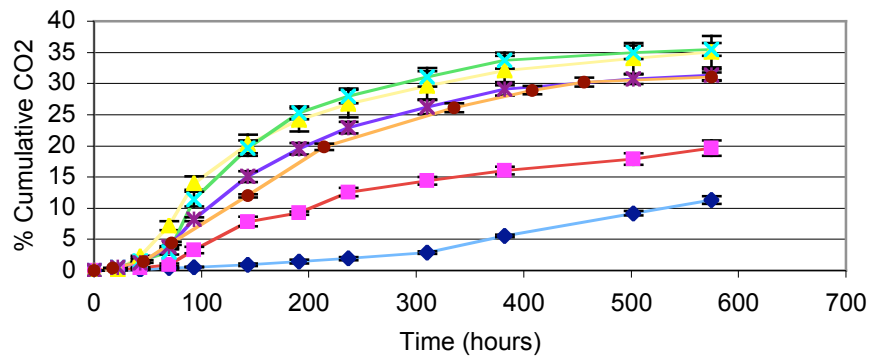
CL-20 Mineralization – exposed to dithionite for 1 day, then oxidized
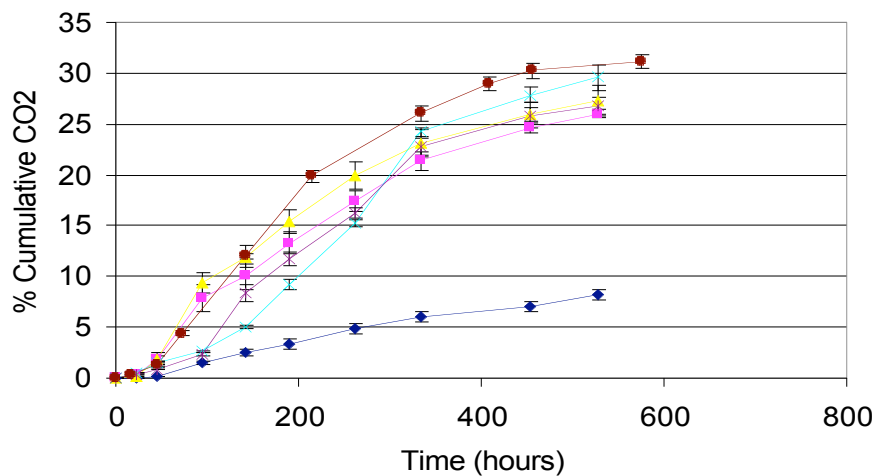
CL-20 Mineralization –exposed to dithionite for 3 days, then oxidized

Treatment 1	Treatment 2	Treatment 3
Treatment 4	Treatment 5	Control-No treatment

treatment	2* di/Fe
1	4.0
2	1.0
3	0.5
4	0.1
5	0.02
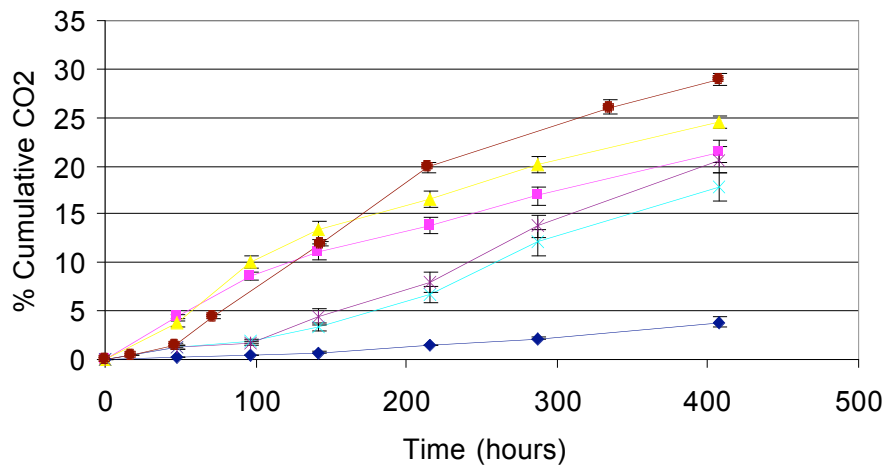
CL-20 Mineralization –exposed to dithionite for 5 days, then oxidized

CL-20 Mineralization –exposed to dithionite for 10 days, then oxidized

E.2
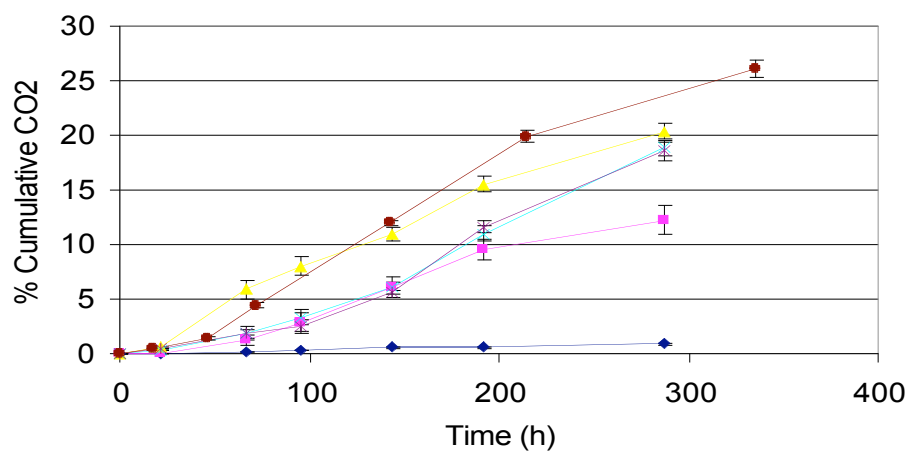
Appendix F: CL-20, RDX, and HMX Oxidation by Persulfate

CL-20 Aqueous Stability

C_0 = 3.5 mg/L

30 C
40 C
50 C
60 C
70 C

det. lim. 0.05 mg/L +/-0.5%

CL-20 oxidation at 30C

aqueous
with 8.1x S_2O_8
with 600x S_2O_8

C_0 = 3.5 mg/L*

det. lim. 0.05 mg/L +/-0.5%

CL-20 oxidation at 40C

aqueous
with 9.6x S_2O_8
with 88x S_2O_8

C_0 = 3.5 mg/L

det. lim. 0.05 mg/L +/-0.5%

F.1

F.2

RDX oxidation at 40C

RDX C/C$_0$

half-life
7000 h
1600 h
800 h

aqueous
with 4.2x S$_2$O$_8$
with 11x S$_2$O$_8$

C$_0$ = 3.5 mg/L
det. lim. 0.05 mg/L +/-0.5%

time (h)

HMX oxidation at 40C

HMX C/C$_0$

half-life
8400 h
3200 h
2000 h

aqueous
with 71x S$_2$O$_8$
with 140x S$_2$O$_8$

C$_0$ = 0.35 mg/L
det. lim. 0.05 mg/L +/-0.5%

time (h)

F.3

Appendix G: HMX Abiotic/Biotic Degradation by Reduced Sediments

R97: HMX Degradation by Red. Sediment
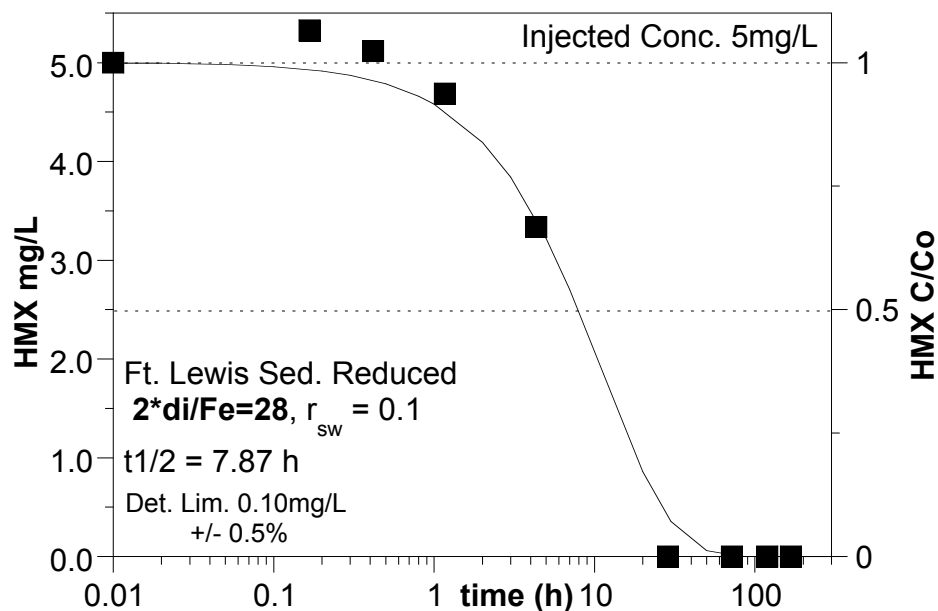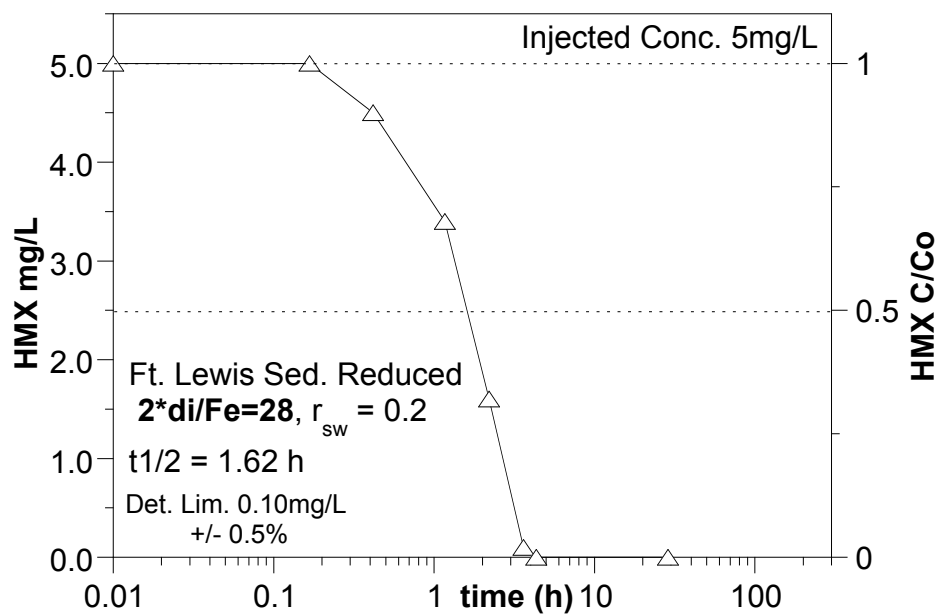
Injected Conc. 5mg/L

Ft. Lewis Sed. Reduced
2*di/Fe=28, r_{sw} = 0.1
t1/2 = 7.87 h
Det. Lim. 0.10mg/L
+/- 0.5%

R98: HMX Degradation by Red. Sediment

Injected Conc. 5mg/L

Ft. Lewis Sed. Reduced
2*di/Fe=28, r_{sw} = 0.2
t1/2 = 1.62 h
Det. Lim. 0.10mg/L
+/- 0.5%

R98: HMX Degradation by Red. Sediment

Injected Conc. 5mg/L

Ft. Lewis Sed. Reduced
2*di/Fe=28, r_{sw} = 0.4
t1/2 = 0.38 h

Det. Lim. 0.10mg/L
+/- 0.5%

HMX mg/L — time (h) — HMX C/Co

R97-99: HMX Degradation by Red. Sediment

Injected Conc. 5mg/L

Ft. Lewis Sed. Reduced
2*di/Fe=28

r_{sw} = 0.1
t1/2 = 7.87 h

r_{sw} = 0.2
t1/2 = 1.62 h

r_{sw} = 0.4
t1/2 = 0.38 h

Det. Lim. 0.10mg/L
+/- 0.5%

HMX mg/L — time (h) — HMX C/Co

G.2
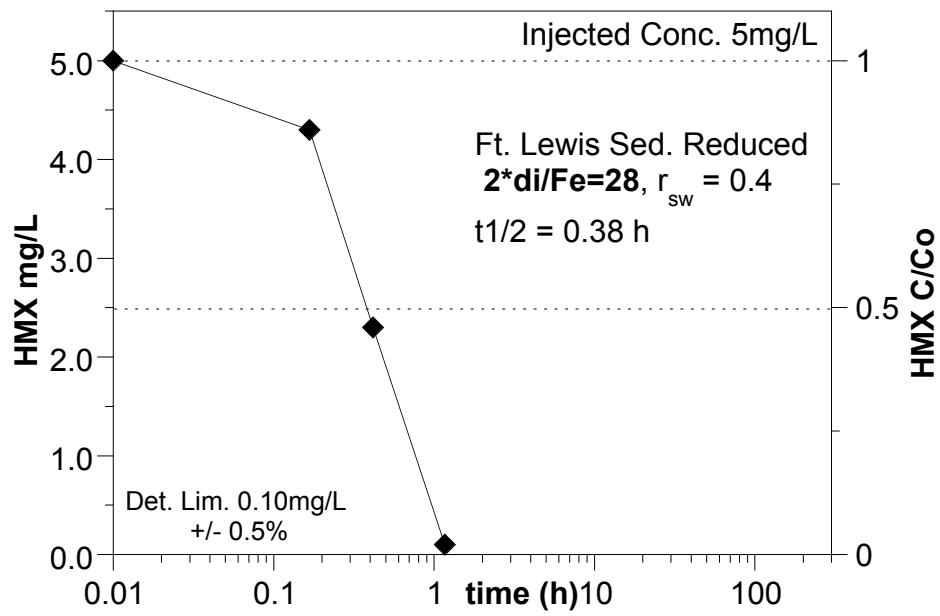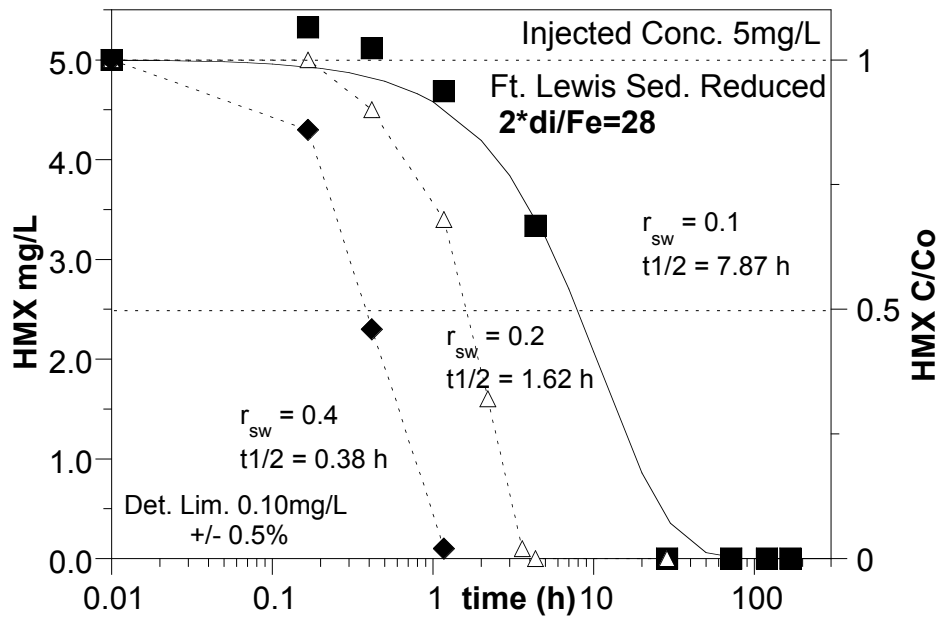
R100: HMX Coupled Biotic Degradation by Red. Sediment

Injected Conc. 4.1 mg/L

Ft. Lewis Sed. Reduced
2*di/Fe=28, r_{sw} = 0.1

+ 0.01 M PIPES

Det. Lim. 0.10mg/L
+/- 0.5%
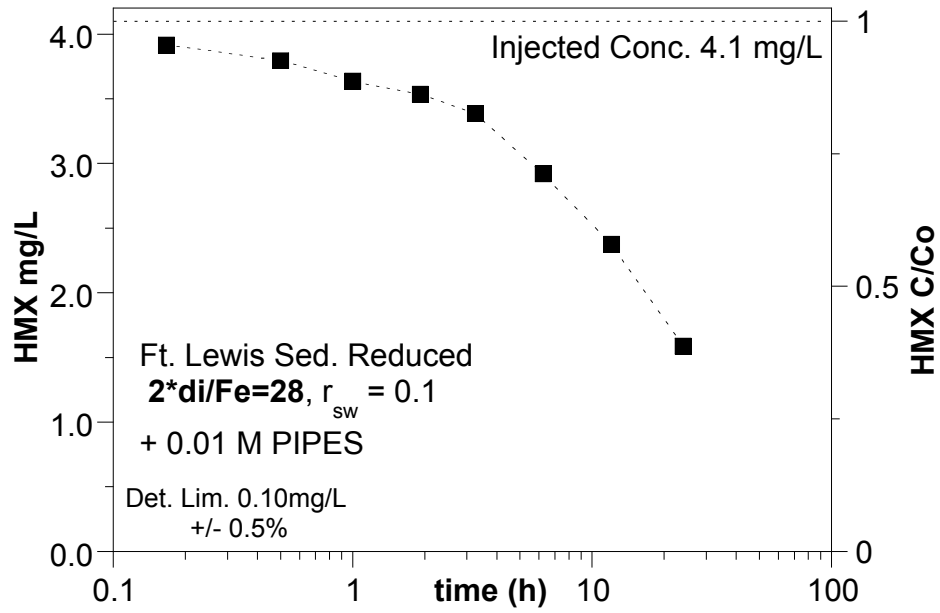
R101: HMX Abiotic Degradation by Red. Sediment + Gluteraldehyde

Injected Conc. 4.1 mg/L

Ft. Lewis Sed. Reduced
2*di/Fe=28, r_{sw} = 0.1

+ 0.01 M PIPES
+ 100 mM gluteraldehyde

Det. Lim. 0.10mg/L
+/- 0.5%

G.3
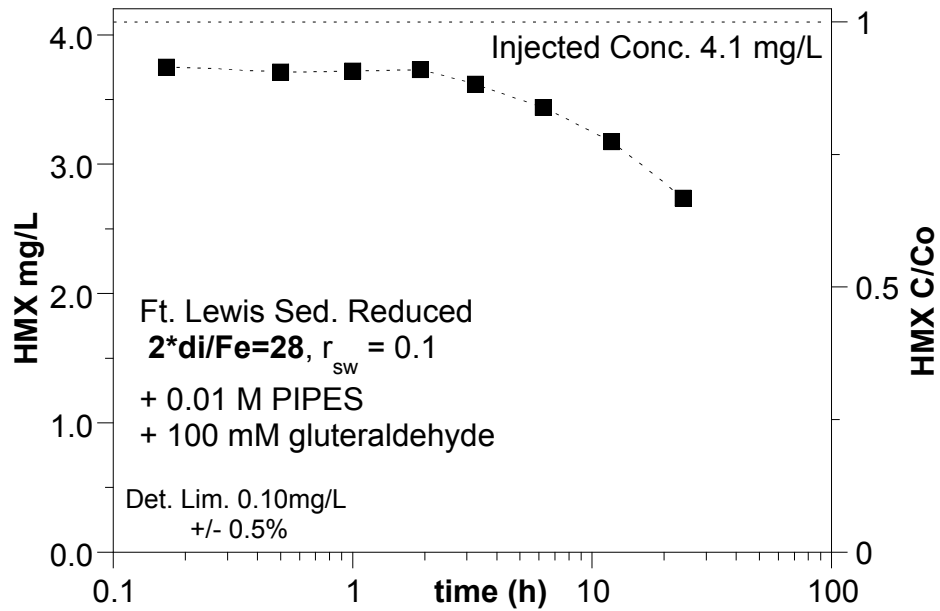
R100/101: HMX Abiotic/Biotic Degradation
by Red. Sediment

Injected Conc. 4.1 mg/L

w/glut.

w/o glut

Ft. Lewis Sed. Reduced

2*di/Fe=28, r_{sw} = 0.1

+ 0.01 M PIPES

Det. Lim. 0.10mg/L
+/- 0.5%

HMX mg/L

HMX C/Co

time (h)

W45; HMX degradation by red. Ft. Lewis
2*dith./Fe = 37, batch r_{sw} = 0.087-0.075

sing. bot.
r_{sw} = 0.087

sep. bot.
r_{sw} = 0.075

HMX
C_0 = 0.0085 mmol/L

Concentration (mmol/L)

Conc. Normalized to RDX Co

det. lim. 0.1 mg/L +/- 0.5%

time (h)

G.4
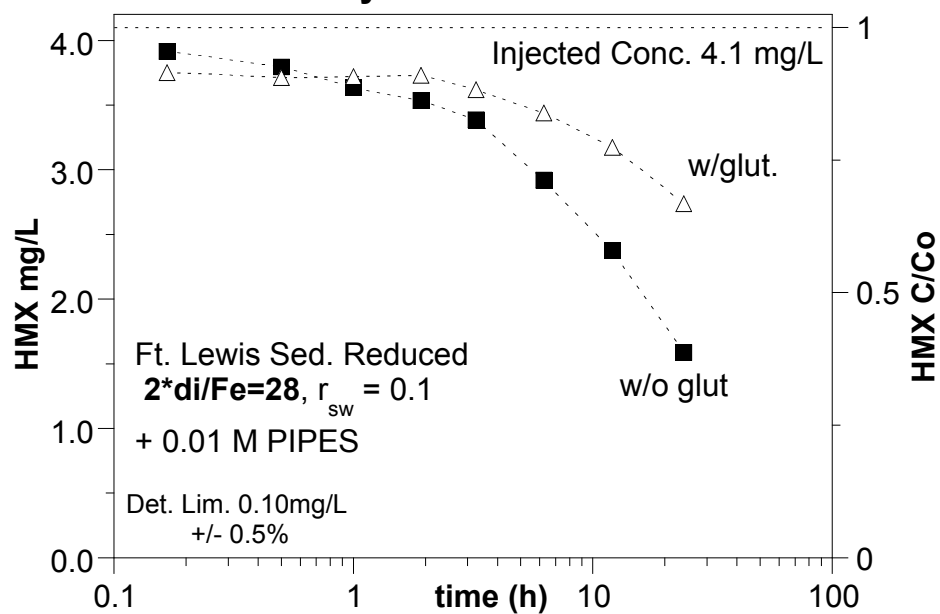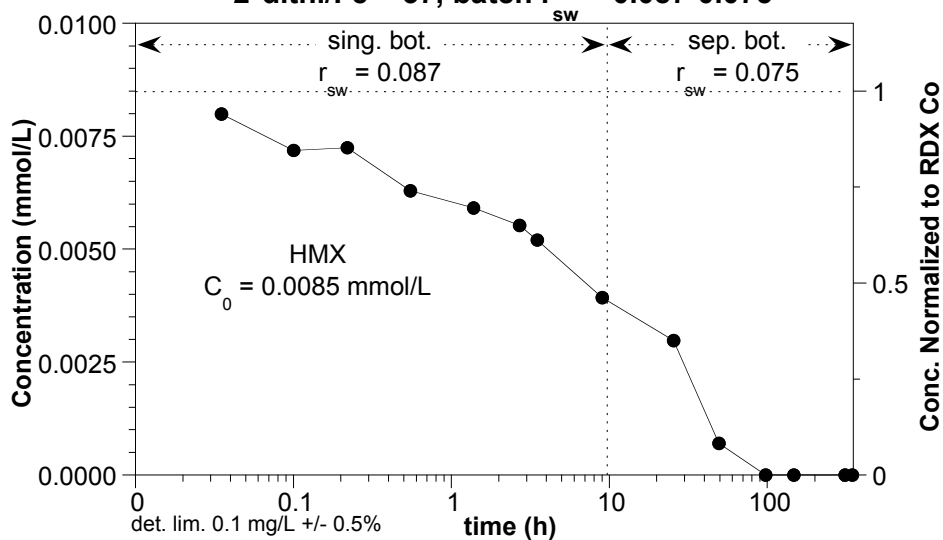
W45; RDX and HMX aqueous stability
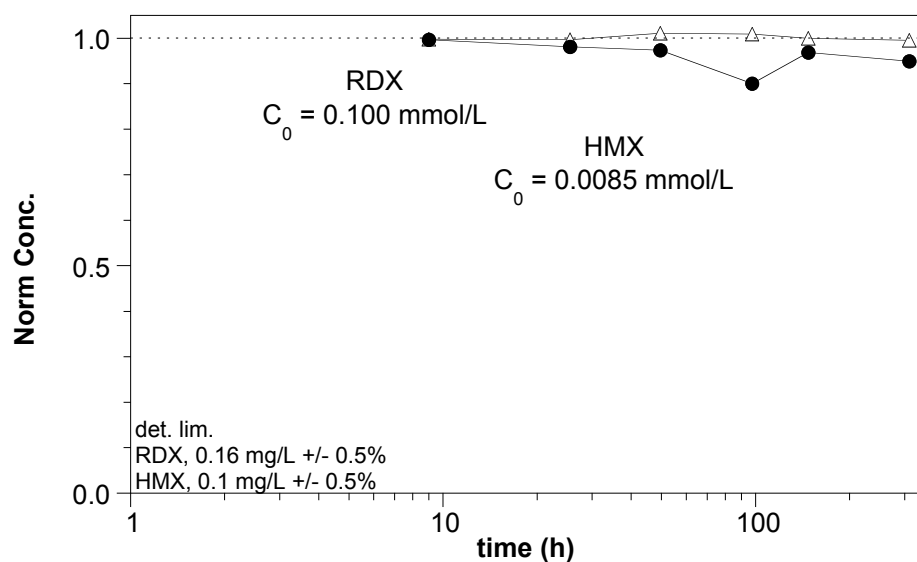
R125 HMX Mineralization in red. sed.(di/Fe=28)

Appendix H: HMX Mineralization by Coupled Abiotic/Biotic Reactions

R127 HMX Mineralization in red. sed.(di/Fe=1.6)

R128 HMX Min. in red. sed.(di/Fe=1.6) +glu+tr.nutr.

R129 HMX Mineralization in red. sed.(di/Fe=0.08)

H.1

R130 HMX Mineralization in untreated sed.

R131 HMX Min. in red.sed. (di/Fe=28) + bactericide

R132 HMX Min. in untr.sed. (di/Fe=28) + bactericide

HMX Mineralization vs Sediment Reduction

dithionite/
ferrous iron:

28

1.6

0.08
untreated

HMX Mineralization: Influence of Nutrients

with trace nutrients
and glucose

no additions

both: dithionite/
ferrous iron = 1.6

HMX Mineralization: Influence of Microbes

reduced sediment only

both: dithionite/
ferrous iron = 28

with bactericides

C/Co

time (h)

HMX Mineralization: Influence of Microbes

untreated sediment only

untreated sed.
with bactericides

C/Co

time (h)

HMX Mineralization Rate in Reduced Sed.

reduced sediment
half-life = 80900 (ratio)^-1.10
r = 0.83

batch reduced

column reduced

HMX mineralization half-life (h)

Fe(II)/HMX ratio (mol/mol)

HMX Mineralization Rate in Reduced Sed.

reduced sediment
half-life = 0.0285(Fe)^-1.102
r = 0.83

HMX mineralization half-life (h)

Fe(II) (mol)

HMX Mineralization vs Sed. Reduction

CO2

untreated sed.
reduced, di/Fe = 0.3
reduced, di/Fe = 1.5
reduced, di/Fe = 30

C/Co

time (h)

Appendix I: TNT Aqueous Stability and Sediment Sorption/Degradation

I.1

R104: TNT Degradation by Red. Sediment

Injected Conc.
25.3 mg/L

Ft. Lewis Sed. Reduced
2*di/Fe=28, r_{sw} = 0.008

Det. Lim. 0.07mg/L
+/- 0.7%

R102-104: TNT Degradation by Red. Sediment

Injected Conc.
25.3 mg/L

r_{sw} = 0.008

r_{sw} = 0.020

Ft. Lewis Sed. Reduced
2*di/Fe=28

r_{sw} = 0.067
t1/2 = 4.7 h

Det. Lim. 0.07mg/L
+/- 0.7%

I.2

X11: TNT Sorption Rate to Untreated Ft. Lewis

aqueous

det. lim. 0.07 mg/L +/- 0.7%

X11: TNT Sorption Rate to Untreated Ft. Lewis

aqueous data

sorption rate:
first-order fit
rate = 2.43/h
half-life 0.2847 h

det. lim. 0.07 mg/L +/- 0.7%

I.3

X13 TNT Sorption Rate to Untreated Ft. Lewis

aqueous

det. lim. 0.07 mg/L +/- 0.7%

C/Co — time (h)

X13: TNT Sorption Rate to Untreated Ft Lewis

aqueous

det. lim. 0.07 mg/L +/- 0.7%

C/Co — time (h)

X13 TNT Sorption-Ft Lewis

sorption rate:
first-order fit
rate= 5.8/h
half-life 0.1678 h

det. lim. 0.07 mg/L +/- 0.7%

Aq. Norm TNT — time (h)

I.4

X14-X20 TNT Degradation by pH Hydrolysis

I.5

X21,X22 TNT Stability at pH 10

no sediment

with sediment

det. limit 0.07 mg/L, ± 0.7%

X23-24: Influence of Sediment on TNT Alkaline Hydrolysis

with sediment

pH=11

no sediment

det. lim. 0.07 mg/L +/- 0.7%

X25-26: influence of sediment on TNT alkaline hydrolysis

pH=12

with sediment

no sediment

det. lim. 0.07 mg/L +/- 0.7%

I.6

TNT/glucose cometabolic deg. in oxic Ft. Lewis sed.

Legend:
- aq. TNT
- aq. ADNT*
- aq. DANT*
- aq. TAT
- total aq.

*combined conc.

X42, rsw = 0.231 g/mL
TNT Co = 105.2 mg/L
4020 mg/L glucose
TNT ± 0.4%
ADNT ± 0.6%
DANT ± 1.5%
TAT ± 5%

TNT/Glucose Cometabolic Deg. in Oxic Sed.

TNT ± 0.4%
ADNT ± 0.6%
DANT ± 1.5%
TAT ± 5%

Legend:
- TNT (aq)
- TNT (sorb) — reversible sorption
- ADNT (aq)
- ADNT (sorb)
- DANT (aq)
- DANT (sorb) — irreversible sorption
- TAT (aq)
- TAT (sorb)

measured sorption

TNT/glucose cometabolic deg. in anoxic Ft Lew. sed.

Legend:
- aq. TNT
- aq. ADNT*
- aq. DANT*
- aq. TAT
- total aq.
- *combined conc.

X43, rsw = 0.275 g/mL

TNT Co = 105.2 mg/L
4020 mg/L glucose

TNT ± 0.4%
ADNT ± 0.6%
DANT ± 1.5%
TAT ± 5%

TNT/Glucose Cometabolic Deg. in Anoxic Sed.

TNT ± 0.4%
ADNT ± 0.6%
DANT ± 1.5%
TAT ± 5%

TNT/glucose cometabolic deg. in reduced Ft Lew. sed.

partial reduction:
2*dith./Fe = 11
soil/water = 0.262 g/mL
TNT = 105.2 mg/L
glucose = 4020 mg/L

X44, part red. sed.
TNT ± 0.4%
ADNT ± 0.6%
DANT ± 1.5%
TAT ± 5%

aq. TNT
aq. ADNT*
aq. DANT*
aq. TAT
total aq.
*combined conc.

TNT/Glucose Cometabolic Deg. in Red. Sed.

TNT (aq)
TNT (sorb)
ADNT (aq)
ADNT (sorb)
DANT (aq)
DANT (sorb)
TAT (aq)
TAT (sorb)

reversible sorb.

irreversible   reversible sorb.

measured sorption

X44, part red. sed.
TNT ± 0.4%
ADNT ± 0.6%
DANT ± 1.5%
TAT ± 5%

I.9

TNT/glucose cometabolic deg. in reduced Ft Lew. sed.

high reduction:
2*dith./Fe = 37

TNT = 105.2 mg/L
glucose = 4020 mg/L
X45, R_{sw} = 0.26 g/mL

aq. TNT
aq. ADNT*
aq. DANT*
aq. TAT
total aq.

*combined conc.

X45, high red. sed.
TNT ± 0.4%
ADNT ± 0.6%
DANT ± 1.5%
TAT ± 5%

TNT/Glucose Cometabolic Deg. in Red. Sed.

TNT (aq)
TNT (sorb)
ADNT (aq)
ADNT (sorb)
DANT (aq)
DANT (sorb)
TAT (aq)
TAT (sorb)

reversible sorb.
irreversible
measured sorption

X45, high red. sed.
TNT ± 0.4%
ADNT ± 0.6%
DANT ± 1.5%
TAT ± 5%

X42-25; TNT cometabolic deg. by Ft. Lewis

W70-73; 2-amino-4,6-dinitrotoluene degradation
by Ft. Lewis sediment, anaerobic batch
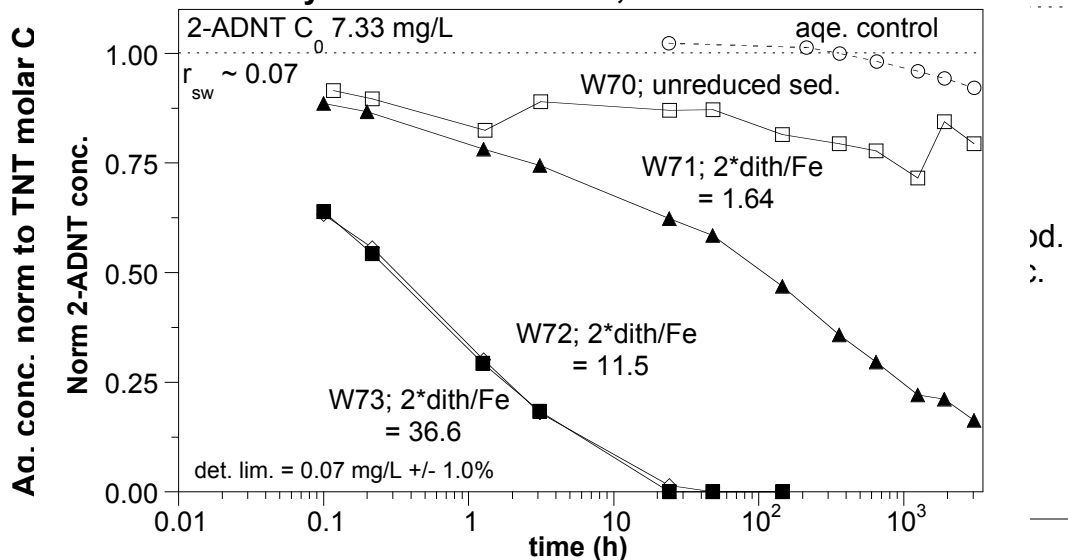
W74-77; 4-amino-2,6-dinitrotoluene degradation
by Ft. Lewis sediment, anaerobic batch
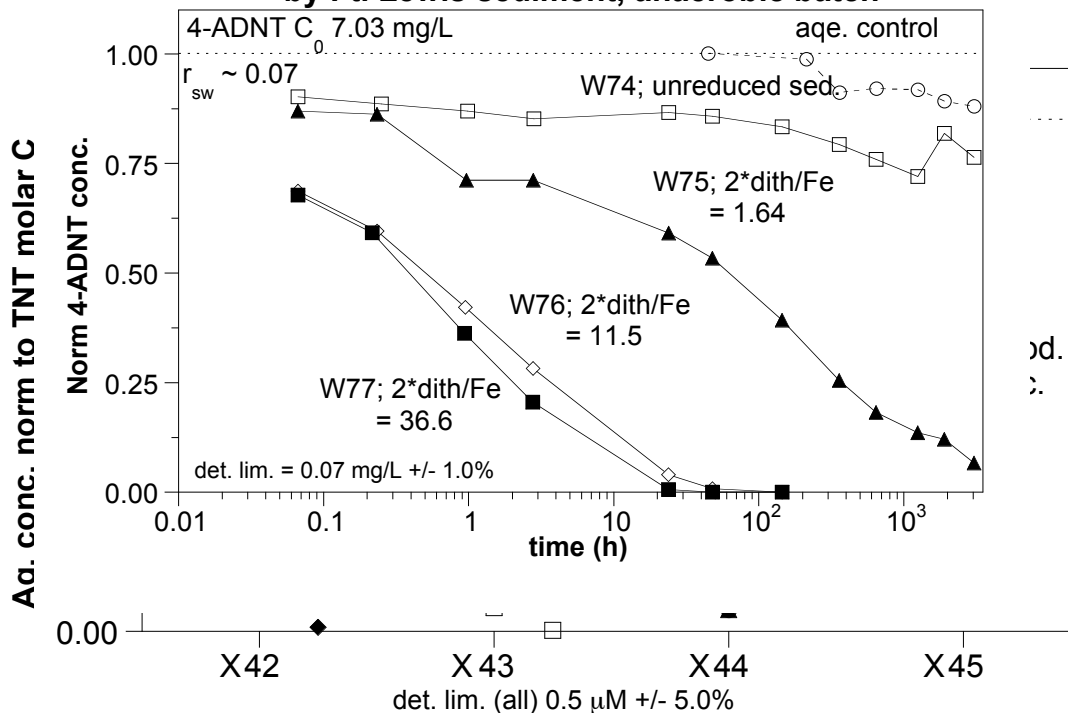
X29 2ADNT Sorption Rate to Untreated Ft. Lewis
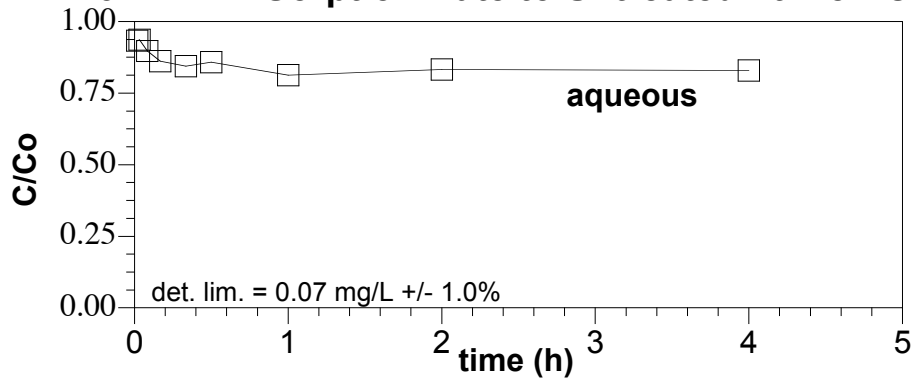
aqueous

det. lim. = 0.07 mg/L +/- 1.0%

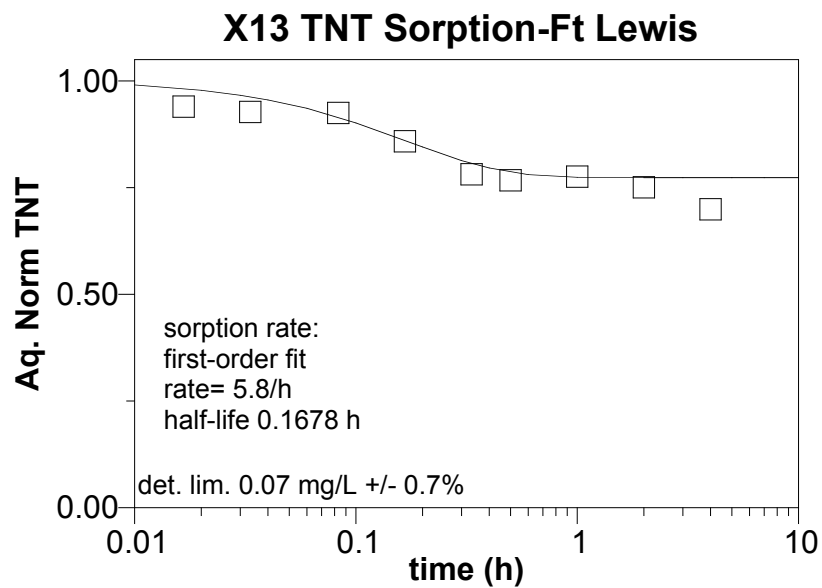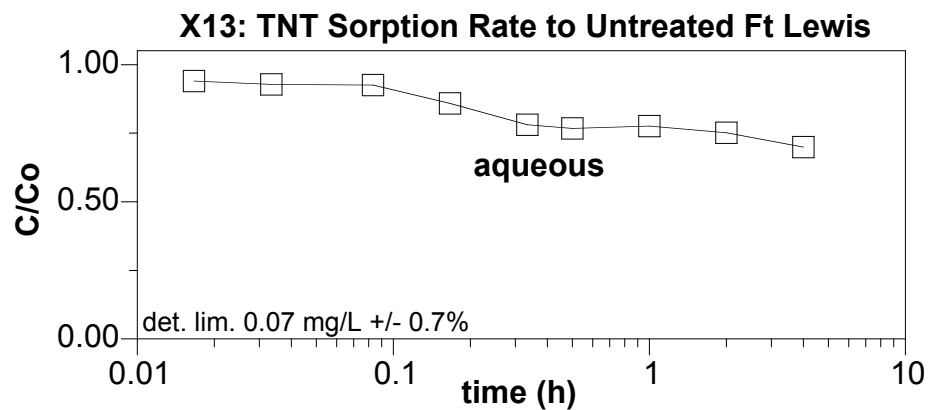**X29: 2ADNT Sorption Rate to Untreated Ft Lewis**

aqueous

det. lim. = 0.07 mg/L +/- 1.0%

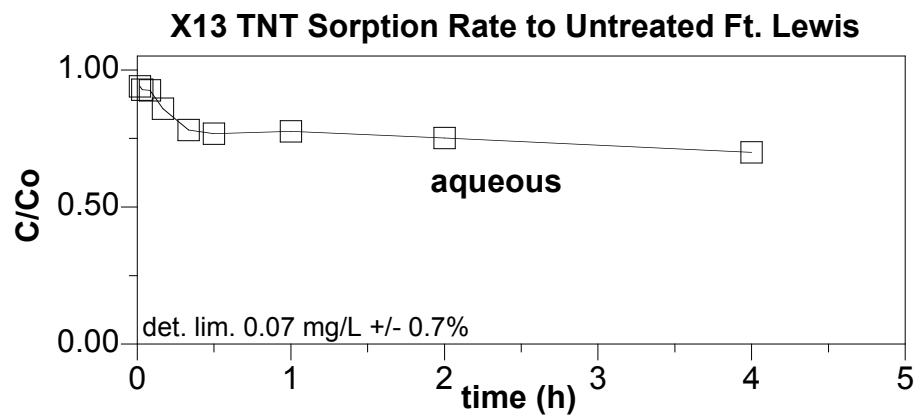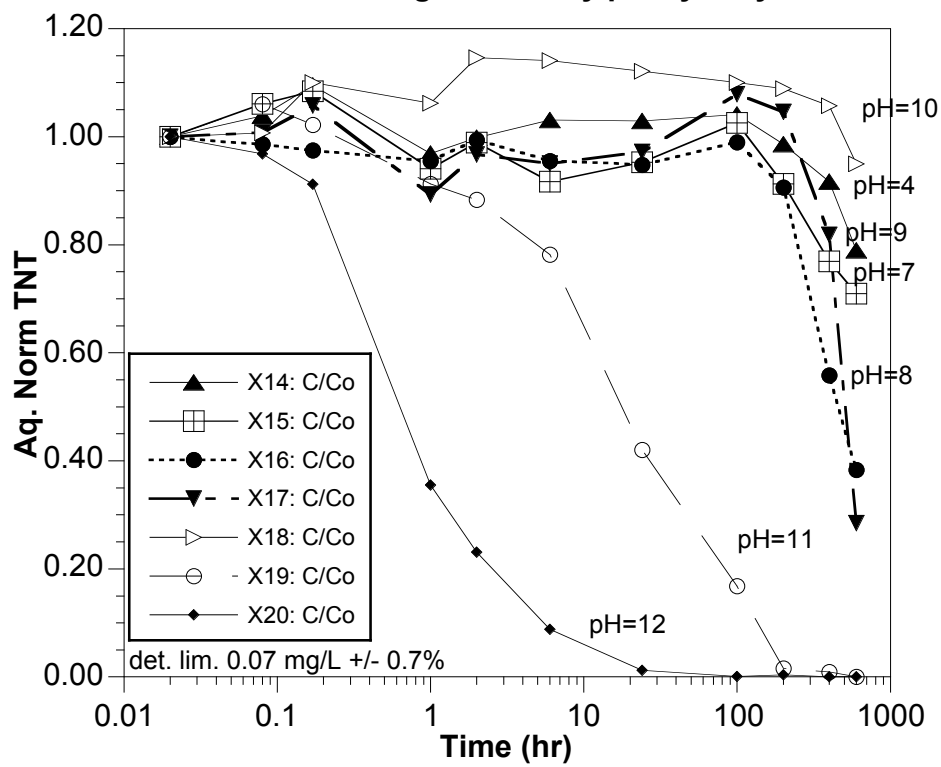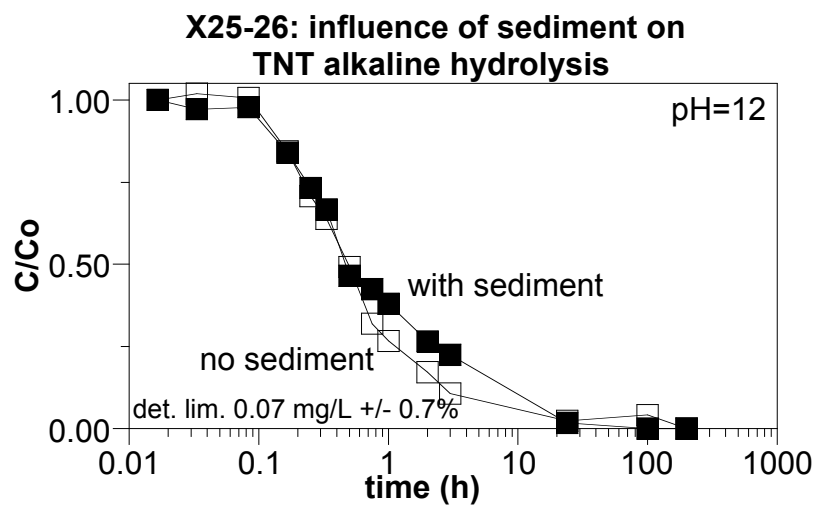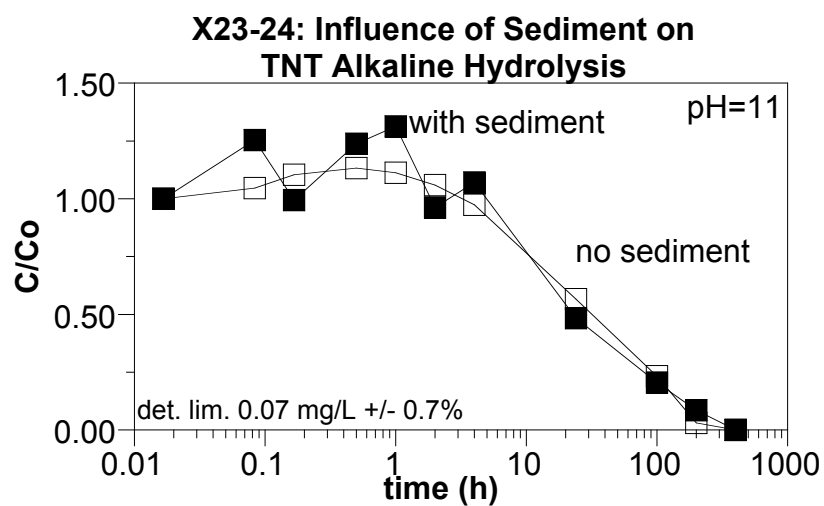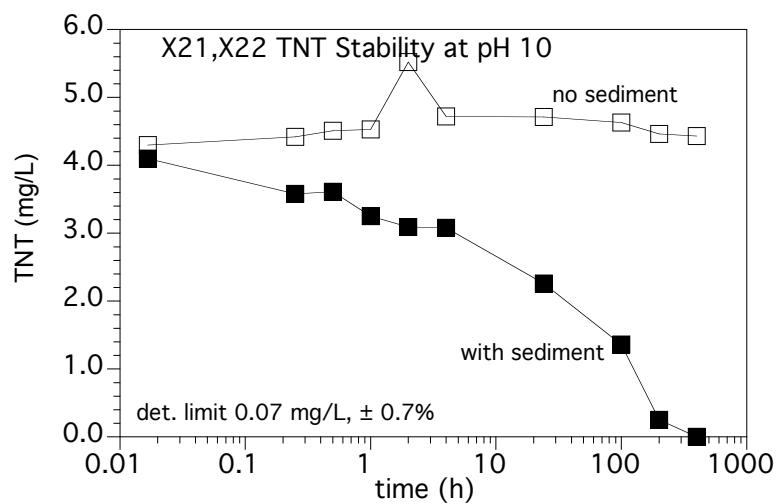**X31 4ADNT Sorption Rate to Untreated Ft. Lewis**

aqueous

det. lim. = 0.07 mg/L +/- 1.0%

X31: 4ADNT Sorption Rate to Untreated Ft Lewis

aqueous

det. lim. = 0.07 mg/L +/- 1.0%

J.2
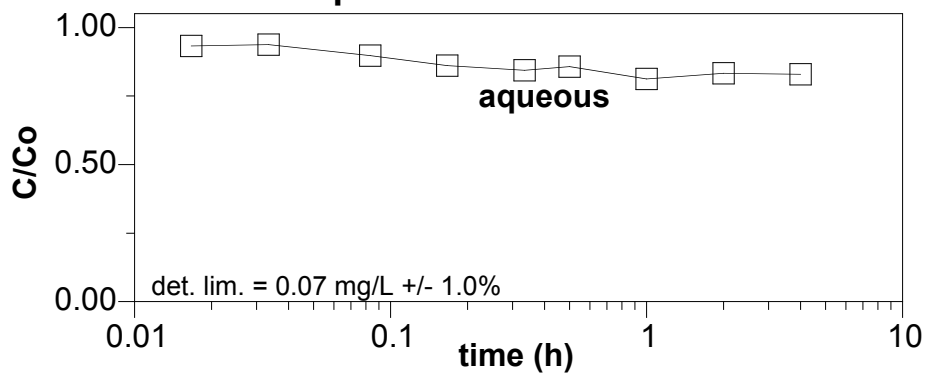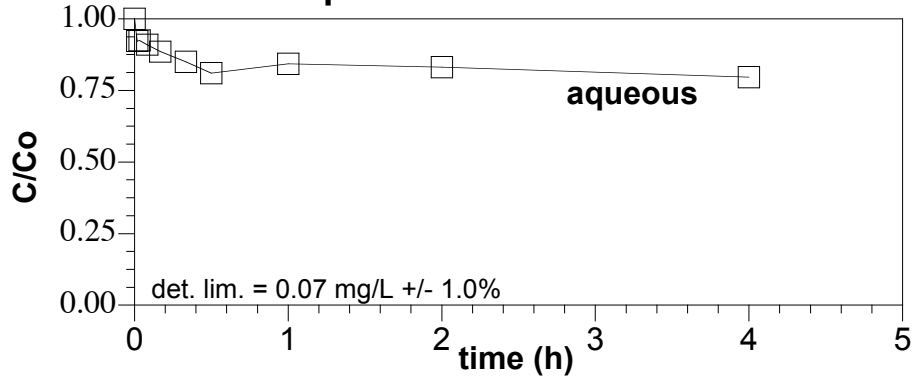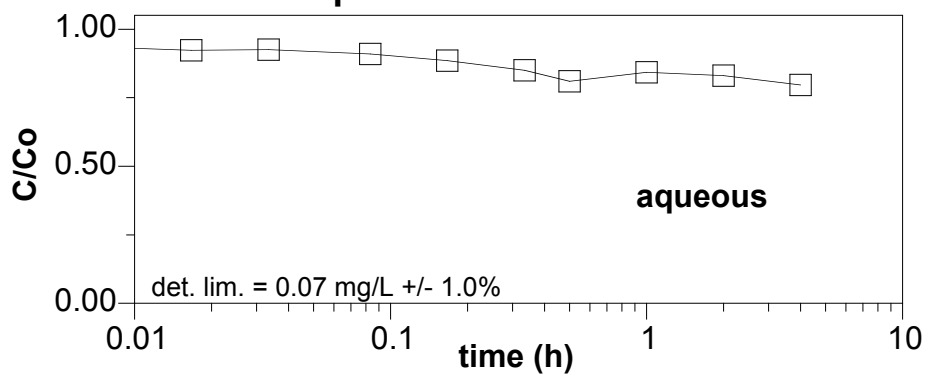
X34 Long term sorption of 2ADNT

C_0 = 12 mg/L

det. lim. = 0.07 mg/L +/- 1.0%

C/Co 2ADNT

Est. Time (h)
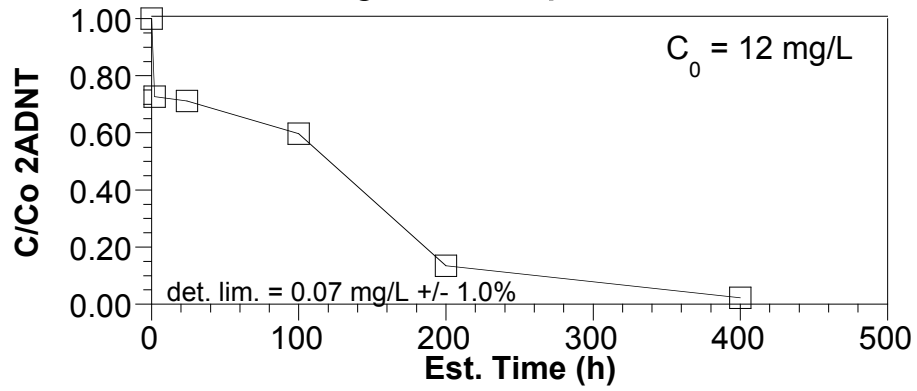
X35 Long term sorption of 4ADNT

C_0 = 12 mg/L

det. lim. = 0.07 mg/L +/- 1.0%

C/Co 4ADNT

Est. Time (h)
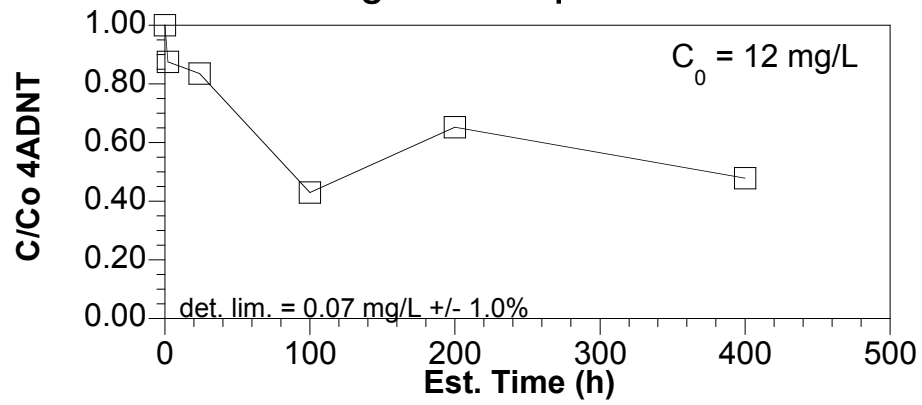
Appendix K: 2,4- and 2,6 Dinitroaminotoluene Sorption and Degradation

W78-81; 2,4-diamino-6-dinitrotoluene degradation by Ft. Lewis sediment, anaerobic batch

2,4-DANT C_0 = 1.99 mg/L

$r_{sw} \sim 0.07$

aqe. control

W78; unreduced sed.

W79; 2*dith/Fe = 1.64

W81; 2*dith/Fe = 36.6

W80; 2*dith/Fe = 11.5

det. lim. = 0.10 mg/L +/- 2.5%

W82-85; 2,6-diamino-4-dinitrotoluene degradation by Ft. Lewis sediment, anaerobic batch

2,6-DANT C_0 = 1.93 mg/L

$r_{sw} \sim 0.07$

aqe. control

W82; unreduced sed.

W83; 2*dith/Fe = 1.64

W84; 2*dith/Fe = 36.6

W85; 2*dith/Fe = 11.5

det. lim. = 0.10 mg/L +/- 2.5%

X39: 2,4-DANT Sorption Rate to Untreated Ft Lewis

aqueous

det. lim. = 0.10 mg/L +/- 2.5%

C/Co

time (h)

X40: 2,6-DANT Sorption Rate to Untreated Ft Lewis

aqueous

det. lim. = 0.10 mg/L +/- 2.5%

C/Co

time (h)

Appendix L: Triaminotoluene Aqueous/Sediment Stability and Degradation

Triaminotoluene Aqueous pH Stability

Triaminotoluene UV Light Sensitivity at pH 3.3, Anaerobic

Dissolved Oxygen and Aqueous Triaminotoluene Stability: No light, pH 3.3
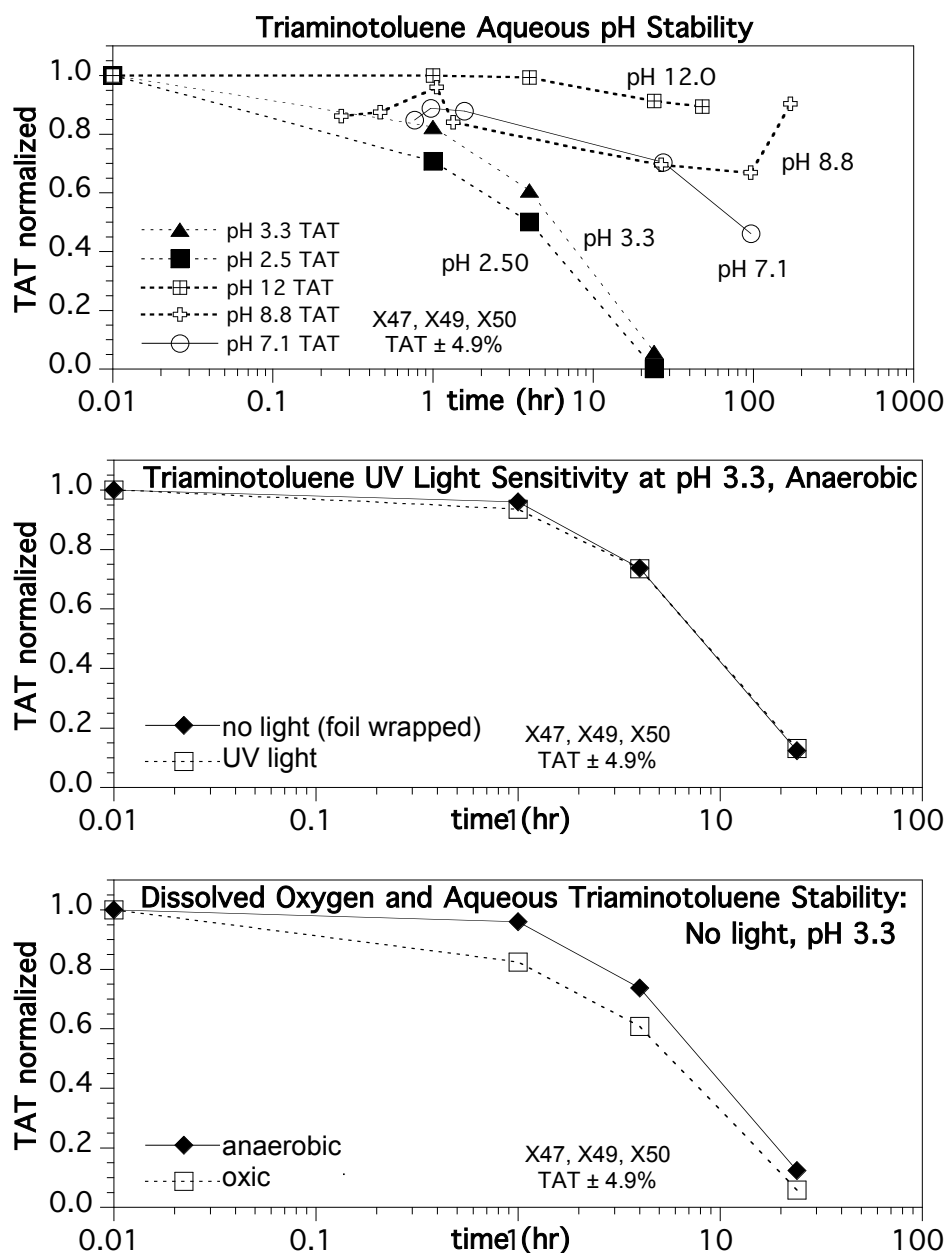
Appendix M: TNT Mineralization in Biostimulated/Reduced Sediments
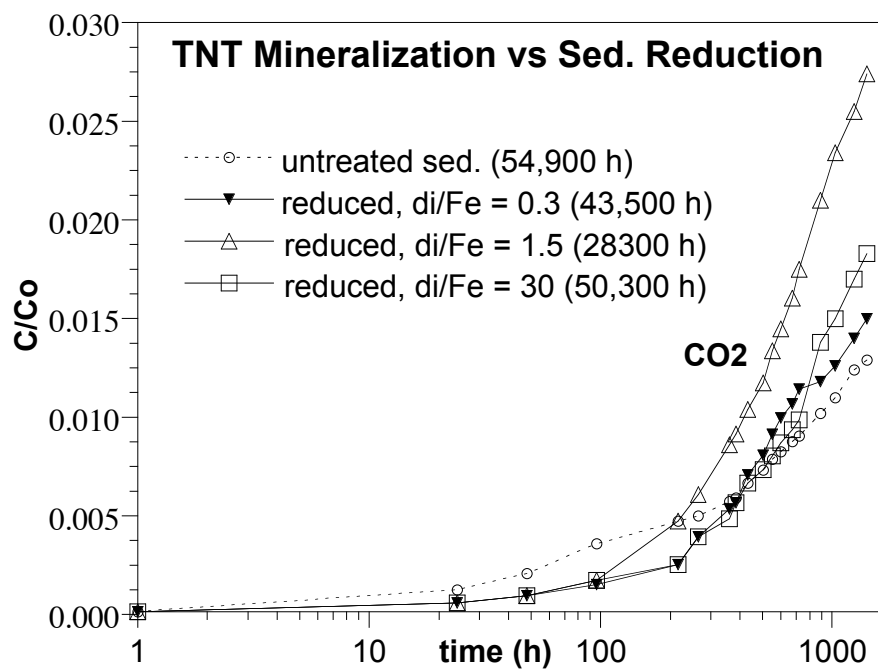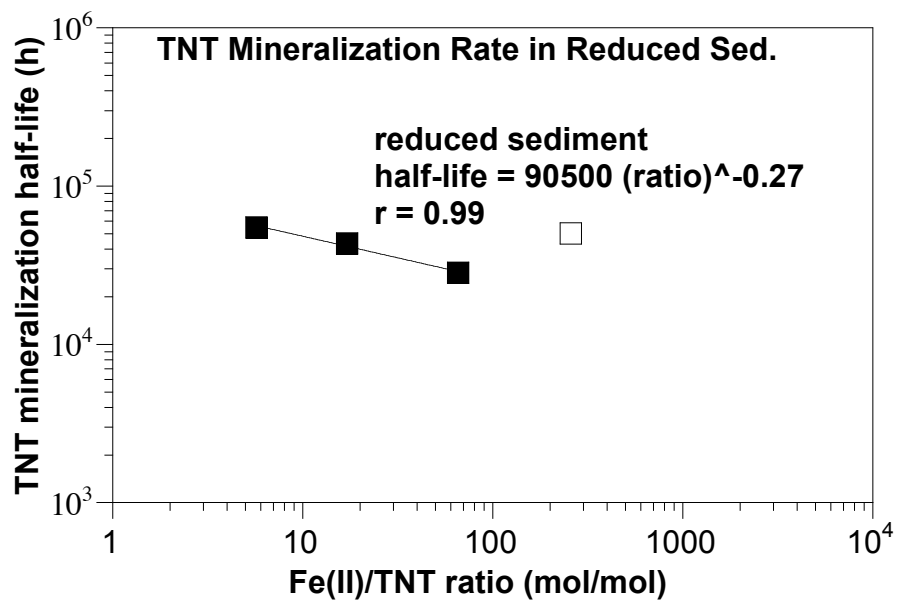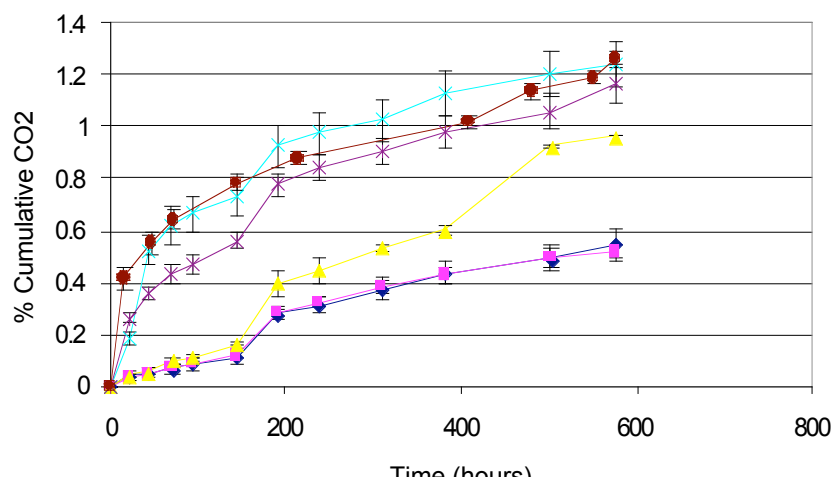
TNT Mineralization –exposed to dithionite for 1 day, then oxidized
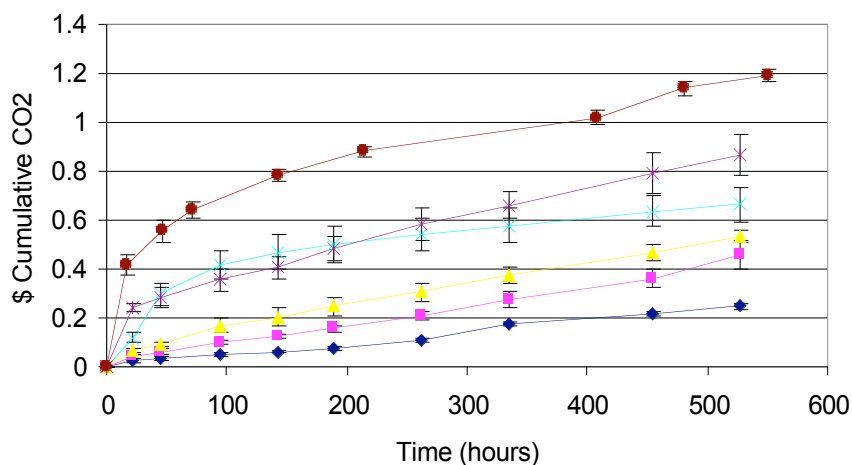
TNT Mineralization –exposed to dithionite for 3 days, then oxidized

◆— Treatment 1	■— Treatment 2	▲— Treatment 3
✕— Treatment 4	✳— Treatment 5	●— Control-No treatment

treatment	2* di/Fe
1	4.0
2	1.0
3	0.5
4	0.1
5	0.02

TNT Mineralization –exposed to dithionite for 5 days, then oxidized

TNT Mineralization –exposed to dithionite for 10 days, then oxidized

M.3

TNT Mineralization in Anoxic, Red. Sed. X56-60

	half-life (h)
X56, anoxic	216,000
X57, red 1.6	238,000
X58 red 6	58,000
X59 red 12	617,000
X60 red 12+C,t	47,000

data ± 0.2%

C/Co

time (h)

TNT Mineral. in Anoxic -> Oxic Sediment

anoxic, no treat.	aq., anoxic 83%
red 1.6	aq.,red 1.6 88%
red 6	aq. red. 6 87%
red 12	aq. red 12 73%
red12t+c	aq. red 12C 44%
gas c trap, red	

aqueous

CO₂ trap

gas phase
carbon trap

data ± 0.2%

C/Co

time (h)

Cometabolic TNT Mineralization with Glucose

Legend: X51, oxic; X52, anoxic; X53, red 1.5; X54, red 36; X55 red36+tr; X55a no sed

data ± 0.2%

Cometabolic TNT Mineralization with Glucose, Oxic

Legend: oxic; anoxic; reduced, 1.6; reduced, 36; reduced,36,tr nut.; control, no sed.; gas C trap, red.; aq., oxic 62%; aq., anoxic 75%; aq., red., 73%; aq., red., 29%; aq., red., 46%; aq., no sed. 99%

aqueous

CO_2 trap

data ± 0.2%

gas phase carbon trap

M.6

Appendix N: RDX, HMX, and TNT 1-D Transport with Sorption/Degradation

W46; HMX+TNT degradation by red. Ft. Lewis
2*dith./Fe = 22, @ 10°C, 1-D flow

1.14 h/PV

HMX, C_0 ~ 5 mg/L

TNT, C_0 ~ 3.5 mg/L

HMX det. lim. = 0.10 mg/L +/- 0.5%
TNT det. lim. = 0.07 mg/L +/- 0.7%

Normalized Concentration

PV
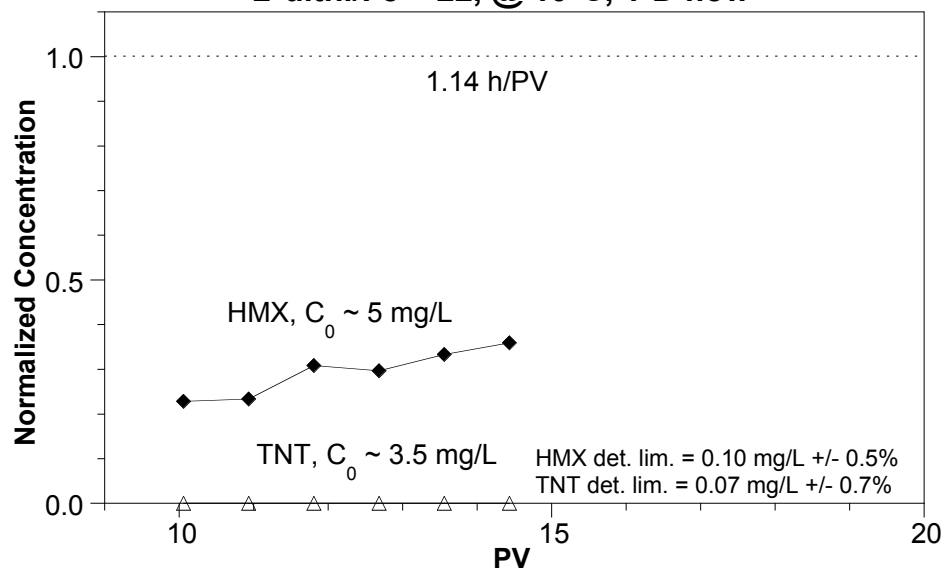
W47; HMX+TNT degradation by red. Ft. Lewis
2*dith./Fe = 4.1, @ 10°C, 1-D flow

1.11 h/PV

HMX, C_0 ~ 5 mg/L

HMX det. lim. = 0.10 mg/L +/- 0.5%
TNT det. lim. = 0.07 mg/L +/- 0.7%

TNT, C_0 ~ 3.5 mg/L

Normalized Concentration

PV
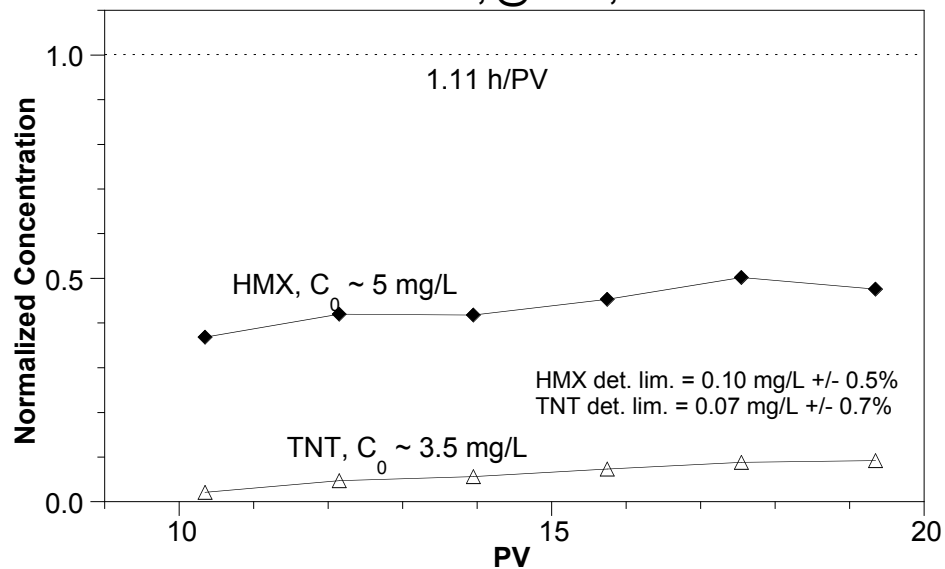
W48; HMX+TNT degradation by red. Ft. Lewis
2*dith./Fe = 1.64, @ 10°C, 1-D flow

1.10 h/PV

TNT, C_0 ~ 3.5 mg/L

HMX, C_0 ~ 5 mg/L

HMX det. lim. = 0.10 mg/L +/- 0.5%
TNT det. lim. = 0.07 mg/L +/- 0.7%

Normalized Concentration

PV
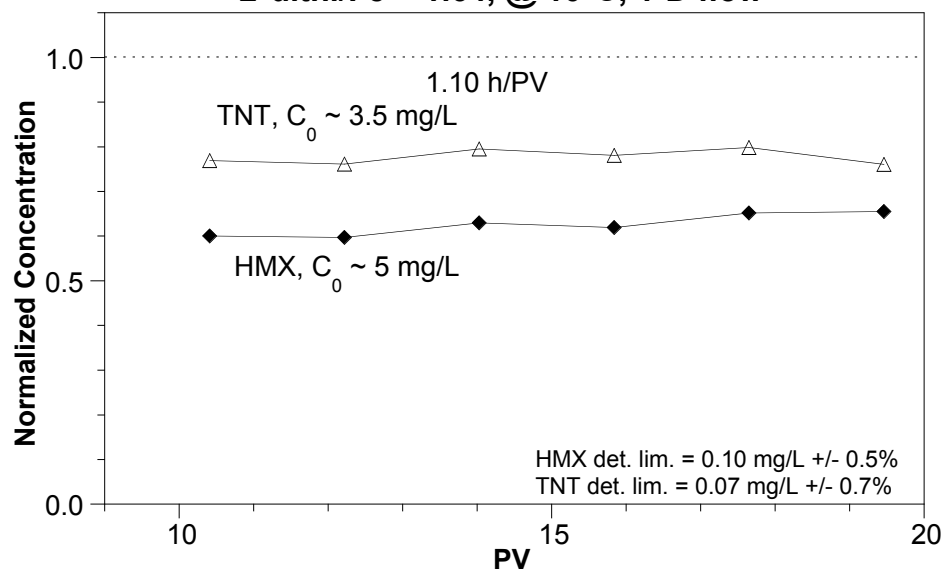
W49; HMX+TNT degradation by red. Ft. Lewis
2*dith./Fe = 0.67, @ 10°C, 1-D flow

1.02 h/PV

TNT, C_0 ~ 3.5 mg/L

HMX, C_0 ~ 5 mg/L

HMX det. lim. = 0.10 mg/L +/- 0.5%
TNT det. lim. = 0.07 mg/L +/- 0.7%

Normalized Concentration

PV

N.2
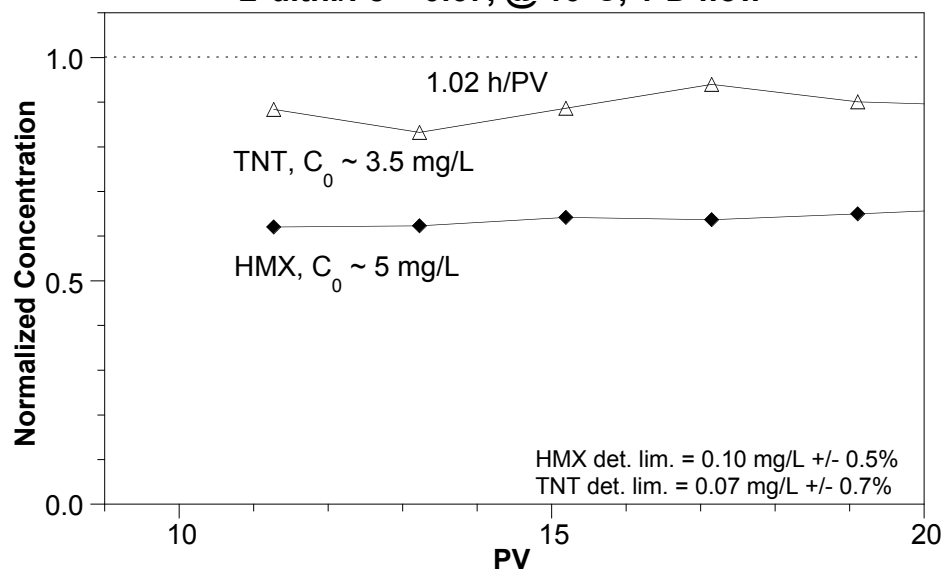
W46-49; HMX degradation by red. Ft. Lewis
2*dith./Fe = 22-0.67, @ 10°C, 1-D flow
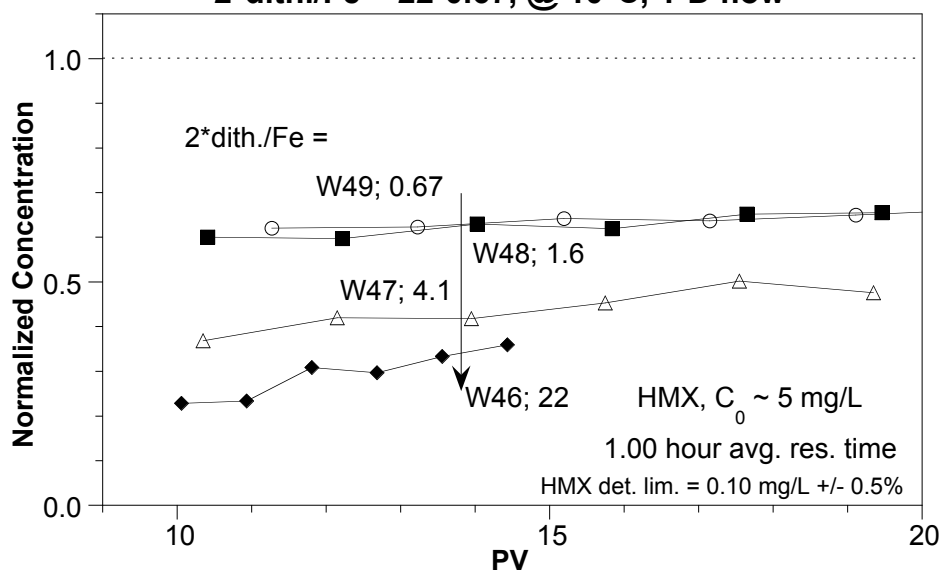
W46-49; TNT degradation by red. Ft. Lewis
2*dith./Fe = 22-0.67, @ 10°C, 1-D flow

W25; HMX and TNT degradation by red. Ft. Lewis
2*dith./Fe = 22, @ 22°C, 1-D flow

W26; HMX and TNT degradation by red. Ft. Lewis
2*dith./Fe = 4.1, @ 22°C, 1-D flow

W27; HMX and TNT degradation by red. Ft. Lewis
2*dith./Fe = 1.6, @ 22°C, 1-D flow

HMX, C_0 = 0.60 mg/L

TNT, C_0 = 0.39 mg/L

1.03 h/PV

1.46 h/PV

HMX det. lim. = 0.10 mg/L +/- 0.5%
TNT det. lim. = 0.07 mg/L +/- 0.7%

W28; HMX and TNT degradation by red. Ft. Lewis
2*dith./Fe = 0.67, @ 22°C, 1-D flow

1.01 h/PV

HMX, C_0 = 0.60 mg/L

TNT, C_0 = 0.39 mg/L

HMX det. lim. = 0.10 mg/L +/- 0.5%
TNT det. lim. = 0.07 mg/L +/- 0.7%

W25-28; HMX degradation by red. Ft. Lewis
2*dith./Fe = 22-0.67, @ 22°C, 1-D flow

HMX, C_0 = 0.60 mg/L

W28; = 0.67

W27; = 1.6

W25; =22

W26; 2*dith./Fe = 4.1

HMX det. lim. = 0.10 mg/L +/- 0.5%

W25-28; TNT degradation by red. Ft. Lewis
2*dith./Fe = 22-0.67, @ 22°C, 1-D flow

TNT, C_0 = 0.39 mg/L

W27; = 1.6

W28; = 0.67

W25; =22

W26; 2*dith./Fe = 4.1

TNT det. lim. = 0.07 mg/L +/- 0.7%

N.6

W29; HMX and TNT degradation by red. Ft. Lewis
2*dith./Fe = 22, @ 22°C, 1-D flow

HMX, C_0 = 5.65 mg/L

TNT, C_0 = 3.40 mg/L

HMX det. lim. = 0.10 mg/L +/- 0.5%
TNT det. lim. = 0.07 mg/L +/- 0.7%

2.16 h/PV · · · · · · 1.27 h/PV

W30; HMX and TNT degradation by red. Ft. Lewis
2*dith./Fe = 4.1, @ 22°C, 1-D flow

2.31 h/PV · · · 1.37 h/PV

HMX, C_0 = 5.65 mg/L

TNT, C_0 = 3.40 mg/L

HMX det. lim. = 0.10 mg/L +/- 0.5%
TNT det. lim. = 0.07 mg/L +/- 0.7%

N.7

W31; HMX and TNT degradation by red. Ft. Lewis
2*dith./Fe = 1.6, @ 22°C, 1-D flow

2.50 h/PV

HMX, C_0 = 5.65 mg/L

TNT, C_0 = 3.40 mg/L

HMX det. lim. = 0.10 mg/L +/- 0.5%
TNT det. lim. = 0.07 mg/L +/- 0.7%

W32; HMX and TNT degradation by red. Ft. Lewis
2*dith./Fe = 0.67, @ 22°C, 1-D flow

2.19 h/PV

HMX, C_0 = 5.65 mg/L

TNT, C_0 = 3.40 mg/L

HMX det. lim. = 0.10 mg/L +/- 0.5%
TNT det. lim. = 0.07 mg/L +/- 0.7%

W29-32; HMX degradation by red. Ft. Lewis
2*dith./Fe = 22-0.67, @ 22°C, 1-D flow

W32; 0.67

W31; 1.6

W30; 4.1

W29; 22

2*dith./Fe

HMX, C_0 = 5.65 mg/L

HMX det. lim. = 0.10 mg/L +/- 0.5%

W29-32; TNT degradation by red. Ft. Lewis
2*dith./Fe = 22-0.67, @ 22°C, 1-D flow

TNT, C_0 = 3.40 mg/L

2*dith./Fe =   W31; 1.6

W32; 0.67

W30; 4.1

W29; 22

TNT det. lim. = 0.07 mg/L +/- 0.7%

W33; HMX+TNT deg. by red. Ft. Lewis
2*dith./Fe = 22, @ 35°C, 1-D flow

HMX, C_0 = 4.50 mg/L

TNT, C_0 = 3.50 mg/L

0.83 h/PV avg.

HMX det. lim. = 0.10 mg/L +/- 0.5%
TNT det. lim. = 0.07 mg/L +/- 0.7%

Normalized Concentration

PV

W34; HMX+TNT deg. by red. Ft. Lewis
2*dith./Fe = 22, @ 35°C, 1-D flow

HMX, C_0 = 4.50 mg/L

TNT, C_0 = 3.50 mg/L

0.89 h/PV avg.

HMX det. lim. = 0.10 mg/L +/- 0.5%
TNT det. lim. = 0.07 mg/L +/- 0.7%

Normalized Concentration

PV

N.10

W35; HMX+TNT deg. by red. Ft. Lewis
2*dith./Fe = 22, @ 35°C, 1-D flow

HMX, C_0 = 4.50 mg/L

TNT, C_0 = 3.50 mg/L

1.4 h/PV avg.

HMX det. lim. = 0.10 mg/L +/- 0.5%
TNT det. lim. = 0.07 mg/L +/- 0.7%

Normalized Concentration

PV

W36; HMX+TNT deg. by red. Ft. Lewis
2*dith./Fe = 22, @ 35°C, 1-D flow

HMX, C_0 = 4.50 mg/L

TNT, C_0 = 3.50 mg/L

1.1 h/PV avg.

HMX det. lim. = 0.10 mg/L +/- 0.5%
TNT det. lim. = 0.07 mg/L +/- 0.7%

Normalized Concentration

PV

N.11

W33-36; HMX degradation by red. Ft. Lewis
2*dith./Fe = 22-0.67, @ 35°C, 1-D flow

W36; 0.67

W35; 1.6

W34; 4.1

W33; 22

2*dith./Fe

HMX, C_0 = 4.50 mg/L

1 hour avg. res. time

HMX det. lim. = 0.10 mg/L +/- 0.5%

Normalized Concentration

PV

W33-36; TNT degradation by red. Ft. Lewis
2*dith./Fe = 22-0.67, @ 35°C, 1-D flow

W36; 0.67

2*dith./Fe =

W35; 1.6

W34; 4.1

W33; 22

TNT, C_0 = 3.50 mg/L

1 hour avg. res. time

TNT det. lim. = 0.07 mg/L +/- 0.7%

Normalized Concentration

PV

N.12

W37; HMX+TNT deg. by red. Ft. Lewis
2*dith./Fe = 22, @ 49°C, 1-D flow

HMX, C_0 = 4.13 mg/L

TNT, C_0 = 5.69 mg/L

0.75 h/PV

HMX det. lim. = 0.10 mg/L +/- 0.5%
TNT det. lim. = 0.07 mg/L +/- 0.7%

Normalized Concentration

PV
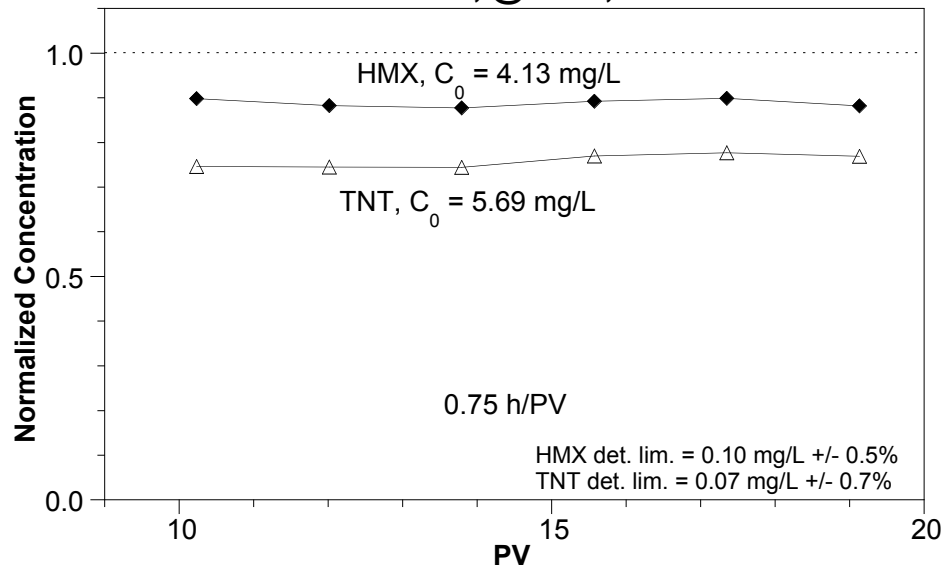
W38; HMX+TNT deg. by red. Ft. Lewis
2*dith./Fe = 4.1, @ 49°C, 1-D flow

HMX, C_0 = 4.13 mg/L

TNT, C_0 = 5.69 mg/L

0.80 h/PV

HMX det. lim. = 0.10 mg/L +/- 0.5%
TNT det. lim. = 0.07 mg/L +/- 0.7%

Normalized Concentration

PV

N.13
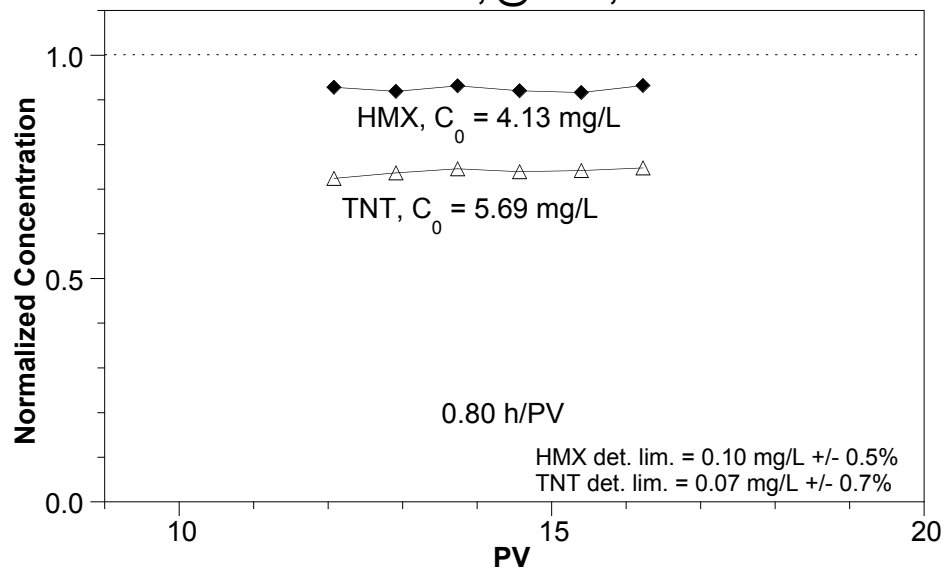
W39; HMX+TNT deg. by red. Ft. Lewis
2*dith./Fe = 1.6, @ 49°C, 1-D flow

HMX, C_0 = 4.13 mg/L

TNT, C_0 = 5.69 mg/L

0.75 h/PV

HMX det. lim. = 0.10 mg/L +/- 0.5%
TNT det. lim. = 0.07 mg/L +/- 0.7%
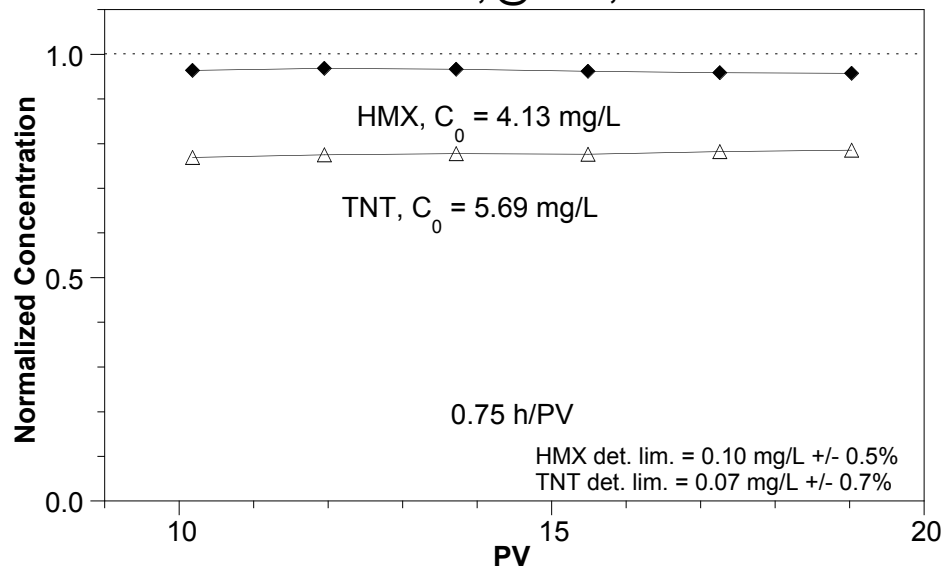
W40; HMX+TNT deg. by red. Ft. Lewis
2*dith./Fe = 0.67, @ 49°C, 1-D flow
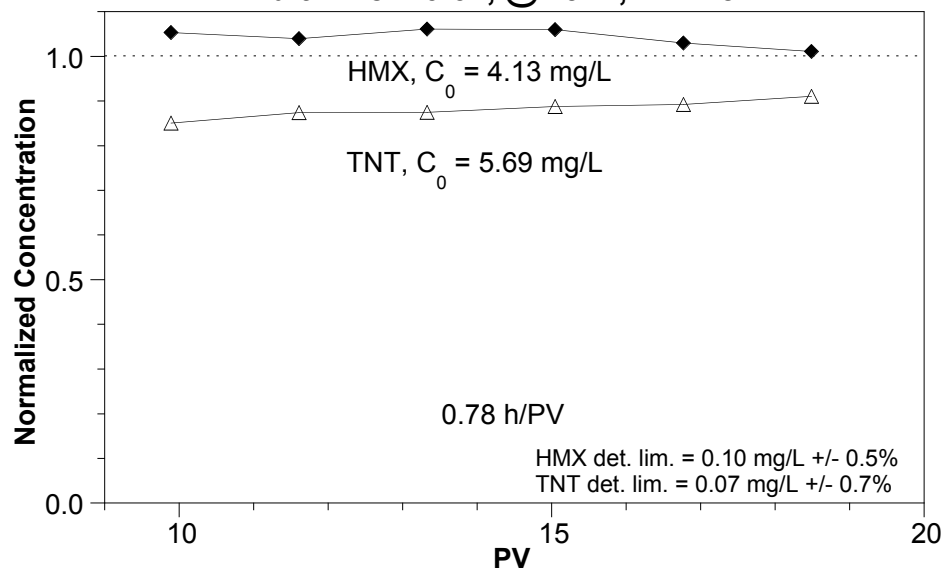
HMX, C_0 = 4.13 mg/L

TNT, C_0 = 5.69 mg/L

0.78 h/PV

HMX det. lim. = 0.10 mg/L +/- 0.5%
TNT det. lim. = 0.07 mg/L +/- 0.7%

W37-40; HMX degradation by red. Ft. Lewis
2*dith./Fe = 22-0.67, @ 49°C, 1-D flow

W40; 0.67
W39; 1.6
W38; 4.1
W37; 22

2*dith./Fe

HMX, C_0 = 4.13 mg/L

0.77 hour avg. res. time

HMX det. lim. = 0.10 mg/L +/- 0.5%

Normalized Concentration

PV

W37-40; TNT degradation by red. Ft. Lewis
2*dith./Fe = 22-0.67, @ 49°C, 1-D flow

W40; 0.67
W39; 1.6
W38; 4.1
W37; 22

2*dith./Fe

TNT, C_0 = 5.69 mg/L

0.77 hour avg. res. time

TNT det. lim. = 0.07 mg/L +/- 0.7%

Normalized Concentration

PV

N.15
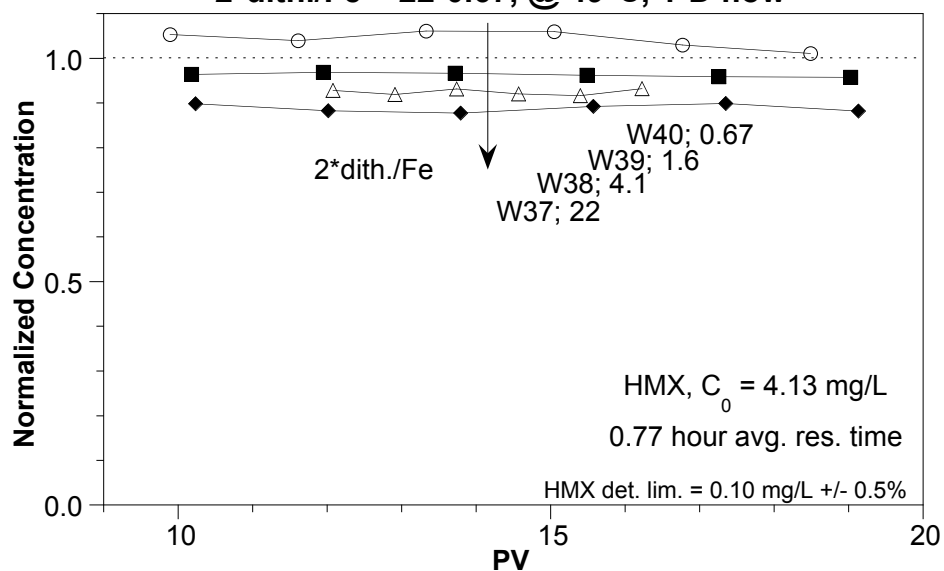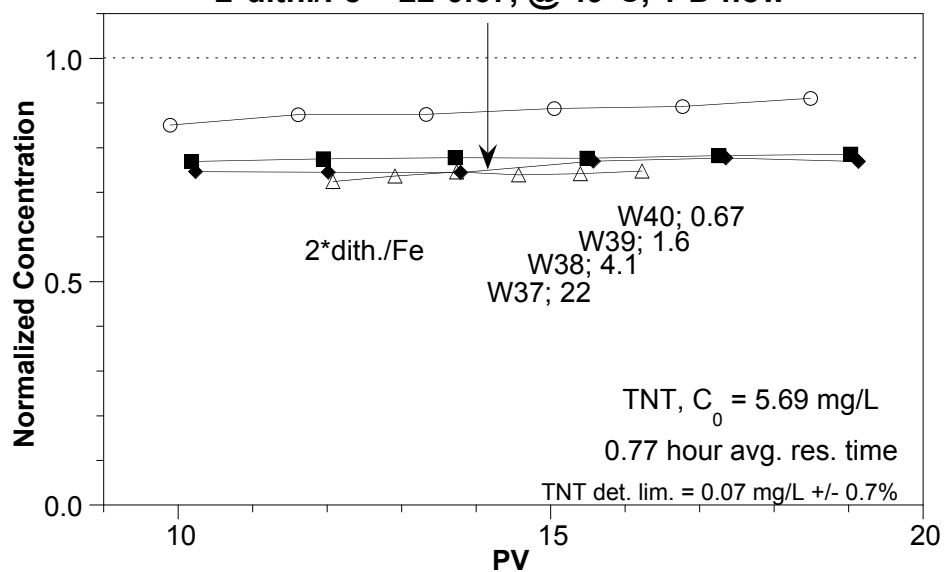
W41; HMX+TNT deg. by red. Ft. Lewis
2*dith./Fe = 22, @ 62°C, 1-D flow

4.56 h/PV

HMX, C_0 = 5.14 mg/L

TNT, C_0 = 3.65 mg/L

HMX det. lim. = 0.10 mg/L +/- 0.5%
TNT det. lim. = 0.07 mg/L +/- 0.7%

Normalized Concentration

PV
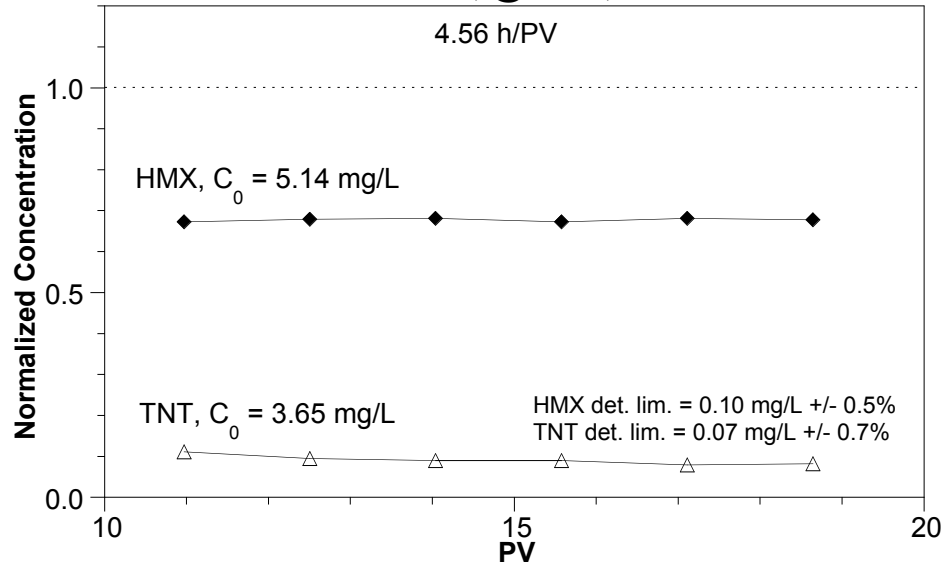
W42; HMX+TNT deg. by red. Ft. Lewis
2*dith./Fe = 4.1, @ 62°C, 1-D flow

6.51 h/PV

HMX, C_0 = 5.14 mg/L

TNT, C_0 = 3.65 mg/L

HMX det. lim. = 0.10 mg/L +/- 0.5%
TNT det. lim. = 0.07 mg/L +/- 0.7%

Normalized Concentration

PV

N.16
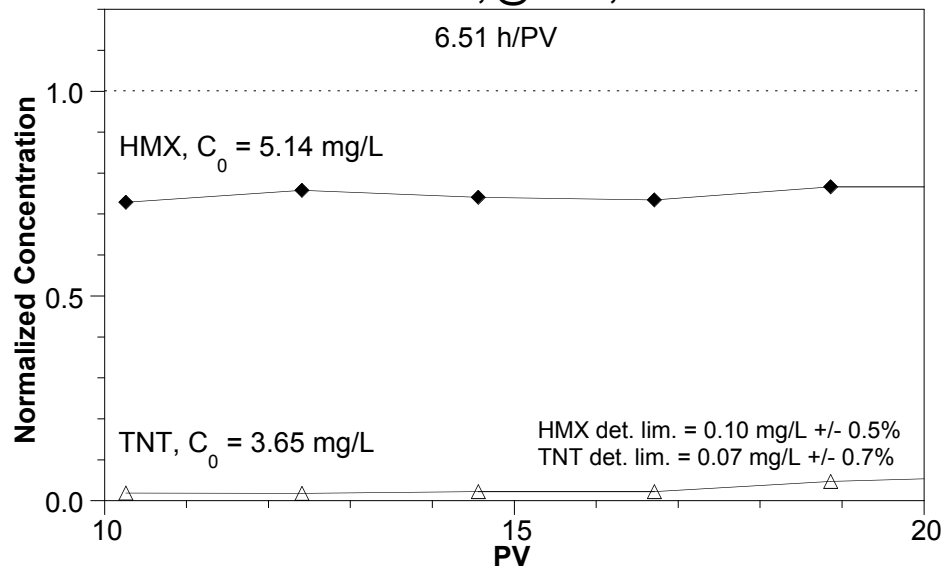
W43; HMX+TNT deg. by red. Ft. Lewis
2*dith./Fe = 1.6, @ 62°C, 1-D flow

8.19 h/PV

HMX, C_0 = 5.14 mg/L

HMX det. lim. = 0.10 mg/L +/- 0.5%
TNT det. lim. = 0.07 mg/L +/- 0.7%

TNT, C_0 = 3.65 mg/L

Normalized Concentration

PV
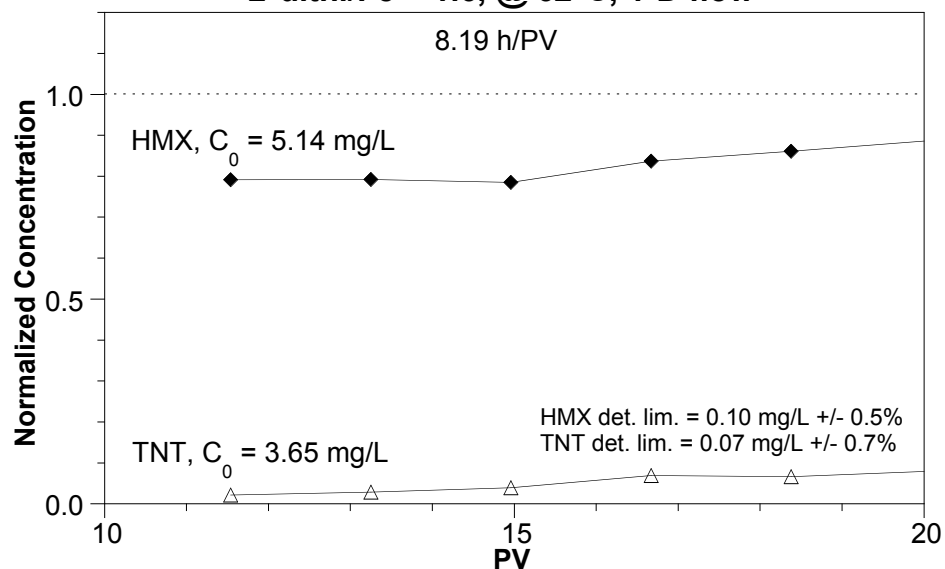
W44; HMX+TNT deg. by red. Ft. Lewis
2*dith./Fe = 0.67, @ 62°C, 1-D flow

HMX, C_0 = 5.14 mg/L

7.25 h/PV

TNT, C_0 = 3.65 mg/L

HMX det. lim. = 0.10 mg/L +/- 0.5%
TNT det. lim. = 0.07 mg/L +/- 0.7%

Normalized Concentration

PV

N.17

W41-44; HMX degradation by red. Ft. Lewis
2*dith./Fe = 22-0.67, @ 62°C, 1-D flow

W44; 0.67

W43; 1.6

W42; 4.1

2*dith./Fe =

W41; 22

HMX, C_0 = 5.14 mg/L

6.63 hour avg. res. time

HMX det. lim. = 0.10 mg/L +/- 0.5%

W41-44; TNT degradation by red. Ft. Lewis
2*dith./Fe = 22-0.67, @ 62°C, 1-D flow

TNT, C_0 = 3.65 mg/L

6.63 hour avg. res. time

TNT det. lim. = 0.07 mg/L +/- 0.7%

2*dith./Fe =

W42; 4.1

W44; 0.67

W41; 22

W43; 1.6

W41-44; HMX degradation by red. Ft. Lewis
2*dith./Fe = 22-0.67, @ 62°C, 1-D flow

W44; 0.67

W43; 1.6

W42; 4.1

W41; 22

2*dith./Fe =

HMX, C_0 = 5.14 mg/L

6.63 hour avg. res. time

HMX det. lim. = 0.10 mg/L +/- 0.5%

Y-axis: Normalized Concentration (0.0, 0.5, 1.0)
X-axis: PV (10, 15, 20)

W41-44; TNT degradation by red. Ft. Lewis
2*dith./Fe = 22-0.67, @ 62°C, 1-D flow

TNT, C_0 = 3.65 mg/L

6.63 hour avg. res. time

TNT det. lim. = 0.07 mg/L +/- 0.7%

2*dith./Fe =

W42; 4.1

W44; 0.67

W41; 22

W43; 1.6

Y-axis: Normalized Concentration (0.0, 0.5, 1.0)
X-axis: PV (10, 15, 20)

N.19

HMX Degradation during 1-D Flow at 10C

di/Fe	half-life
22	0.66 h
4.1	1.04 h
1.6	1.6 h
0.67	1.8 h

more sed. reduction

HMX, C_0 = 5.65 mg/L, data ± 0.5%

HMX Degradation during 1-D Flow at 22C

sorption, Rf

more sed. reduction

di/Fe	half-life	Kd (L/Kg)
22	2.10 h	0.08
4.1	3.46 h	0.10
1.6	16.4 h	0.11
0.67	49.8 h	0.09

HMX, C_0 = 5.65 mg/L, ± 0.5%

HMX Degradation during 1-D Flow at 35C

more sed. reduction

di/Fe	half-life
22	2.73 h
4.1	4.43 h
1.6	25.7 h
0.67	50.4 h

HMX, C_0 = 5.65 mg/L, data ± 0.5%

N.20

TNT Degradation during 1-D Flow at 10C

di/Fe	half-life
22	0.18 h
4.1	0.30 h
1.6	2.9 h
0.67	6.7 h

TNTo = 3.50 mg/L, ± 0.7%

more sed. reduction

TNT Degradation during 1-D Flow at 22C

di/Fe	half-life	Kd (L/Kg)
0.67	2.79 h	1.70
1.6	2.65 h	0.32
4.1	1.74 h	1.97
22	0.96 h	0.98

sorption, Rf

more sed. reduction

TNTo = 3.40 mg/L, ± 0.7%

TNT Degradation during 1-D Flow at 35C

more sed. reduction

TNTo = 3.50 mg/L, ± 0.7%

di/Fe	half-life
22	1.35 h
4.1	1.24 h
1.6	3.73 h
0.67	6.48 h

HMX Degradation Rate by Reduced Sediment

high reduction

low reduction

di/Fe	Ea
0.67	2.6 kJ/mol
1.6	54.4 kJ/mol
4.1	38.1 kJ/mol
22	37.0 kJ/mol

ln k_f

1/T (1/°K)

TNT Degradation Rate by Reduced Sediment

di/Fe	Ea
0.67	2.3 kJ/mol
1.6	1.3 kJ/mol
4.1	48.4 kJ/mol
22	65.0 kJ/mol

high reduction

low reduction

ln k_f

1/T (1/°K)

RDX 1-D Transport in Reduced Sediment Column, 4.4 h/pv

pore vol

influent RDX 10 mg/L, 45 umol/L

RDX ± 0.5%
MNX ± 0.5%
DNT ± 1.6%
TNX ± 0.5%
MDNA ± 0.5%

- ◆ RDX in
- ▣ RDX
- ◯ MNX
- ◆ DNT
- ◦ TNX
- ▲ methylene dinitramine

conc (umol/L)

time (h)

RDX 1-D Transport in Reduced Sediment Column, 4.4 h/pv

pore vol

influent RDX 10 mg/L, 45 umol/L

RDX ± 0.5%
MNX ± 0.5%
DNT ± 1.6%
TNX ± 0.5%
MDNA ± 0.5%

- ◆ RDX in
- ▣ RDX
- ◯ MNX
- ◆ DNT
- ◦ TNX
- ▲ methylene dinitramine

conc (umol/L)

time (h)

RDX 1-D Transport in Reduced Sediment Column, 0.44 h/pv

influent RDX 10 mg/L, 45 umol/L

RDX in
RDX
MNX
DNT
TNX
methylene
dinitramine

RDX ± 0.5%
MNX ± 0.5%
DNT ± 1.6%
TNX ± 0.5%
MDNA ± 0.5%

RDX 1-D Transport in Reduced Sediment Column, 0.44 h/pv

influent RDX 10 mg/L, 45 umol/L

RDX
MNX
DNX
TNX
MDNA

RDX ± 0.5% MNX ± 0.5% DNT ± 1.6%
TNX ± 0.5% MDNA ± 0.5%

10 mg/L RDX Injection into Reduced Sediment, 89 h/pv

pore vol.

aqueous species

data ± 0.15%

carbon dioxide

5.0E-3
138 h

6.0E-3
115 h

% CO2

time (h)

10 mg/L RDX Injection into Reduced Sediment, 4.56 h/pv

pore vol.

aqueous species

data ± 0.15%

carbon dioxide

6.9E-3
100 h

5.9E-3
118 h

% CO2

time (h)

10 mg/L RDX Injection into Reduced Sediment, 8.38 h/pv

8.38 h residence time

data ± 0.15%

carbon dioxide

1.16E-3/h
598 h

7.0E-4/h
985 h

3.7E-4/h
1900 h

% CO2

Pore Volumes

Appendix O: HPLC Calibration Curves for Energetics and Intermediates

Compound	Full Name	CAS	MW	Density	Solubility in Water	Co-Solvent	Retention time	Calibration Constant	Detection Range		
Energetics											
CL-20	2,4,6,8,10,12-Hexanitro-2,4,6,8,10,12-Hexaazaisowurzitane	135285-90-4	438.23 g/mol	2.044 g/cm^3 (solid)	5.0 mg/L	55% MeOH	7 min.	166.6 Area/mg/L	0.150 -3.5	mg/L	+/- 0.5%
HMX	1,3,5,7-tetranitro-1,3,5,7-tetrazocane, $C_4H_8N_8O_8$	2691-41-0	296.16 g/mol	~1.91 g/cm^3 (solid)	5.0 mg/L	45% MeOH 60% MeOH	5.81 min. 4.9 min.	237.1 Area/mg/L	0.105 -5.7	mg/L	+/- 0.5%
TNT	trinitrotoluene, 2,4,6-trinitromethylbenzene, $C_6H_2(NO_2)_3CH_3$	118-96-7	227.13 g/mol	1.654 g/cm^3 (solid)	45 mg/L	55% MeOH 60% MeOH	11 min. 6.9 min.	327.0 Area/mg/L	0.076 -11.0	mg/L	+/- 0.7%
RDX	hexahydro-1,3,5-trinitro-1,3,5-triazine, $(CH_2-N-NO_2)_3$	121-8-24	222.12 g/mol	1.83 g/cm^3 (solid)	45 mg/L	45% MeOH 55% MeOH	8.4 min. 5.9 min.	159.0 Area/mg/L	0.157 -10.2	mg/L	+/- 0.5%
Degradation Products											
MNX (RDX deg.)	hexahydro-1-nitroso-3,5-dinitro-1,3,5-triazine, peaks at 10% RDX mass		206.12 g/mol			45% MeOH 55% MeOH	7.2 min. 5.1 min.	39.3 Area/mg/L	0.636 -19.7	mg/L	+/- 0.5%
DNX (RDX deg.)	hexahydro-1,3-dinitroso-5-nitro-1,3,5-triazine, peaks at 10% of RDX mass		190.12 g/mol			45% MeOH 55% MeOH	6.15 min. 4.3 min.	149.4 Area/mg/L	0.167 -9.5	mg/L	+/- 1.6%
TNX (RDX deg.)	hexahydro-1,3,5-trinitroso-1,3,5-triazine, peaks at 40% of RDX mass		174.12 g/mol			45% MeOH 55% MeOH	5.4 min. 3.8 min.	282.5 Area/mg/L	0.088 -16.8	mg/L	+/- 0.5%
2-ADNT (TNT deg.)	2-amino-4,6-dinitrotoluene, $C_6H_2(NH_2)(NO_2)_2CH_3$	035572-78-2	197.13 g/mol		> 10 mg/L	60 % MeOH	7.3 min.	354.0 Area/mg/L	0.071 -10.4	mg/L	+/- 2.0%
4-ADNT (TNT deg.)	4-amino-2,6-dinitrotoluene, $C_6H_2(NH_2)(NO_2)_2CH_3$	001946-51-0	197.13 g/mol		> 10 mg/L	60 % MeOH	7.7 min.	408.0 Area/mg/L	0.061 -9.0	mg/L	+/- 0.6%
2,4-DANT (TNT deg.)	2,4-diamino-6-nitrotoluene, $C_6H_2(NH_2)_2(NO_2)CH_3$	6629-29-4	167.13 g/mol		> 5 mg/L	60 % MeOH	5.0 min.	240.3 Area/mg/L	0.104 -9.3	mg/L	+/- 3.3%
2,6-DANT (TNT deg.)	2,6-diamino-4-nitrotoluene, $C_6H_2(NH_2)_2(NO_2)CH_3$	59229-75-3	167.13 g/mol		>5 mg/L	60 % MeOH	4.9 min.	293.3 Area/mg/L	0.085 -8.8	mg/L	+/- 0.8%
TAT(3-HCl) (TNT deg.)	2,4,6-triaminotoluene trihydrochloride, $C_6H_2(NH_2)_3CH_3(HCl)_3$, *Note: 1g TAT(3-HCl) => + 0.556g TAT 0.0122 mol HCl*	634-87-7	246.57 g/mol (137.13 w/o HCl)		soluble in anoxic base pH~12+	60 % MeOH	5.5 min	436.9 Area/mg/L	0.057 -58.6	mg/L	+/- 4.9%
MEDINA	methylene dinitramine, $CH_4N_4O_4$		136.07 g/mol		> 50 mg/L	40% MeOH	2.7 min.	218.0 Area/mg/L	0.115 -50.0	mg/L	+/- 0.5%
NDMA	N-nitrosodimethylamine $C_2H_6N_2O$		74.1 g/mol		~50 mg/L	40% MeOH	5.1 min.	344.0 Area/mg/L	0.073 -3.0	mg/L	+/- 1.0%
DMA	dimethylamine (derivativazation with 50:1 M DNFB req. for HPLC)	124-40-3	45.08 g/mol	0.89 g/cm^3		60%MeOH/ 40%(0.2%) acetic acid pH=4	8.0 min	1029.0 Area/mg/L	0.024 -58.6	mg/L	+/- 4.9%
DMA (HCl)	dimethylamine hydrochloride *Note: 1g DMA(HCl) => 0.553g DMA + 0.0122 mol HCl*	53170-19-7	81.54 g/mol (45.08 w/o HCl)	0.89 g/cm^3		+50:1 M DNFB					

RDX standard in water from Acetonitrile Stock, 09/24/04 BJD

Phenomonex Bondclone 10, C-18, 100A, 300x3.9mm column
50 µL injection, 0.8 mL/min flow 55% MeOH/45% water.

RDXin water from RDX Stock in Acetonitrile
New Co-Solvent Used
Conducted 09/24/04 by BJD
(average RT 6.2 min)

y = 341.83x + 1.15
r = 99.974%
(accuracy is 98% for all concentrations)

Y-axis: RDX area response (10 to 10000)
X-axis: RDX (mg/L) (0.1)
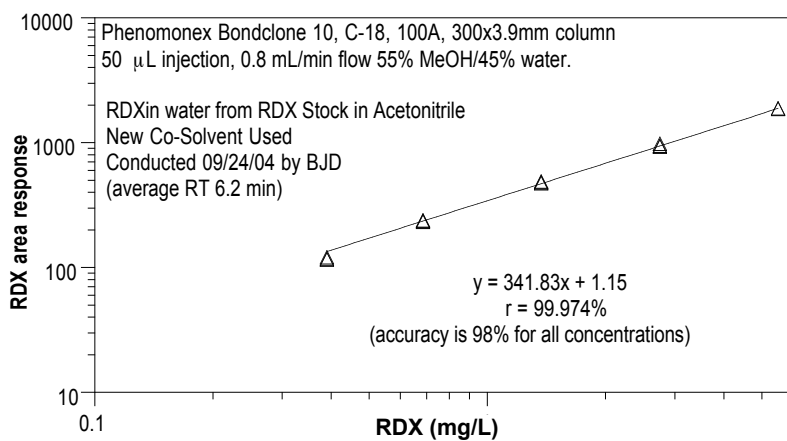
RDX (mg/L)	HPLC area
0.39	121
0.39	116
0.39	117
0.685	237
0.685	239
0.685	233
1.37	481
1.37	473
1.37	489
2.75	978
2.75	948
2.75	932
5.5	1872
5.5	1868
5.5	1881

Q11.1; HPLC Calibration for RDX from Stock#3 (11769.2 mg/L in Acetonitrile)

Phenomonex Bondclone 10, C-18, 100A, 300x3.9mm column
50 µL injection, 0.8 mL/min flow 40% MeOH/60% DI water.

RDXin water from RDX Stock in Acetonitrile
Conducted 12/15/04 by BJD
(average RT 10.3 min)

y = 71.223x +0.13699
r = 0.9999

Y-axis: HPLC area response (mAU) (10 to 1000)
X-axis: RDX Calc. (mg/L) (0.1 to 10)
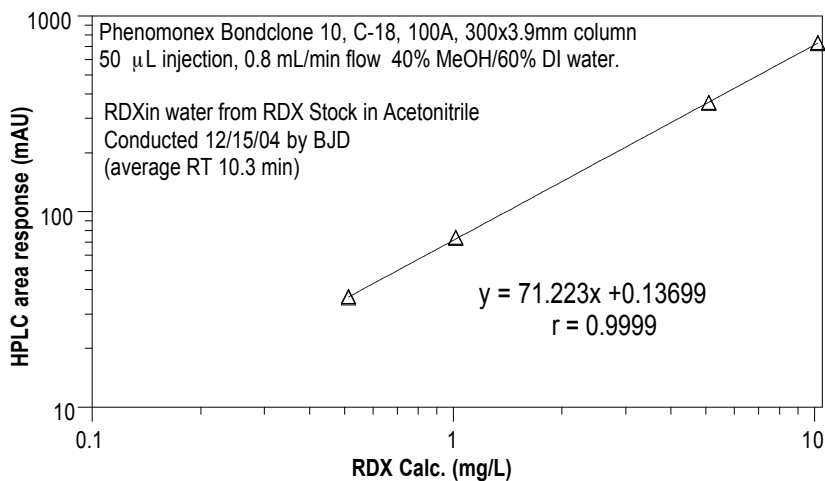
RDX (mg/L)	HPLC area
10.21	732.68
10.21	729.1
10.21	723.75
5.1	359.68
5.1	360.53
5.1	363.21
1.02	73.56
1.02	74.07
1.02	73.13
0.51	36.34
0.51	36.86
0.51	36.78

Q12.1; HPLC Calibration for RDX from Stock#3 (RDX and trace HMX in Acetonitrile)

Phenomonex Bondclone 10, C-18, 100A, 300x3.9mm column
50 μL injection, 0.8 mL/min flow 45% MeOH/55% DI water.
12/28/04 by BJD

RDX in water
(average RT 8.4 min)

RDX = 3308.5 mg/L
(y = 3308.5x -0.2458
r = 0.9951)

HMX in water
(average RT 5.8 min)

HMX = 386.15 mg/L
(y = 386.15x -0.0673
r = 0.9960)
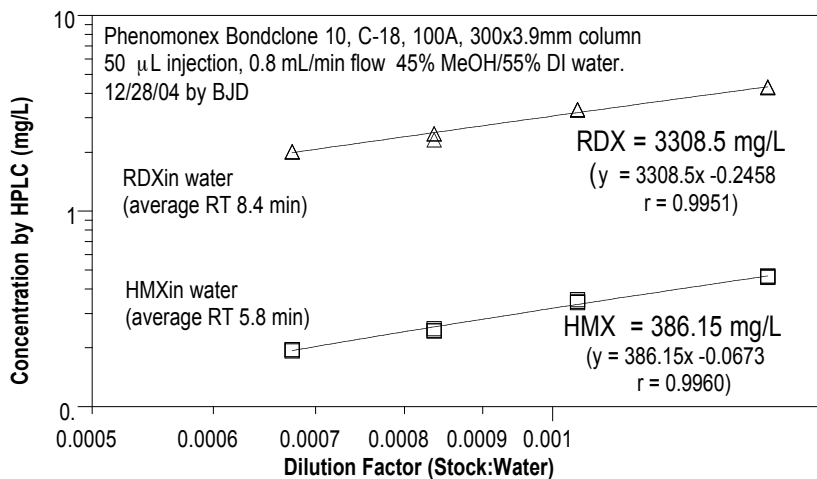
RDX (mg/L)	HMX (mg/L)
4.28	0.46
4.31	0.47
4.29	0.46
3.31	0.35
3.3	0.35
3.28	0.34
2.49	0.25
2.48	0.24
2.31	0.25
2.01	0.2
2.01	0.19
2.01	0.2

W62B; HPLC Calibration for MEDINA from Stock#1 (500 mg/L in Acetonitrile)

Phenomonex Bondclone 10, C-18, 100A,
300x3.9mm column 50 μL injection,
0.8 mL/min flow 40% MeOH/40% DI water.

methylenedinitramine (MEDINA) water
pH adjusted to >11 with NaOH
Conducted 6/20/06 by BJD
(average RT 2.7 min)

y = 217.56x +2.547

r^2 = 0.99994

lower detection limit ~ 0.01 ppm (0.08 uM)
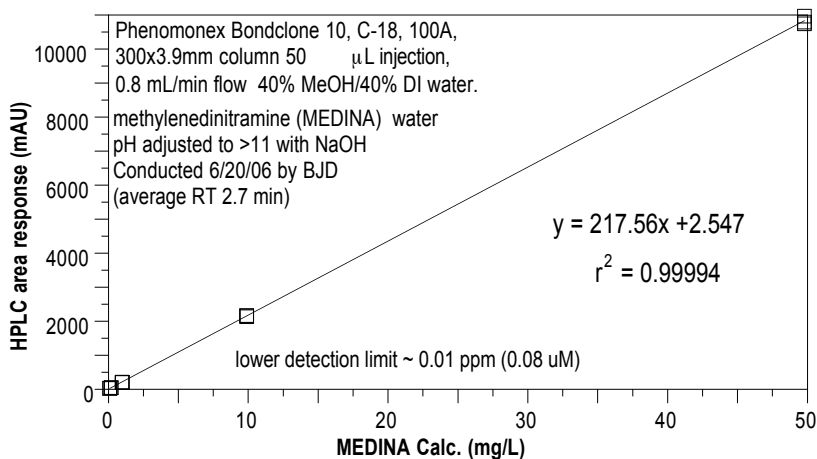
MEDINA (mg/L)	HPLC area
49.79	10967
49.79	10743
49.79	10795
9.9	2172
9.9	2138
9.9	2163
0.99	208
0.99	200
0.99	208
0.2	49
0.2	52
0.2	48
0.1	33
0.1	29
0.1	28

W62B; HPLC Calibration for MEDINA from Stock#1 (500 mg/L in Acetonitrile) for new lamp installed 06/21/06

Phenomonex Bondclone 10, C-18, 100A, 300x3.9mm column 50 μL injection, 0.8 mL/min flow 40% MeOH/40% DI water.

methylenedinitramine (MEDINA) water pH adjusted to >11 with NaOH Conducted 6/22/06 by BJD (average RT 2.7 min)

$y = 221.98x - 20.799$

$r^2 = 0.99998$

lower detection limit ~ 0.1 ppm (0.5 uM)

HPLC area response (mAU) vs **MEDINA Calc. (mg/L)**
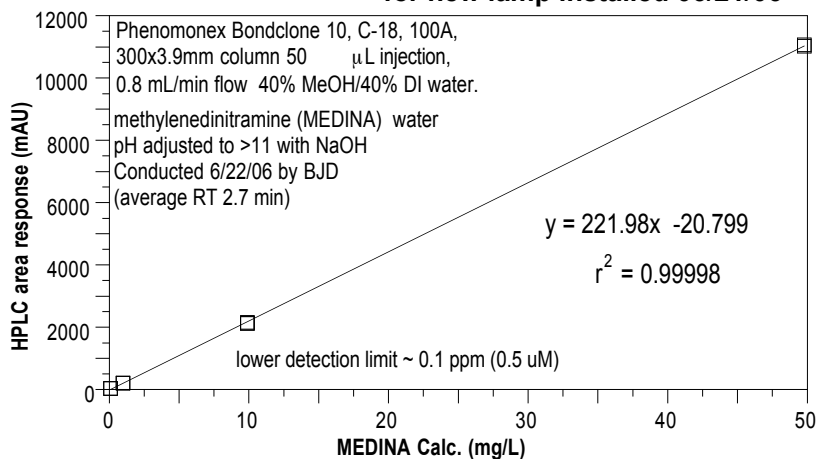
MEDINA (mg/L)	HPLC area
49.79	11016
49.79	11071
9.9	2157
9.9	2129
9.9	2126
0.99	207
0.99	206
0.99	202
0.1	31
0.1	45

CL-20 standard in water from MeOH Stock

Initial calibration for aqueous CL-20 in water for new column; Phenomonex Bondclone 10, C-18, 100A, 300x3.9mm column 50 μL injection, 0.8 mL/min flow 55% MeOH/5% water.

CL-20 in water from CL-20 Stock in Methanol Conducted 09/22/04 by BJD (average RT 8.8 min)

$y = 203.06x - 3.10$

$r = 99.932\%$

CL-20 area response vs **CL-20 (mg/L)**
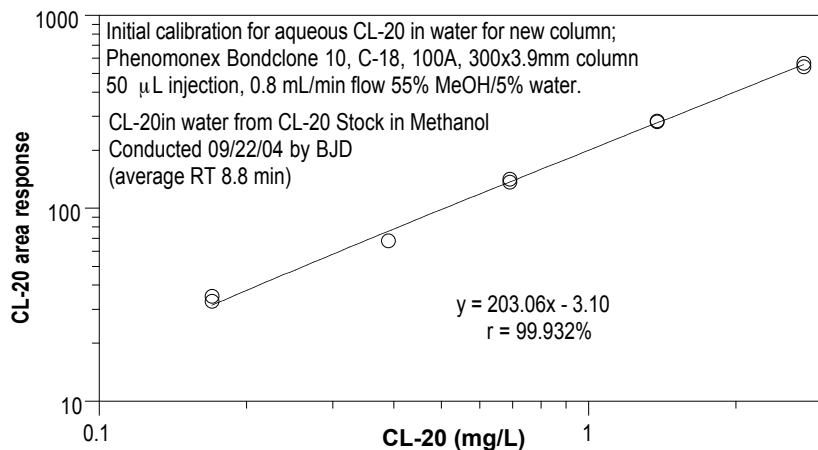
CL20 (mg/L)	HPLC area
0.17	35
0.17	33
0.39	68
0.39	68
0.69	137
0.69	142
1.38	281
1.38	284
2.75	542
2.75	564

O.4

CL-20 standard in water from MeOH Stock, 09/24/04 BJD

Phenomonex Bondclone 10, C-18, 100A, 300x3.9mm column
50 μL injection, 0.8 mL/min flow 55% MeOH/45% water.

CL-20in water from CL-20 Stock in Methanol
New Co-Solvent Used
Conducted 09/24/04 by BJD
(average RT 8.8 min)

$y = 213.01x - 2.13$
$r = 99.819\%$
(accuracy ranges from 92% at 0.1 mg/L
to 95% at3.0 mg/l)

X-axis: **CL-20 (mg/L)**
Y-axis: **CL-20 area response**
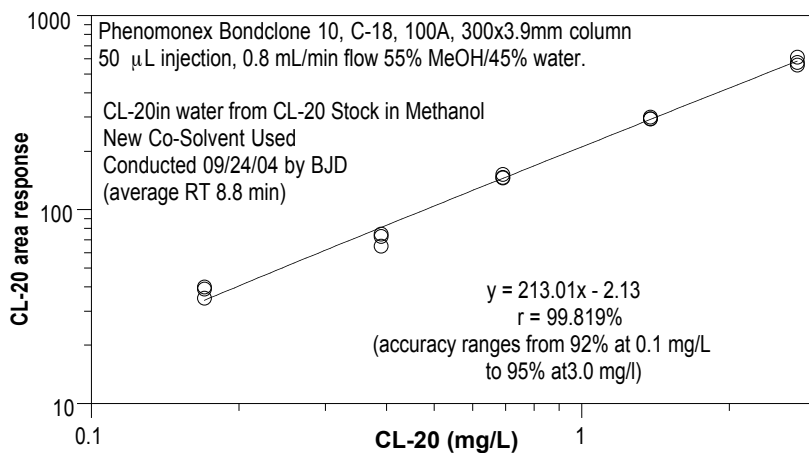
CL20 (mg/L)	HPLC area
0.17	40
0.17	35
0.17	39
0.39	75
0.39	65
0.39	73
0.69	152
0.69	146
0.69	147
1.38	294
1.38	301
1.38	294
2.75	557
2.75	612
2.75	576

Q10.1; HPLC Calibration for CL-20 from "910" Stock (910 mg/L in MeOH)

Phenomonex Bondclone 10, C-18, 100A, 300x3.9mm column
50 μL injection, 0.8 mL/min flow 55% MeOH/45% water.

CL-20in water from CL-20 Stock in Methanol
Conducted 12/13/04 by BJD
(average RT 8.8 min)

$y = 166.68x - 5.152$
$r = 0.9999$

X-axis: **CL-20 (mg/L)**
Y-axis: **HPLC area response (mAU)**
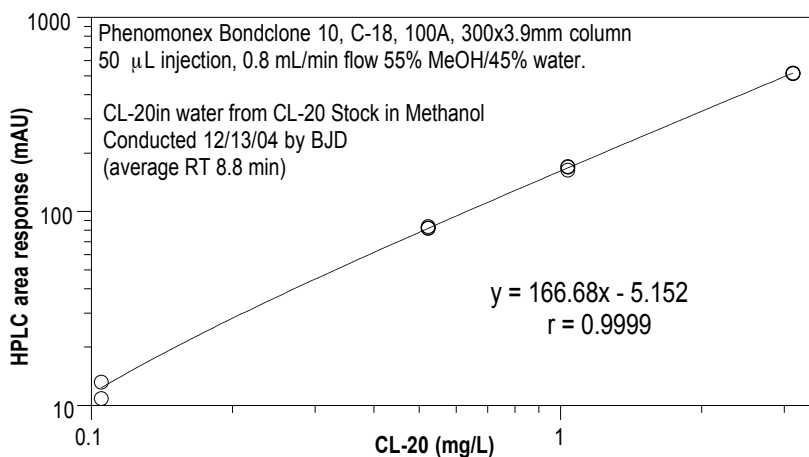
CL20 (mg/L)	HPLC area
3.13	514.43
3.13	516.25
3.13	517.95
1.035	170.97
1.035	164.09
1.035	169.43
0.522	82.11
0.522	82.47
0.522	83.65
0.105	8.87
0.105	10.9
0.105	13.23

O.5

Q10.2; HPLC Calibration for CL-20 from CL-20 Stock#7 (5354 mg/L in MeOH)

Phenomonex Bondclone 10, C-18, 100A, 300x3.9mm column
50 µL injection, 0.8 mL/min flow 55% MeOH/45% water.

CL-20in water from CL-20 Stock in Methanol
Conducted 12/13/04 by BJD
(average RT 8.8 min)

y = 165.26x - 19.17
r = 0.9972
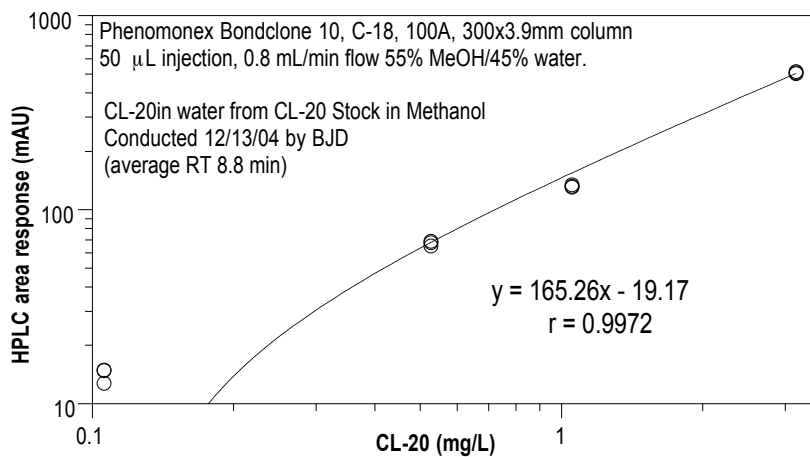
CL20 (mg/L)	HPLC area
3.159	504.05
3.159	516.88
3.159	508.75
1.053	131.14
1.053	132.17
1.053	134.41
0.527	67.88
0.527	68.83
0.527	65.37
0.106	14.86
0.106	14.95
0.106	12.79

Q10.3; HPLC Calibration for CL-20 from CL-20 Stock#10 (5993.7 mg/L in MeOH)

Phenomonex Bondclone 10, C-18, 100A, 300x3.9mm column
50 µL injection, 0.8 mL/min flow 55% MeOH/45% water.

CL-20in water from CL-20 Stock in Methanol
Conducted 12/13/04 by BJD
(average RT 8.8 min)

y = 167.09x - 11.568
r = 0.9990
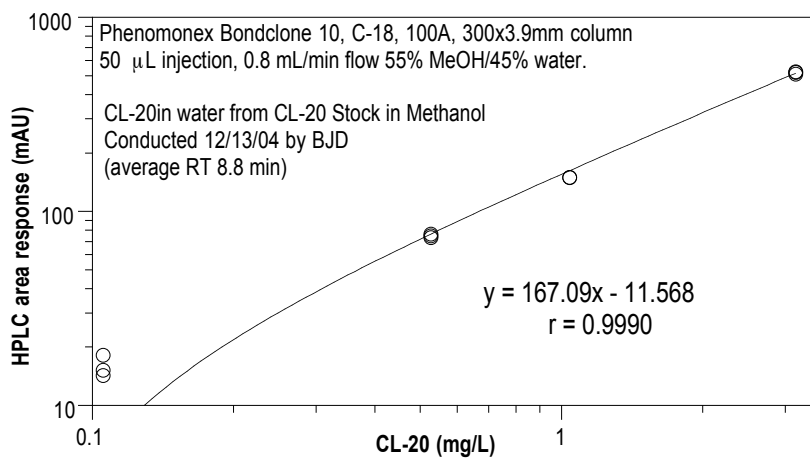
CL20 (mg/L)	HPLC area
3.155	511.08
3.155	521.73
3.155	525.99
1.04	149.97
1.04	150.22
1.04	149.42
0.526	74.87
0.526	76.51
0.526	73.37
0.105	18.18
0.105	14.28
0.105	15.21

O.6

W111.A; HPLC Calibration for CL-20 from Stock # 10, CL-20 (5993.7 mg/L) in MeOH (0.01-6.5 mg/L)

Phenomonex Bondclone 10, C-18, 100A, 300x3.9mm column 50 μL injection, 0.8 mL/min flow 55% MeOH/45% DI water.

CL-20 in water
Conducted 01/04/07 by BJD
(average RT 7.2 min)

$y = 160.66x - 1.3056$

$r^2 = 0.99978$

lower detection limit ~ 0.05 ppm (0.1 uM)
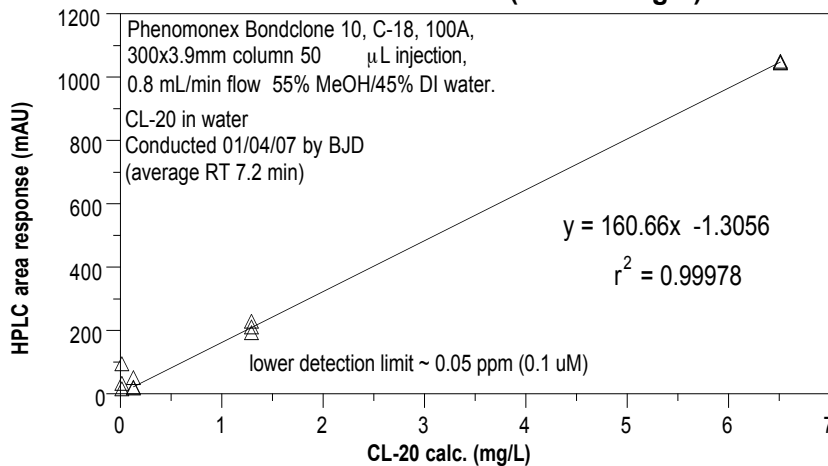
CL-20 (mg/L)	HPLC area
6.513	1045
6.513	1050
6.513	1047
1.292	229
1.292	211
1.292	193
0.129	51*
0.129	18
0.129	21
0.016	95*
0.016	33*
0.016	16*
	*not used in fit

Q10.4; HPLC Calibration for TNT from TNT Stock#1 (10,597 mg/L in Acetonitrile)

Phenomonex Bondclone 10, C-18, 100A, 300x3.9mm column 50 μL injection, 0.8 mL/min flow 55% MeOH/45% water.

TNT in water from TNT Stock in Acetonitrile
Conducted 12/13/04 by BJD
(average RT 10.6 min)

$y = 264.64x - 23.467$
$r = 0.99995$
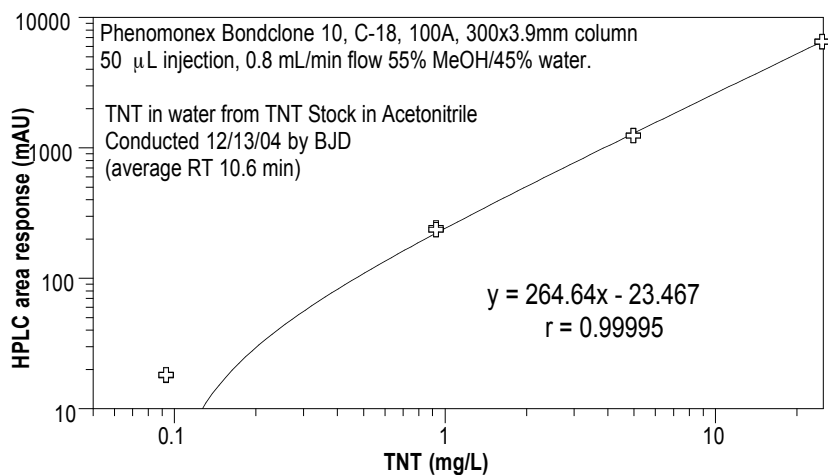
TNT (mg/L)	HPLC area
24.74	6522.98
24.74	6552.46
24.74	6518.77
4.962	1248.29
4.962	1248.54
4.962	1245.32
0.927	236.33
0.927	244.56
0.927	236.89
0.093	18.31
0.093	18
0.093	18.24

W25C; HPLC Calibration for TNT from Stock#1 (10597 mg/L in Acetonitrile)

Phenomonex Bondclone 10, C-18, 100A,
300x3.9mm column 50 μL injection,
0.8 mL/min flow 60% MeOH/40% DI water.

TNT in water from HMX Stock in Acetonitrile
Conducted 3/28/06 by BJD
(average RT 6.9 min)

$y = 395.1x + 10.991$
$r = 0.99983$
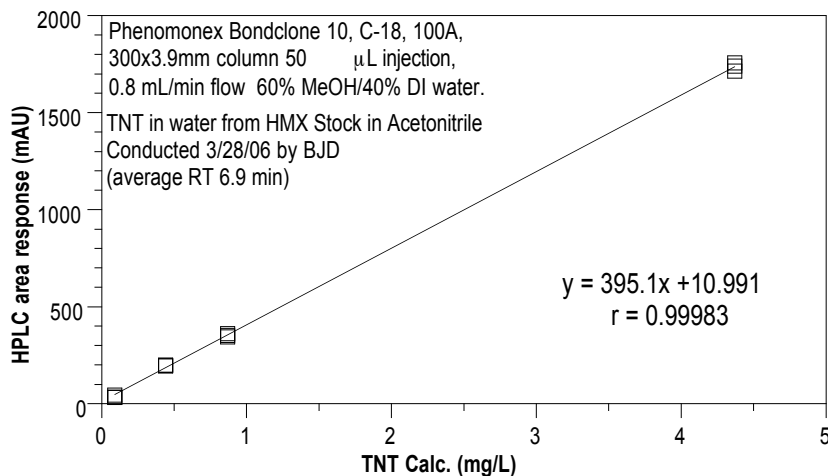
TNT (mg/L)	HPLC area
4.37	1740
4.37	1714
4.37	1757
0.87	361
0.87	344
0.87	352
0.44	199
0.44	194
0.44	198
0.09	45
0.09	33
0.09	34

X27-A; HPLC Calibration for TNT from Stock#1 (10,597 mg/L in Acetonitrile)

Phenomonex Bondclone 10, C-18, 100A,
300x3.9mm column 50 μL injection,
0.8 mL/min flow 60% MeOH/40% DI water.

2,4,6-trinitrotoluene in water
Conducted 6/19/06 by BJD
(average RT 7.0 min)

$y = 326.91x - 20.031$
$r^2 = 0.99978$
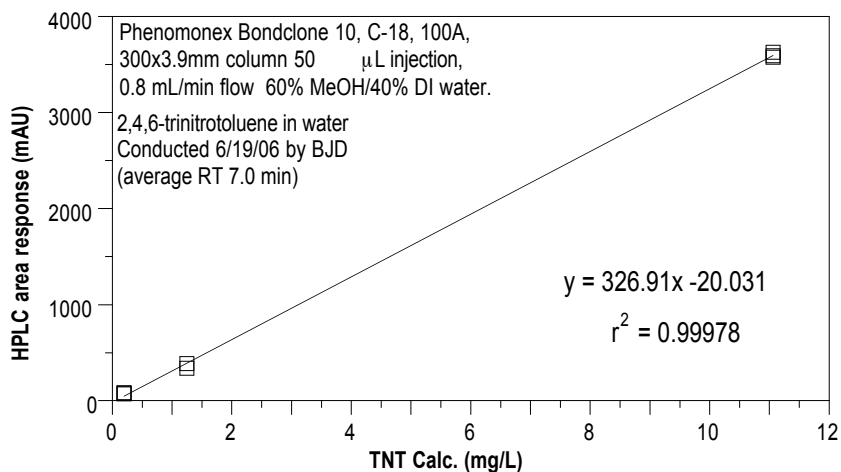
TNT (mg/L)	HPLC area
11.06	3629
11.06	3592
11.06	3577
1.25	335
1.25	339
1.25	385
0.2	77
0.2	71
0.2	82

X27-B; HPLC Calibration for 2-ADNT from stock ampule (1,000 mg/L in Acetonitrile)

Phenomonex Bondclone 10, C-18, 100A,
300x3.9mm column 50 μL injection,
0.8 mL/min flow 60% MeOH/40% DI water.

2-amino-4,6-dinitrotoluene in water
Conducted 6/19/06 by BJD
(average RT 7.7 min)

$y = 353.55x - 2.8909$

$r^2 = 0.99975$
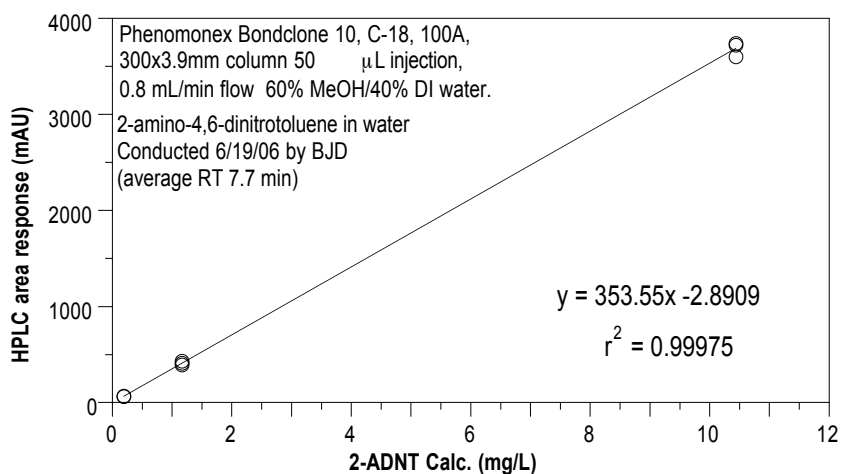
TNT (mg/L)	HPLC area
10.44	3602
10.44	3740
10.44	3721
1.17	410
1.17	393
1.17	430
0.19	61
0.19	67
0.19	67

X27-C; HPLC Calibration for 4-ADNT from stock ampule (1,000 mg/L in Acetonitrile)

Phenomonex Bondclone 10, C-18, 100A,
300x3.9mm column 50 μL injection,
0.8 mL/min flow 60% MeOH/40% DI water.

4-amino-2,6-dinitrotoluene in water
Conducted 6/19/06 by BJD
(average RT 7.3 min)

$y = 407.49x - 13.145$

$r^2 = 0.99996$
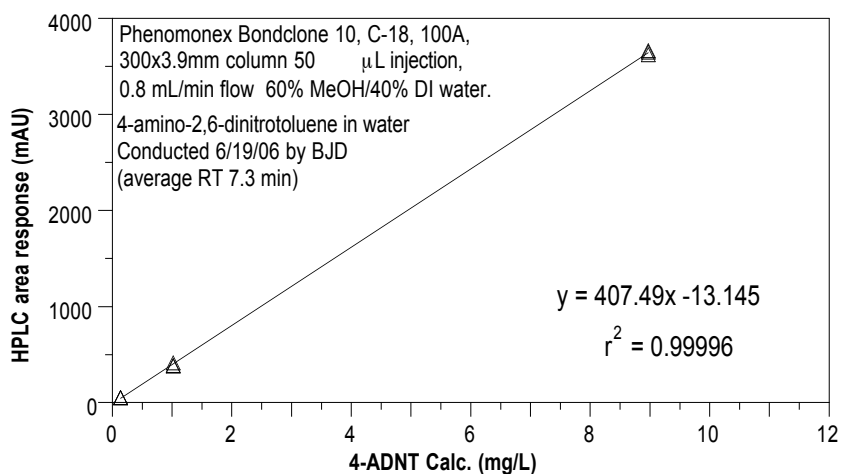
TNT (mg/L)	HPLC area
8.97	3621
8.97	3664
8.97	3648
1.02	386
1.02	381
1.02	414
0.14	50
0.14	53
0.14	50

X36-A; HPLC Calibration for 2,4-DANT from stock ampule (100 mg/L in Acetonitrile)

Phenomonex Bondclone 10, C-18, 100A,
300x3.9mm column 50   μL injection,
0.8 mL/min flow 60% MeOH/40% DI water.

2-,4-diamino-6-nitrotoluene in water
Conducted 07/07/06 by LMD
(average RT 5.0 min)

$y = 240.34x - 30.012$

$r^2 = 0.99878$

Lower detection limit~ 0.125 mg/L
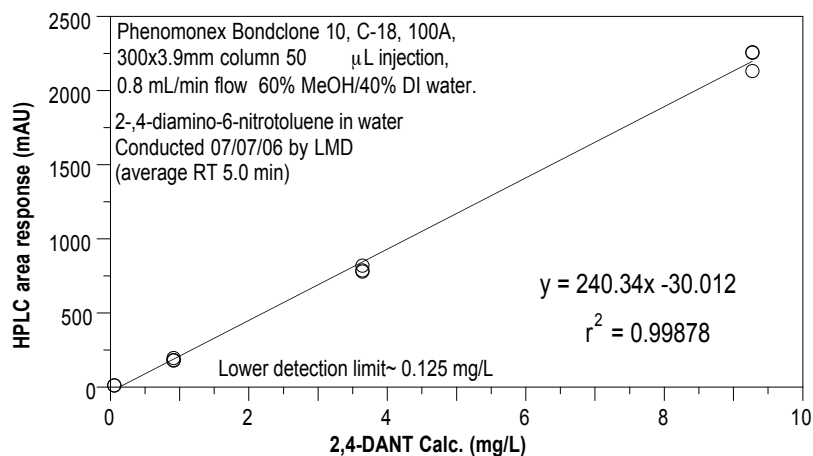
2,4-DANT (mg/L)	HPLC area
9.272	2132.7
9.272	2256.5
9.272	2260.6
3.637	822.1
3.637	788.4
3.637	781.2
0.91	198.2
0.91	184.7
0.91	180.2
0.055	14.3
0.055	12.7
0.055	11.7

X36-B; HPLC Calibration for 2,6-DANT from stock ampule (100 mg/L in Acetonitrile)

Phenomonex Bondclone 10, C-18, 100A,
300x3.9mm column 50   μL injection,
0.8 mL/min flow 60% MeOH/40% DI water.

2-,6-diamino-4-nitrotoluene in water
Conducted 07/07/06 by LMD
(average RT 5.0 min)

$y = 293.31x - 7.1773$

$r^2 = 0.9999$

Lower detection limit~ 0.02 mg/L
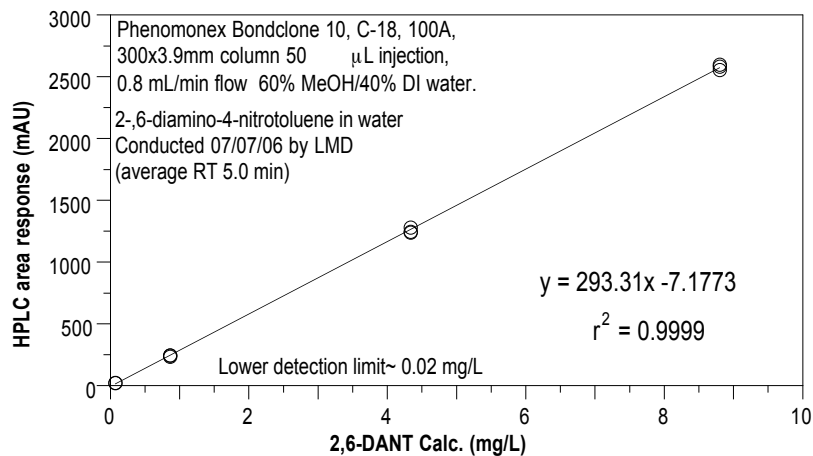
2,6-DANT (mg/L)	HPLC area
8.801	2598
8.801	2556.8
8.801	2582.5
4.338	1280.3
4.338	1239.6
4.338	1247.8
0.862	243.7
0.862	244.7
0.862	235.2
0.07	23.9
0.07	22.1
0.07	20.5

O.10

X49.4; HPLC Calibration for Triaminotoluene (TAT) from dry TAT(3HCl), (0.34-58.6 mg/L)

Phenomonex Bondclone 10, C-18, 100A,
300x3.9mm column 50 μL injection,
0.8 mL/min flow 60% MeOH/40% DI water.

triaminotoluene in anaerobic water
+ 0.01M NaOH (pH12.5)
Conducted 10/04/06 by BJD
(average RT 5.4 min)

$y = 436.93x - 35.931$

$r^2 = 0.99877$

lower detection limit ~ 0.06 ppm (0.4 uM)
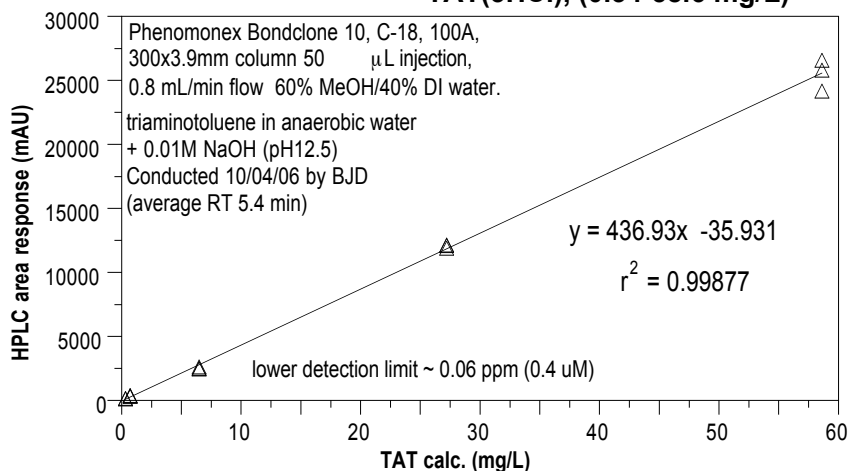
TAT (mg/L)	HPLC area
58.61	24151
58.61	25803
58.61	26581
27.21	12095
27.21	12148
27.21	11887
6.50	2627
6.50	2509
6.50	2471
0.71	342
0.71	324
0.71	407
0.34	181
0.34	178
0.34	128

Q11.2; HPLC Calibration for HMX from Stock#1 (6460 mg/L in Acetonitrile)

Phenomonex Bondclone 10, C-18, 100A, 300x3.9mm column
50 μL injection, 0.8 mL/min flow 40% MeOH/60% DI water.

HMX in water from HMX Stock in Acetonitrile
Conducted 12/15/04 by BJD
(average RT 6.7 min)

$y = 220.03x + 10.119$
$r = 0.9999$
(without 10 ppm point)

$y = 150.15x + 100.94$
$r = 0.8503$
(with 10 ppm point)
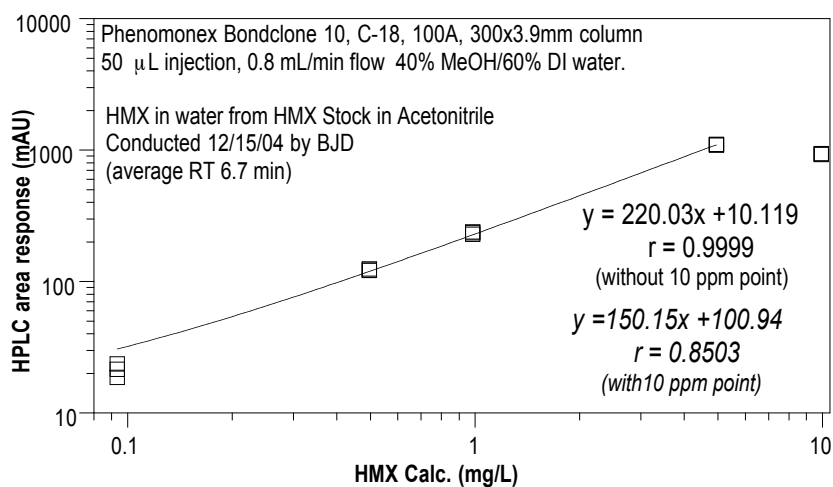
HMX (mg/L)	HPLC area
9.91	936.96
9.91	927.26
9.91	937.47
4.95	1092.09
4.95	1105.31
4.95	1095.94
0.98	229.23
0.98	234.8
0.98	239
0.5	121.43
0.5	124.86
0.5	122.32
0.09	23.68
0.09	21.57
0.09	18.6

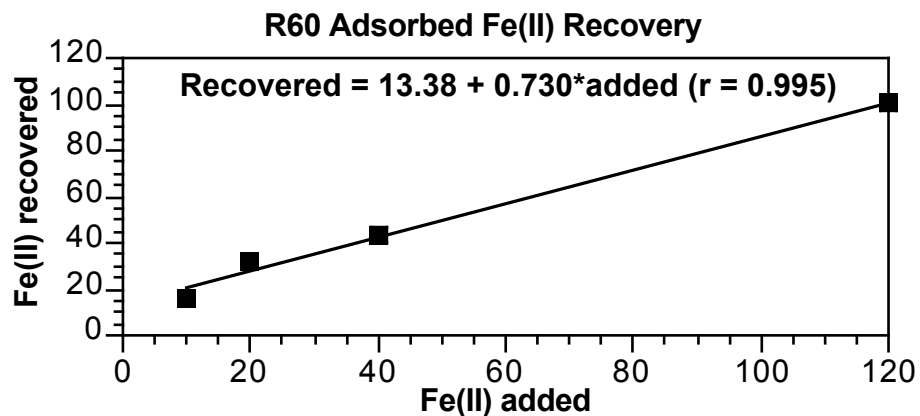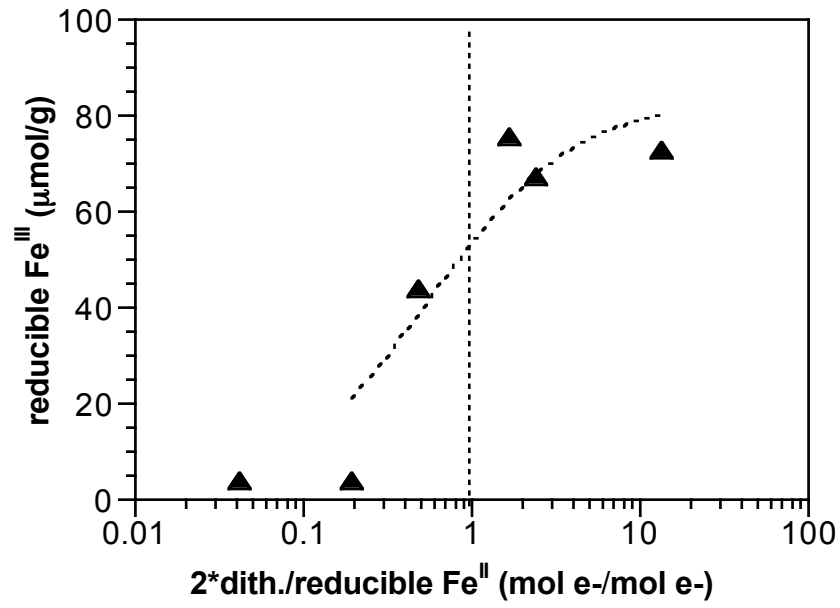## Q12.2; HPLC Calibration for HMX from Stock#1 (6460 mg/L in Acetonitrile)

Phenomonex Bondclone 10, C-18, 100A, 300x3.9mm column
50 µL injection, 0.8 mL/min flow 45% MeOH/55% DI water.

HMX in water from HMX Stock in Acetonitrile
Conducted 12/28/04 by BJD
(average RT 5.8 min)

$y = 237.1x + 3.5212$
$r = 0.9999$
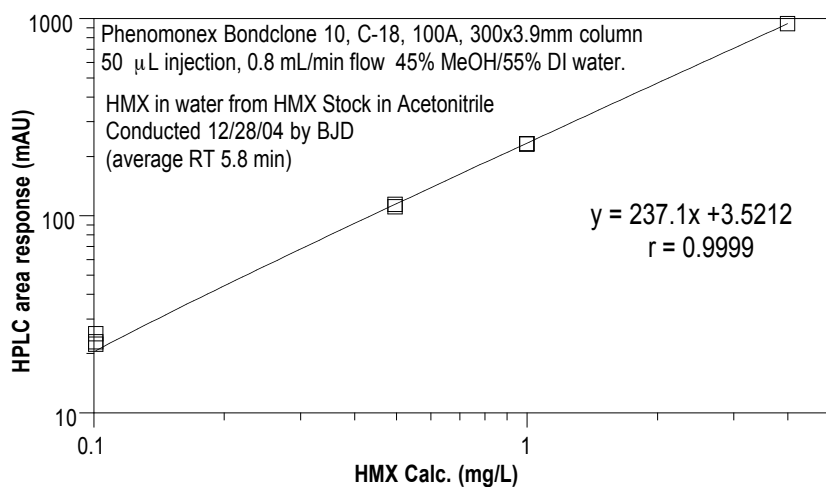
HMX (mg/L)	HPLC area
3.99	945.14
3.99	942.21
3.99	945.3
1	232.39
1	231.89
1	232.04
0.5	111.33
0.5	111.21
0.5	114.3
0.1	22.97
0.1	22.3
0.1	25.31

W25C; HPLC Calibration for HMX from Stock#1 (6460 mg/L in Acetonitrile)

Phenomonex Bondclone 10, C-18, 100A, 300x3.9mm column
50 µL injection, 0.8 mL/min flow 60% MeOH/40% DI water.

HMX in water from HMX Stock in Acetonitrile
Conducted 3/28/06 by BJD
(average RT 4.8 min)

$y = 225.88x - 3.0709$
$r = 0.99956$
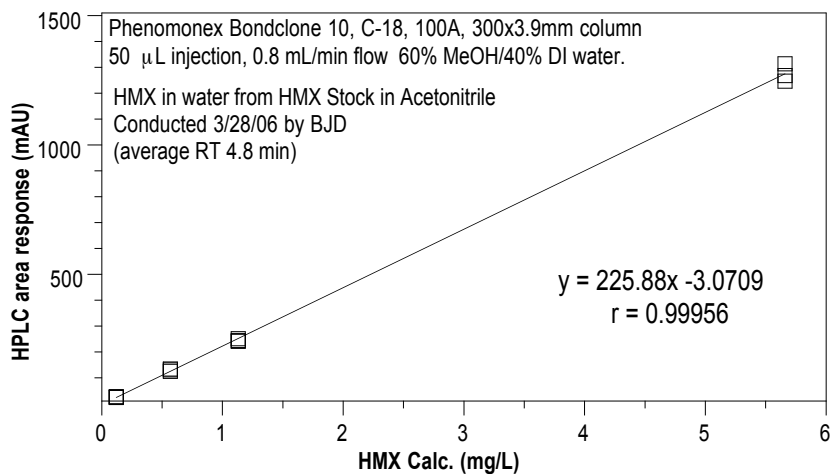
HMX (mg/L)	HPLC area
5.66	1268
5.66	1314
5.66	1247
1.13	251
1.13	244
1.13	241
0.57	131
0.57	134
0.57	125
0.12	24
0.12	28
0.12	25

Appendix P: Sediment Abiotic Characterization: Iron Extraction, pH, Eh, and Reductive Capacity Measurements
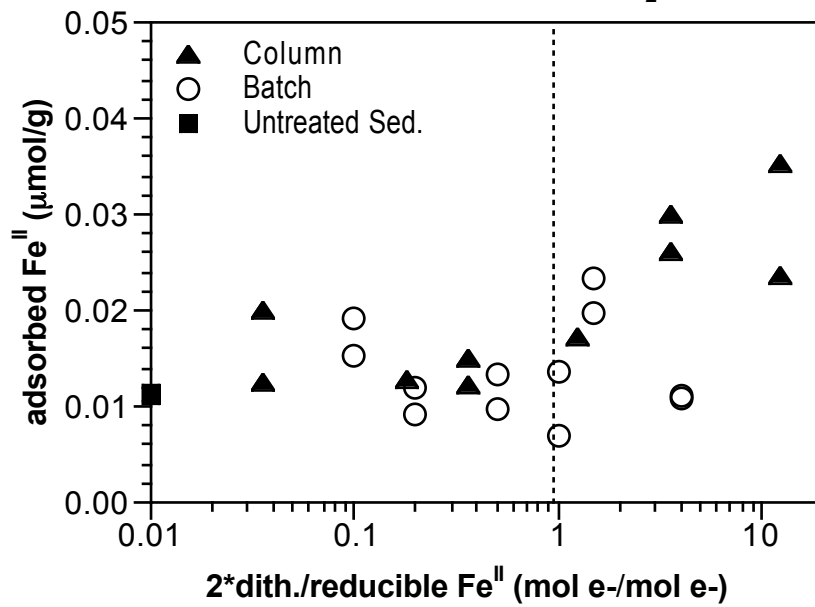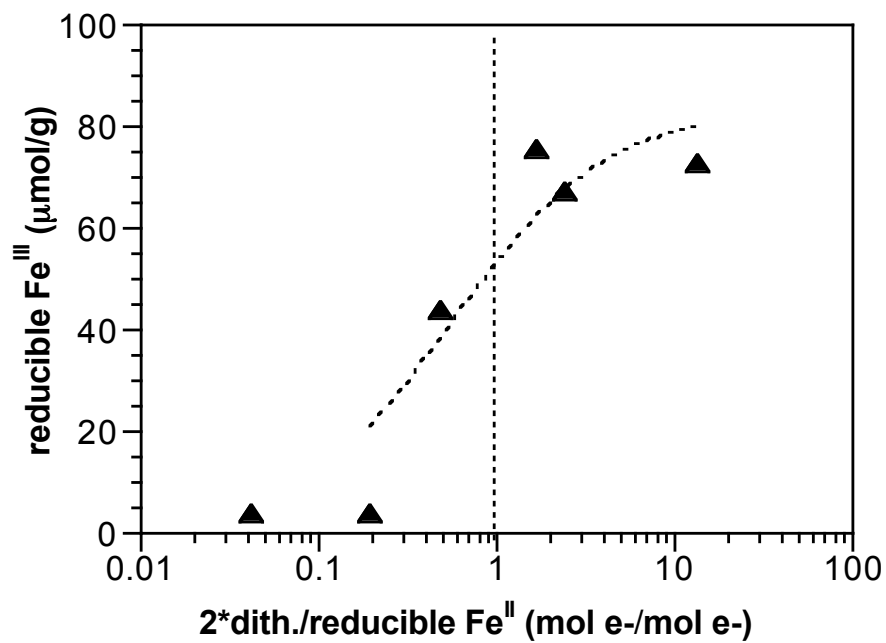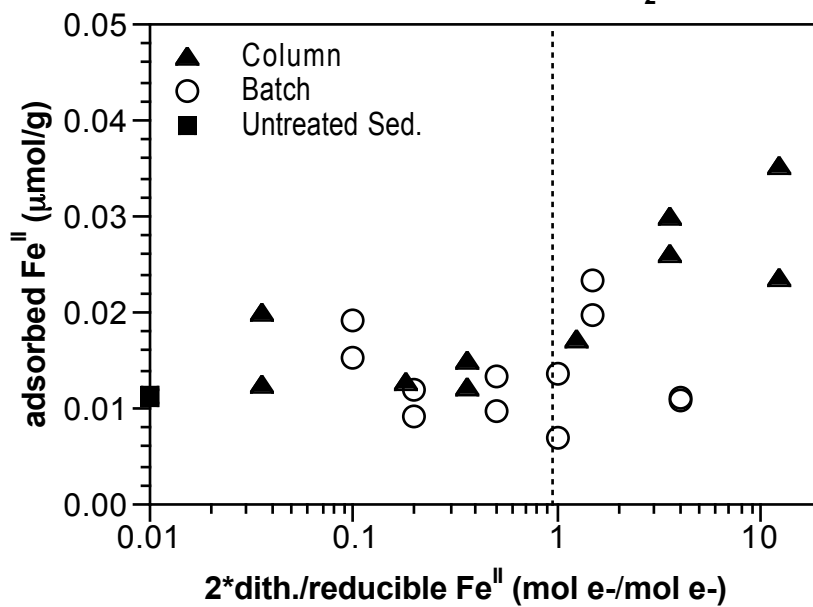
0.5M HCl Extraction

**reductive capacity
by column reduction/oxidation**

Eh of Dithionite-reduced Sediment

Eh (mv) vs 2*dithionite/Fe

y-axis: Eh (mv), 0 to -600
x-axis: 2*dithionite/Fe, 0.01 to 100

Eh of Dithionite-reduced Sediment

Eh (mv) vs Time (h)

2*di/Fe:
0.078
0.23
1.12
0.54
26.8

Eh vs Time (R24, 2di/Fe = 26)

2*di/Fe:
0.078
0.35
0.8
26
1.1

x-axis: Time (h)

R60 Adsorbed Fe(II) Recovery

Recovered = 13.38 + 0.730*added (r = 0.995)

y-axis: Fe(II) recovered, 0 to 120
x-axis: Fe(II) added, 0 to 120

P.2

Column Reduction/Column Oxidataion

Column + Batch Reduction/CaCl$_2$ Extraction

P.3

Column Reduction/Column Oxidataion

Column + Batch Reduction/CaCl$_2$ Extraction
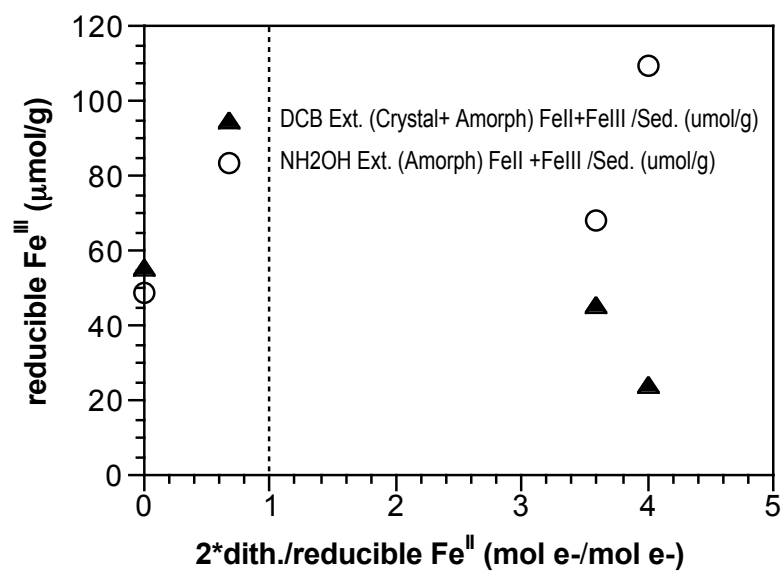
Column + Batch Reduction/0.5M HCl Extraction

Column + Batch Reduction/5.0M HCl Extraction
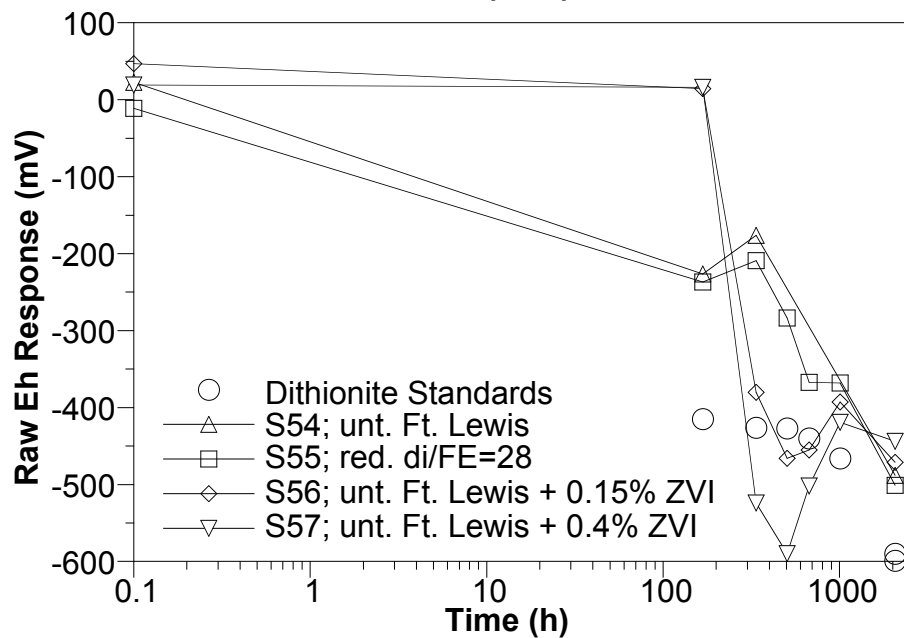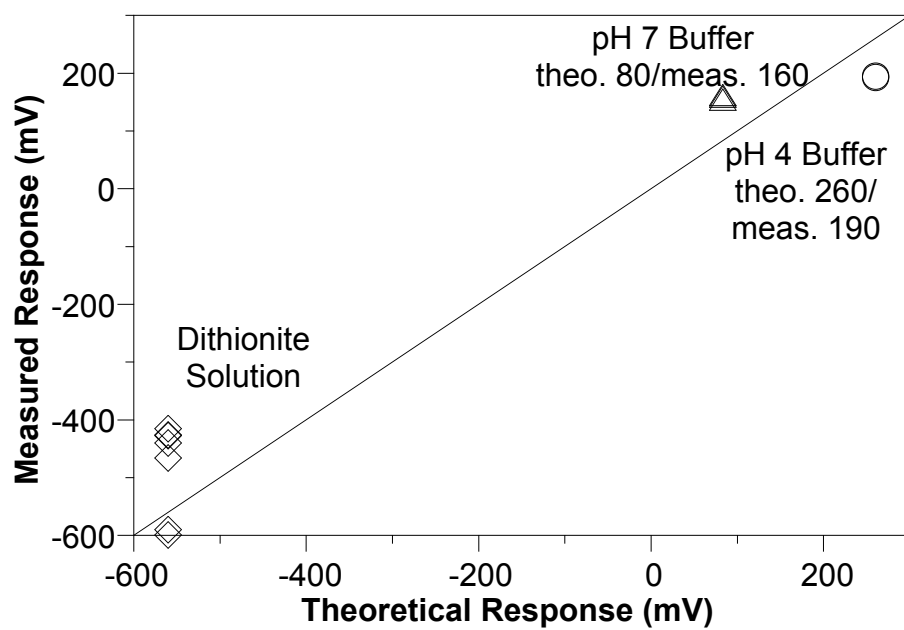
Column + Batch Reduction/5.0M HCl Extraction
Total Fe

Column + Batch Reduction/NH$_2$OH HCl Extraction

P.6
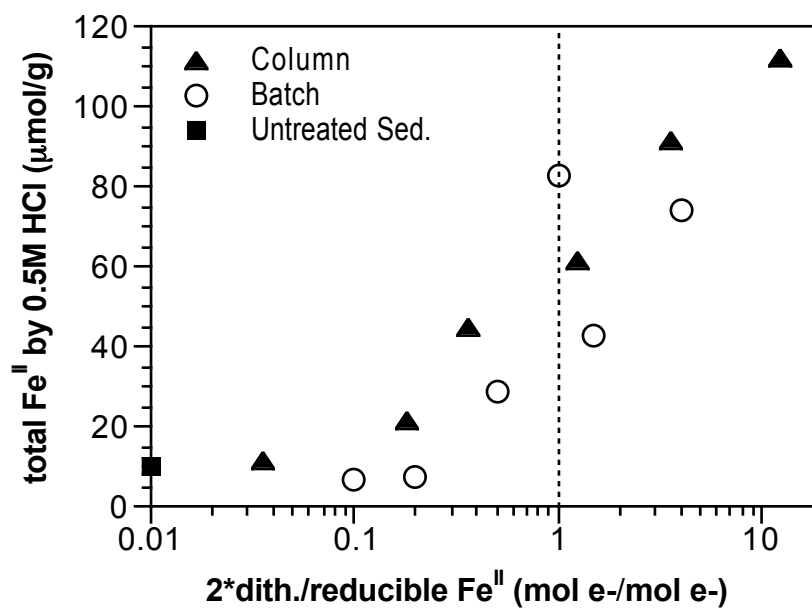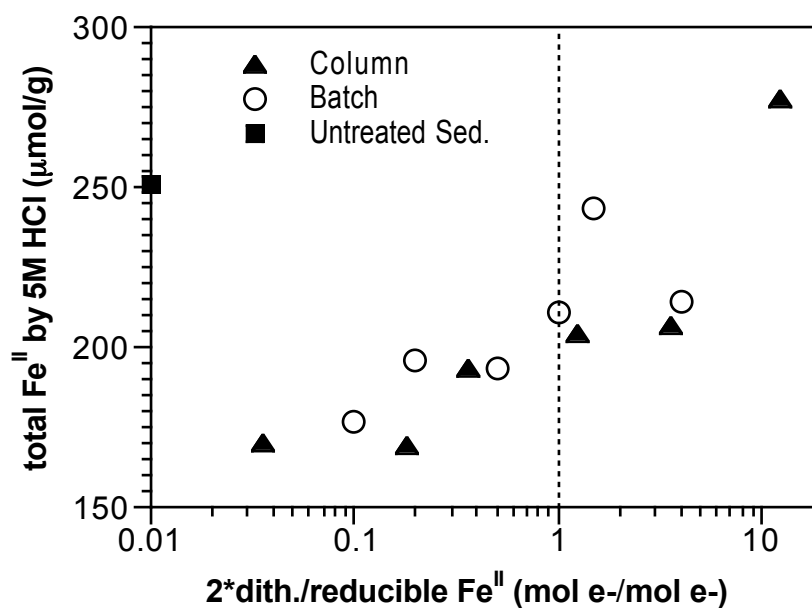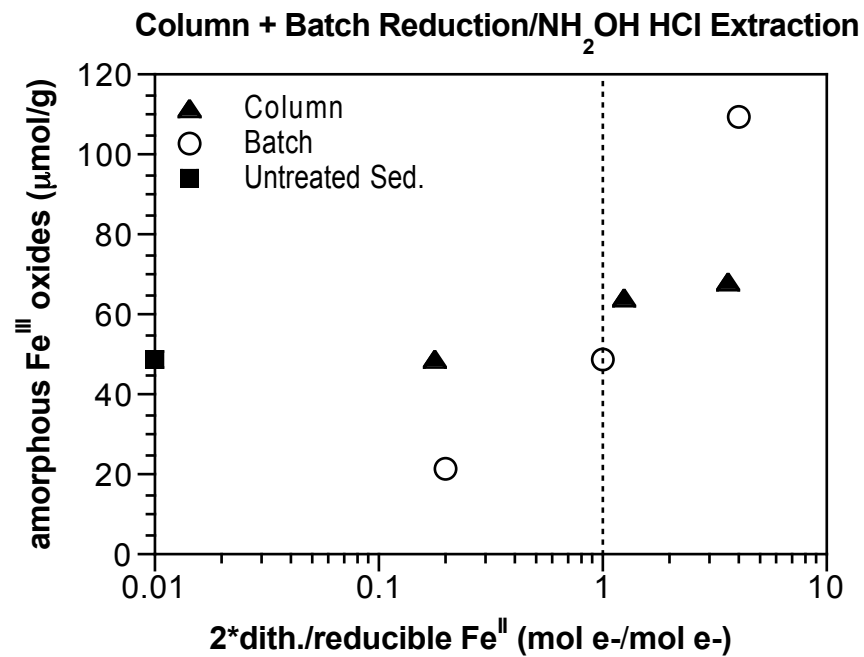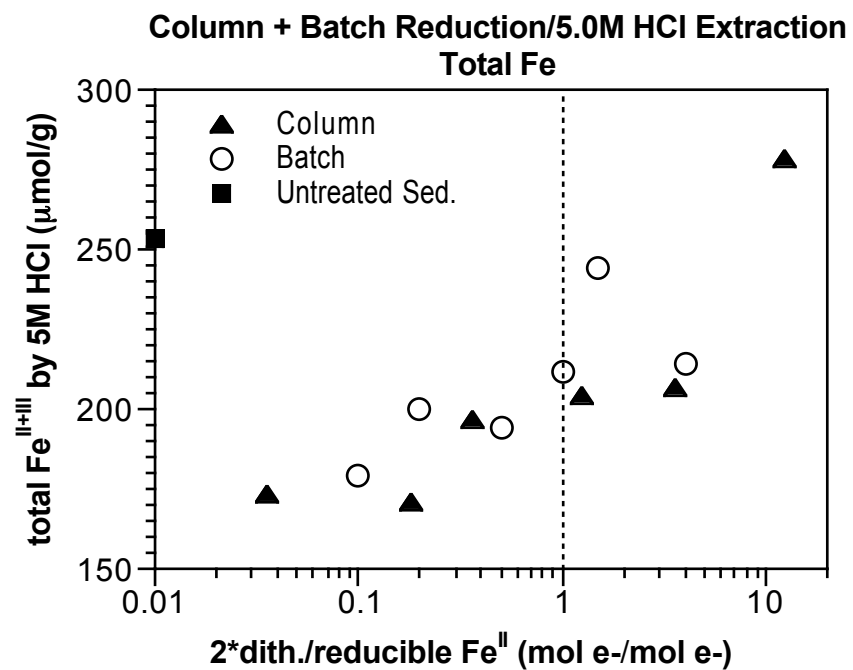
Column + Batch Reduction/NH$_2$OH HCl and DCB Extraction

Plot — y-axis: reducible Fe^{III} (µmol/g), ranging 0 to 120; x-axis: 2*dith./reducible Fe^{II} (mol e-/mol e-), ranging 0 to 5.

Legend:
▲ DCB Ext. (Crystal+ Amorph) FeII+FeIII /Sed. (umol/g)
○ NH2OH Ext. (Amorph) FeII +FeIII /Sed. (umol/g)

S54-57: Eh (raw) vs. Time

Legend:
- ○ Dithionite Standards
- △ S54; unt. Ft. Lewis
- □ S55; red. di/FE=28
- ◇ S56; unt. Ft. Lewis + 0.15% ZVI
- ▽ S57; unt. Ft. Lewis + 0.4% ZVI

X-axis: Time (h)
Y-axis: Raw Eh Response (mV)

S54-57: Eh Electrode Calibration

pH 7 Buffer
theo. 80/meas. 160

pH 4 Buffer
theo. 260/
meas. 190

Dithionite
Solution

X-axis: Theoretical Response (mV)
Y-axis: Measured Response (mV)

X1-4 AND X6-9 Fe conc.

X1-X4

X6-X9

X1-X4 ppm

Est. Time (h)

X1-10 Chg.in Eh during TNT deg.

Eh (X10)

Eh (X5)

Eh (mV)

Est. time (h)

X1-10 Chg.in pH during TNT deg.

pH (X10)

pH (X5)

pH

Est. time (h)

Coupled Degradation: pH Changes

biostimulation for all:
  10 mg/L RDX (N source)
  glucose addition
  trace nutrient addition

pH

— ▲— S54; untreated sediment
— □— S55; dith. reduced sediment
— ◇— S56; anaerobic sed. + 0.15% ZVI
— ▼— S57; anaerobic sed. + 0.4% ZVI

Time (h)

Appendix Q: Sediment Reductive Capacity 1-D Column Experiments

R15: Dissolved Oxygen Column, Probe 1
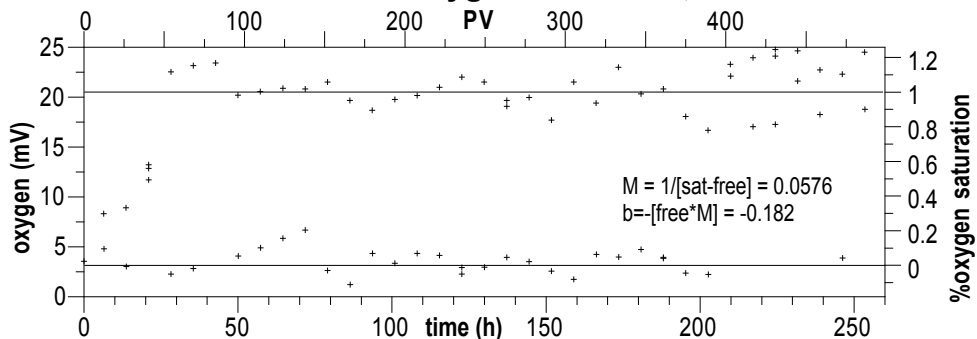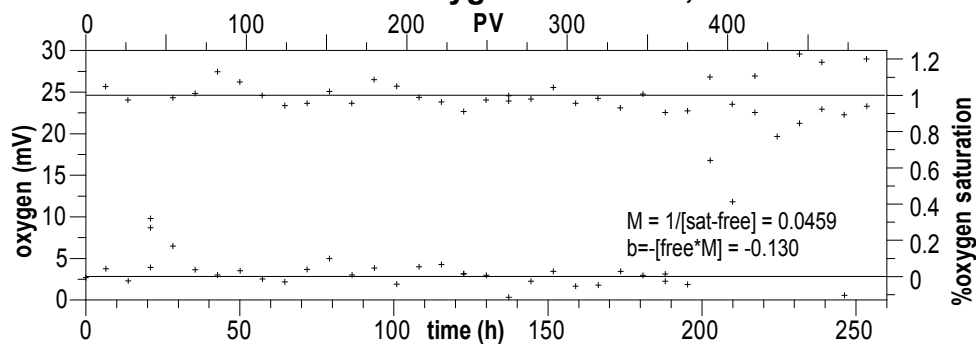**Ft Lewis Comp., red. w/0.1M dith +0.4M K** $_2$**CO**$_3$ **~33.5 PV @ 3.4**
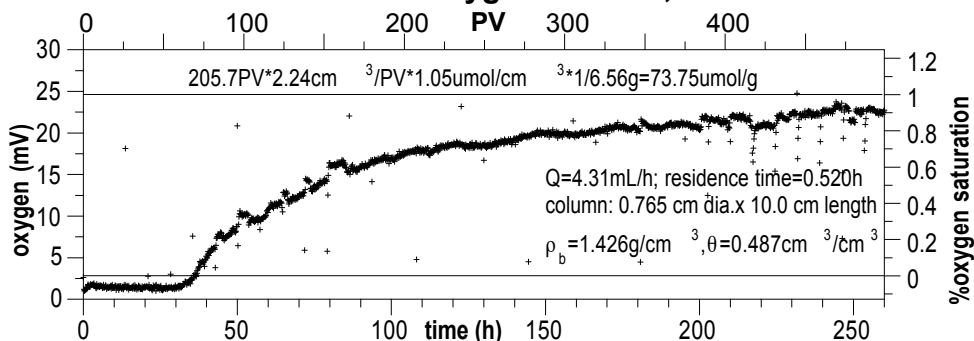
200.2PV*2.24cm^3/PV*1.05umol/cm^3*1/6.56g=71.79umol/g

Q=4.31mL/h; residence time=0.520h
column: 0.765 cm dia.x 10.0 cm length
ρ_b=1.426g/cm^3,θ=0.487cm^3/cm^3

R15: Dissolved Oxygen Column, Probe 2

205.7PV*2.24cm^3/PV*1.05umol/cm^3*1/6.56g=73.75umol/g

Q=4.31mL/h; residence time=0.520h
column: 0.765 cm dia.x 10.0 cm length
ρ_b=1.426g/cm^3,θ=0.487cm^3/cm^3

R15: Dissolved Oxygen Standards, Probe 1

M = 1/[sat-free] = 0.0576
b=-[free*M] = -0.182

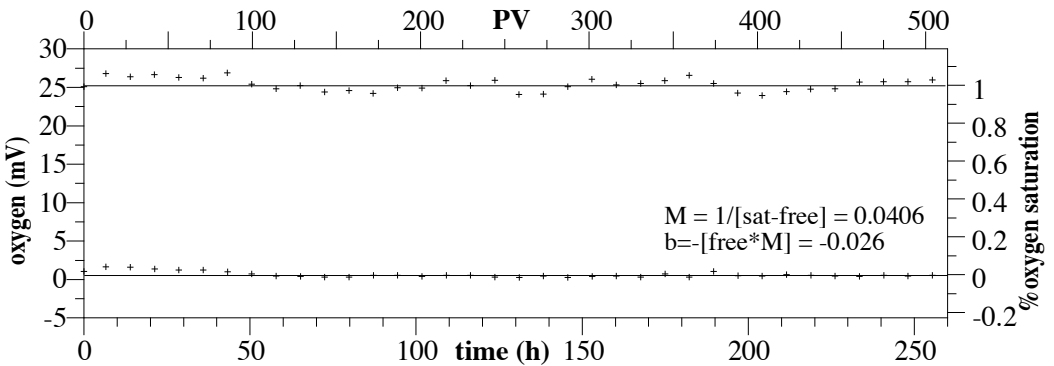### R15: Dissolved Oxygen Standards, Probe 2

M = 1/[sat-free] = 0.0459
b=-[free*M] = -0.130

Q.1

R17: Dissolved Oxygen Column, Probe 1

Ft Lewis Comp., red. w/0.03M dith +0.12M K CO_3 **~21 PV @ 5.45 h/P**

227.0PV*2.12cm^3/PV*1.05umol/cm^3*1/7.28g=69.41umol/g

Q=4.183mL/h; residence time=0.506h
column: 0.765 cm dia.x 10.0 cm length
$\rho_b \pm 1.583g/cm^3, \theta=0.461cm^3/cm^3$

R17: Dissolved Oxygen Column, Probe 2

212.1PV*2.12cm^3/PV*1.05umol/cm^3*1/7.28g=64.87umol/g

Q=4.183mL/h; residence time=0.506h
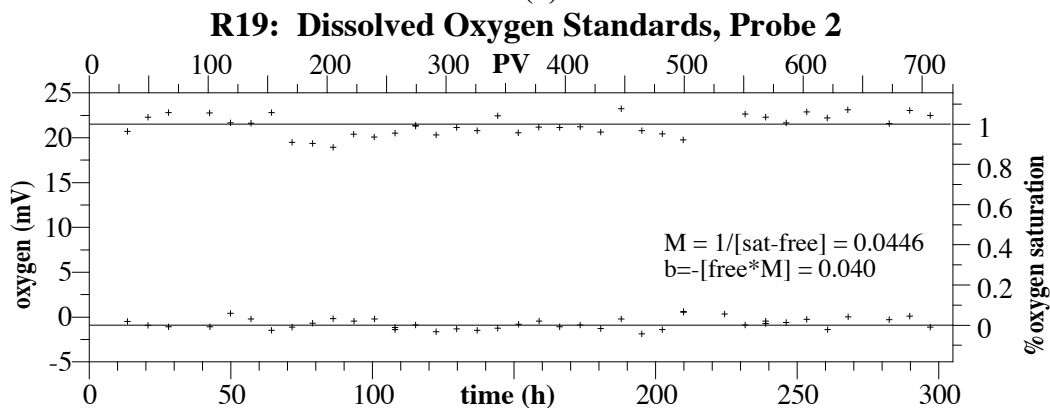column: 0.765 cm dia.x 10.0 cm length
$\rho_b \pm 1.583g/cm^3, \theta=0.461cm^3/cm^3$

R17: Dissolved Oxygen Standards, Probe 1

M = 1/[sat-free] = 0.0411
b=-[free*M] = -0.052

R17: Dissolved Oxygen Standards, Probe 2

M = 1/[sat-free] = 0.0406
b=-[free*M] = -0.026

Q.2

R19: Dissolved Oxygen Column, Probe 1

Ft Lewis Comp., red. w/0.01M dith +0.04M K **CO_2CO_3 ~19.5 PV @ 7.39 h**

Q=4.91mL/h; residence time=0.420h
column: 0.765 cm dia.x 10.0 cm length

ρ_b=1.548g/cm^3,θ=0.448cm^3/cm^3

71.0PV*2.06cm^3/PV*1.05umol/cm^3*1/7.12g=21.57umol/g

R19: Dissolved Oxygen Column, Probe 2

Q=4.91mL/h; residence time=0.420h
column: 0.765 cm dia.x 10.0 cm length

ρ_b=1.548g/cm^3,θ=0.448cm^3/cm^3

117.4PV*2.06cm^3/PV*1.05umol/cm^3*1/7.12g=35.67umol/g

R19: Dissolved Oxygen Standards, Probe 1

M = 1/[sat-free] = 0.0528
b=-[free*M] = -0.053

R19: Dissolved Oxygen Standards, Probe 2

M = 1/[sat-free] = 0.0446
b=-[free*M] = 0.040

Q.3

R21: Dissolved Oxygen Column, Probe 1

Ft Lewis Comp., red. w/0.003M dith +0.012M K CO_3 ~42.55 PV @ 3.38

PV
0   100   200   300   400   500   600

oxygen (mV): 25, 20, 15, 10, 5, 0, -5
% oxygen saturation: 1, 0.8, 0.6, 0.4, 0.2, 0, -0.2

Q=4.23mL/h; residence time=0.467h
column: 0.765 cm dia.x 10.0 cm length

ρ_b=1.530g/cm^3,θ=0.428cm^3/cm^3

247.5PV*1.97cm^3/PV*1.05umol/cm^3*1/7.04g=72.72umol/g

time (h): 0, 50, 100, 150, 200, 250, 300

R21: Dissolved Oxygen Column, Probe 2

PV
0   100   200   300   400   500   600

oxygen (mV): 25, 20, 15, 10, 5, 0, -5
% oxygen saturation: 1, 0.8, 0.6, 0.4, 0.2, 0, -0.2

Q=4.23mL/h; residence time=0.467h
column: 0.765 cm dia.x 10.0 cm length

ρ_b=1.530g/cm^3,θ=0.428cm^3/cm^3

267.4PV*1.97cm^3/PV*1.05umol/cm^3*1/7.04g=78.58umol/g

time (h): 0, 50, 100, 150, 200, 250, 300

R21: Dissolved Oxygen Standards, Probe 1

PV
0   100   200   300   400   500   600

oxygen (mV): 25, 20, 15, 10, 5, 0, -5
% oxygen saturation: 1, 0.8, 0.6, 0.4, 0.2, 0, -0.2

M = 1/[sat-free] = 0.0459
b=-[free*M] = -0.031

time (h): 0, 50, 100, 150, 200, 250, 300

R21: Dissolved Oxygen Standards, Probe 2

PV
0   100   200   300   400   500   600

oxygen (mV): 25, 20, 15, 10, 5, 0, -5
% oxygen saturation: 1, 0.8, 0.6, 0.4, 0.2, 0, -0.2

M = 1/[sat-free] = 0.0472
b=-[free*M] = -0.047

time (h): 0, 50, 100, 150, 200, 250, 300

Q.4

R27: Dissolved Oxygen Column, Probe 1^3

Q=4.077mL/h; residence time=0.471h
column: 0.765 cm dia.x 10.0 cm length
ρ_b=1.517g/cm^3,θ=0.417cm^3/cm^3

11.75PV*1.92cm^3/PV*1.05umol/cm^3*1/6.98g=3.39umol/g

R27: Dissolved Oxygen Column, Probe 2

14.65PV*1.92cm^3/PV*1.05umol/cm^3*1/6.98g=4.23umol/g

Q=4.077mL/h; residence time=0.471h
column: 0.765 cm dia.x 10.0 cm length
ρ_b=1.517g/cm^3,θ=0.417cm^3/cm^3

R27: Dissolved Oxygen Standards, Probe 1

M = 1/[sat-free] = 0.0543
b=-[free*M] = -0.243

R27: Dissolved Oxygen Standards, Probe 2

M = 1/[sat-free] = 0.0459
b=-[free*M] = -0.145

Q.5

R29: Dissolved Oxygen Column, Probe 2

Q=3.45mL/h; residence time=0.588h
column: 0.765 cm dia.x 10.0 cm length

ρ_b=1.574g/cm^3,θ=0.441cm^3/cm^3

14.57PV*2.03cm^3/PV*1.05umol/cm^3*1/7.24g=4.29umol/g

Ft Lewis Comp., red. w/0.3 mM dith +1.2 mM K   **CO$_2$**   **~28.14 PV @ 4.23**

R29: Dissolved Oxygen Column, Probe 1

Q=3.45mL/h; residence time=0.588h
column: 0.765 cm dia.x 10.0 cm length

ρ_b=1.574g/cm^3,θ=0.441cm^3/cm^3

13.33PV*2.03cm^3/PV*1.05umol/cm^3*1/7.24g=3.92umol/g

R29: Dissolved Oxygen Standards, Probe 1

M = 1/[sat-free] = 0.0500
b=-[free*M] = -0.0525

R29: Dissolved Oxygen Standards, Probe 2

M = 1/[sat-free] = 0.0447
b=-[free*M] = -0.0353

Q.6
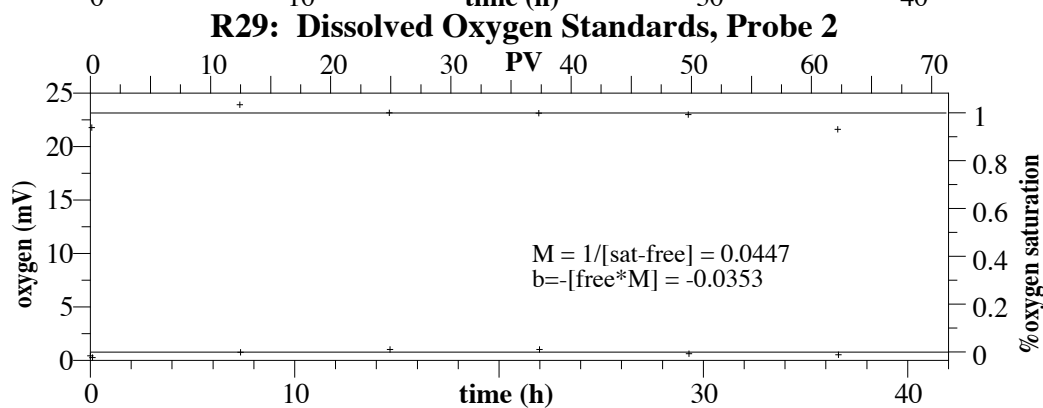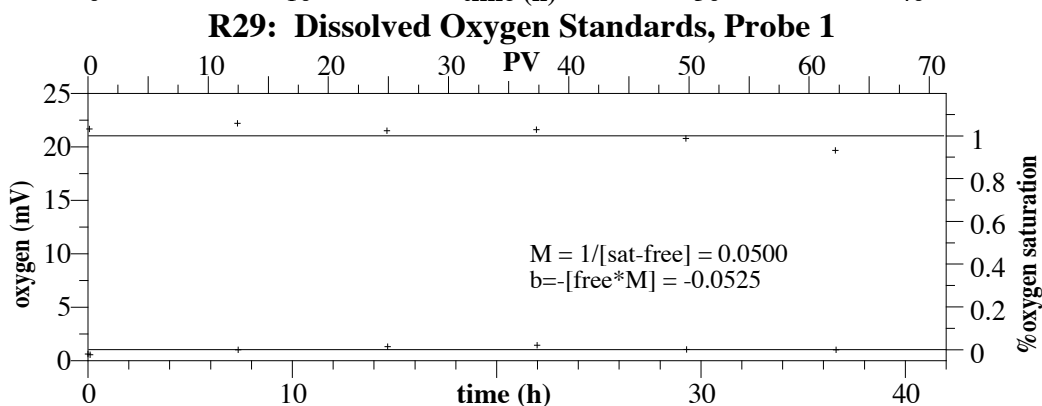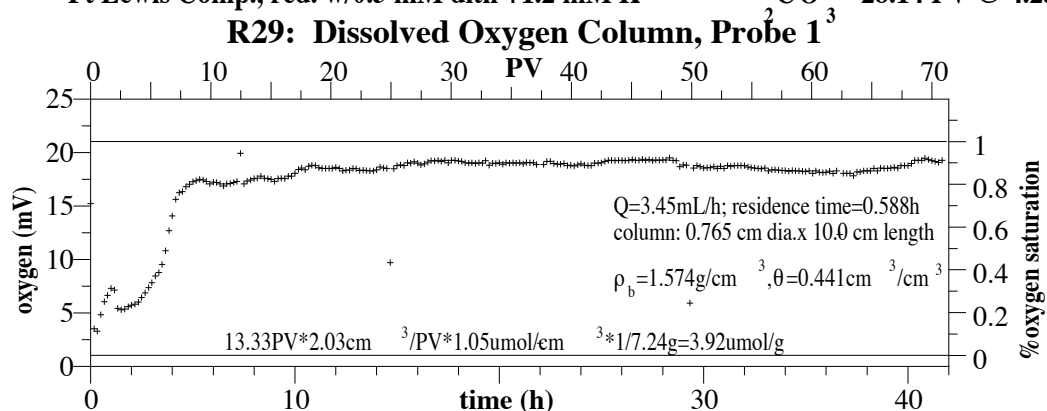
Ft Lewis Comp., reduced with 2*Dith./Fe = 1.118
R44: Dissolved Oxygen Column, Probe 1
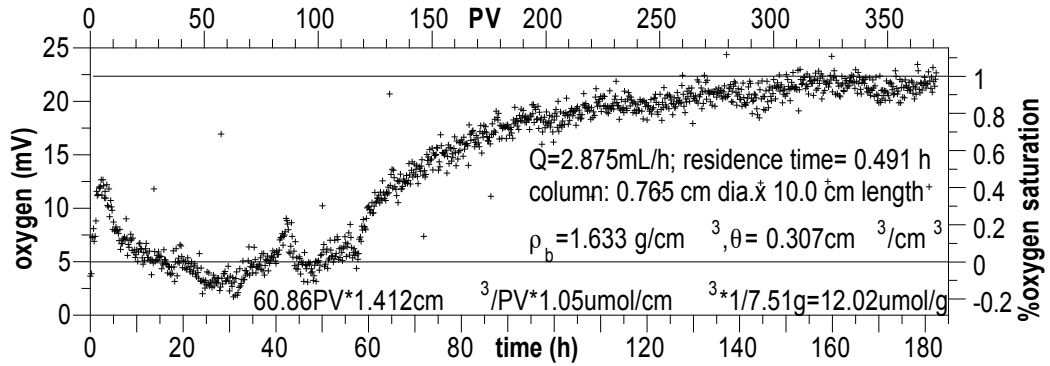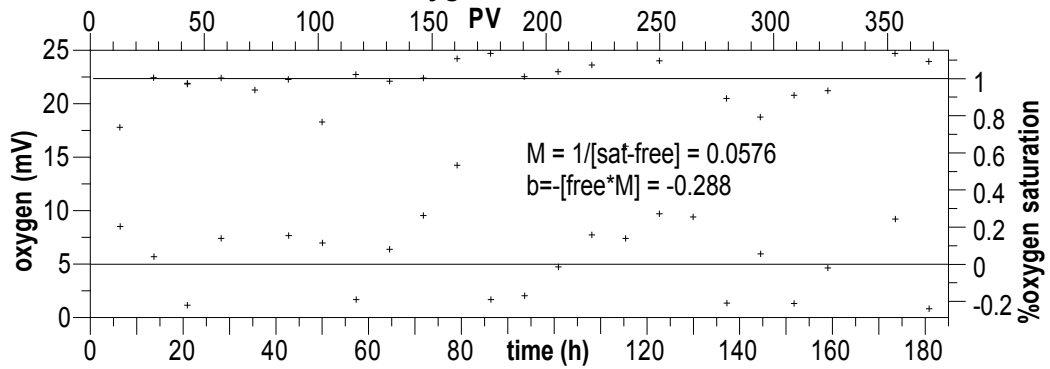
PV

oxygen (mV)

%oxygen saturation

Q=2.875mL/h; residence time= 0.491 h
column: 0.765 cm dia.x 10.0 cm length

ρ_b=1.633 g/cm^3, θ= 0.307cm^3/cm^3

60.86PV*1.412cm^3/PV*1.05umol/cm^3*1/7.51g=12.02umol/g

time (h)

R44: Dissolved Oxygen Standards, Probe 1

PV

oxygen (mV)

%oxygen saturation

M = 1/[sat-free] = 0.0576
b=-[free*M] = -0.288

time (h)

R44: Dissolved Oxygen Column, Probe 2

PV

oxygen (mV)

%oxygen saturation

Q=2.875mL/h; residence time= 0.491 h
column: 0.765 cm dia.x 10.0 cm length

ρ_b=1.633 g/cm^3, θ= 0.307cm^3/cm^3

107.6PV*1.412cm^3/PV*1.05umol/cm^3*1/7.51g=21.24umol/g

time (h)

R44: Dissolved Oxygen Standards, Probe 2

PV

oxygen (mV)

%oxygen saturation

M = 1/[sat-free] = 0.0521
b=-[free*M] = -0.178

time (h)

Q.7
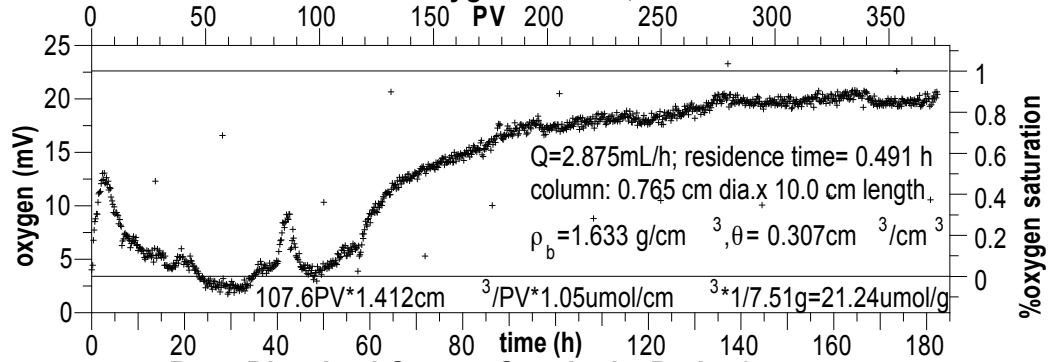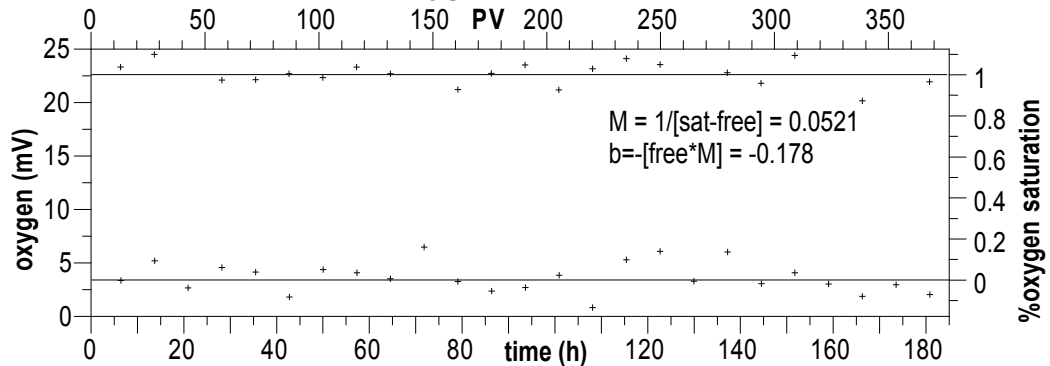
Ft Lewis Comp., reduced with 2*Dith./Fe = 0.541
R46: Dissolved Column Standards, Probe 1
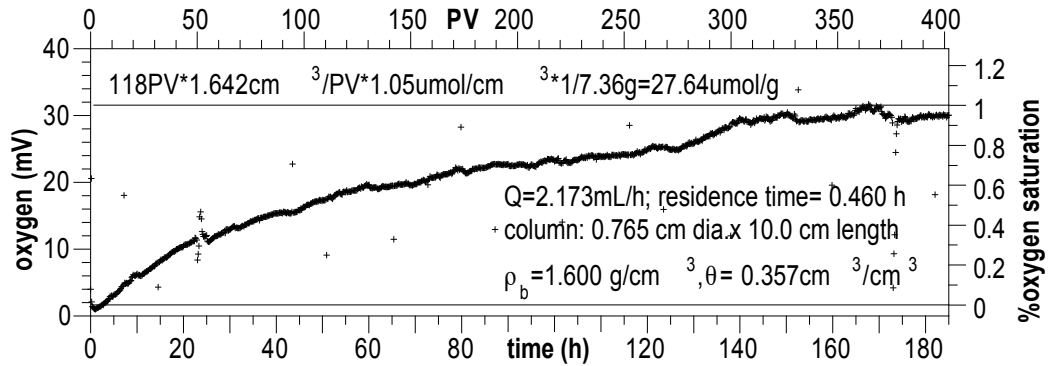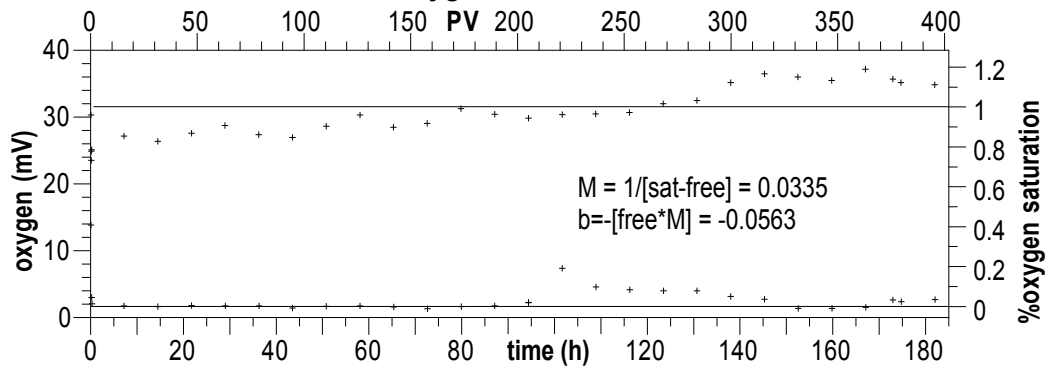
$118PV*1.642cm^3/PV*1.05umol/cm^3*1/7.36g=27.64umol/g$

Q=2.173mL/h; residence time= 0.460 h

column: 0.765 cm dia.x 10.0 cm length

ρ_b=1.600 g/cm^3, θ= 0.357cm^3/cm^3

R46: Dissolved Oxygen Standards, Probe 1

M = 1/[sat-free] = 0.0335

b=-[free*M] = -0.0563

R46: Dissolved Oxygen Column, Probe 2

Q=2.173mL/h; residence time= 0.460 h

column: 0.765 cm dia.x 10.0 cm length

ρ_b=1.600 g/cm^3, θ= 0.357cm^3/cm^3

electrode not
responding
after 78 h

R46: Dissolved Oxygen Standards, Probe 2

M = 1/[sat-free] = 0.0528

b=-[free*M] = -0.0697

electrode not
responding
after 78 h

Q.8
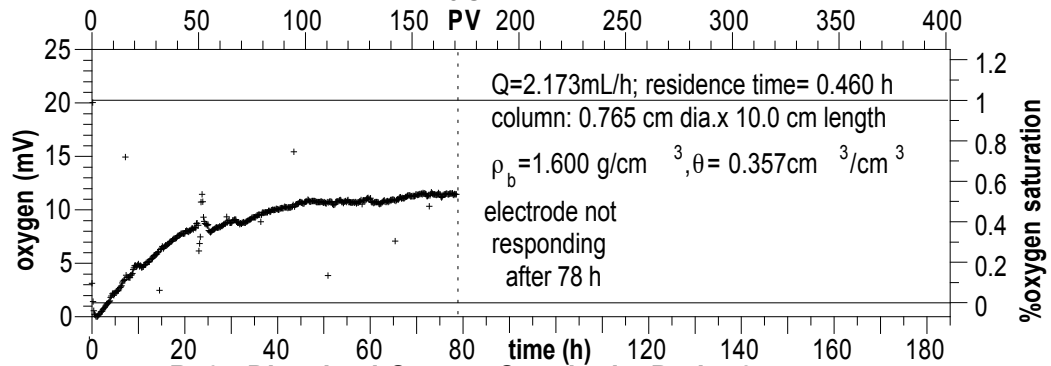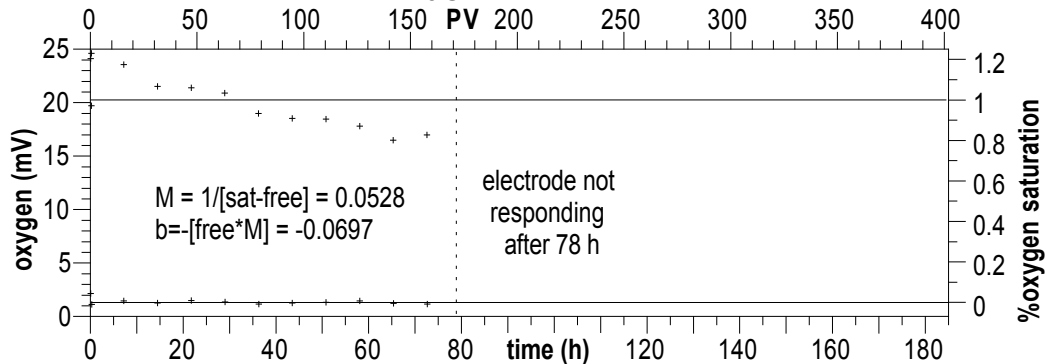
Ft Lewis Comp., reduced with 2*Dith./Fe = 0.237

R48: Dissolved Oxygen Column, Probe 1
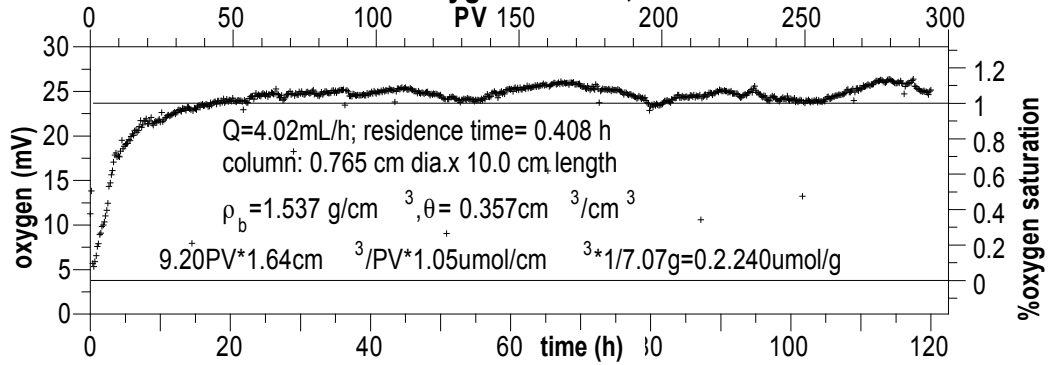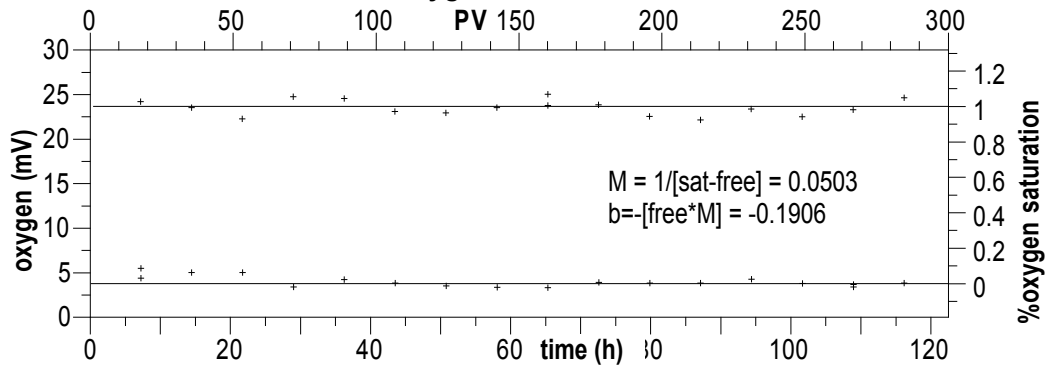
Q=4.02mL/h; residence time= 0.408 h

column: 0.765 cm dia.x 10.0 cm length

ρ_b=1.537 g/cm^3, θ= 0.357cm^3/cm^3

9.20PV*1.64cm^3/PV*1.05umol/cm^3*1/7.07g=0.2.240umol/g

R48: Dissolved Oxygen Standards, Probe 1

M = 1/[sat-free] = 0.0503

b=-[free*M] = -0.1906

R48: Dissolved Oxygen Column, Probe 2

Q=4.02mL/h; residence time= 0.408 h

column: 0.765 cm dia.x 10.0 cm length

ρ_b=1.537 g/cm^3, θ= 0.357cm^3/cm^3

41:16PV*1.64cm^3/PV*1.05umol/cm^3*1/7.07g=10.03umol/g

R48: Dissolved Oxygen Standards, Probe 2

M = 1/[sat-free] = 0.0428

b=-[free*M] = -0.1485

Q.9
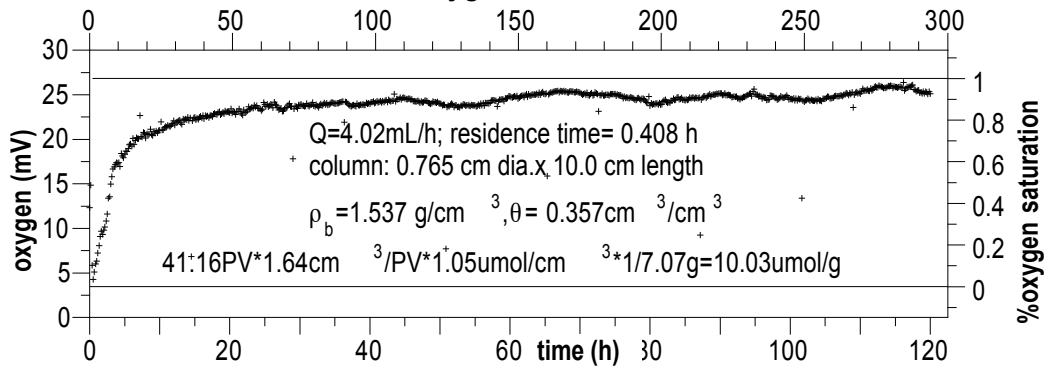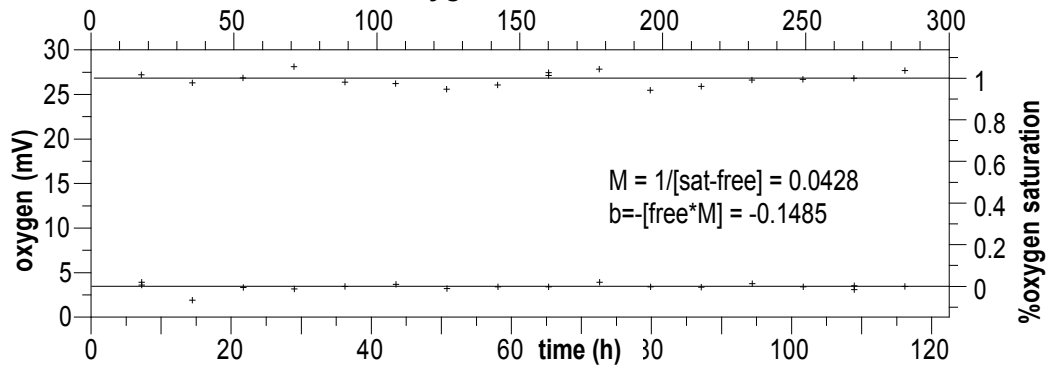
Ft Lewis Comp., reduced with 2*Dith./Fe = 0.10
R50: Dissolved Oxygen Column, Probe 1
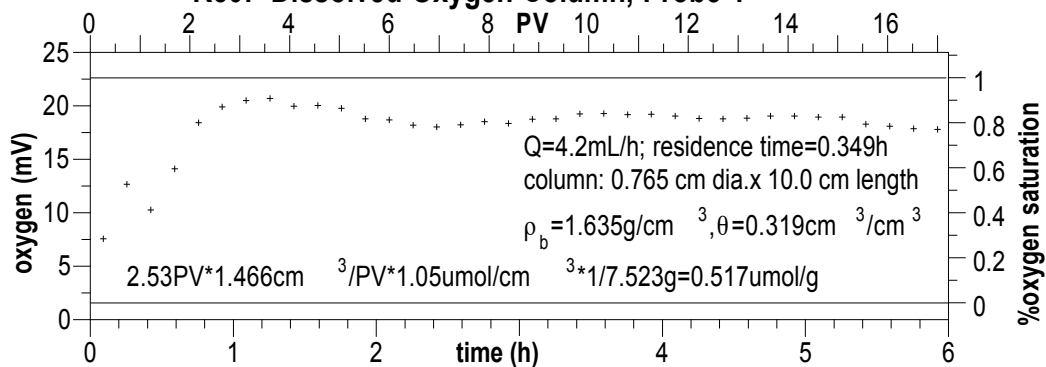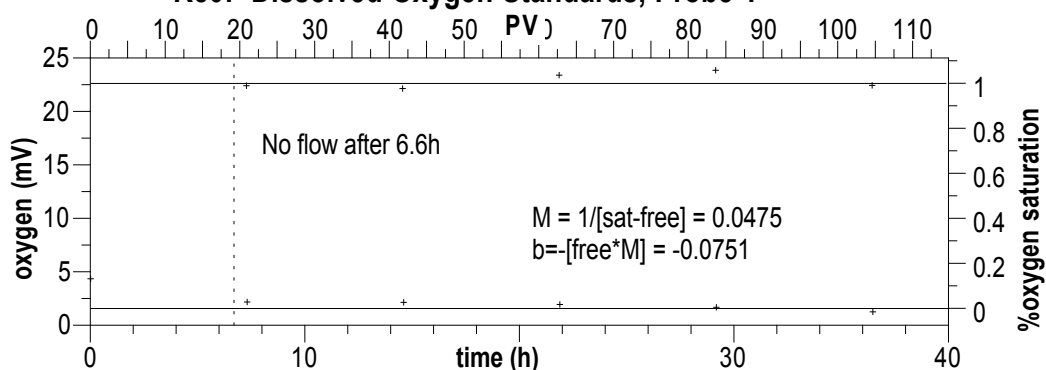
Q=4.2mL/h; residence time=0.349h
column: 0.765 cm dia.x 10.0 cm length

ρ_b=1.635g/cm^3,θ=0.319cm^3/cm^3

2.53PV*1.466cm^3/PV*1.05umol/cm^3*1/7.523g=0.517umol/g

R50: Dissolved Oxygen Standards, Probe 1
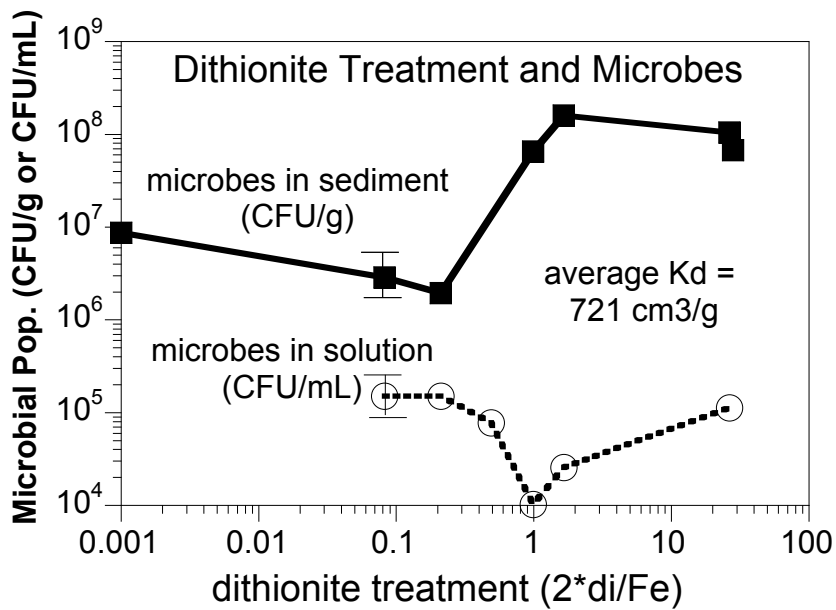
No flow after 6.6h

M = 1/[sat-free] = 0.0475
b=-[free*M] = -0.0751

R50: Dissolved Oxygen Column, Probe 2

Q=4.2mL/h; residence time=0.349h
column: 0.765 cm dia.x 10.0 cm length

ρ_b=1.635g/cm^3,θ=0.319cm^3/cm^3

5.21PV*1.466cm^3/PV*1.05umol/cm^3*1/7.523g=1.066umol/g

R50: Dissolved Oxygen Standards, Probe 2

No flow after 6.6h

M = 1/[sat-free] = 0.0399
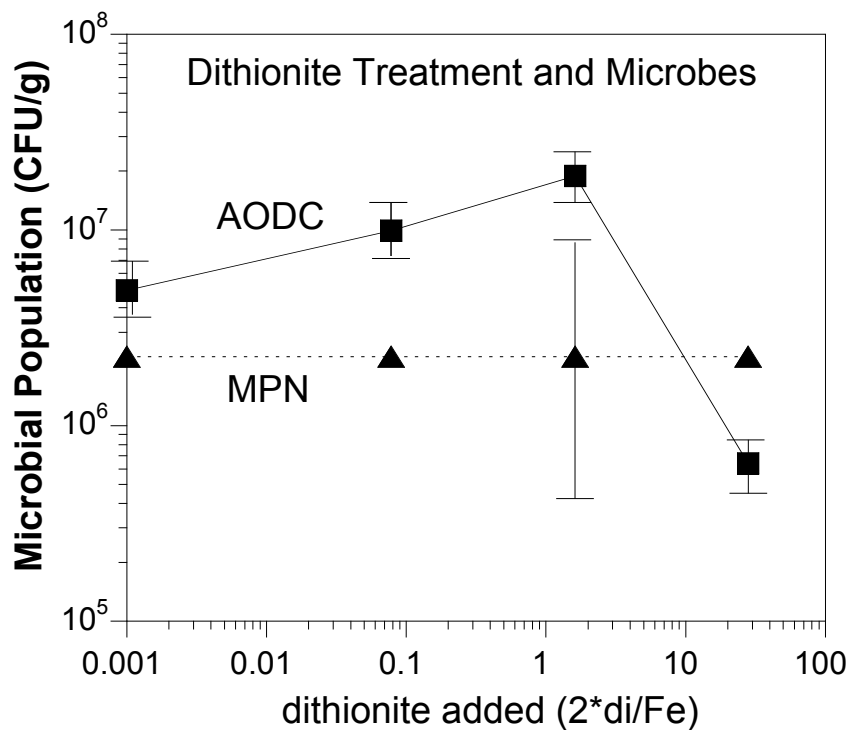b=-[free*M] = 0.0084

Q.10
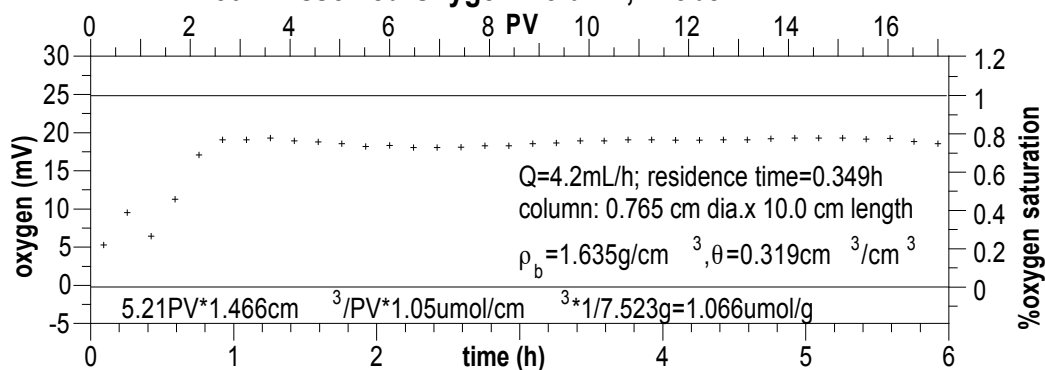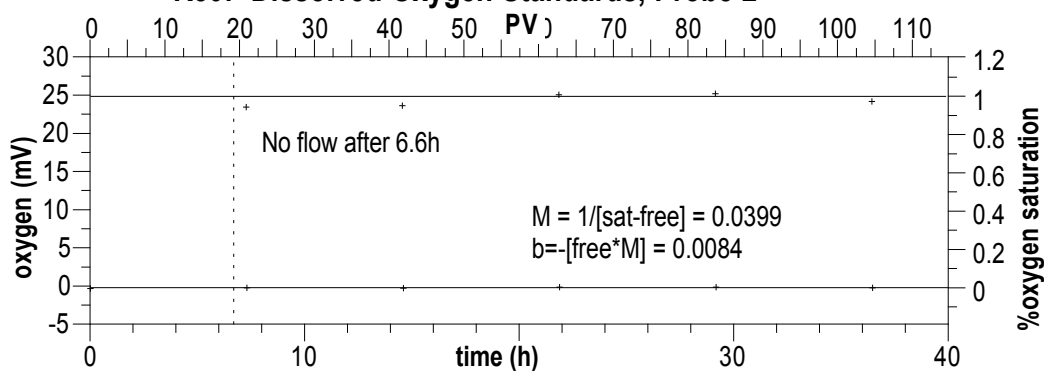
Ft Lewis Comp., reduced with 2*Dith./Fe = 0.078
R52: Dissolved Oxygen Column, Probe 1
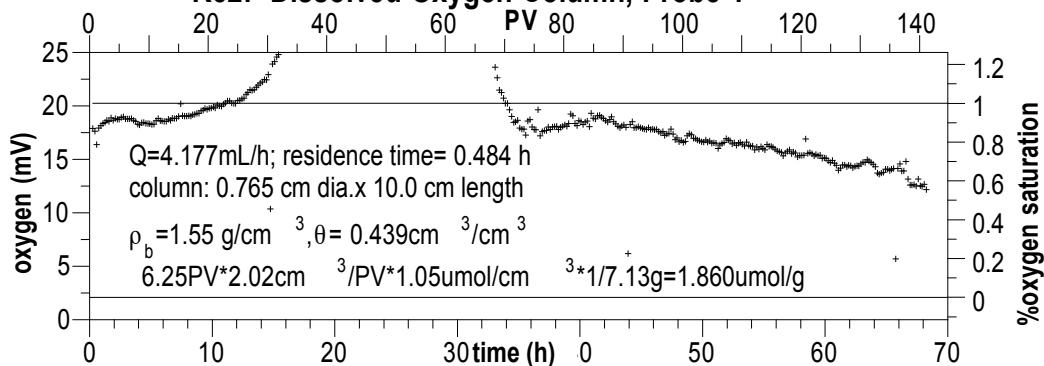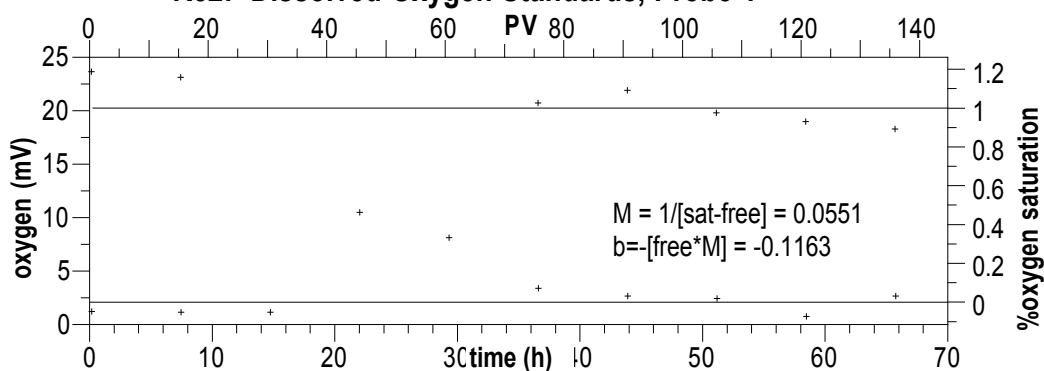
Q=4.177mL/h; residence time= 0.484 h

column: 0.765 cm dia.x 10.0 cm length

ρ_b=1.55 g/cm^3,θ= 0.439cm^3/cm^3
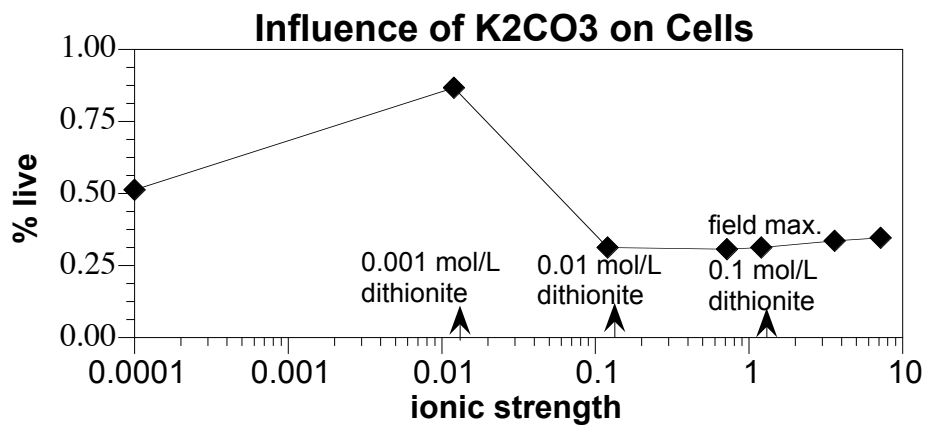
6.25PV*2.02cm^3/PV*1.05umol/cm^3*1/7.13g=1.860umol/g

R52: Dissolved Oxygen Standards, Probe 1

M = 1/[sat-free] = 0.0551

b=-[free*M] = -0.1163

R52: Dissolved Oxygen Column, Probe 2

18.48PV*2.02cm^3/PV*1.05umol/cm^3*1/7.13g=5.393umol/g

Q=4.177mL/h; residence time= 0.484 h

column: 0.765 cm dia.x 10.0 cm length

ρ_b=1.55 g/cm^3,θ= 0.439cm^3/cm^3

R52: Dissolved Oxygen Standards, Probe 2

M = 1/[sat-free] = 0.0422

b=-[free*M] = -0.0532

Q.11
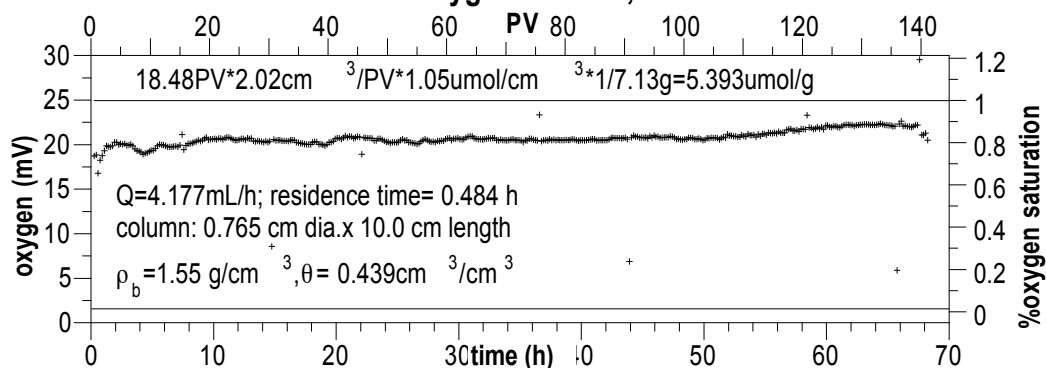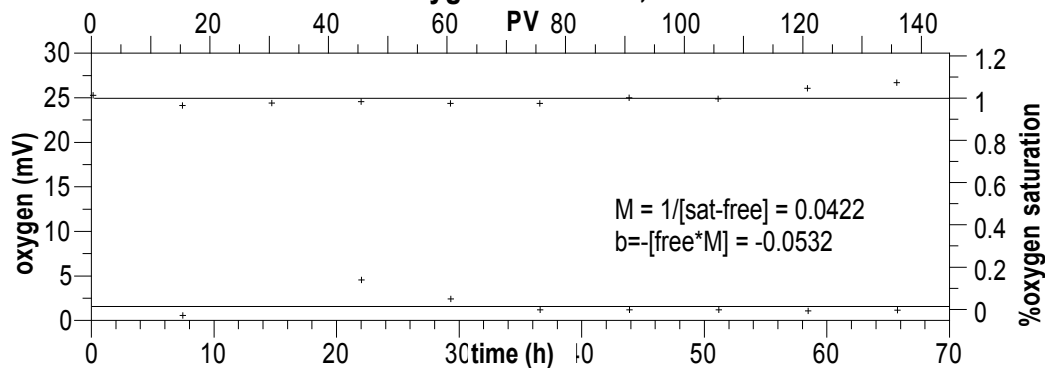
Appendix R: Sediment Microbial Biomass and Dithionite Treatment

Influence of Na2S2O4 + K2CO3 on Cells

% live

0.001 mol/L dithionite

0.01 mol/L dithionite

field max.
0.1 mol/L dithionite

ionic strength

Influence of Na2S2O4 on Cells

% live

0.001 mol/L dithionite

0.01 mol/L dithionite

field max.
0.1 mol/L dithionite

ionic strength

Influence of K2CO3 on Cells

% live

0.001 mol/L dithionite

0.01 mol/L dithionite

field max.
0.1 mol/L dithionite

ionic strength

Apparent Microbial Attachment

Kd (L/Kg) vs ionic strength

0.001 mol/L
dithionite

0.01 mol/L
dithionite
(typical)

0.1 mol/L
dithionite
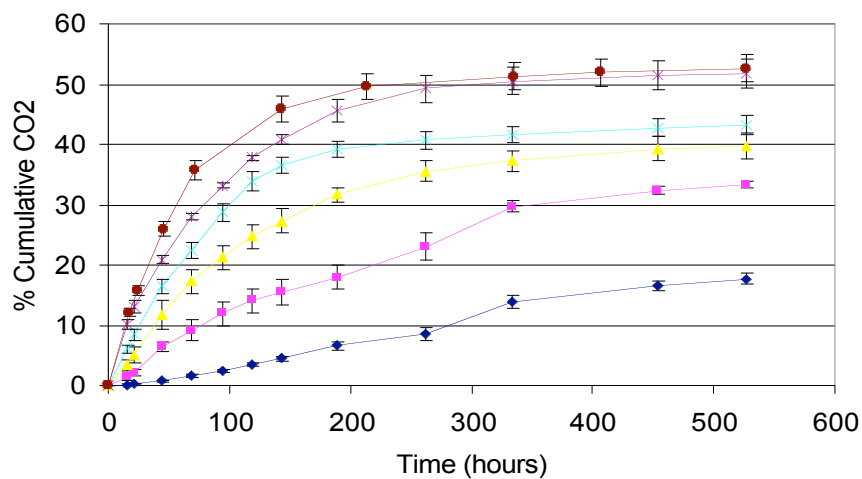field max.

PNNL/Szecsody
SERDP ER1376

R.3

Appendix S: Sediment Microbial Activity Characterization: Acetate Mineralization and Dithionite Exposure
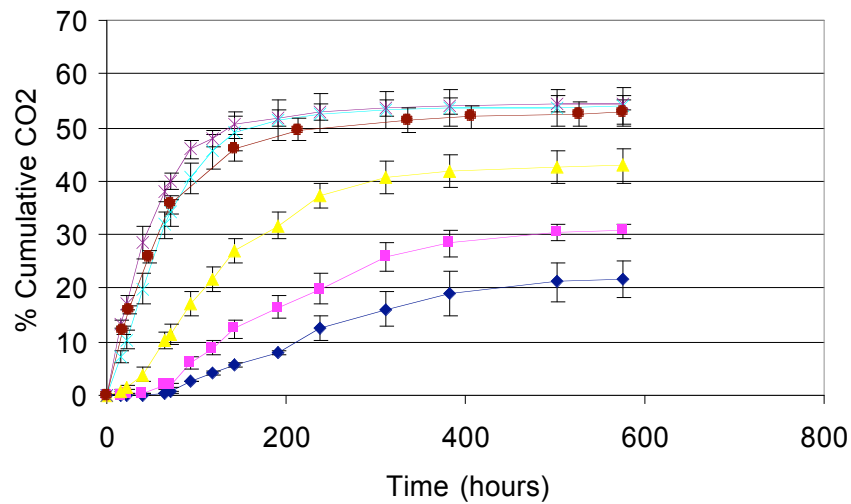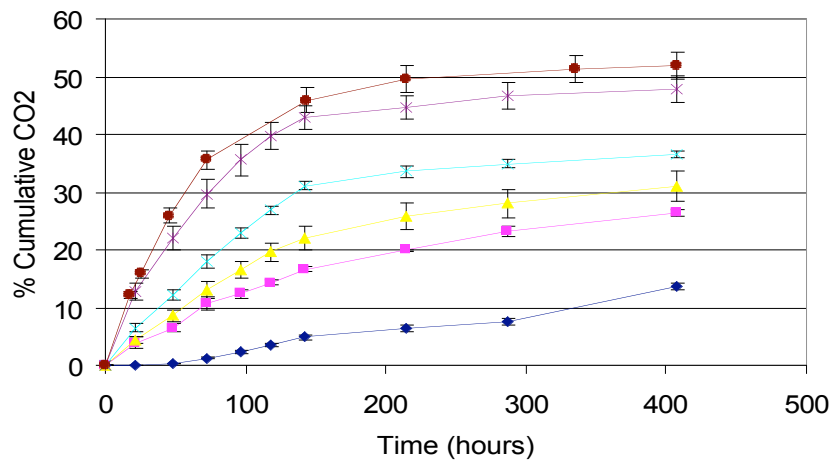

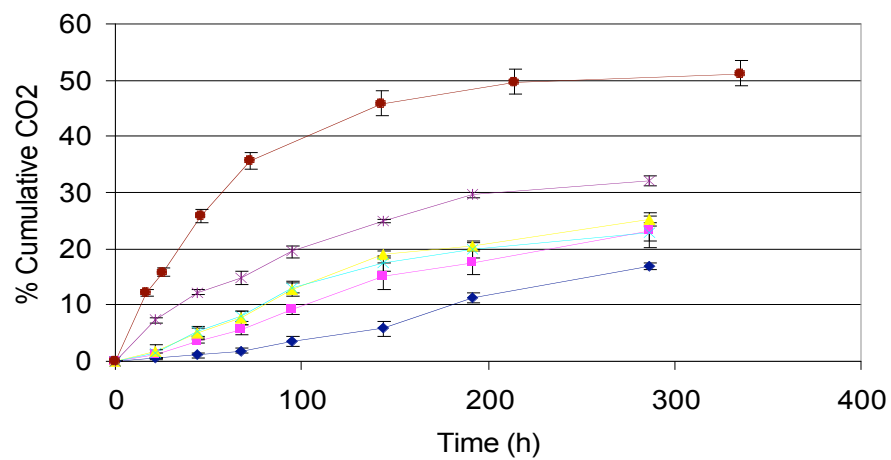Acetate Mineralization – exposed to dithionite for 1 day, then oxidized

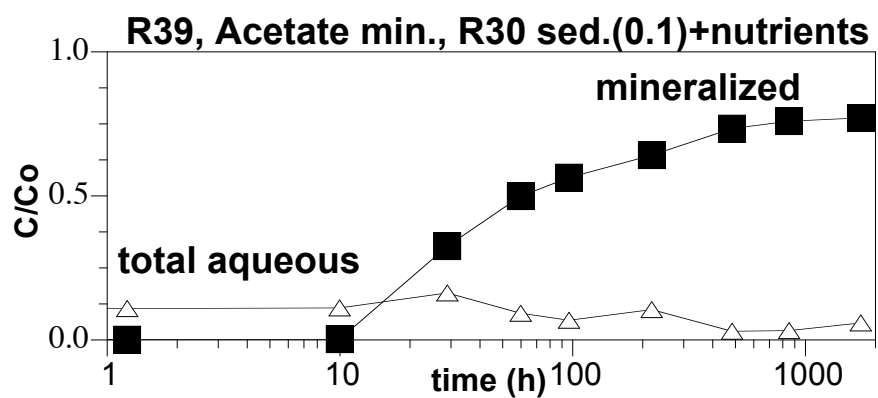Acetate Mineralization – exposed to dithionite for 3 days, then oxidized

◆ Treatment 1	■ Treatment 2	▲ Treatment 3
✕ Treatment 4	✱ Treatment 5	● Control-No treatment
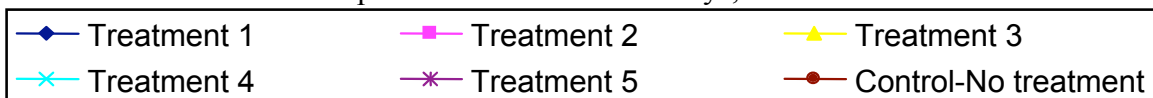
Acetate Mineralization – exposed to dithionite for 5 days, then oxidized

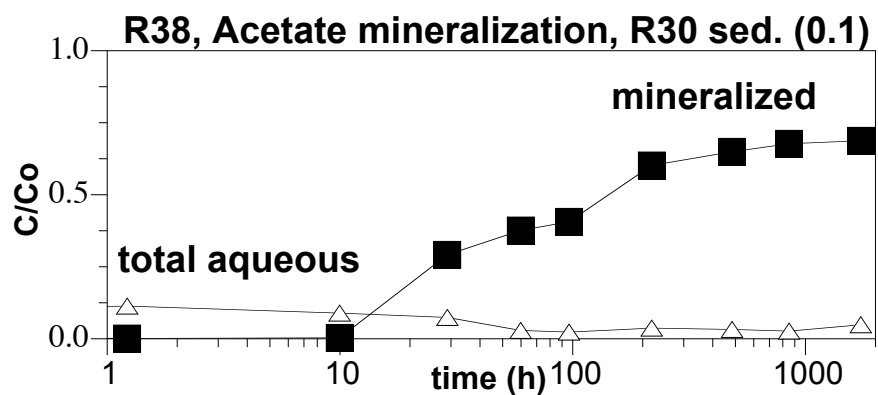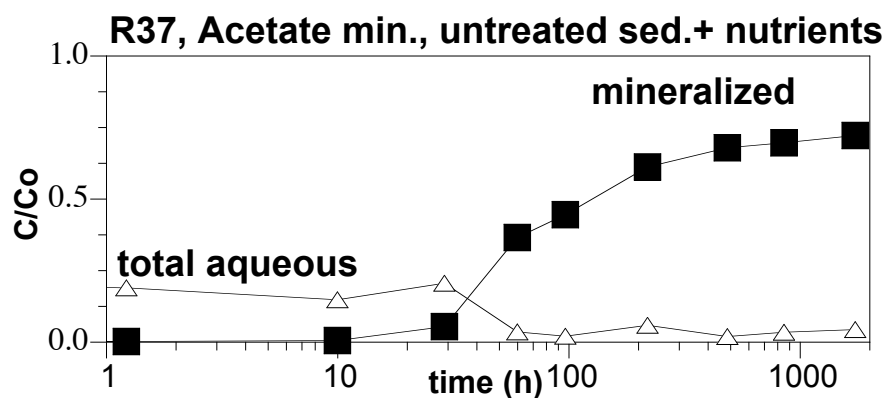Acetate Mineralization – exposed to dithionite for 10 days, then oxidized

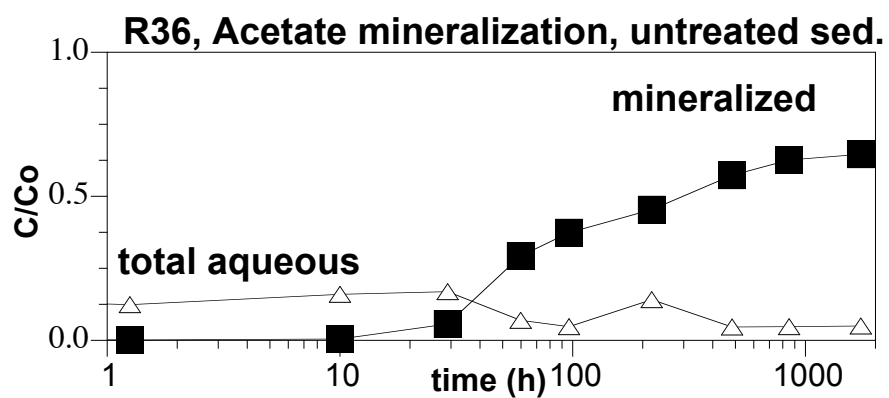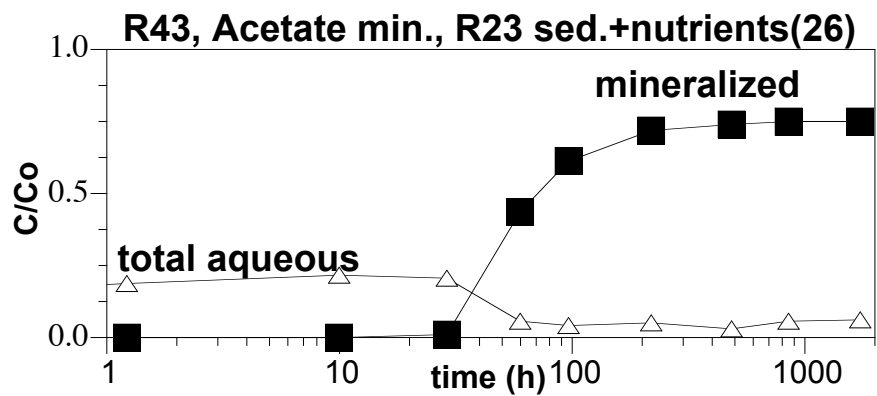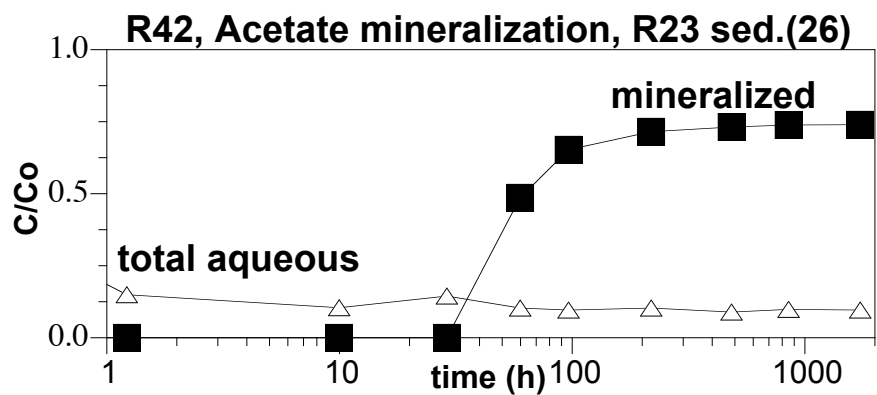| treatment	2* di/Fe
1	4.0
2	1.0
3	0.5
4	0.1
5	0.02

R36, Acetate mineralization, untreated sed.

R37, Acetate min., untreated sed.+ nutrients

R38, Acetate mineralization, R30 sed. (0.1)

R39, Acetate min., R30 sed.(0.1)+nutrients

S.3

R40, Acetate mineralization, R26 sed.(1.0)

mineralized

total aqueous

C/Co

time (h)

R41, Acetate min., R26 sed.(1.0)+nutrients

mineralized

total aqueous

C/Co

time (h)

R42, Acetate mineralization, R23 sed.(26)

mineralized

total aqueous

C/Co

time (h)

R43, Acetate min., R23 sed.+nutrients(26)

mineralized

total aqueous

C/Co

time (h)

R62/63, Acetate mineralization controls

gluteraldehyde added: 0.4 mL/g; 0.1 mL/5 mL

mineralized

◆ untreated sediment
☐ reduced sediment (2di/Fe = 26)

C/Co

time (h)

R77: Acetate Mineralization by Red. Sediment + Bacteriacides

Ft. Lewis Sed. Reduced 2*di/Fe=28, r_{sw} = 0.167

In anaerobic environment
10 mg/L 14C-Acetate + 0.17 mL 0.5M PIPES
+ 0.1mL/5mL 25% gluteraldehyde
+ 2mM molbdate tetrahydrate
+ 6mM sodium 2-bromoethanesulfonate

Mineralized C/Co

time (h)

RDX, Acetate Mineralization in Reduced Sediment with Bactericide (R76, 77)
sediment: 26x (R66)

C/Co

mineralized

time (h)

S.5

Acetate Mineralization vs Iron Reduction + nutrients

hypothesis: acetate mineralization is a measure
  of microbial reductase. There should be less
  with stronger dithionite treatment.
  With nutrients, should see faster min.
results: ~no difference with treatments
- but nutrients did increase rate:
half-life (no nutr.): 52-300h
half-life (+nutr.): 48-93 h

2*di/Fe = 26

1.0

0.1

0.00

C/Co

time (h)

Acetate Mineralization vs Iron Reduction

2*di/Fe = 26

0.1

1.0

0.00

C/Co

time (h)